A Study of Low head Hydropower using a siphon system and conversion to air pressure

A thesis submitted for the degree of Doctor Philosophy

Engineering Department, Lancaster University

By

Esti Mardiani-Euers

Submitted: August 2013

ProQuest LLC.
789 East Eisenhower Parkway
P.O. Box 1346
Ann Arbor, MI 48106 – 1346

Declaration

I hereby declare that this submission is my own work and that, to the best of my knowledge and belief, it contains no material previously published or written by another person nor material which to a substantial extent has been accepted for the award of any other degree or diploma of the university or other institute of higher education, except where due to acknowledgement has been made in the text.

Esti Mardiani-Euers

December, 2012

Abstract

This thesis describes an investigation into a technique for converting the energy available at low head (2m) hydro sites into an air flow that could be used to generate electricity. After giving a rationale for the uses of this design at the many available sites in the U.K., a brief history of the development of water power and of the more recent research into this process is outlined.

The investigation focused on the equipment employed in using a water siphon to induce air flow. The testing of various aerator configurations in a full scale laboratory experiment is described, and the difficulties encountered in the two phase flow that occurs in the process are examined. The on- site experiment at the Yorkshire Treatment Plant that is discussed, proved that this siphon system was robust and reliable.

The laboratory experiment (with restrictions of space availability) results show that more than 30% of the energy available at such sites can be converted into a form of air flow energy. While this is a slight improvement over the previous work done in the field it must be noted that the highest power output of 460 Watts occurred at 32.3% efficiency in the high siphon. Suggestions of improvement on aerator design that could increase more power output and efficiency are given, while recognizing that there will be some further losses of energy when the system is used to generate electricity. The results indicate the technique devised is environmentally advantageous and economically feasible.'

Acknowledgement

This project was funded by the Joule Centre, and thanks to the Director, Professor Peter Crossley PhD, MIET, CEng, for this opportunity. It was also partly funded by Yorkshire Water authority to test the siphon operation onsite and thanks to Mr. Ilyas Dawood, Director of R and D Energy at the Yorkshire Water who has provided facilities to make the experiment run smoothly.

I would like to take this opportunity to express my gratitude to all those who have assisted in this project and have given their tremendous support during my PhD study.

I have received academic supervision and support from many people; I list them hear with all my gratitude, in chronological order: Dr. Nick Baker, Mr. Martin B. Widden, Dr. Phil Leigh, Mr. George Agiddis, Dr. Michael Moore, Dr. James C Taylor, Prof. Xi Jiang, Dr. Wlodeck Tych, Dr Lesleyann, Dr. Dhany Arifianto, and Dr. Maria Angeles Solera Garcia.

Encouragement, support, advice, and coaching were provided in numerous occasions by, Dr. Will Med, Dr. Cheryl Simmill Binning, Mrs. Genevieve Moore, Mrs. Jacqueline Williams, and Dr. Vina Adriany.

Many times technical support was given by Mr. Peter Caley and Mr. Barry Nobel, my colleagues: Adam Bedford, Kester Gunn, Yudhi Ariadi, Jeremy Pie, Haikal Bekti Anggoro, and Muhammad Maskuri.

At the final stage of my study, I have also received several grants from some awarding bodies; my gratitude to the Fund for Women Graduates, the Royal British Legion, the Scots Guards Association, ABF The Soldier's Charity, the Southdown Trust, the Worshipful Company of Engineers, the Lancaster University through Access for Learning Fund and the Graduate College.

Finally my husband John, for his patience and silent support, especially at the end stage of my study period where morale boosting and motivation needed, and I have left him alone at home almost every day until late at night.

We cannot do great things on this earth,
we can only do small things with great love
Mother Teresa

Contents

List of Tables

List of Figures

Chapter 1

Introduction

This chapter describes the background, the aims and objectives of the research, and the methodology used.

1.1 Background and Rationale

Renewable energy is an integral part of government strategy to tackle climate change in order to reduce carbon emissions, as well as to ensure the provision of energy that is clean and affordable. In March 2007 the European Council agreed to a binding target of 20% of renewable energies in overall EU consumption by 2020 (Arnott, 2010).

The following paragraphs describe the forecasted energy demand resources, up to 2035, extracted from World Energy Outlook Factsheets 2010 and 2011 (OECD/IEA, 2010, 2011).

Between 2008 and 2035, the yearly average of the world primary energy demand will increase, and oil will remain the dominant fuel. Coal will continue to be the second largest energy source with a total reserve of 1 trillion tonnes. This can supply energy for another 150 years.

However, the ongoing Middle East crisis, the unstable situations in Arab countries, and the giant Chinese booming economy have resulted in high and continuously changing oil prices. These factors will force the government into seeking alternative energy sources in order to replace oil, possibly with nuclear power or renewable sources.

The Outlook Factsheets (OECD/IEA, 2010, 2011), cited above, stated that the world nuclear power generation led by China, Korea and India, and more recently by Iran (which has caused controversy and political tension with Israel) will grow up to 70% from the 2008 nuclear power. The tragedy of Fukushima Daiichi nuclear disaster has made people think that nuclear energy is not one hundred percent safe, and that to operate current and new nuclear power plants will cost more due to the increased requirements for safety.

Lord Turner, the chairman of the independent Committee on Climate Change (CCC) stated that '*meeting the 20% share of renewable energy target in the UK by 2020 requires a step change in the rate of progress and entails significant delivery risks, which should be addressed as a matter of urgency*'. (Arnott, 2010)

Thus, renewable energy will have an important role in any future choices to meet the continuously growing energy demand.

The following paragraphs show the reasons why we have to look at renewable energy as an alternative energy source in the future to replace oil and coal.

1. To build nuclear power stations is extremely expensive and the companies which build and operate nuclear power plants have to cover the costs of waste management and of ultimately decommissioning the existing sites.

   As an example, it is estimated that to build The Olkiluoto project, Western Europe's first new reactor, will cost £2.25b. In comparison, the cost of building a gas-fired

power station by RWE npower in the UK is approximately £800m, almost one-third of the cost of a nuclear power plant (BBC News, Jan 2008).

2. To keep using oil and coal as energy sources will put the world on unsustainable energy paths, as well as cause continuously increasing oil prices, carbon emissions, and more global warming.

3. Even though coal will be abundant for over one hundred years, it causes pollution and results in secondary, hidden long-term adverse effects on health conditions in the community surrounding the plant. This will burden the NHS with extra costs.

4. The constant population growth will increase energy consumption.

Therefore, water companies in partnership with research centres and universities have good incentives to take an active role in developing renewable energy, especially hydropower that is available to them. (Joule Centre, 2008).

Thus to meet the target of 20% renewable energy by 2020, the binding agreement set by the European Council, it will be necessary to explore and develop new renewable energy technologies.

In the UK wind is the most potential renewable source, followed by small-scale hydro power (DECC, 2007). Wind energy development has been occurring since the 1970s and is close to reaching its full potential. In 2011, offshore and onshore wind energy in the UK contributed about an average of 4300 MW of electricity. (RenewableUK, 2012).

Even though small-scale hydro power is the second most potential renewable source, this technology has not yet been developed. Therefore, more research and development is needed in this area.

1.1.1 Hydro power potential in the UK

It is estimated that 400MW of potential hydro power exists in the UK that has not been exploited. Approximately 100MW is generated by existing small hydro plants which are spread over 120 sites, most of them concentrated in Scotland and Wales. However, there are thousands of small low-head potential sites in England. These could generate over 10 MW of electricity. (Paish, 2002).

Figure 1.1 Map of potential hydro power sites in the UK

(Source: Friend of the Earth, 2012)

Table 1.1 shows the locations of low head potential hydro power sites in the North West of England. These were studied by Salford University (1989). They were not considered for further study because their power generation potential was less than 25 kW. In many cases the hydraulic head available was less than 2 m.

Table 1.1 Potential power sites in the NW of England selected for further study

River	Location	Town	Potential	Head (estimate)
River Kent	Scroggs Farm	Staveley	< 25 kW	
	Oak Mill	Burnside	< 25 kW	2-3 m
	Kentmere	Staveley	25 kW	
	Heslington Mills	Kendal		< 2 m
	Low Sizergh Mill	Kendal		< 2 m
River Lune	Broad Raine Mill	High Oaks	< 25 kW	2-3 m
	Killington New	High Oaks		< 2 m
	Weir 1	Halton		< 2 m
	Weir 2	Halton		< 2 m
River Mint	Patton Bridge	Patton Bridge	< 25 kW	
	Weir	Kendal		< 2 m

(Source: extracted from Salford University Civil Engineering Ltd report, 1989)

From the above table, we can see that even though some locations have an estimated head of less than 2 m, they still have the potential to be developed. As an example one on the River Lune in Halton, Weir 1, has sufficient water flow throughout the year to warrant further study. A recent study by Fishtek Consulting Ltd. (2012) showed that at Weir 1. The mean discharge was 36.9 m3/s. The proposed hydro scheme by Halton Lune Hydro plans to install two Kaplan turbines that will generate 160 kW electricity. These will use only one third of the mean flow, i.e. approximately 12 m3/s to generate this power.

Some locations such as Oak Mill in Burneside and Broad Raine Mill in High Oaks have 2-3 m of head available and are therefore suitable to be considered for further study.

Paish and others have stated that the existing low head hydro plants using conventional water turbines are not considered to be economical and eco-friendly. (Wiemann et al, 2006; Paish, 2002; Date and Akhbarzadeh, 2009). This is because in a conventional low head hydro, the costs for mechanical and civil works are very expensive and the blades of the water turbine was considered harmful for fish. Thus other means of exploiting the available low head potential sources are needed.

1.1.2 Electricity generation and consumption in the UK

The latest Digest of the UK Energy Statistics (DUKES) 2010 issued by DECC (July, 2011) reported that total electric plant capacity in the UK was 90,208 MW, of which 4,268 MW represented by hydro-electric stations (natural flow and pump storage), that was about 4.7% of the total. Wind energy contributed 2,260 MW and other renewable energy sources contributed 1,960 MW (1093 MW).

Thus, overall renewable energy represented 8488 MW (or about 9.4% of the total electric capacity). This means, in order to achieve the target of 20% of renewable energy contribution by 2020, renewable energy will need to generate another 10.6%, that is 9562 MW.

Therefore if the 400 MW of low head hydro power can be exploited it will contribute 0.45% of renewable energy to the goal. While not a large amount this is still a significant contribution to a more sustainable energy path in the future.

Another reason why it is crucial to speed up the exploration of potential renewable energy available is, as the DUKE 2010 data showed, that the total electricity demand in

2010 was 384 TWh where 1.8% or 7.1 TWh was imported. In fact the statistical data since 1998 showed that the amount of electrical energy the UK has been importing has ranged between 5 TWh and 14.5 TWh. In the last two years (2008, 2009) it dropped significantly to approximately half the maximum rate, i.e. to 7 TWh.

The problems mentioned above show that there is an opportunity for and a challenge to researchers to explore, develop, and study to find solutions using new technology that is green, renewable, eco-friendly and economically viable while utilizing the available hydro power in the UK.

One of the technologies that could be developed using a low head hydro power is the siphon hydro system.

1.2 Aim and Objectives of the Project

The aim of this research project is to study the siphon hydro system based on conversion from water to air pressure, and if possible to develop, or at least to recommend, a way of doing this reasonably efficiently. This is a technique of harnessing the potential energy in a river which is not the same as a conventional system. The research focuses on the assessment of the performance of three different aerator designs which were installed in a siphon system. Also to understand the behavior of two phase flow during the aeration process that might affect on the performance of the aerators.

It was conducted using a laboratory investigation and a field experiment. The aim was to improve the siphon system to a level where it is a practical and economically viable

technology, i.e. the overall capital cost is less than the conventional system cost, and to make a system that is easy to operate and maintain, and is eco-friendly.

Low head hydro plant using the siphon system is different from conventional low head hydro systems. The conventional system uses a water turbine to generate power, whereas this siphon system uses an air turbine to generate power. This is achieved by introducing air into the siphon, using the fact that at its highest point the water pressure in the siphon is less than atmospheric pressure. Thus at the top of the vertical down shaft of the siphon (See Figure 1-2), air at atmospheric pressure will enter the siphon. The continuous water flow carries the entering air away and allows more air to be drawn in thus allowing an air turbine to operate continuously.

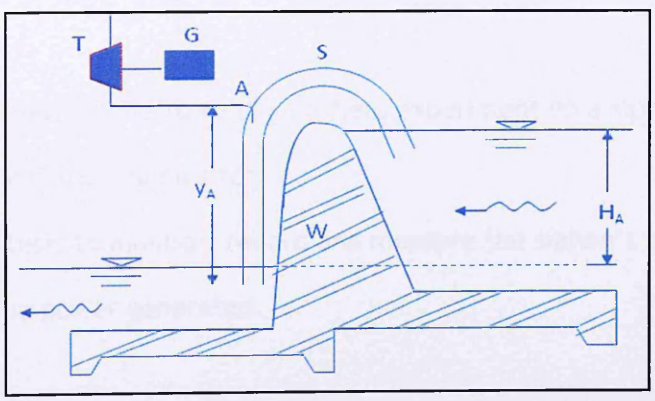

Figure 1.2 Siphon systems with aeration

(H_A= driving head, S=siphon, A= aerator, G=Generator, T=air turbine, W = weir, y_A= vertical height of down leg)

1.3 Research Methods

This research was carried out by conducting experiments in the laboratory and then in a field site.

Three different types of aerators were tested, then some modified aerators were made and tested in both the laboratory and on site.

1.3.1 Laboratory experiments

They involved:

- Developing and building a siphon system rig for laboratory scale experiments;
- Investigating the performance of various types of aerators;
- Conducting a separate experiment on a single hole aerator;
- Observing the aeration process in the siphon systems.

1.3.2 Field experimentation

This encompassed

- Finding a potential site to conduct a field experiment on a siphon system;
- Installing the siphon rig on site;
- Conducting tests to monitor, record and measure the siphon's performance;
- Measuring the power generated.

1.3.3 Overview

An experimental rig was designed and built in the laboratory to be able to simulate the run-of-river condition with a weir (hydraulic structure) where a siphon can be installed over it. This was completed by some measuring devices that allow measurement of various water and air flow rates, and also measurement of the air pressure in the siphon. The rig can also be modified or partly dismantled to change the aerator, and to run the aeration using a pump system and a siphon system.

1.4 Chapter Organisation

There are 8 chapters in the thesis, and described into 4 areas i.e. i) Introduction and studies of literature review on previous works (Chapter 1 and Chapter 2) ; ii) Rig development and head losses analysis in the pipe system (Chapter 3 and Chapter 4); iii) Experimental work and results (Chapter 5, Chapter 6 and Chapter 7); iv) Conclusions and recommendations for further work (Chapter 8).

Chapter 2

Reviews of previous studies

2.1 Introduction

This chapter discusses low head hydro power and gives a brief overview of conventional low head hydro power plus current developments and technology. It also contains reviews of previous work on the conversion of water energy to air flow for the use in air turbines. It also describes some characteristics of the two phase flow that occurs in this process especially void fraction, drift velocity and flow patterns. In particular the focus is on the downward flow in vertical pipes.

2.1.1 Small hydro power

By definition, a river site can be classified as a low head hydropower one if the difference in the water levels that occur upstream and downstream of a weir or any natural drop is less than 10m (as defined by BHA, 2005) or, less than 15 m (Dragu and Sels, 2002; Tung et al, 2006).

If the head between such locations ranges from 15 m to 100 m it is classified as a medium hydro power site. Above 100 m it is classified as a high head hydro power site.

Using the amount of power that can be generated, the hydro power plants located at the low head sites are categorized into three groups; Small hydro plants (2 MW-5 MW), Mini hydro plants (500 kW-2 MW), Micro hydro plants (less than 500 kW) and Pico hydro

plants (less than 10 kW). (Kirk,1999; Paish, 2002). Most of the power plants at low head sites fit into the small hydro category, generating less than 5 MW.

The classification given above is not universal. China defines small hydro plants as ranging from 0.5 MW to 25 MW. France defines micro hydro as being from 0.5 MW to 5 MW, whilst India classifies them as ranging from 2001 kW to 25 MW, and Mini hydro from 101 kW to 2 MW, Micro hydro up to 100kW. (Kirk, 1999, Das and Bhati 2010).

Small hydro power plants contribute 40 GW to world power generation, 50 % of this comes from low head plants that are costly to install. (Paish, 2002). To maximize the amount of energy captured at such sites it would be necessary to install a larger diameter turbine, a costly undertaking that would not be economic. It may also affect the passage of fish migrating upstream and be against Environment Agency policy.

Thus, a different type of hydro power plant is needed. The siphon system provides one alternative approach. Details about siphon systems with aeration are discussed in Chapter 3.

2.2 Low-head Hydro power potential in the UK

There are a lot of existing weirs and natural drop sites in the rivers which are potential to be developed as low head hydro power resource. Study in East of England showed that there are about 525 sites of various old mills and weir which have potential to produce 13 MW electricity (DECC, 2010).

The recent report from the Environment Agency (2011) identified that there are about 26000 barriers in the UK in the form of weirs, other man-made structures and natural sites which could be used to generate power. Over 4000 sites were identified as suitable for small hydro schemes, potentially generating 580 MW. Most of these sites were found in the Severn, Thames, Aire and Neath river catchments.

As 50% of the above sites are considered to be in high sensitivity areas for fish movement, especially salmon and eel, a design which allows fish passage and a fish friendly environment is required. The siphon system is a technology choice that fits these requirements.

Between May 1987 and October 1988, Salford University Civil Engineering Limited conducted a study on the economic potential for small scale hydro electric generation in the UK. Of these 203 locations in the North West and 174 in Yorkshire were rejected for further study because they were too small, the estimated generation being less than 25 kW of electricity, or having a potential head drop of less than 2 m. The study was carried out more than 20 years ago. Now, due to greater demand for electricity and new technological developments the opportunity for local communities to initiate hydro power projects may be possible. Thus further studies to establish the feasibility of using these sites is warranted.

2.3 Technology Development of Conventional Low-head Hydro Power

The use of large hydro power systems is well established; low head hydro needs to be developed to achieve high efficiency and be economically viable. Normally low head hydro sites are not at locations where there is water storage, where the water flow rate is low and the water level fluctuates with the seasons. These sites are not suitable for conventional hydro schemes. Some examples of low head technology already available or being installed on such sites are discussed below.

Water wheels have been used since the industrial revolution with low efficiency. Today, a lot of water wheels are made using new technology, which can reach 75-89% efficiency. (Muller, 2003).

Still at the early stage of development, The Beck Mickle Company near to Kendal has designed a mini water wheel which can utilise a water fall as little as 8 inches high (see Figure 2-1c) . This mini water wheel was designed for use in homes close to small streams or creeks.

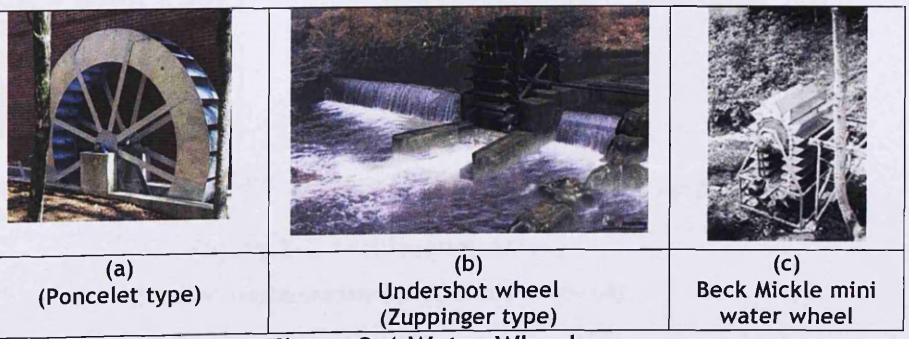

(a) (Poncelet type)	(b) Undershot wheel (Zuppinger type)	(c) Beck Mickle mini water wheel

Figure 2-1 Water Wheel

(Source: waterwheelfactory.com; coenergydiy.com; theherald.co.uk; picoenergy.co.uk)

Another conventional system that was also not new in principle but functionally changes in the usage is the Archimedes screw (see Figure 2-2). It has been used for centuries to lift water from rivers for irrigation, but now a days it is used to generate electricity. To construct an Archimedes screw requires considerable civil work. It can operate efficiently on heads that range between 1 m and 8 m. The smallest screw is 1 m in diameter and uses a flow rate of 250 l/s. It is not economically viable at heads of less than 1.5 m. (Renewable First, 2012)

Muller and Kauppert (2002) reviewed the latest development of water wheels and Archimedes screws in Germany. They reported that an Archimedes screw with a maximum flow rate of 3.5 m^3/s reached its optimum operation when the angle to the horizontal was 30°. It achieved 70% efficiency when the flow rate was 40% of the maximum flow, and 80% with flow rates of 60 - 100% of the maximum flow.

Archimedes screw in River Bain
Bainbridge North Yorkshire

Archimedes Screw in River Dart
National Park

Figure 2-2 Archimedes Screw

(Sources: westernrenew.co.uk; Scotland.gov.uk)

Another conventional system is using a water turbine. It can be found in two types i.e. impulse turbines and reaction turbines. The same as Archimedes Screw, the water

turbine also needs a considerable amount of civil and mechanical work for installation. Therefore it is not economical. Besides, the highest efficiency only occurs at its maximum flow and it reduces when the flow is less than maximum flow.

Pelton, Crossflow or Ossberger are examples of Impulse turbines. Francis and Kaplan turbines are examples of reaction turbine. Kaplan turbines with regulated guide vanes achieve up to 90% efficiency at 70% of maximum flow, and drop to 75% efficiency at 20% of maximum flow.

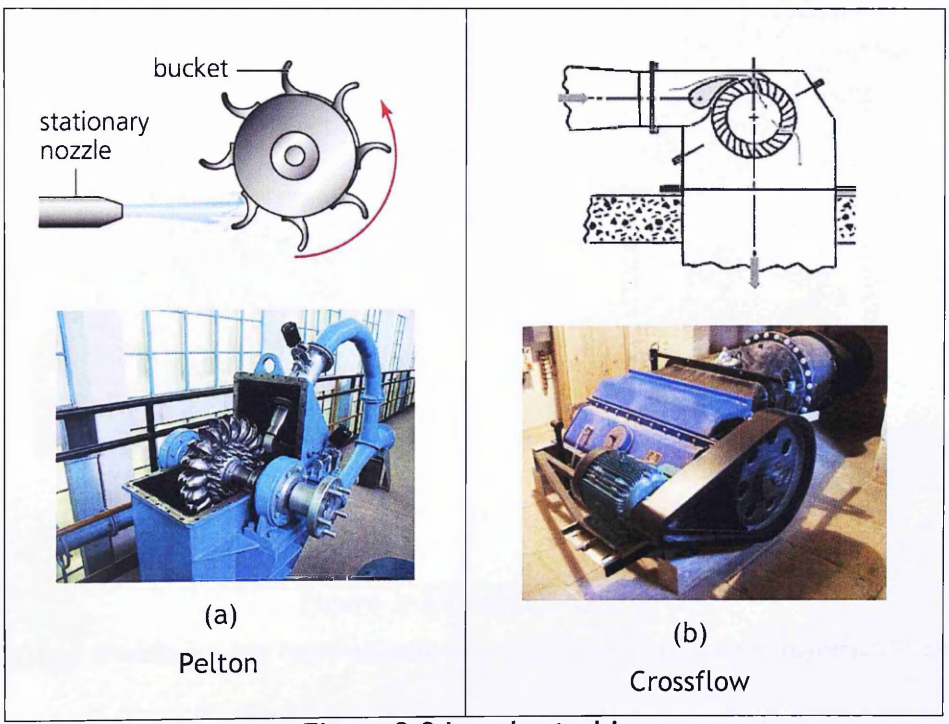

Figure 2-3 Impulse turbine

(*Source*: brighthubengineering.com; turbinesinfo.com; mechanical-engineering-info.blogspot.com; british-hydro.org)

Impulse turbines produce power by jetting a fluid flow through a nozzle hitting the vanes of a turbine wheel (or runner) one at a time. (Crow, 2001) They operate in air, (see Fig. 2.3).

In reaction turbines the fluid flow is under pressure and fills the chamber where the impeller is located (Crow et al, 2001). Water flows through a volute casing, the flow cross section of the casing decreasing, with guide vanes directing the water onto the runner blades, (see Fig.2.4). The rotor of the reaction turbine is submerged in the water and enclosed in a pressure casing (Paish, 2002).

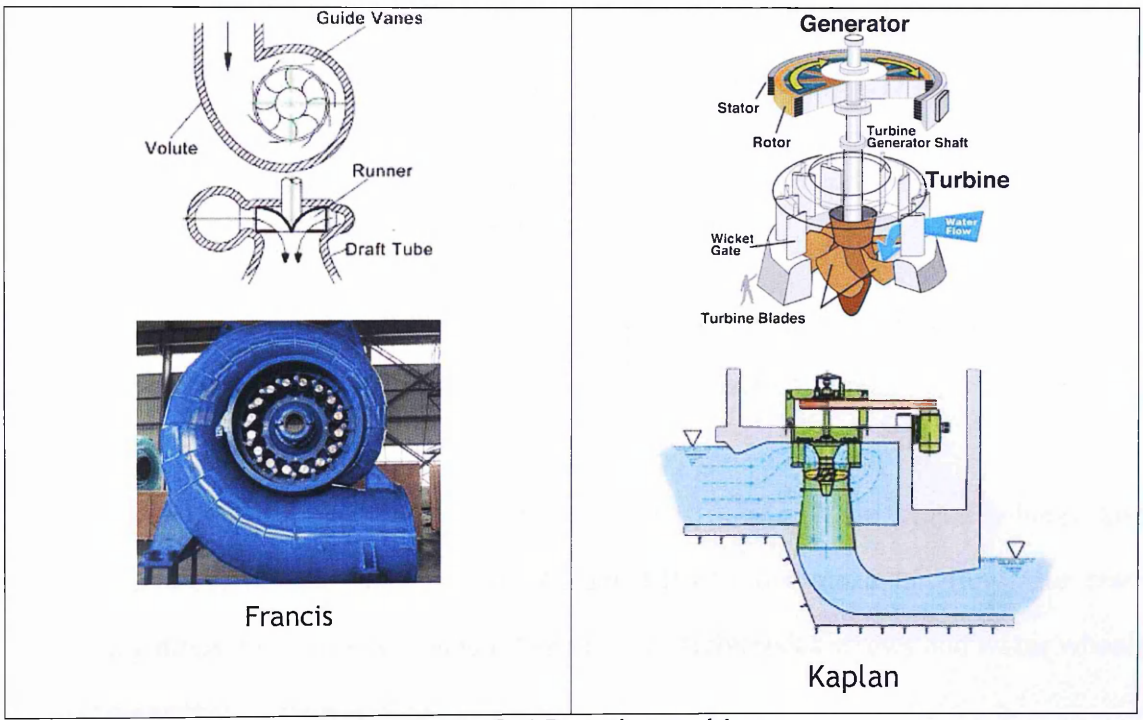

Figure 2-4 Reaction turbine

(*Source*: tradeboss.com; renewablesfirst.co.uk; newmillshydro.com; roymech.co.uk)

Kaplan turbines can operate in low head situations ranging from 3 m to 10 m and with flow rates from less than 0.5 m^3/s to 20 m^3/s. Cross flow turbines can operate with 3 m to above 10 m head and in flows ranging from 0.5 m^3/s to 5 m^3/s. See Figure 2.5.

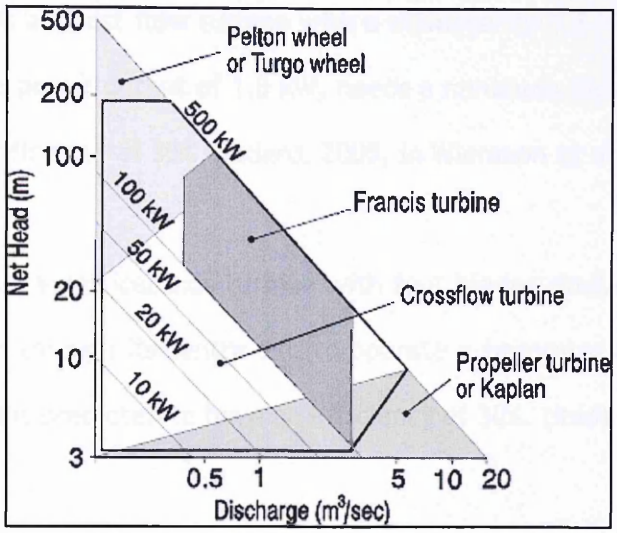

Figure 2-5 Head-flow ranges of small hydro turbines

(Source: british-hydro.org)

Kaplan turbines with regulated guide vanes achieve up to 90% efficiency at 70% of maximum flow, and drop to 75% efficiency at 20% of maximum flow.

Thus water turbines can reach efficiencies (90%) higher than water wheels and Archimedes screws at maximum flow. At one fifth of the maximum flow rate their efficiency drops down to 75%, is about the same as Archimedes screws and water wheels operating at their maximum flow.

The above technologies are classified as conventional systems and require major construction work.

Other technologies developed as a result of tidal power research include the Gorlov-Turbine, the Davis turbine, and the Underwater Electric Kite (UEK). Their generation efficiency is about 30% (Bedard in Wiemann et al, 2007).

The Gorlov turbine is a direct flow turbine with a diameter of 1.5 m and a length of 2.5 m. It can generate a power output of 1.5 kW, needs a minimum flow velocity of 1.5 m/s and has an overall efficiency of 33% (Bedard, 2005, in Wiemann et al, 2007).

The Davis turbine has a vertical axis turbine with four blades similar to hydrofoils. It is connected to a rotor through its centre axis to operate a generator (Blue Energy 2006 in Wiemann, 2007) and is predicted to have an efficiency of 30%. (Ibid)

The UEK turbine has a propeller on a horizontal axis. It is covered by an augmenter ring which protects the turbine and controls the water flow in such a way to keep a low pressure zone behind the turbine to achieve a maximum efficiency of 57% (Bedard, 2005 in Wiemann, 2007).

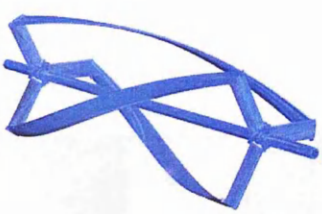

Gorlov Turbine

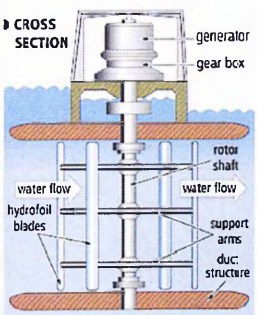

Davis turbine

UEK prototype, Bedard (2005)

Figure 2-6 Gorlov, Davis, and UEK turbines

(Sources: Bedard, 2005, in Wiemann et al,2007)

2.4 Studies on Two Phase Flow

Many experiments involving two phase flow and air entrainment process have been conducted in Chemical Engineering, in the Mining Industry, and in Nuclear power plant

industries. Little research on the two phase flow process in producing electricity from hydro head situations has occurred.

2.4.1 Flow pattern and flow regimes

There are four types of two phase flow, i.e. gas -liquid, gas-solid, liquid-liquid, and liquid-solid. Gas-liquid is the most complex because of the different characteristics of the two components; a deformable interface, and compressibility of one of the components. (Hetsroni, 1982).

In the case of gas-liquid there are two physical parameters that determine the flow pattern, i.e. surface tension and gravity. The gravity tends to pull the liquid to the bottom, and the surface tension tends to make the liquid form small droplets and to form small spherical bubbles.

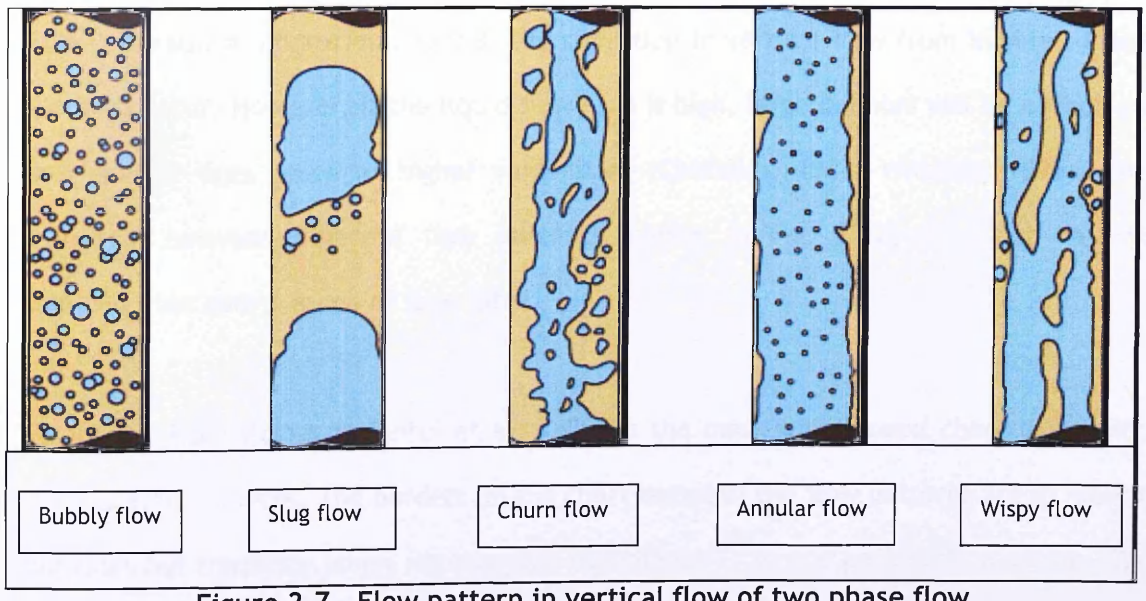

Figure 2-7. Flow pattern in vertical flow of two phase flow

*(Source: **Victoria Kippax**, http://www.waterworld.com, **2011**)*

The geometric configurations in a vertical pipe with a two-phase flow of gas and liquid (the flow patterns), can be split into five common categories (Hetsroni, 1982). They are: (see Figure 2-7)

1) Bubbly flow - the gas bubbles are enclosed in a continuous liquid phase and are of relatively uniform size;

2) Plug or slug flow - the bubbles coalesce and form large bullet-shaped bubbles;

3) Churn flow - with increasing flow velocity, the motion of the liquid becomes oscillating in upward and downward directions;

4) Annular flow - the liquid forms a film round the wall, and the gas core may contain small liquid drops;

5) Wispy flow - as liquid flow rate increases the concentration of liquid drops in the centre of cross section increases, and they may coalesce. This is characteristic of flow with a high mass flux.

At a void ratio of approximately 0.3, the transition in vertical flow from bubble to slug starts to occur. However, if the liquid flow rate is high, large bubbles will be broken up into smaller ones, even at higher void ratios (Chisholm, 1983, Whalley, 1996). The transition between adjacent flow patterns (shown in Fig. 2.12) does not happen suddenly, but over a range of flow rates.

Figure 2.8 from Govier in Taitel et al, 1980, is the most widely used chart to predict vertical flow patterns. The borders on the chart between the flow patterns are in reality not lines but transition zones representing the change from one pattern to another. The

chart was developed using a small smooth pipe diameter of 25.625mm, with air and water at 70 degrees F (21.1° C) at 36 psia (248 N/m2).

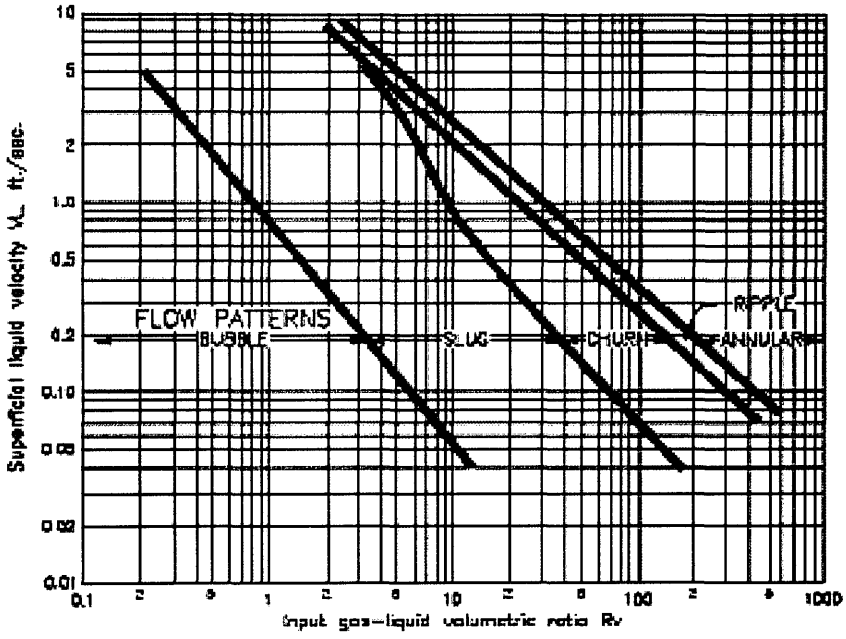

Figure 2-8 Superficial liquid velocity vs gas-liquid volumetric ratio

(Sources: Govier in Taitel et al,)

The flow pattern of most interest for the research is bubbly flow. It produces greater pressure suction than other flow patterns (Hanser, 2005) and can thus generate more electricity.

2.4.2 Vertical two phase flow

Many studies have been carried out on two phase flow in horizontally and vertically upward flows in small diameter pipes (1 cm diameter to 5 cm). Very little research has been done on vertically downward two phase flow, especially in large diameter pipes (Kashinsky and Randin, 1999).

Kundu et al (1995) conducted research on vertically downward, two phase flow using a 51.6 mm diameter pipe, 2.030 m long. They wanted to evaluate the gas void ratio and total pressure gradient. An ejector jets the water from the top of the system and mixes with the air in the ejector assembly and enters the down shaft (the contactor) through a diffuser. The upper part of the contactor was an intense mixing zone and the lower part had a bubbly flow pattern zone. The lower end of the contactor was submerged into a separator tank.

The experimental results indicated that at a low value of flow ratio (φ_R), the void ratio (α) increases rapidly with an increase in liquid flow rate up to certain value of flow ratio (φ_R) then remains constant. Their set-up had a nozzle diameter of 4.76 mm, and water flow rates ranged from 0.070 l/s to 0.340 l/s. This achieved a constant void ratio of 0.32 at flow ratio above 0.54 (Kundu, 1995, p 899).

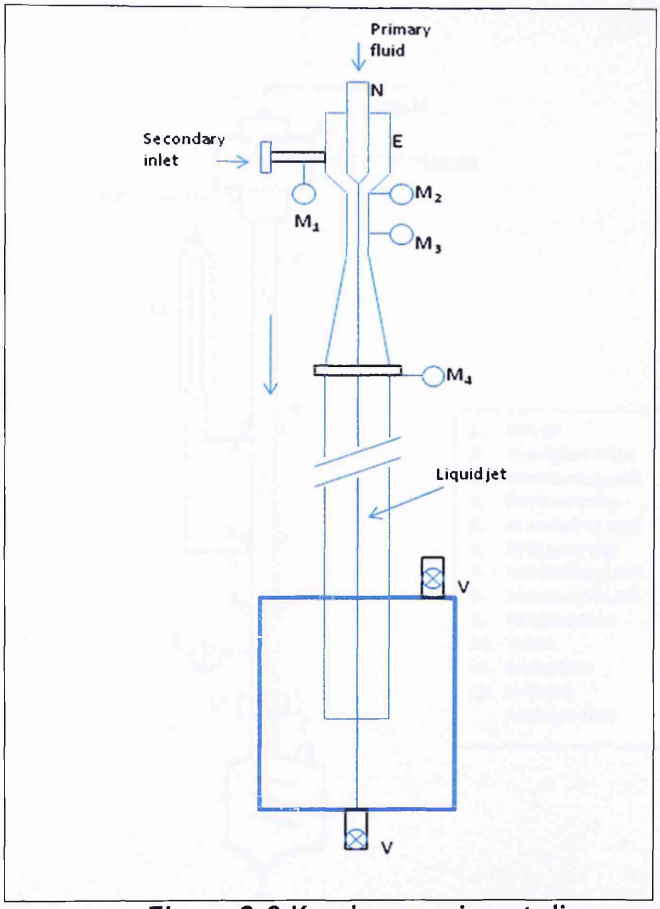

Figure 2-9 Kundu experiment diagram

(M = manometer; V= valve; N = nozzle; E= ejector)

Kashinsky and Randin (1999) studied local characteristics of downward bubbly flow using 42.3 mm diameter pipes of 4.8 m lengths. They concluded that downward bubbly flow was characterized by a centrally peaked void profile. Another important finding was that the wall shear stress in downward bubbly flow was higher than in single phase flow for the same liquid velocity.

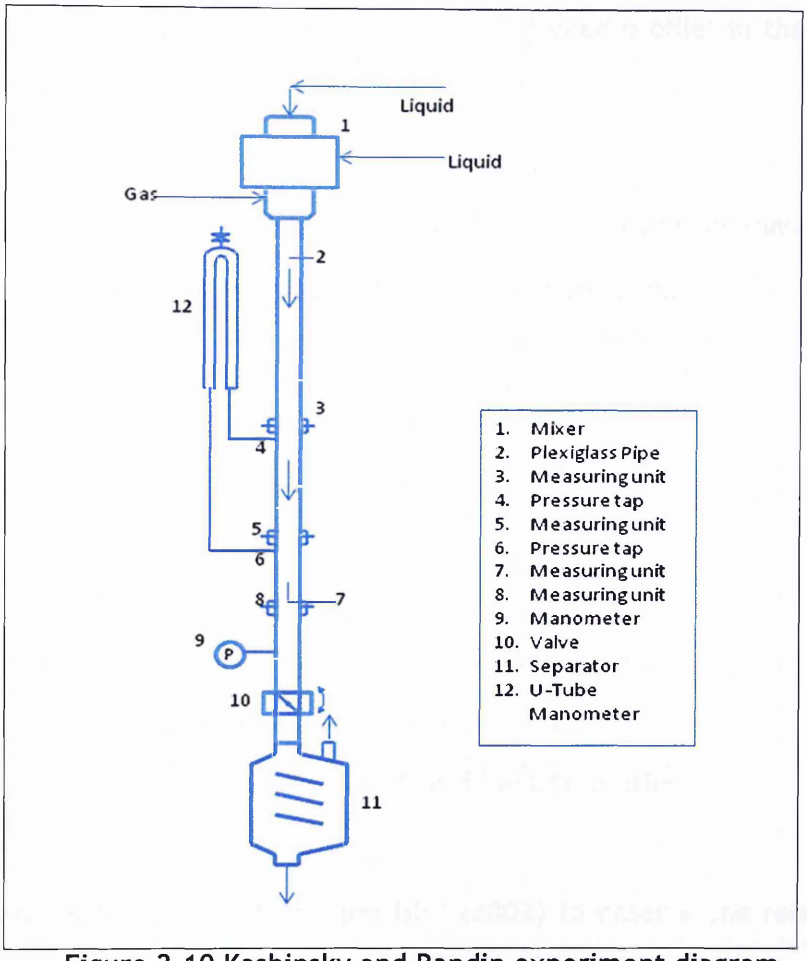

Figure 2-10 Kashinsky and Randin experiment diagram

Hibiki et al (2004) studied the radial phase distribution pattern of void fraction in column diameters of 25.4 mm and 50.8 mm, and column lengths of 3.175m and 2.7178m. In their experiment, they used a sparger unit of porous material with 10μm diameter holes to produce uniform bubbles of 1-2 mm. These were injected into the mixing injection chamber before diffusing into the down pipe. In the same experiment, they also observed the radial profile of flow distribution for upward vertical flow.

Hibiki et al confirmed the Kashinky and Randin results that in downward flow, the void ratio profile tends to be a bell shape (with a central peak), while in vertically upward

flow, it tends to have a 'near wall peak and/or flattened profile' in the centre of the pipe (Hibiki, 2004). See Figure 2-11.

In their experiment it was also found that for fluid velocity greater than 2.01 m/s, the distribution of void fraction was bell shaped with a central peak.

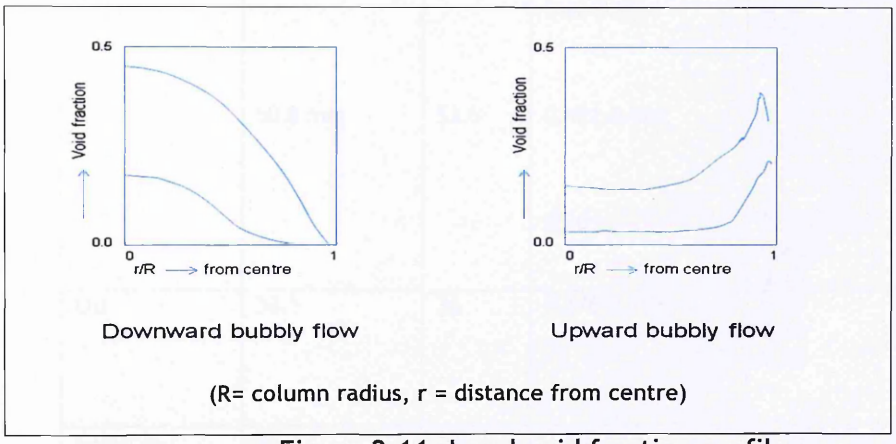

Figure 2-11. Local void fraction profile

Research was carried out by **Hibiki and Ishii (2002)** to observe the relation between void fractions and drift velocity in vertically downward flow (in 25.4 mm and 50.8 mm diameter pipes). The results of this experiment showed that drift velocity decreases with the increase in void fraction in bubbly flow. Other studies on bubbly flow carried out by Liu and Kalcach-Navarro (Liu, 1989, Kalcach-Navarro, 1992, in Hibiki and Ishii, 2002) showed similar trends.

Table 2-1 shows drift velocity (the upward velocity of the bubbles) from some studies carried out by various investigators.

Table 2-1. Values of drift velocity in bubbly flow

Investigators	Pipe diameter mm	z/D	Superficial liquid velocity m/s	Void fraction	Drift velocity m/s
Hibiki and Ishii	25.4	125	0.872 -1.75	0.30 0.20 0.10	0.125 0.163 0.188
			2.62-3.49	0.30 0.20 0.10	0.275 0.400 0.350
	50.8 mm	53.5	0.491-0.986	0.30 0.20 0.10	0.133 0.169 0.200
			0.201	0.30 0.20 0.10	0.225 0.300 0.275
Liu	38.1	36	0.376-0.753	0.30 0.20 0.10	0.130 0.169 0.200
Kalcach-Navarro	38.1	50	0.3-0.8	0.30 0.20 0.10	0.170 0.210 0.280

(z= the axial location measured from the test inlet; D= column diameter)

Source: extracted from Hibiki and Ishii(2002)

According to Govier (Figure 2-8), in a bubbly flow superficial liquid velocity decreases when void fraction increases. Superficial velocity is defined as total liquid flow rate divided by cross section area.

The table above indicates that the drift velocity also decreases when void fraction increases. It shows that the higher the fluid velocity, the higher the drift velocity. The above table shows that drift velocity ranges from 0.125 m/s to 0.400 m/s.

Hibiki and Ishii (2002) reported that the drift velocity was relatively constant in slug, churn, and annular flow. Their experiments found that in slug flow, the drift velocity was 0.175 m/s in 25.4 mm pipe diameter. In 50.8 mm, the drift velocity was 0.25 m/s.

The slug flow regime gave relatively constant drift velocity in the range of 0.2 m/s to 0.25 m/s (Liu, Kalcach-Navarro,1992; Grossetete, 1995; Serizawa et al, 1991; in Hibiki and Ishii, 2002).

Thus, in order to reduce the drift velocity significantly, it is important to develop a full bubbly flow condition. Unfortunately, this is not possible to achieve in the siphon system, which needs to be operating at a very high air flow rate. Chapter 5 gives more information on this.

Jain (1988) conducted experiments on a vortex-flow drop shaft in a 292 mm diameter pipe. Water from a constant head tank flows through a horizontal pipe and then enters a vertical drop shaft through a tangential vortex inlet. At the top of the vertical shaft a hole allows air to enter the drop shaft. A control valve in the horizontal pipe sets water discharge rates so the air-water ratios in the vertical shaft can be changed. The experiment showed that the air concentration increases with an increase in water discharge up to a maximum value after which it decreases, and also, that for a constant water discharge the air concentration decreases with decreasing vertical drop.

He reported that air concentration increased with an increasing water velocity. The circulation and the water velocity increased with increasing water discharge. However the increase in circulation caused a reduction in the air concentration. Thus there is an

optimum water flow rate that achieves the maximum air concentration. The siphon system with aeration that was studied in this thesis was a vertically downward two phase flow in a 200 mm diameter pipe that was 6 m long.

Using a scheme similar to Shapiro's HAC/GT investigation, **Aissa** et al (2010) conducted research on vertical downward two phase flow to analyse the performance of a low head hydraulic compressor rig. They used a small diameter pipe (25.4 mm) that varied from 8.25 m to 8.60 m in length. The air tube length had diameters ranging from 1.4 cm to 1.9 cm, and form 25 cm to 60 cm air tube.

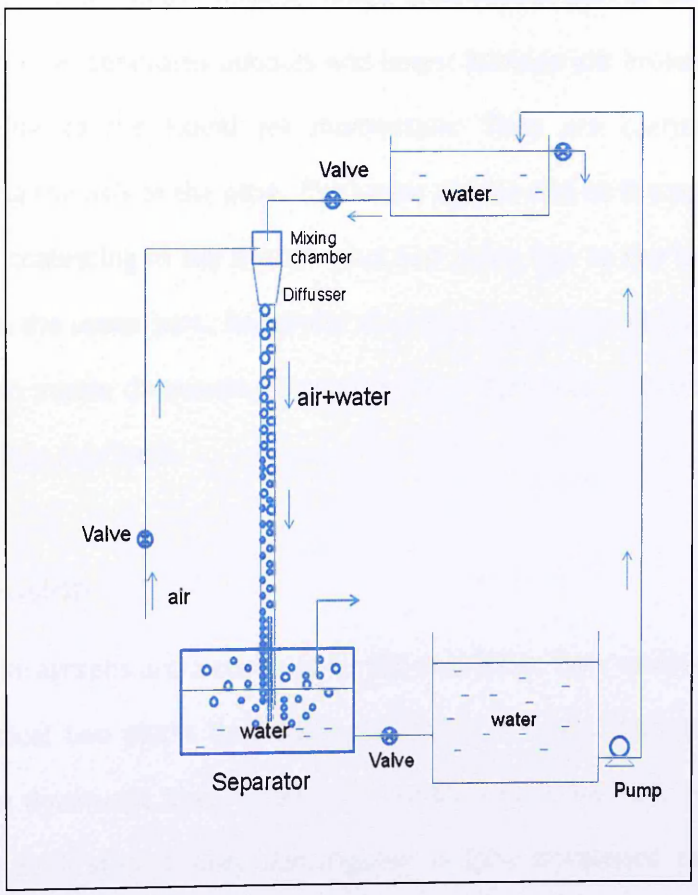

Figure 2-12 Schematic of Aissa HAC

Several points of their experimental findings are:

- Mean diameter of air bubbles increases with increasing air tube diameter and decreasing air tube length.
- Mean air bubble diameter decreases along the down pipe.
- HAC efficiency increases with an increase in the air tube length.
- The compression ratio increases with an increase in the length of the down pipe up to certain limit.

Majumder et al (2006) studied the bubble size distribution using 50 mm diameter of 1.60 m pipe. This confirmed the Aissa finding that bubble size decreases along the down pipe length. They stated that in the intense mixing zone (upper part of the column) high rate of energy dissipation generates bubbles and larger bubbles are broken up into a smaller size bubbles due to the liquid jet momentum. They are carried downwards and distributed along the axis of the pipe. The larger bubble size at the upper part is a result of the bubbles coalescing in the bottom part and rising due to the buoyancy effect and accumulating in the upper part. Majumder et al also reported that bubble size decreases with decrease in nozzle diameters. They also found that void fraction up increases with increase in the gas flow rate.

2.4.3 Conclusion

The following paragraphs are a summary of the two phase flow reviews. All of the above studies on vertical two phase flow were conducted in small diameter pipes (less than 100 mm) and in downward flow, except Jain (1988) which used 292 mm diameter. Most of the experimental studies were investigated in fully developed bubbly flow using a mixing chamber and diffusive ejector connected to the vertically down pipe as shown in Fig. 2-12.

The water level in the upper tank was maintained at a constant head. The fluid enters the mixing chamber where air is injected. Some other experiments were made using a pumped system to inject the water into the mixing chamber. The fluid discharge into the mixing chamber was controlled with a valve.

Results from the above studies are:

- The distribution of void fraction was a bell shape and or centre peak in a vertical downward flow and wall peak and flattened in the centre in an upward vertical flow.(see Figure 2-15)
- Drift velocity decreases with the increase in void fraction for bubbly flow, but remains relatively constant in slug, churn and annular flow.
- The bubble diameter decreases with decrease in nozzle diameters
- The bubble diameter in the lower part of the vertical down ward flow is smaller than in the upper part because the pressure is higher in the lower part.
- In the intensive mixing zone (the top upper pipe), there were a lot of coalesced bubbles due to bubbles coming from the bottom part and drifting upward due to the effect of buoyancy.

2.5. Conversion water to air power

Another alternative way of harnessing water power is to convert water energy to air energy.

The objective of water air conversion systems is to use the water head to create a moving column of air that can drive a turbine. The air motion is caused by either creating a low pressure point in the water that induces the air flow, or by compressing the air and forcing it through a turbine. In these processes the following terms are often used:

Aeration - the mixing of the air and water;

Bubble drift velocity - The air bubbles tend to drift vertically upwards rather then match the velocity of the water flow.

Void fraction - The ratio of the air volume to total volume of mixed air and water. The higher the ratio is, the more air available for the turbine operation, the optimum value being that with the highest efficiency.

Two phase flow - The mixture of air and water that is moving. Ideally this is homogeneous with the air bubbles evenly distributed throughout the water. In practice this rarely occurs. The flow is complex because one compound is compressible, and because the inter-phase between the two compounds is deformable. Various types of the flow are described below.

Examples of this conversion process are hydraulic air compressors, hydraulic venturis, and siphons using aeration.

2.5.1 Hydraulic air compressor (HAC)

The idea of obtaining compressed air from hydraulic power is not new. It was used extensively in the nineteenth century in large mining, lumbering and canal lock operations in America and Canada (Rice, 1976). It was reported that efficiencies between 40% and 85% were achieved in large systems.

Hartenberg (1960) reported that a hydraulic air compressor was used in Italy as a trompe in a forge. Figure 2-13 shows the schematic diagram of a trompe working. Air is drawn into the down pipe by the water flow. It is compressed by the increase in pressure in the water column as it reaches lower levels. When the column of mixed air and water reaches the wind box the air separates from the water. The compressed air is drawn off at the top of the wind box while the water is settling at the bottom. The increased air pressure pushes the water out through the discharge pipe while that at the top operates a furnace.

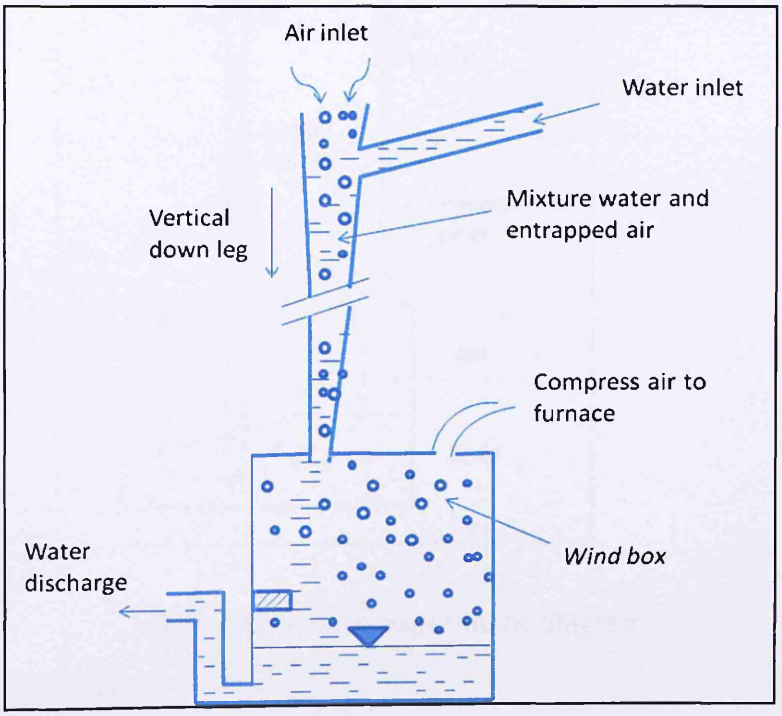

Figure 2-13 The schematic trompe

Rice conducted a laboratory scale experiment with a very small diameter pipe of 19 mm and 0.43 m hydraulic head. Air was blown rather than induced into the down pipe (Fig.2.14). He achieved a maximum efficiency of 45%. Based on this experiment he

carried out theoretical calculations using computer programming to predict the HAC performance in a large scale set up. He predicted that a 3.05 m diameter pipe with hydraulic heads ranging from 3.05 m to 18.3 m would achieve an efficiency of 65% to 70%.

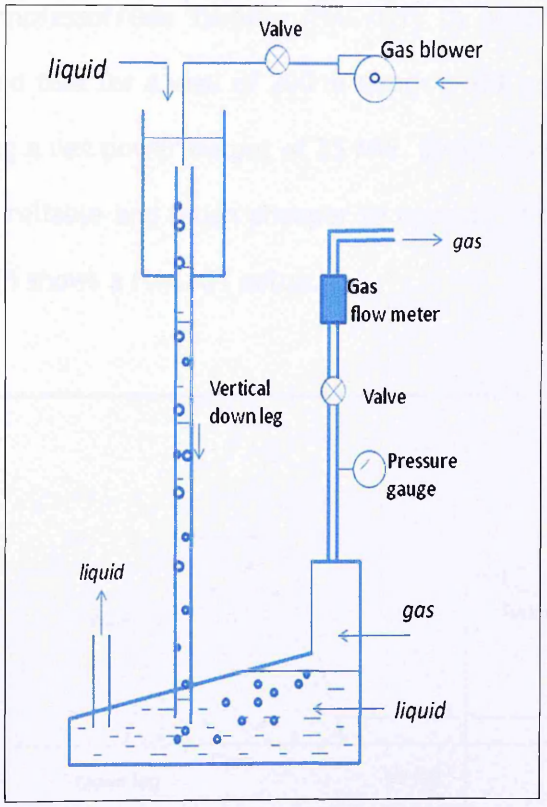

Figure 2-14. Rice experiment diagram

Rice (1976) concluded:

1. the compressed air flow rate in the outlet pipe is determined by the air-water ratio in the down pipe;
2. This flow rate is directly proportional to the hydraulic head and the cross sectional area of the down pipe.

Rice did not examine the different characteristics in flow patterns in the two phase flow in small diameter rather than very large diameter pipes are used. This affects the void fraction which is related to the efficiency achieved.

Using the same principle as described by Rice (1976), Shapiro (1994) proposed a Hydraulic Air Compressor/Gas Turbine (HAC/GT) to generate electricity. Preliminary calculation showed that for a well of 200 m depth a 90% compression efficiency can be reached producing a net power output of 25 MW. Shapiro also claimed that this HAC/GT system would be reliable and much cheaper to operate and maintain than other power plants. Figure 2.15 shows a HAC/GT setup.

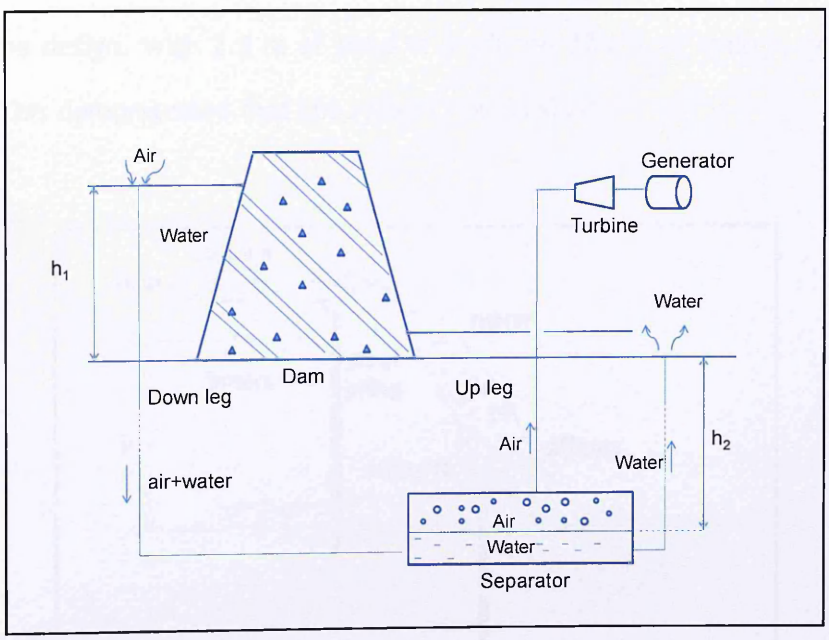

Figure 2-15 Schematic open water loop HAC/GT

2.5.2 Siphon system using aeration

Bellamy (1986) at Coventry University conducted research and experiments to produce electric power from low head river sites by converting water energy to air energy. He tested it at Borrowash on the River Derwent.

Bellamy combined a siphon with a venturi at the high point of the siphon and called it a Syfogen. Air was drawn in at this point, the air flow powering a turbine. (Fig. 2-20) Theoretical calculation showed that the Syfogen would achieve an efficiency of 50%. The prototype was tested in March 1992 and reached an efficiency of 25%. The prototype was left operating until July 1993. This showed that the system was reliable and easy to operate. A second experiment was carried out in February 1994 after a significant review of the design. With 2.3 m of head it produced 22 kW of energy, achieving 30% efficiency. This demonstrated that the system was feasible.

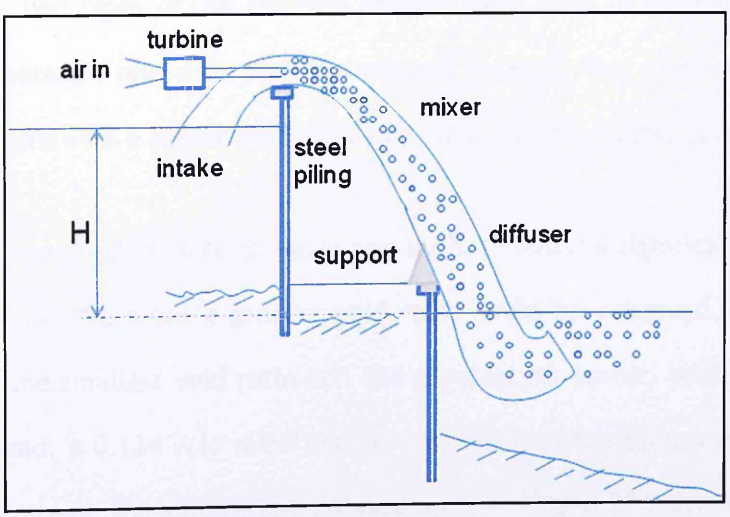

Figure 2-16 Syfogen hydro electric system

(H = hydraulic head)

French and Widden (2001, 2004, 2005) conducted a series of experiments on converting water to air pressure based on pumped systems. They assumed that the process is isothermal and that the bubble drift velocity is constant. The first experiment in 2001 used 2 siphon rigs, one of 2 m length and the other 4 m with pipes of 78 mm diameter. The void ratio was less than 0.3.

In 2004 another experiment was conducted using 150 mm diameter pipe with a pumped system to study the aeration process in order to reach maximum air entrapment. It achieved a 0.20 void ratio. In another experiment in 2005, the void ratio reached 0.23. This is close to what Hasan achieved. (Hasan in French and Widden, 2001). French and Widden (2001) stated that theoretically the overall efficiency could be above 60%. There was no observation of the flow patterns in their experiments.

Hanser (2005) used a pumped system to study aerator performance. He used 150 mm diameter pipes. Two types of the aeration process were tried in the vertical leg of the pipe above an aerator, one with and one without a mesh. The mesh was to create a bubbly flow pattern with a higher void ratio that would produce more power.

The mesh created a good mixture of water and air but caused a significant pressure loss. He found that with the mesh a greater void ratio could be achieved. Using a double mesh produced the smallest void ratio and the greatest air power. With no mesh and a 0.9 m driving head, a 0.124 void ratio occurred with an estimated power production of 17.7 Watts. With mesh, the void ratio increased up to 0.17 and 22 Watts were produced. The mesh creates smaller bubbles and produces bubbly flow in the down pipe.

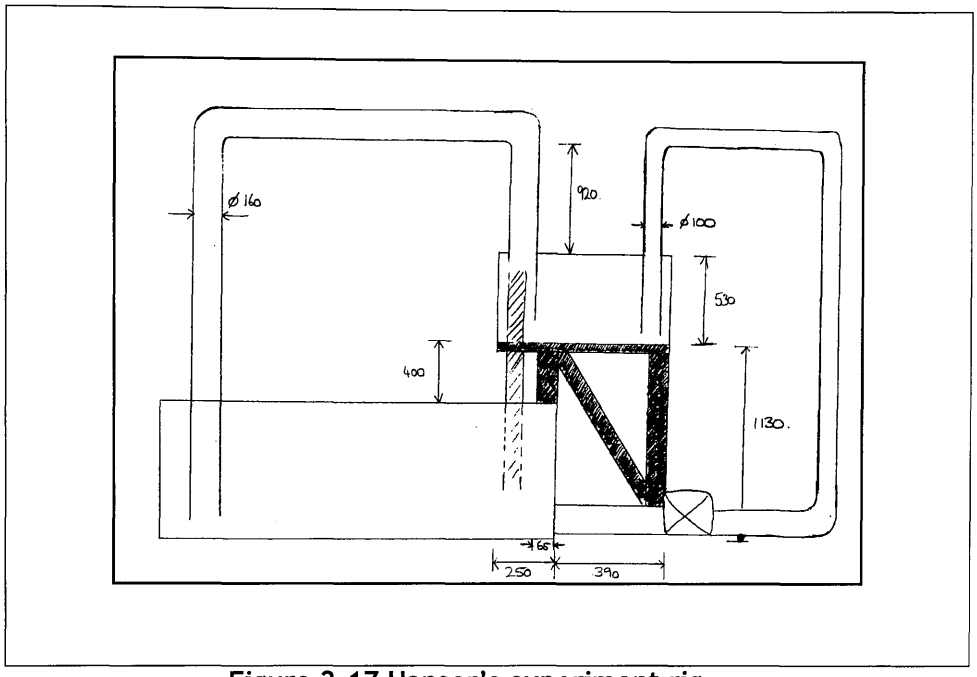

Figure 2-17 Hanser's experiment rig

(Source: Hanser, 2005)

He introduced a second tank to create a siphon system, but could only produce a low water flow rate because the second tank was not large enough to create a high water flow in the siphon. With the aerator height of approximately 2 m and a 0.9 m driving head, 0.1165 void ratio was reached. In unstable condition it reached 0.291.

The presence of 'void' caused a reduction of the pressure suction. He found that every 10 cm drop of void in the siphon column will reduces about 1200 N/m^2 (0.012 bar).

The term 'void' in Henser's work was a transition region, or a bubbly flow development zone, i.e. a region between an intensive air stream flow pattern around the aerator and the bubbly flow region at the lower part of the siphon.

It can be explained that a bubbly flow pattern could only happen in a relatively small air flow rate compared to the water flow rate. However, if the air flow rate increases the flow pattern will change. In a high air flow rate, the flow pattern change i.e. from an intensive jet air flow pattern around the aerator, followed by a churn flow in the middle and then a bubbly flow. Henser (2005) named the distance from the aerator to the location where the bubbly flow begins as 'void'. Chapter 7 describes in more detail about the changes in flow pattern along the downward leg of the siphon.

Several conclusions can be drawn from Hanser's experiments:

- Using two meshes produced the highest air flow and the highest power output however, losses were high.
- Increasing the water flow will increase the air flow. This also increases the 'void', which reduces the suction pressure, and thus reduces the power output.

The objective of this siphon experiment was to get the water flow as high as possible in order to maximise air flow. This produces the highest power output. At the same time it is necessary to reduce the void as much as possible in order to create the highest suction pressure. The key to achieving this will be in the design of the aerator.

Howey and Pullen (2008) conducted research using a similar experiment to that carried out by French and Widden (2001), and Hanser (2005). They combined a siphon and a hydraulic air compressor (HAC) to power an air turbine and generator. In this experiment they used a 100 mm pipe diameter siphon with a bell mouth inlet and a diffuser in the down pipe. Air was entrained through a manifold and introduced into the water flow at 8 points along the outer edge of the siphon.

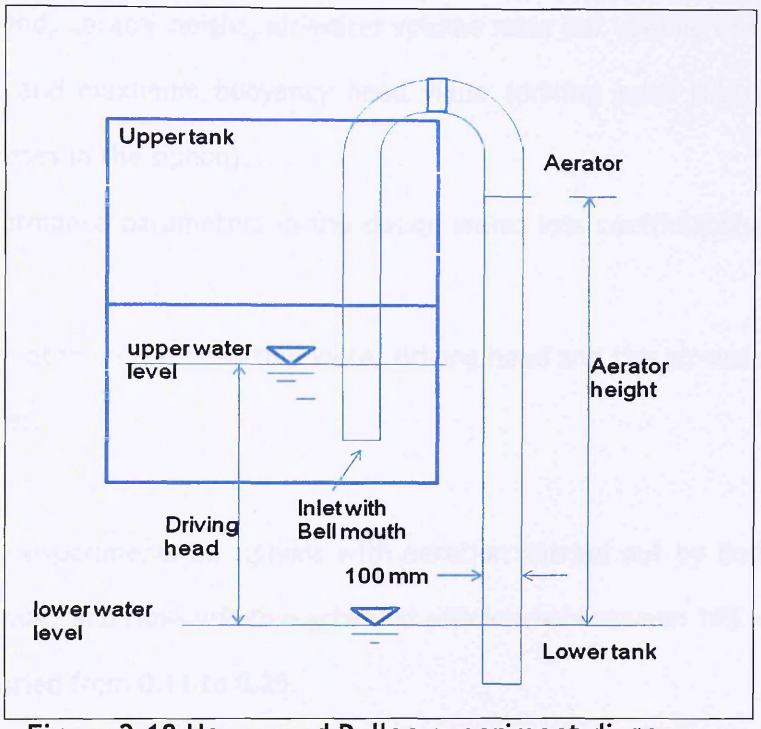

Figure 2-18 Howey and Pullen experiment diagram

With the driving head of 1 m and an aerator height of 2 m, this system achieved a maximum void ratio of 0.116 and a power output of 20 Watts, with an efficiency of 10%, about 50% less than was predicted. The void ratio and the power output are similar to Hanser's experimental results, which were 0.1165 void fraction, and 22 watts power output for a driving head of 1 m and an aerator head of about 2 m in 150 mm pipe diameter. Howey and Pullen also calculated theoretically the effect of the diffuser if it is applied at the outlet, and found that it will increase the power output but not the efficiency.

Conclusions from the Howey and Pullen experimental results are

- Air power increases with an increase in driving head.

- The efficiency of the Hydraulic Air Compressor (HAC) system is dependent on driving head, aerator height, air-water volume ratio (air volume divided by water volume), and maximum buoyancy head value (driving head subtracted by the overall losses in the siphon).
- Key performance parameters in the design were: loss coefficient(s) and aerator height.
- Key parameters in the operation were: driving head and the air-water volumetric in the inlet.

In summary, the experiments on siphons with aeration carried out by Bellamy, French and Widden, Henser, and Howey-Pullen achieved efficiencies between 10% -30%.
The void ratio varied from 0.11 to 0.25.

Thus siphon systems with aeration are feasible, reliable, and deserve to be investigated further. The challenge is to design a siphon system with the maximum air flow, producing maximum power and at a high efficiency. It is necessary to maintain the continuity and stability of the siphon flow, while minimizing the losses in the system.

Chapter 3

Design and development of a Siphon Test Rig

3.1. Introduction

This chapter describes the design and the development of the siphon experimental rig, the aerators' design and the measuring devices. This experimental rig was designed and developed by the author from scratch. On the way to the construction, slight modification and small changes were done to adjust with the space availability and for practicality.

There are two stages of rig development, i.e. a rig using a pumped system to test three different aerators, and a rig using natural siphons of two different heights to find which performed the best.

Some differences between the previous studies and this experiment are:

1) In the siphon system, the top part of vertical down leg pipe where air was injected is in a higher location than the position of the upper tank.
2) There is no separation between the mixing zone and the down leg part of the siphon. Water and air were mixing in the down leg pipe. Only Jain (1988) had the similar system.
3) This siphon system used a large diameter of 200 mm, whereas the above studies, except Jain (1988) used much smaller diameters (less than 100 mm)

4) Some of the studies above were set in a full developed bubbly condition in the down leg pipe after the mixing zone by adjusting the water discharge and air flow, whereas in the siphon system, air was entered as much as possible in order to produce high void fraction. There was an attempt and expectation to create bubbly flow by designing an aerator with small holes diameter of 2-4 mm, and also using an air chamber.

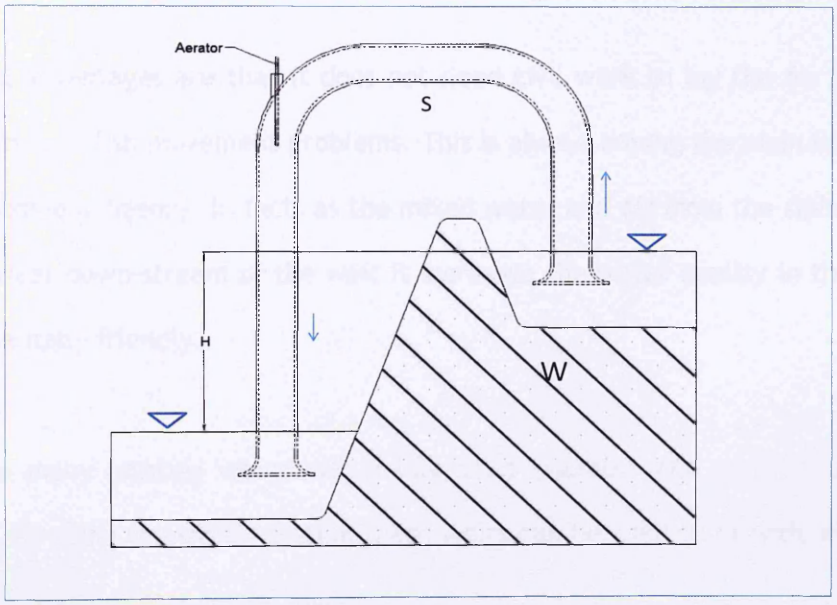

Figure 3.1 Siphon system

(W=Weir, S=Siphon, H= potential head)

In the low head hydro power using a siphon system, the siphon is installed over the weir (or any suitable structure) to carry the water from upstream to downstream, the head difference, H (see Fig.3.1) driving the siphon.

In the vertically down part of the siphon, air at atmospheric pressure is introduced at the top point of the siphon where the pressure is less than atmospheric pressure. By

maintaining this continuous air flow, the system can be connected to an air turbine to generate electricity.

As this turbine is in the air instead of submerged in the river, it is easier to install, maintain and operate. Thus it reduces the capital cost compared to a conventional system.

Additional advantages are that it does not need civil work to lay the air turbine in the river and avoids fish movement problems. This is always among the main issues raised by the Environment Agency. In fact, as the mixed water and air from the siphon flows back into the river down-stream of the weir it increases the water quality in the river and is environmentally friendly.

There are many existing weirs with a low head available and which are not utilised anymore. By using the siphon system these weirs can be used to provide electricity and create jobs for the local community.

3.2 Development of Test Rig

In order to simulate the upper and the downstream part of the weir, two tanks were built in the laboratory. A lower (bottom) tank represents the water level downstream of the weir; an upper tank represents the water level upstream of the weir. The lower tank also functions as a storage tank, so water can be circulated from there to the upper tank. (See Fig. 3.2)

Flow between the tanks was controlled by a valve and by reducing or increasing the RPM of the pump with a digital electronic control.

The water level in the upper tank was maintained at a set level by installing a circular weir (an overflow pipe) that allowed overflow back to the third chamber of the storage tank.

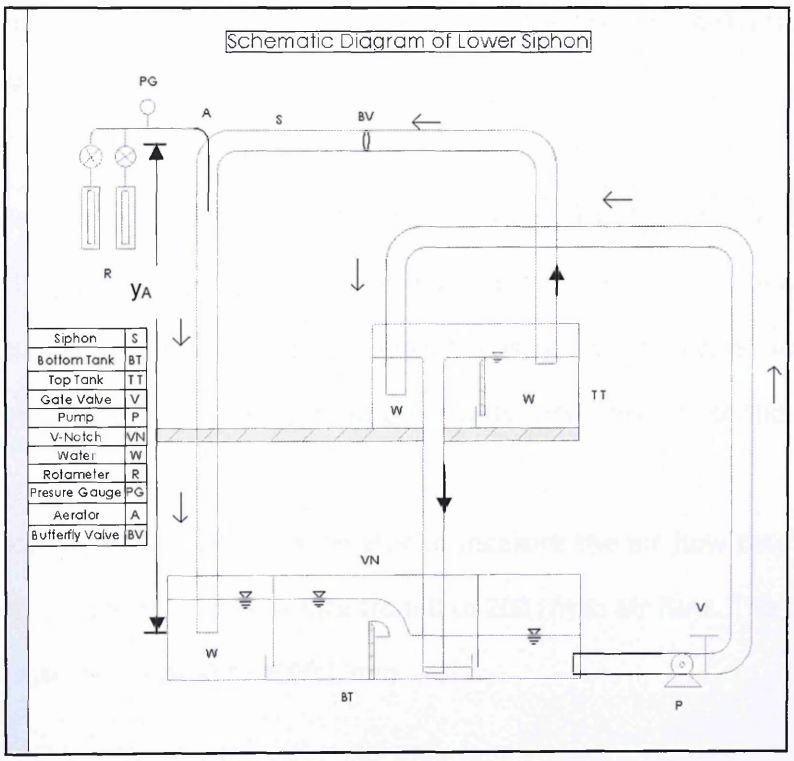

Figure 3.2 Schematic diagram of Siphon Rig

There are four chambers in the bottom tank. The first chamber (from the left) is the chamber where the water flows back to the bottom tank. It also operated as a stilling basin before the water entered the second chamber.

In the second chamber, a V-Notch was installed to measure the water flow from the siphon. In both the first and second chambers, the water level is the same. This water level was monitored to ensure it remained constant. A V-notch weir allowed the water to enter the third chamber of the lower tank and the flow rate to be measured. The third chamber of the lower tank also received an overflow from the circular weir in the top tank and acted as a stilling basin for the fourth chamber where the pump water was pumped to the upper tank. The third chamber of the bottom tank also allowed air bubbles to exit the flow.

The upper tank has two chambers separated by a gate or a weir with a rectangular cross section. The first chamber (from the left) is where the water from the bottom tank was pumped to fill the top tank. The second chamber is where the siphon inlet takes the water. The siphon outlet discharges the water into the first chamber of the bottom tank.

Two rotameters were put before the aerator to measure the air flow rate. The smaller rotameter (right) measures the flow rate from 0 to 200 l/min air flow. The big rotameter measures the flow rate from 0 to 1000 l/min.

A valve between the rotameters and aerator is used to control the air flow rate. The valve is adjusted gradually to allow more air to enter the siphon until it reaches the maximum air flow rate that causes the siphon to break.

A pressure gauge is put at the inlet of the aerator to measure the air pressure at this point.

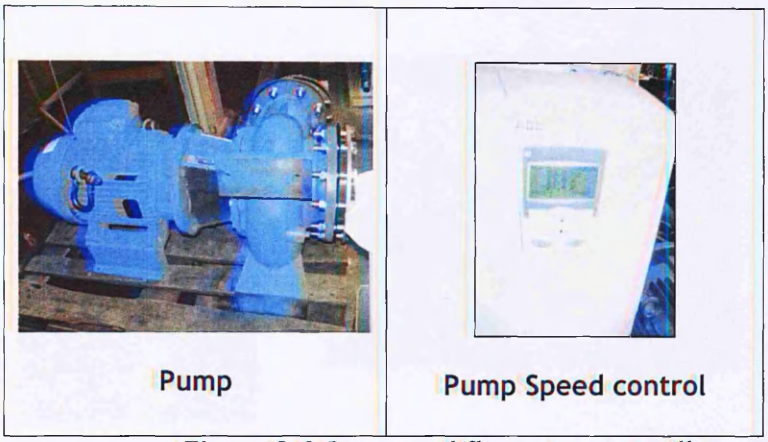

Pump | Pump Speed control

Figure 3.3 Pump and flow rate controller

Various types of aerators were installed to investigate their performance. In this experiment, the flow pattern, the air flow rate and the pressure at the aerator point were recorded.

Three different designs of aerators were tested; Orifice and spargers, an aeration ring using a cylindrical air chamber in the down pipe, and an aerator using an air chamber in the horizontal pipe of the siphon.

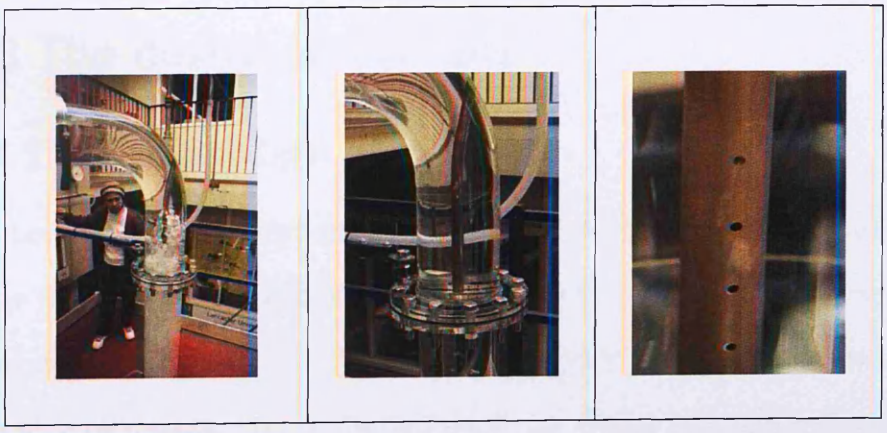

Figure 3.4 Aerator-1

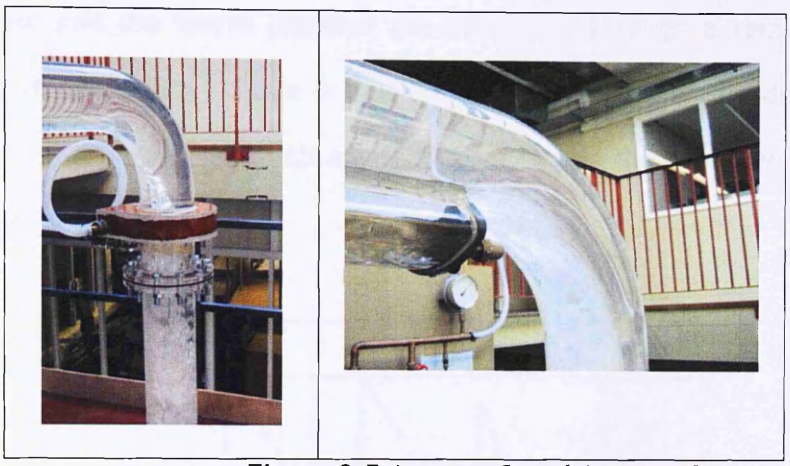

Figure 3.5 Aerator-2 and Aerator-3

To start siphoning, a suction (vacuum) pump is used. Once the siphon is working, the vacuum pump is switched off, and the natural siphon flows continuously.

In order to understand the performance of the aerators, without the disruption of siphon breaks, a pumped system was used. Chapter 6 will discuss in detail the experiment using a pumped system.

3.3 The design of the tank

3.3.1 The bottom tank

The bottom tank (see Fig 3.6) was divided into four chambers to allow the turbulent water from the first chamber to calm down before measuring the flow in the second chamber using the V-Notch. The first chamber and the second chamber are connected through a rectangular hole at the bottom of the divider and with a thin end sill in front of it to slow down the flow at the bottom tank so that the second chamber has relatively calm water before it passes through the V-Notch.

The third and the fourth chamber are connected through a rectangular hole at the bottom of the divider. There is also an end sill in front of the divider to reduce the velocity of the water as it falls over the V-Notch and the overflow water falls from the top tank.

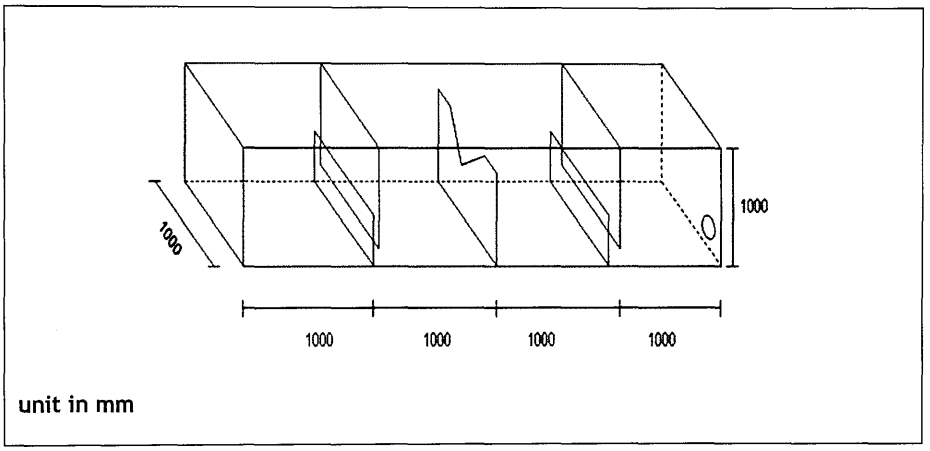

Figure 3.6 Storage Tank

The storage tank dimension: 1.0 m x 1.0 m x 1.0 m (=4.0m^3)

3.3.2 The top tank

The top tank was designed to be the supply source for the siphon inlet. The water then flows throughout the siphon. At the top of the down pipe of the siphon it is mixed with air, and discharges into the first chamber of the bottom tank.

It was important to ensure that there is enough water available so that a continuous siphon flow can be maintained.

It was decided to build the siphon tank with two chambers of 1 m^3 each. The first chamber is where the inlet of the siphon takes the water for the siphon system. The

second segment is where the water from the bottom storage tank is pumped and allowed to settle.

There is a rectangular crest weir in between the two chambers to control the water level. The overflow of the water is drained back to the storage tank.

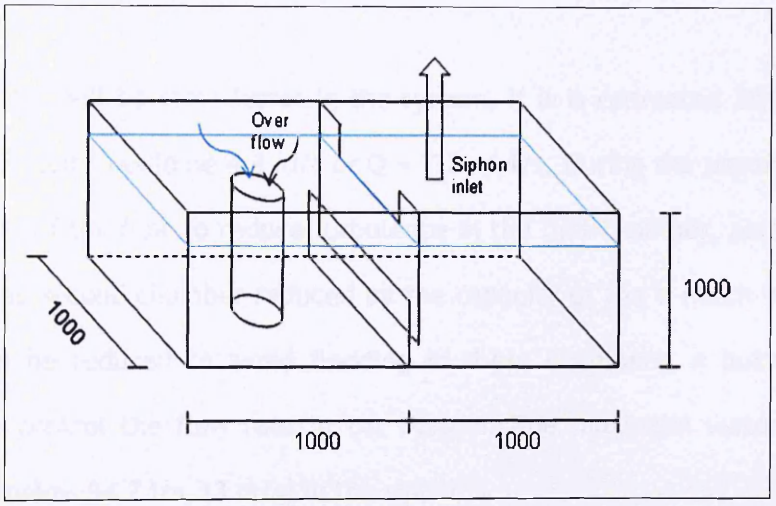

Figure 3.7 Top tank with two chambers

This second tank was located on a platform as a reservoir to store water so there is enough to be siphoned. The storage tank dimension: 2 m x 1.0m x 1.0m =2m^3.

To avoid over flow or to control the water level at the siphon tank, a circular weir is put in the second chamber, so whenever the water rises above the water level weir, it will flow back to the third chamber of the storage tank.

3.4 Water Discharge and Velocity

During the siphon operation, the volume of the bottom tank was such that it could not cope with the maximum flow rate in the siphon. For a 2 m driving head (h), if there are no losses in the system, the water velocity in the siphon would be:

$$v = \sqrt{(2gh)} = \sqrt{(2x9.81x2)} = 6.26 \text{ m/sec}$$

The flow rate in the siphon (Q) with a 200 mm diameter is:

$$Q = v(\pi r^2) = 6.26 \times \pi \times (0.1)^2 \approx 200 \text{ l/sec.}$$

In reality there will be some losses in the system. If it is estimated 30% losses in total, the siphon velocity would be 4.4 m/s or Q = 138.16 l/s. During the experiment there is a slowing down of the flow to reduce turbulence in the first chamber, and with the outlet flow from the second chamber reduced by the capacity of the V-notch weir, the rate of flow had to be reduced to avoid flooding in these chambers. A butterfly valve was installed to control the flow rate in the system. The maximum water flow rate was maintained below 94.7 l/s, (3 m/s) in the siphon.

The siphon pipe is 200 mm diameter. Experimental measurement were taken for two different heights of siphon (y_A). The lower siphon was 3.5 m, and the higher siphon was 4.7 m. It was measured from the top of the vertical pipe where the aerator was located to the bottom pipe to the bottom tank direction (see Figure 3-2).

3.5 Aerator Design

Three different types of aerators were installed for the tests using the pump, and their performances were observed. The aerators were designed with the objective of producing small bubbles that were evenly distributed in the down pipe, (see Fig. 3.9).

1. Aerator-1 - A. An orifice with straight line spargers. B, An orifice with spiral spargers.

2. Aerator-2 - A ring structure formed an air chamber around the down pipe. The air entered the down pipe through holes in the pipe wall.
3. Aerator-3 - An air chamber was attached to the lower side of the horizontal pipe.

Using air chambers gives a uniform pressure to the air entering the pipe through the holes so that, ideally, the distribution of the air is uniform.

The objective was to see the flow pattern of two phase flow in the down pipe, and to find the aerator which produces the maximum air flow rate. This aerator is expected to produce the maximum power. The following diagrams show the different types of aerator used in the down pipe.

Figure 3-8 shows the details of Aerator-1, A. with the straight line spargers, and B. with the spiral spargers. Figure 3-9 shows aerators with air chambers.

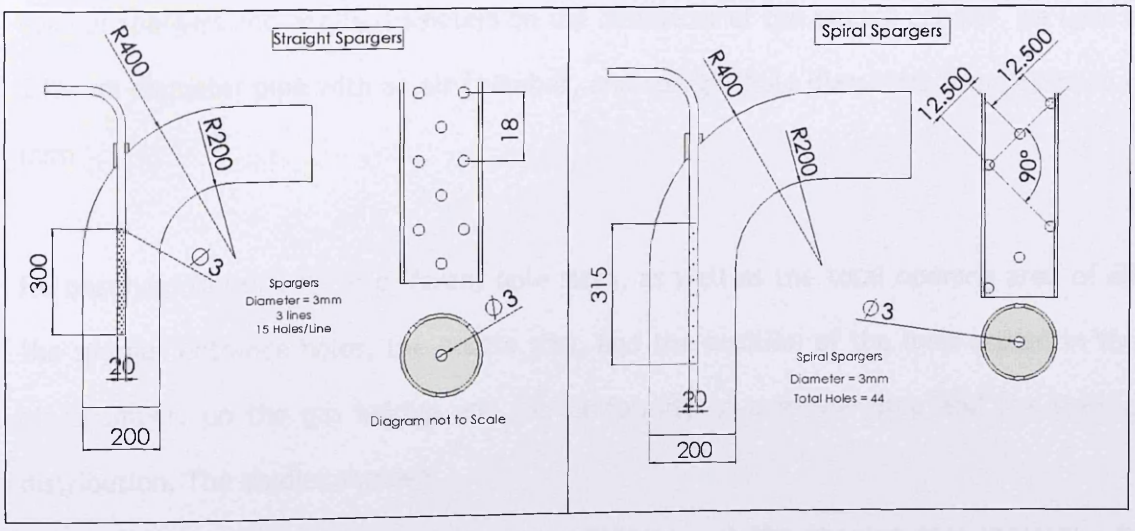

Figure 3.8 Orifice spargers with A. straight and B. spiral line holes

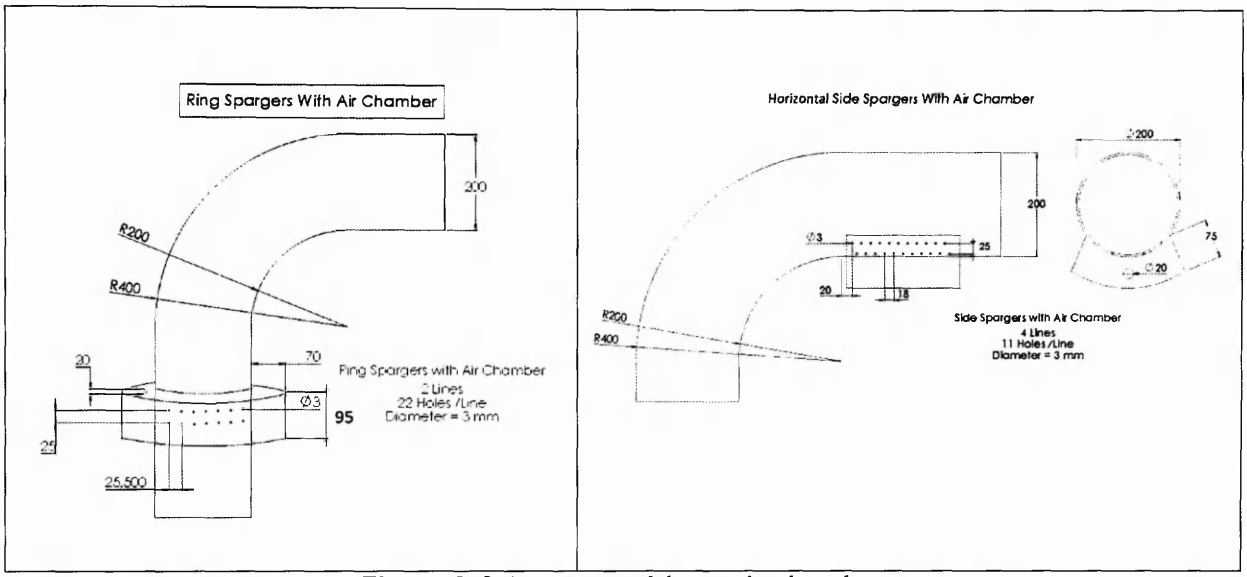

Figure 3.9 Aerators with an air chamber

3.5.1 Sparger diameter and air chamber

The design of sparger hole diameters was based on the study conducted by Dhotre (Dhotre, 2006). He carried out very comprehensive 3D simulation studies using CFD of upward, two phase flow to simulate the flow pattern, and to investigate the effect of various spargers and nozzle diameters on the behaviour of the bubble column. He used a 200 mm diameter pipe with an air chamber, and sparger hole diameters from 2 mm to 4 mm.

He observed the effects of different hole sizes, as well as the total opening area of all the sparger entrance holes, the nozzle size, and the position of the inlet nozzle in the air chamber, on the gas holdup and the uniformity of pressure drop and gas bubble distribution. The studies showed:

1) The average gas holdup (void ratio) decreases as the opening area increases. It also decreases when the opening area of the sparger holes is greater than the nozzle cross section area.

2) As the hole-size of the spargers increase, the pressure drop across the sparger area decreases, and the uniformity of bubble distribution decreases.
3) As hole diameter increases the average gas hold-up decreases. Conversely, smaller sparger holes will create smaller bubbles resulting in a larger gas holdup.
4) An increase in nozzle size increases the uniformity of bubble distribution.

From his results it can be concluded that smaller bubble size results in a higher void fraction (gas holdup). However, this increases the pressure drop, which, ideally, should be as small as possible to limit the energy loss. Therefore, there has to be a balance between having an aerator where the hole size is small enough to produce a large as possible void fraction without having too great a pressure drop. Chapter 5 describes in more detail the relation between the hole size of the spargers and the pressure loss.

Dhotre also found that it is important that the total opening area is the same or smaller than the cross sectional area of the nozzle in order to maintain the uniformity of gas distribution from the spargers.

Futher, Dhotre suggested that to get a relatively uniform distribution, the nozzle should not (as on the left in Fig.3.10) be directly facing the holes (spargers). His simulation produced a maximum void fraction of 0.22.

Based on Dhotre studies, the following design of the spargers for the siphon system was chosen:

The diameter of the nozzle of air tube is 20 mm diameter;

the cross sectional area = π x10 x 10 = 314 mm^2.

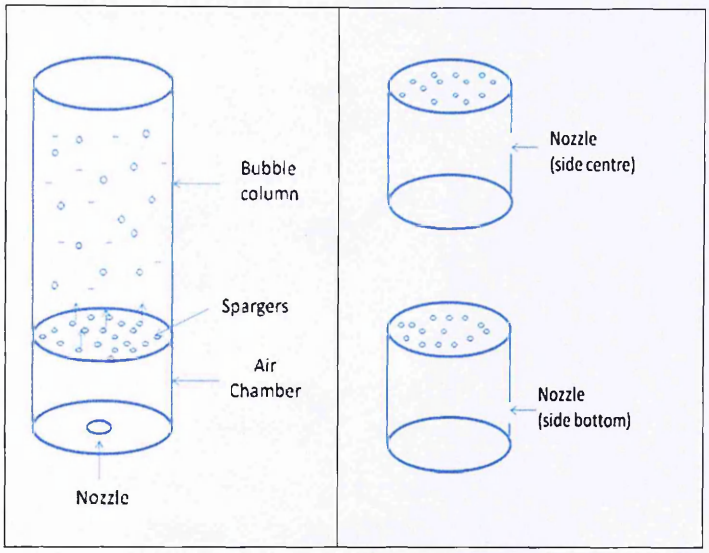

Figure 3.10 Bubble column and air chamber - Dhotre

To maintain the total area of opening of the spargers the same as the cross sectional area of the air tube:

For a hole's diameter of 2 mm,

The number of holes needed = 314 mm^2 ÷ (π x1 x 1 mm^2) = 64

For a hole diameter of 3 mm,

The number of holes needed = 314 mm^2 ÷ (π x1.5 x 1.5 mm^2) = 44

3.6 Measuring Devices

3.6.1 V-Notch Weir

A critical aspect of the project is in achieving the correct measurement of water flow rates. If these values are consistently incorrect, all calculations will be affected and thus meaningless. The flow rate is dependent on the angle of the v-notch and the level of water above the sharp crest of the weir:

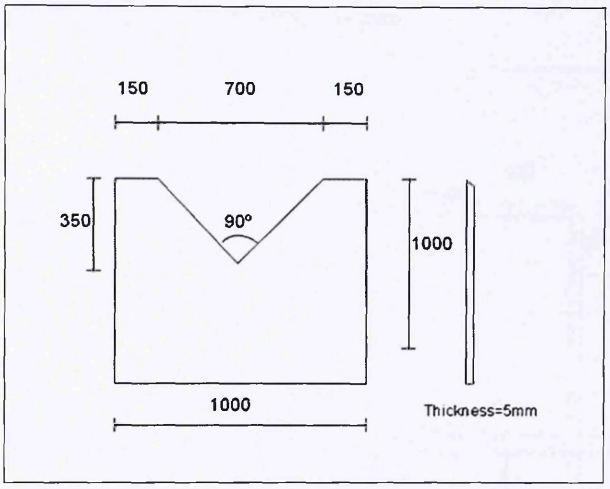

Figure 3.11 Detail of V-Notch

Figure 3.12 V-Notch detail

Chapter-4 discusses in detail how to calculate the water discharge using a V-Notch weir.

3.6.2 Pressure gauge and manometer tap

Manometers were installed to measure the pressure within the pipe, at the locations shown in the Fig. 3-13 below; M1, M2, M3, M4 and M5. These pressure measurements were made to find the losses due to friction and other causes when water was pumped through the pipe.

An air pressure gauge was installed between the rotameter and the aerator to measure the air pressure at this point during the aeration process.

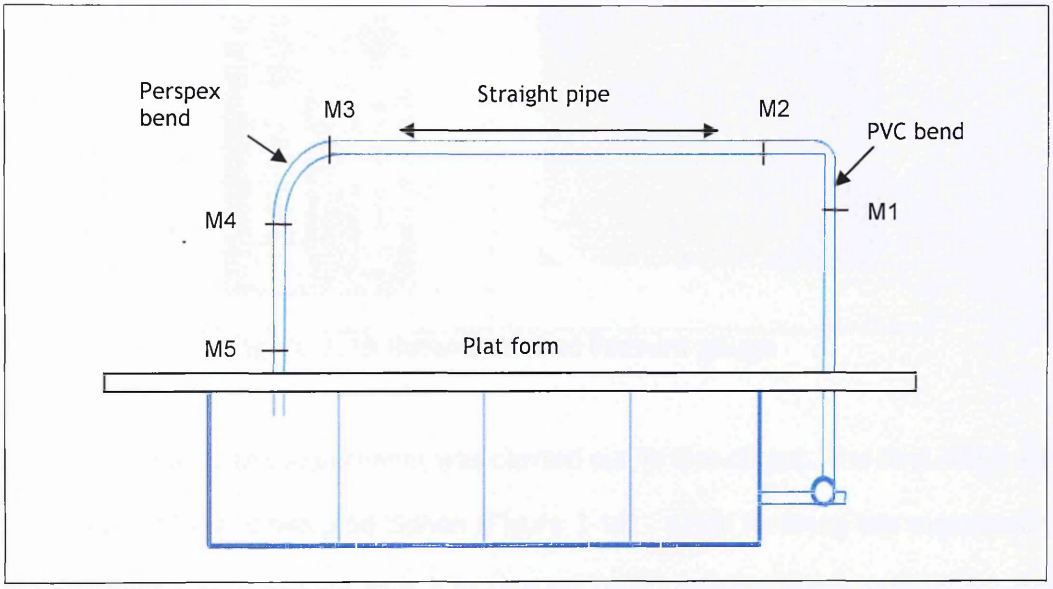

Figure 3.13 Positions of Manometer taps

Figure 3.14 Manometer

3.6.3 Rotameter

A rotameter is used to measure the air flow rate. The flow rate is controlled by a valve. The rotameter is calibrated to read for air at atmospheric pressure.

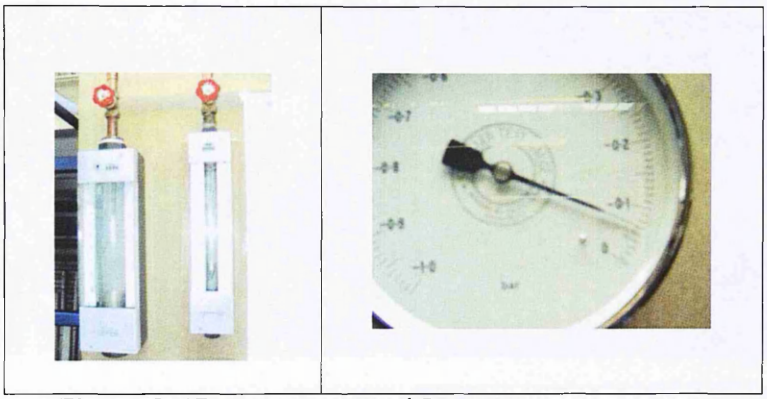

Figure 3.15 Rotameter and Presure gauge

For the siphon system, the experiment was carried out in two stages. The first stage was using a 3.5 meter long, down pipe siphon (Figure 3-16) . After finishing the experiment, the siphon height was raised up to 4.7 m (Figure 3-17), and the same experiment was carried out. Chapter 6 describes in more detail the siphon experiment.

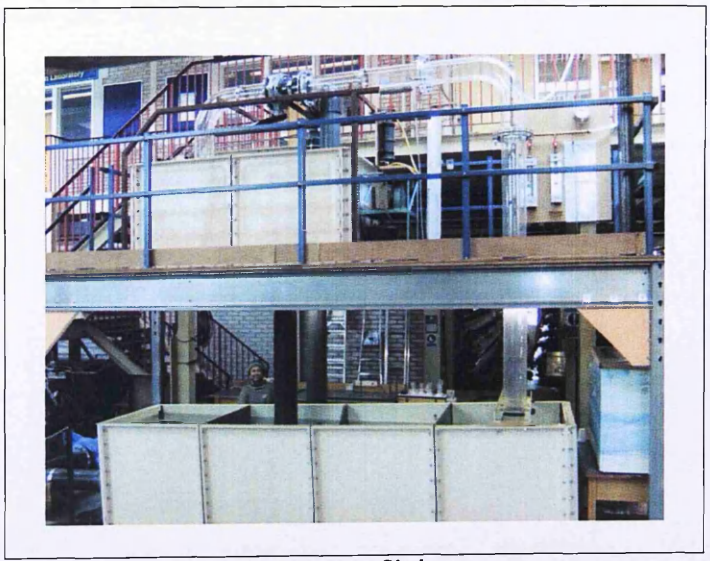

Figure 3.16 Low Siphon

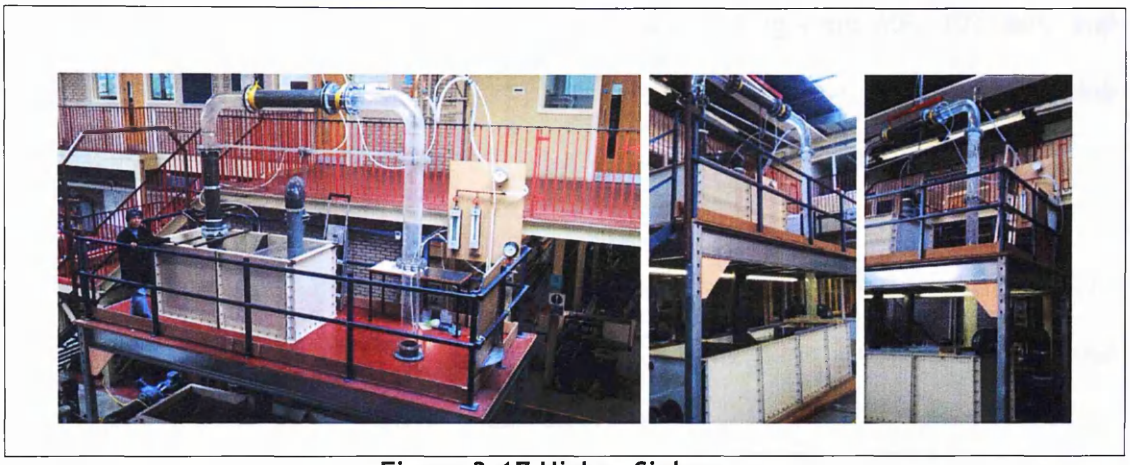

Figure 3.17 Higher Siphon

3.7 Butterfly Valve

Due to the V-Notch weir, the water flow rate into the second chamber was relatively small. Operation at higher flow rates causes the first chamber of the bottom tank to overflow. Thus, a butterfly valve was installed on the horizontal part of the pipe system to control the flow rate. See Fig, 3-18.

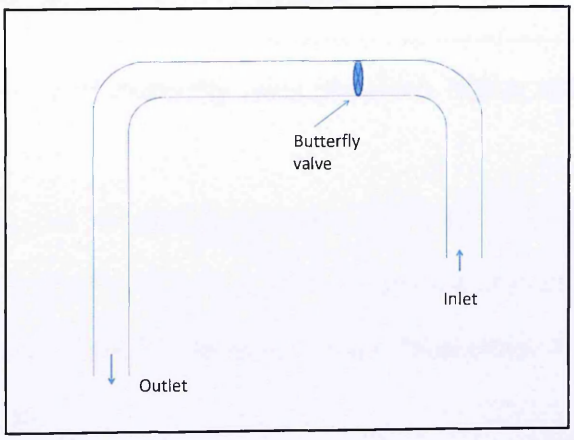

Figure 3.18 Butterfly valve position - lower siphon

The siphon was run with various butterfly openings starting from 60°, 70°, 80°, and eventually full opening. To avoid flooding in the bottom tank, a full butterfly opening was used only when the air flow rate was sufficient to prevent flooding.

For the low siphon, the butterfly valve was located in the horizontal part of the siphon. For the higher siphon, the butterfly valve was located in the vertical pipe between the inlet and the first bend of the siphon. See Fig. 3-19.

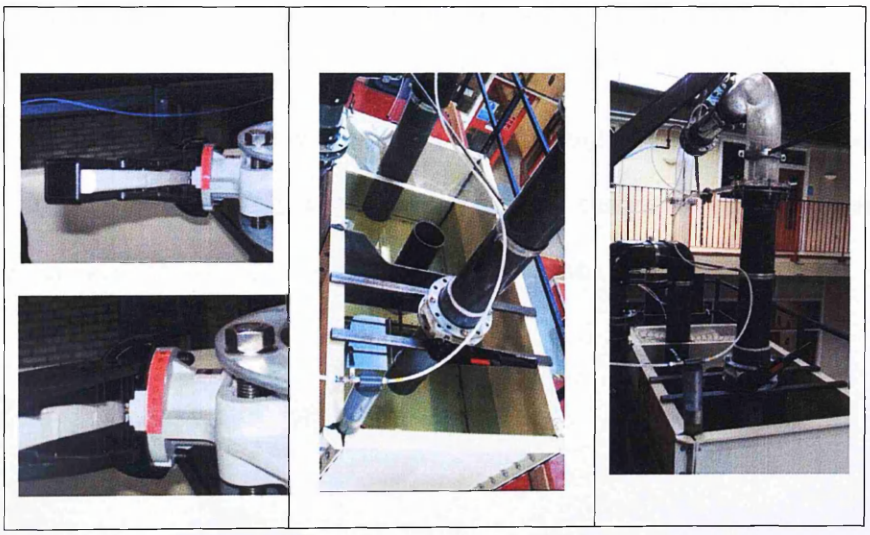

Figure 3.19 Butterfly valve position - higher siphon

All the equipment, i.e. the Perspex pipe system, the tanks, the pump with flow meter and its manifold, the butterfly valve and other measuring devices were purchased from UK companies and then assembled together in the laboratory. It was installed by the departmental technicians.

Chapter 4

Pre Experimental Work

4.1 Introduction

This chapter describes the calibration of the V-Notch weir i.e. to find its discharge coefficient in order to measure the water flow rate; the calculation of the loss coefficients in the pipe system due to friction and other losses due to the inlet and outlet, the pipe bends and the butterfly valve.

To calibrate the V-notch weir measurements of volume flow were timed, converted to flow rates, and a rating curve was drawn to show the relationship between the height of the water level above the V-notch and the flow rate.

4.2 V-Notch Measurement

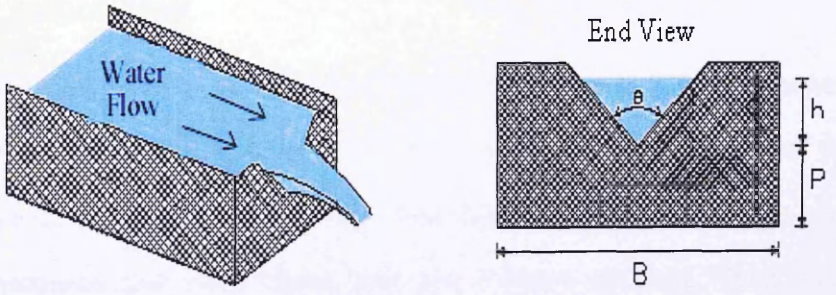

Figure 4.1 Flow measurement over V-notch

The flow over the V-notch is dependent on the angle of the V-notch and the level of water ('h' in Fig 4-1) above the sharp crest of the weir (Sastraatmadja, 1981).

Theoretically, the flow rate over the V-notch is:

$$Q = 8/15\ (\sqrt{2g})\ \tan(\Theta/2)\ h^{2.5} \qquad (4.1)$$

This formula has to be corrected by coefficient of discharge (Cd) for the V-notch weir. (Subramaya,1982; Fox and Mc Donald, 2001). This depends on the physical condition of the crest weir. Thus:

$$Q = Cd * 8/15\ (\sqrt{2g})\ \tan(\Theta/2)\ h^{2.5} \qquad (4.2)$$

Where: Q = discharge, m3/s

Θ = angle of V-notch, deg

h = head on apex of notch, m

The angle of the V-notch is 90°. Thus, the only variable which can alter the flow rate is the height of water above the crest, h (**Figure 4-1**)

4.2.1 Cd calculation

Young et al (1997) found that typical Cd for triangular weirs is in the range of 0.58 to 0.62. To find out exactly the value of Cd, first we measure the volume of flow (in m^3) using flow meter in 60 seconds, so we can find the water flow rate in litre per second. It was also measured the water level over the V-Notch (in cm). Then the discharge coefficient of the V-notch (Cd) was calculated using formulae (4.3).

This combination reading of flow meter volume and the V-Notch height were carried out for 28 readings, then Cd was calculated of flow rate and water level.

$$Cd = Q/[8/15\ (\sqrt{2g})\ \tan(\Theta/2)\ h^{2.5}] \qquad (4.3)$$

Table 4.1 shows the calculation of Cd for 28 water level reading (h) and flow meter reading. The result from the reading flow meter and calculation from **(4.3)** was Cd= 0.598 ≈ 0.6. (See **Table 4.1**).

Table 4.1 Cd calculation

Height (m)	Flow-meter (l/sec)	Cd
0.295	65.548	0.5865
0.290	63.524	0.5947
0.285	60.190	0.5942
0.280	57.976	0.6041
0.275	55.548	0.6006
0.270	52.976	0.6056
0.265	50.095	0.6067
0.260	49.407	0.5939
0.255	46.067	0.5982
0.250	44.160	0.5959
0.245	41.824	0.5939
0.240	39.590	0.5916
0.235	37.610	0.5929
0.230	35.610	0.5920
0.225	34.271	0.5866
0.220	32.210	0.5870
0.210	28.911	0.5937
0.200	25.310	0.5876
0.190	22.357	0.5989
0.180	19.478	0.6014
0.170	16.885	0.6020
0.160	14.510	0.6098
0.150	12.348	0.5955
0.140	10.392	0.5945
0.130	8.857	0.5978
0.120	7.214	0.6153
0.110	5.667	0.6122
0.100	4.595	0.6151
	Cd (average) =	**0.5981**

4.2.2 Flow meter reading

The volume discharges of flow meter (in m^3) were recorded in 60 second period of time, and then the flow rate was calculated. These readings were repeated 7 times for each flow rate calculation, and then calculate the mean as follows:

$$(\text{Flow rate})_i = 1000*(\text{Vreading-2} - \text{Vreading-1})/60 \quad (\text{l/s}) \tag{4.4}$$

$$\text{Mean of flow rate} = (\Sigma(\text{Flow rate})_i)/7 \tag{4.5}$$

The maximum error for each flow rate was estimated as ± 0.03%.

4.2.3 Flow rate over V-notch calculation

Based on this Cd, then the flow rate in the V-notch is calculated using (4.2) formulation with Cd=0.6.

$$Q = 0.6 * 8/15 (\sqrt{2g}) \tan(\Theta/2) h^{2.5} \tag{4.6}$$

Giving g=9.81, $\Theta = 90^{o,}$ $\tan(\Theta/2) = 1$:

$$Q = 1.417 * (h\text{^}2.5) *1000 \quad (\text{l/s}) \tag{4.7}$$

and **Figure 4.2** shows the rating curve of the V-notch. V-notch and flow-meter correlation can be seen on **Figure 4.3.**

The error of reading on the V-Notch height is estimated to be 1 mm.

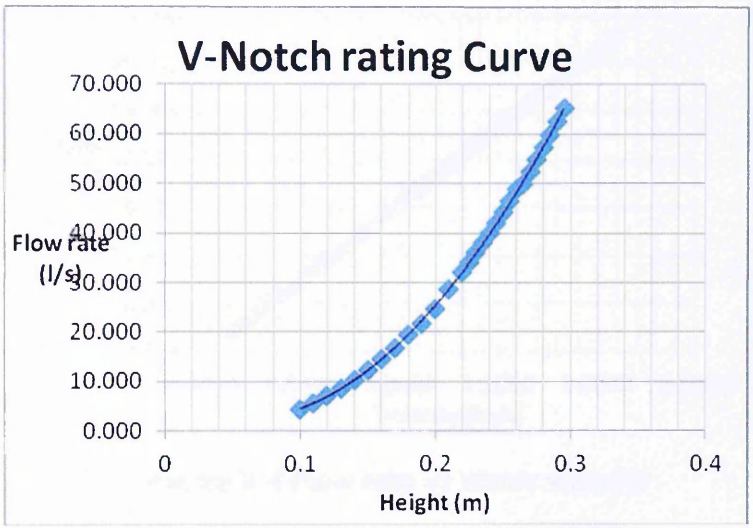

Figure 4.2 Rating curve of V-notch

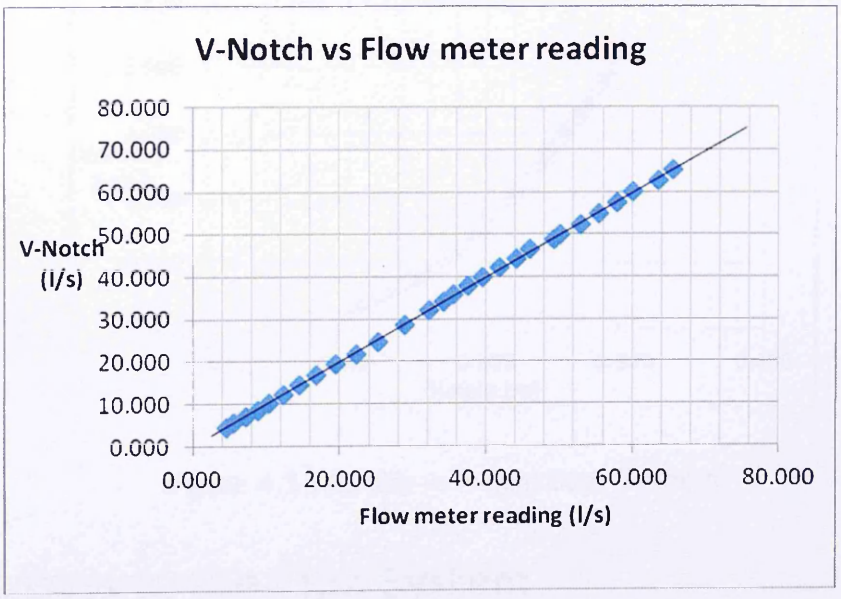

Figure 4.3 V-Notch vs Flow-meter

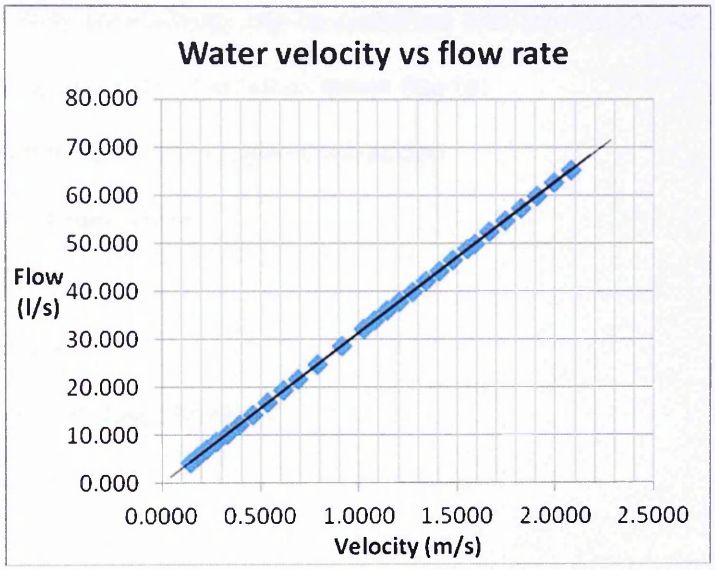

Figure 4.4 Flow rate vs Water velocity

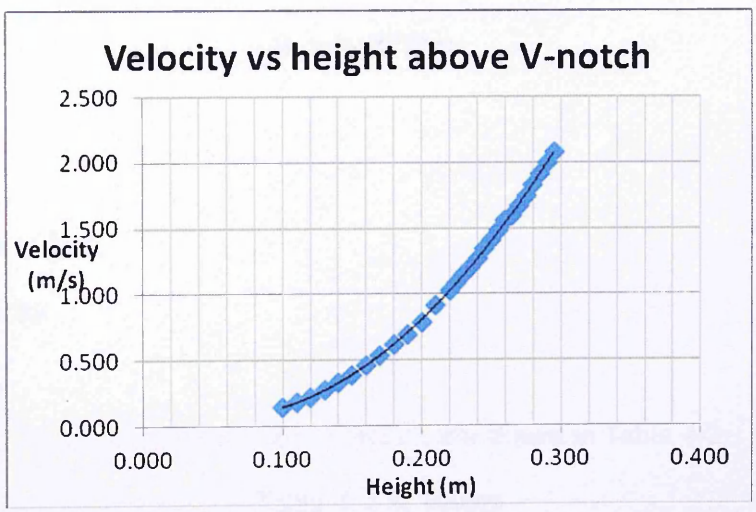

Figure 4.5 Velocity vs Height over V-Notch

4.3. Losses in the Pipe System

It is important to find the pressure losses for the various flow rates. This data will be used to find the loss component when aeration flows are carried out.

Losses in a water flow pipe system can be classified into two components i.e. major loss due to friction along the pipe, and minor losses due to:

- sudden enlargement and sudden contraction
- the pipe inlet and outlet
- pipe bends
- pipe junctions
- divergent and diffuser sections
- joints
- valves

In fully developed turbulent flow these losses are given by the following simple formula:

$$H_L = K_L (V^2/2g) \qquad (4.8)$$

Where:

H_L = head loss

K_L = coefficient of loss

V = water velocity

The value of K_L for the above common situations are shown in Table 4-2

Table 4.2 K_L values

	K_L value in practice
Bell-mouth entry	0.10
Sharp edge entry	0.5
Sharp edge exit	1.0
Diffuser outlet	0.2
90° bend	0.4
90° Tees :	
- In-line flow	0.4
- Branch to line	1.5
- Gate valve	0.25

Source: Sleigh and Goodwill, (2009), Miller (1996)

Table 4.3 shows other K_L values. (White, Streeter, and Hydraulic Institute in Munson, 2002).

Table 4.3 K_L values

	K_L value in practice
a) Elbow:	
Regular 90°, flanged	0.3
Regular 90°, threaded	1.5
Long radius 90°, flanged	0.20
Long radius 90°, threaded	0.7
b) Union, threaded	0.08
c) Valve	.
Gate, fully open	0.15
Gate, ¼ closed	0.26
Gate, ½ closed	2.1
Gate, ¾ f closed	17

Source: Munson (2002), Miller (1996)

4.3.1 Friction loss in pipe

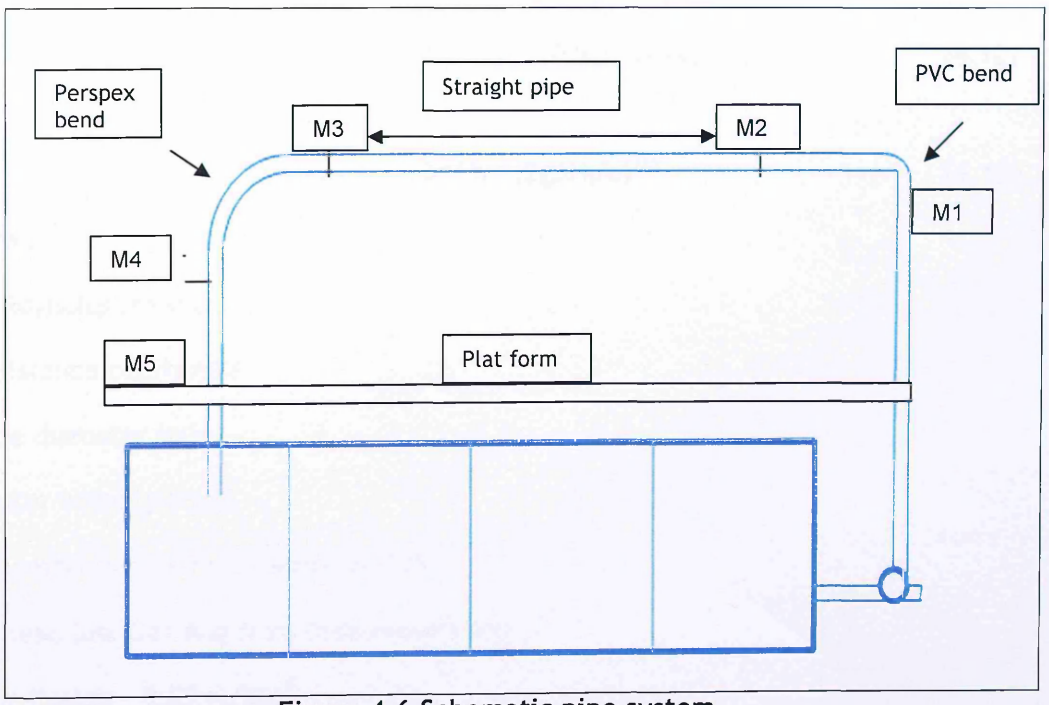

Figure 4.6 Schematic pipe system

Loss due to the friction in the straight pipe section (between the PVC bend and the Perspex pipe bend) was measured. (See Figure 4-6). The length of the straight pipe between M2 and M3 is 0.80 m. By reading manometers 2 and 3 for various flow rates, we can find the head losses (ΔH_f).

These values are then used to find the resistance coefficient, f, (Moody resistance coefficient) (See Appendix 4-1) from equation 4.9.

$$\Delta H_f = f\,(L/D)\,V^2/2g \qquad (4.9)$$

$$V=(2g\,\Delta H_f\,/L)^{1/2}\,(D/f)^{1/2} \qquad (4.10)$$

Since the Reynolds number:

$$\mathbf{Re = VD/v} \qquad \mathbf{(4.11)}$$

Where: v= kinematic viscosity

By substituting V in equation (4.10) into (4.11) (see Crowe et al 2001);

$$\mathbf{Re=}\,(2g\,\Delta H_f\,/L)^{1/2}\,(D/f)^{1/2}\,(D/v) \qquad (4.12)$$

$$\mathbf{Re}f^{1/2} = (D^{3/2}/v)*(2g\Delta H_f/L)^{1/2} \qquad \mathbf{(4.13)}$$

Where :

Re = Reynolds number

f= resistance coefficient

D=pipe diameter (m)

V= water velocity (m/s)

v= kinematic viscosity for water at 20°C

ΔH_f= head loss (reading from manometer) (m)

g= gravitation = 9.81 m/sec^2

L = length between manometer (m)

The head loss ΔH_f is measured from various flow rates between 19 l/s to 57 l/sec reading. Then the values of $Re\sqrt{f}$ were calculated based on equation (4.13). By calculating k_s/D, i.e. k_s is pipe roughness and D is pipe diameter, the Moody diagram can be used to find the value of resistance coefficient (f).

Table 4-4 gives various values of pipe roughness.

Table 4.4 Roughness coefficient (k_s)

	k_s value for perspex, plastic, glasses
DS Miller (1996) Sleigh and Goodwin (2009) Colebrook (in Munson 2002)	0.0025 0.0030 0.0 (smooth glass)

For k_s=0.003 then k_s/D = 0.000015. Referring to the Moody diagram (Crow at al, 2001, p 418, Mc Kinney, p 418), the coefficient of resistance (f) of the perspex pipe ranges from 0.013 to 0.018. It varies with the flow velocity in the pipe. The f increases with a decrease in flow velocity. **Appendix A-2** shows the detail calculation for the values of $Re\sqrt{f}$.

4.3.2. Loss in PVC bend

In the experimental rig, there are two bends to be measured, i.e. the vertically upward pipe (PVC bend) and the Perspex transparent pipe bend at the down pipe. The pressure loss at the PVC bend was measured using Manometers 1 and 2, and for the perspex bend it is measured using Manometers 3 and 4. The water flow in the pipe is measured by

reading V-notch level height and then it is converted using the Rating Curve (Figure 4-2), or Figure 4-5 to find the velocity.

The difference in the manometer readings between the bend (M1 and M2) gives the pressure head loss in the bend, i.e.:

Different pressure head (ΔH) = Reading1- Reading2 (m)

$$\Delta H_{bend} = K_B v^2/2g \qquad (4.14)$$

Reading-1 and Reading-2 are read from the manometer. The V-notch height is also read. By using the Rating Curve in Figure 4.2 the flow rate is calculated (in m^3/sec) from the corresponding V-notch height. Then the $v^2/2g$ is found using the following formula:

$$V^2/2g = (Q/A)^2/2g \qquad 4.15)$$

A is the area of the pipe and g is gravitational acceleration. Manometer readings were made for different values of the flow rate. The results were then plotted into the ΔH_p versus $v^2/2g$ graph (See Figure 4.7 and Figure 4.8).

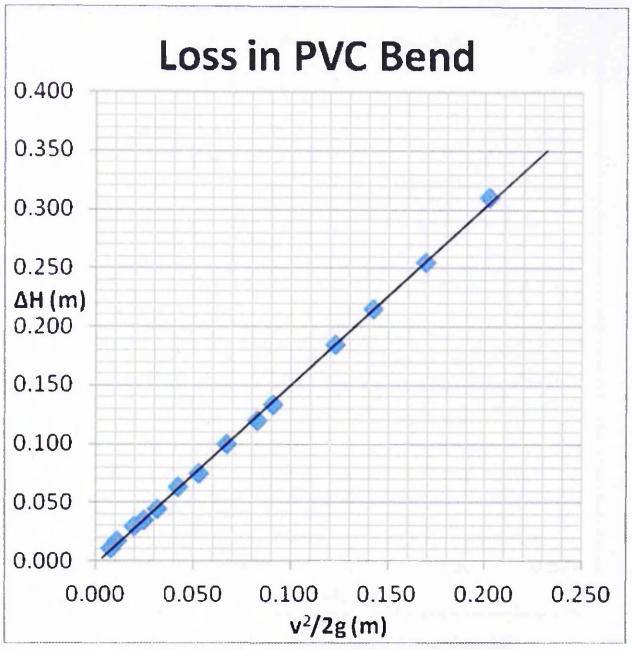

Figure 4.7 Loss in PVC bend

The Loss Coefficient in PVC bend (K_B) was found from the gradient of the graph, i.e.:

$$K_{B\text{-}PVC} = \Delta H_p/(V^2/2g) \qquad (4.16)$$

From Figure 4.7 it is found that $K_{B\text{-}PVC}$ = 1.5 for PVC bend.

Reading the manometer is not easy because it keeps fluctuating. In order to minimize error on the reading, for every single fluid flow rate, it was taken 3 times then the average of the three readings was taken.

4.3.3. Loss in Perspex pipe bend

Figure 4-8 plots the difference in manometer readings (ΔH) between the bends versus the velocity head ($V^2/2g$). The gradient of the graph represents the loss coefficient for the perspex bend, $K_{B\text{-}Perspex}$ = 0.36.

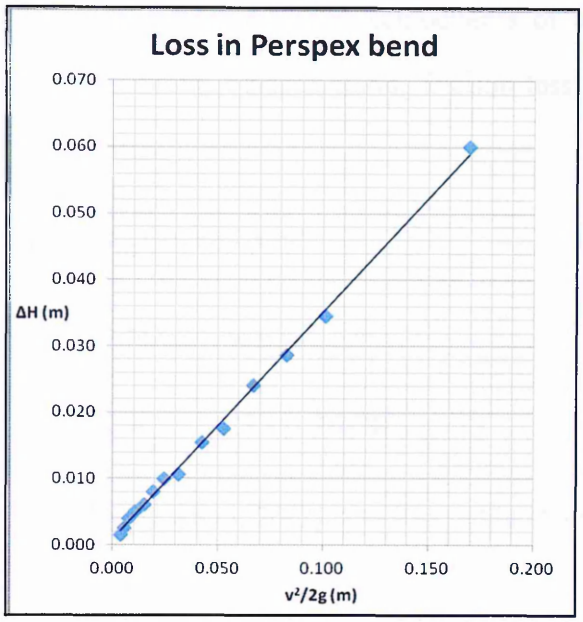

Figure 4.8 Loss in Perpex bend

This value should be slightly less because there are joints (union) next to Manometer 3 and Manometer 4. From Table 4.3, $K_{union} = 0.08$, then:

$$K_{B\text{-}Perspex} = 0.36 - (2\ K_{union}) \qquad (4.17)$$

$$K_{B\text{-}Perspex} = 0.36 - (2*0.08) = 0.20$$

According to Miller (Miller 2001, p 81) the value of K_B ranges from 0.20 - 0.50, or i.e. K_B ranges from 0.15 - 0.27 for r/D= 2-3 (bend radius, D= pipe diameter), , and K_B ranges between 0.24-0.5 for r/D=1. The value of the Reynolds number ranges between 10^4 and 10^6.

The value of $K_{B\text{-}Perspex}$ will be checked again after measuring the loss between two bends.

4.3.4 Loss between two bends

The total loss between the two bends, i.e. from the PVC bend, along the horizontal pipe, and the Perspex pipe bend was measured. From the graph (Figure 4.9), it shows

that the total loss coefficient is $K_{b\text{-}b} \approx 2.1$. The components of losses in this segment come from, losses due to PVC bend, Perspex bend, friction loss, and the three joints between the manometer readings.

Thus the loss due to joints (ΣK_j) can be found.

$$\Sigma K_j = K_{b\text{-}b} - K_{B\text{-}PVC} - K_{B\text{-}Perspex} - K_f \quad (4.18)$$

$$\Sigma K_j = 2.1 - 1.5 - 0.20 - Kf \quad (4.19)$$

Using Darcy-Weisbach equation (Munson, 2002), the loss in the straight pipe with circular cross section is:

$$\Delta H_f = f\,(L/D)\,(V^2/2g) = K_f\,(V^2/2g) \quad (4.20)$$

$$K_f = f\,(L/D) \quad (4.21)$$

For f= 0.013, L= 0.80 m, and D= 0.20m:

$$K_f = 0.013 * (0.80/0.20) = 0.052$$

Back to equation (4.18)

$$K_j = (2.1 - 1.5 - 0.36 - 0.052)/3 = 0.063 \approx 0.06$$

For f= 0.018, L= 0.80 m, and D= 0.20:

$$K_f = 0.018 * (0.80/0.20) = 0.072$$

$$K_j = (2.1 - 1.5 - 0.36 - 0.072)/3 = 0.056 \approx 0.06$$

Back to equation (4.11), using $K_j = 0.06$

$$K_{B\text{-}Perspex} = 0.36 - (2 * 0.06) = 0.24.$$

It was found that the value $K_{B\text{-}Perspex}$= 0.24, for 90° radius bend with r/D = 1. This value agrees with the reference value from Miller (2001) which ranges between 0.24-0.5 for r/D=1. This means that for any other experiment, the use of values published in reference works can be used with confidence. Calculation showed that K_j = 0.063, which is slight smaller compared to the reference, i.e. K_j = 0.08 (Munson 2002).

If the measurements are made lower down in the vertical pipe, the total loss from the PVC bend to this point is not very different giving K = 2.2 as shown in **Figure 4.9.**

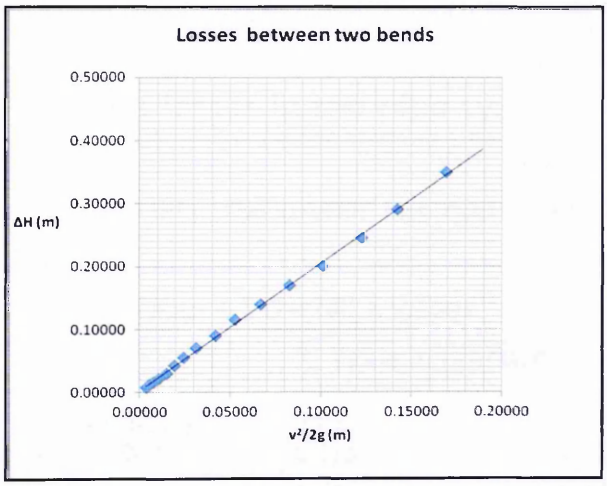

Figure 4.9 Losses between PVC bend and perspex bend

4.3.5 Losses in inlet and outlet

Ideally, the inlet is a well rounded entry to minimize the entry loss. It was not possible to build this in the experimental rig, so it has a sharp edged entry. Due to the small space available in the rig, the outlet also has a sharp edge. The value of K_L for entry and exit is taken from Table 4.2, i.e. K_{entry}=0.5 and K_{exit}=1.0.

4.3.6 Losses in joints (union)

Within the pipe system, there are some joints (union) in the straight pipe. Based on the calculation from the previous section the value of K_j = **0.06.**

4.3.7 Gate valve loss

To control and set various flow rates, a gate valve was put between the pump and the vertically up pipe. During experiments, the valve was opened between 40% and 70% of full opening, and with its loss coefficient K_L values ranging between 0.26 and 2.1.

4.3.8 Overall coefficient losses in the pipe system

Based on the experimental results, the overall loss coefficient (K) in the system is summarised in Table 4-5.

Table 4.5 Overall K values

	K_L value in practice
Friction loss (L= 0.80 m)	0.052
Friction loss (L=5.0m)	0.325
PVC bend	1.50
Perspex bend	0.24
Joint (one joint)	0.06
Joints (9 joints)	0.54
Inlet (sharp edge entry)	0.50
Outlet (sharp edge exit)	1.0
Gate valve (40% opening)	2.1
Gate valve (70% opening)	0.26

Table 4.5 shows that the biggest losses were contributed by PVC bend, inlet-outlet, valve openings. All these losses happened because of the restriction of space in the laboratory. On site experiment, where there are no space restrictions, these losses can be minimized by some improvements, i.e. by using a bell mouth or diffusion inlet and outlet, reducing the number of joints i.e. by using only one single large radius bend. It is

possible to operate in full siphon mode, so there is no need to put a butterfly valve to control the flow rate.

4.3.9 Losses due to Butterfly valve

As it was mentioned in the Chapter 3 section 3.8, the butterfly valve was used to control the water flow rate. The energy loss due to the butterfly valve varies depending on the degree of the opening and the flow velocity.

A series of experiments using various openings were carried out and the different pressures across the butterfly valve were measured (between Point-D and Point-C in Figure 4-10).

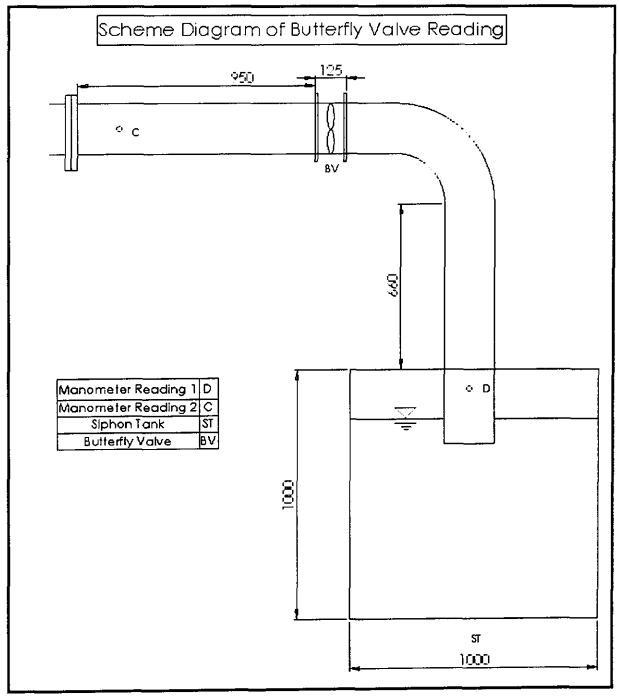

Figure 4.10 Butterfly Valve

Total pressure drop across the butterfly valve (between Point D and Point C) and using the following equation gives the pressure loss cefficient.

$$(p_1-p_2)/\rho g = v^2/2g\ (K_f+K_B+K_J) + v^2/2g\ (K_{but}) \qquad (4\text{-}22)$$

$$K_{but} = \{[(p_1-p_2)/\rho g] - [v^2/2g\ (K_f+K_B+K_J)]\} \ /\ v^2/2g \qquad (4\text{-}23)$$

Where:

(p_1-p_2) = different pressure between Point D and Point C

ρ_w = water density

K_f = friction loss coefficient = 0.013, L = 1.80 m

K_B = bend coefficient (one bend)

K_J= joint coefficient (two joints)

Table 4-6 shows the loss coefficient for butterfly valve openings (K_{but}).

Table 4.6 Loss Coefficient of butterfly valve

Butterfly opening	K_{but}	Log (K_{but})
20°	166.1	2.22
30°	86.3	1.94
40°	43.4	1.64
50°	21.2	1.33
60°	9.7	0.99
65°	5.8	0.76

Figure 4-11 shows a graph of various butterfly valve openings and the values of its loss coefficient. Calculation details can be seen in Appendix A-3.

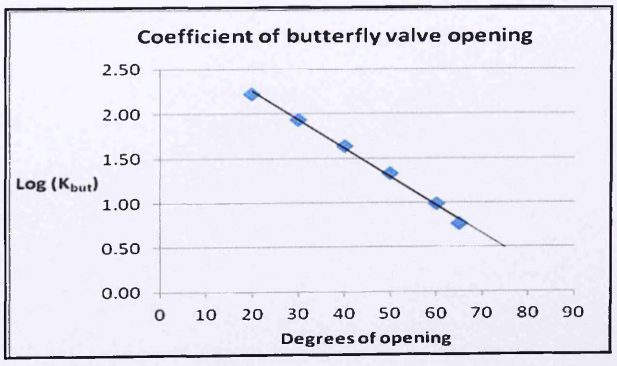

Figure 4.11 Coefficient of butterfly valve

It can be seen that the loss coefficient of the butterfly valve is not linear. The value increases exponentially as the degree of opening decreases. For 20° the K value reaches above 100, and at 65° opening, K reduces significantly to 5.8. In full butterfly valve opening, the value of Log K_{but} = 0, or K_{but} = 1. This butterfly valve also contributes a significant loss in the pipe system.

As a summary, the overall total loss coefficient in the system due to the water flow in the siphon was estimated to be (see also Table 4.5 -and Table 6.2 - Chapter 6):
K= 3.60 for the low siphon and K = 3.9 for the higher siphon.

As it was mentioned above, on site experiment, we can run a full siphon flow with no restriction. Therefore, we do need a butterfly valve to control the siphon flow.

Chapter 5

SINGLE-HOLE AERATOR EXPERIMENT

5.1 Introduction

This chapter describes a single-hole aerator experiment that was carried out to observe the bubble formation, the flow pattern surrounding the nozzle, and the pressure loss due to bubble development and detachment from the nozzle. In order to carry out this experiment, a single-hole aerator experimental rig was set up separately from the main siphon experimental rig.

In the siphon system with aeration, there are two groups of head loss components, as summarised in Figure 5-1 i.e.:

- losses in the pipe system which can be represented as a function of velocity head ($v^2/2g$)
- losses due to aeration, i.e. air entering the siphon, and bubble development which can be represented as a function of pressure head (p/γ)

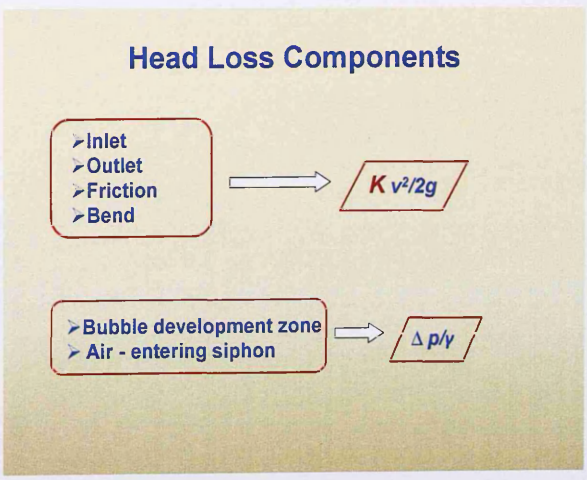

Figure 5.1 Loss components in the siphon system with aeration

The values of K for the first group of loss components have been discussed in Chapter 4.

This experiment was set up separately from the main siphon experiment in order to observe the air pressure drop due to bubble formation only, without the effects caused by the various pipe system losses. This experiment was carried out in still water.

An open top hexagon tank of transparent material of 35 cm height and 16 cm sides was filled with water. Through an air regulator, air flows into the water in the cylinder, the flow being measured by a rotameter. Air was then released into the water through a circular hole. The KDG 1100 rotameter used has a maximum capacity of 10 l/min. The pressure difference in the air before and after it was released into the water was measured by a U-tube manometer. A total of nine hole types were tested, consisting of three different diameters (2 mm, 3 mm and 4 mm) with edge cuts being either straight, or with an inner chamfer, or with an outer chamfer (see Figures 5-4). As shown in Fig. 5-5 these holes were machined into the one circular plate that could be positioned with the air inlet pipe so only one hole was releasing air into the chamber.

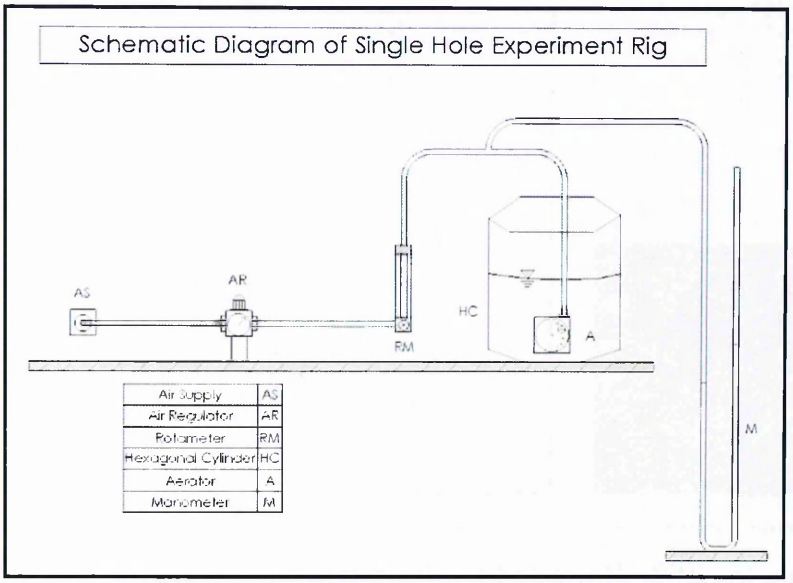

Figure 5.2 Schematic diagram of Single-hole Rig

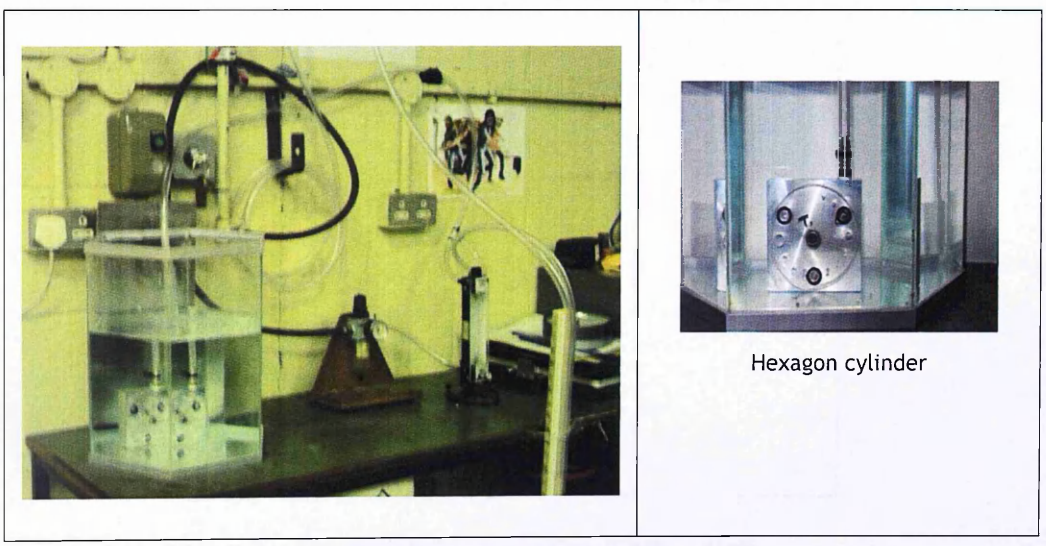

Figure 5.3 Single-hole aeration rig

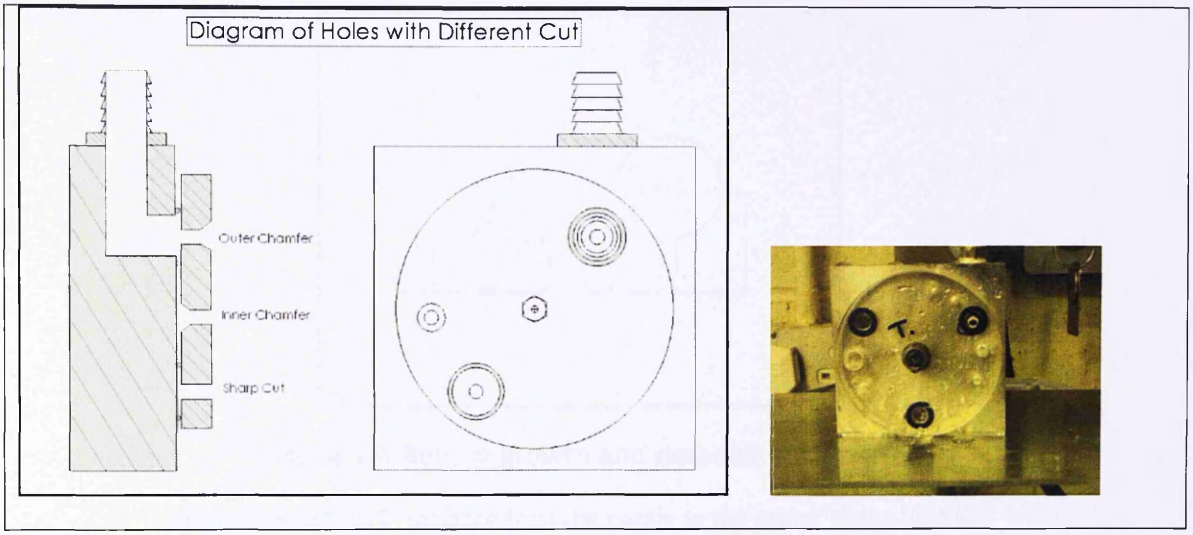

Figure 5.4 Cross section of the holes with different cut

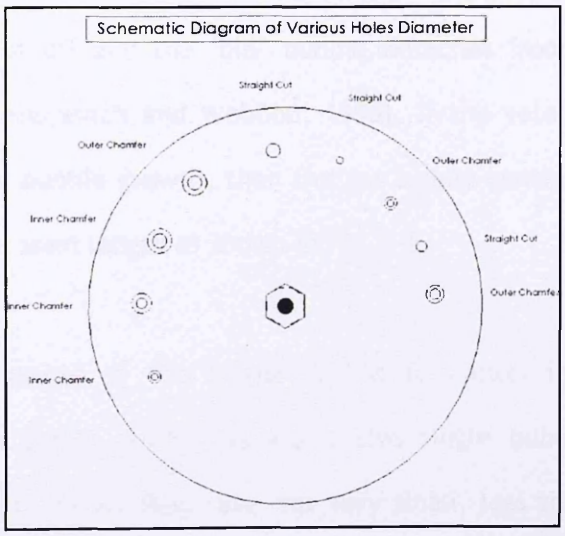

Figure 5.5 various holes' types

5.2. Bubble Formation

5.2.1. Theory and observation of bubble formation

There are two stages in the formation of a bubble, i.e. bubble growth and bubble detachment.

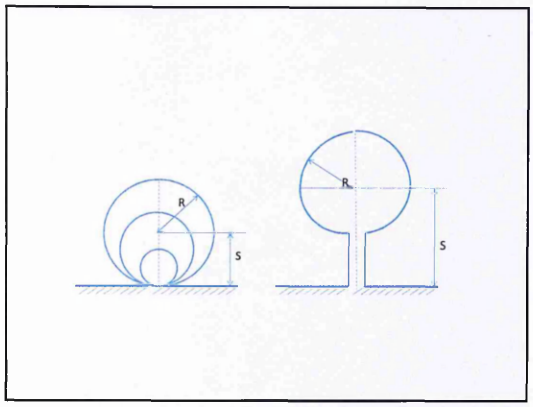

Figure 5.6 Bubble growth and detachment stages

(R= bubble radius, S= distance from the nozzle to the center of the bubble)

If the velocity of the bubble centre (dS/dt) is larger than bubble expansion rate (dR/dt), then the gas supply is cut off and the 'old' bubble detaches from the nozzle, thus creating a single bubble (Buyevich and Webbon, 1996). If the velocity of the bubble centre is smaller than the bubble growth, then the gas supply continues to expand the bubble and to build up the stem length as shown in Fig. 5-6.

Figure 5-7 shows an example of the single bubble formation in the single hole experimental rig for the 2 mm nozzle diameter. This single bubble formation and detachment occurred when the air flow rate was very small, less than 2 l/min, dS/dt being greater than dR/dt. As the aim of a low head siphon system is to increase the air flow to the maximum possible, this situation is unlikely to occur in a real system.

The white arrow shows the bubble that has been detached from the nozzle.

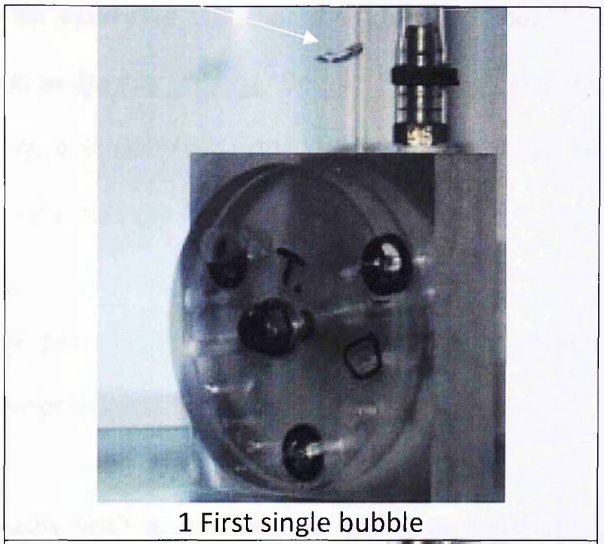

1 First single bubble

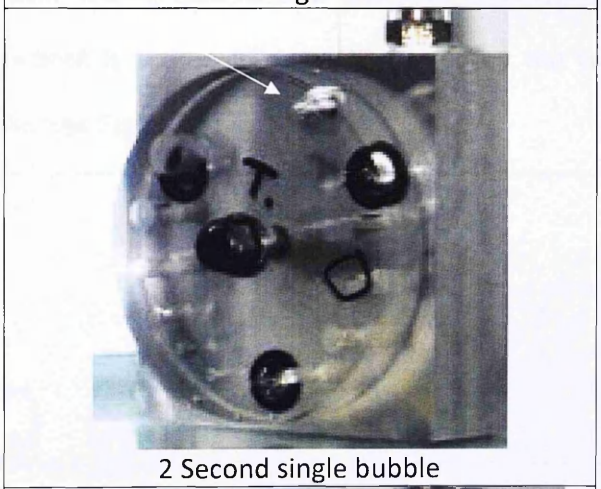

2 Second single bubble

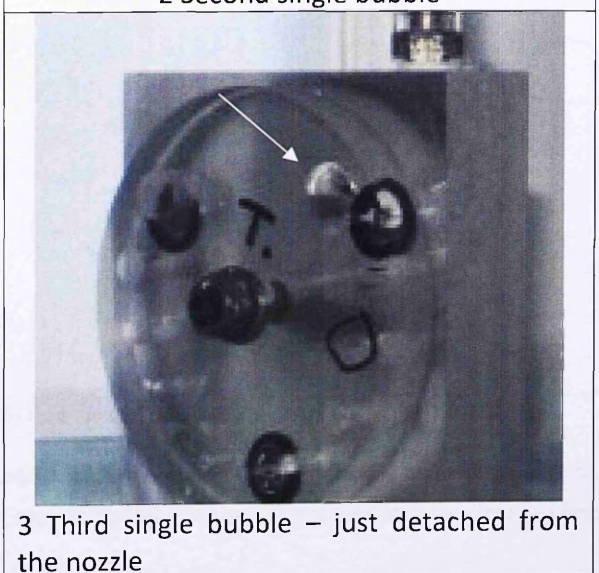

3 Third single bubble – just detached from the nozzle

Figure 5.7 Single bubble formation

McCann (1971) has made an extensive study of the 'delay' of bubble detachment. He identified this phenomenon as Bubble Pairing, Double Bubbling, and the combination of pairing and double bubbling, e.g. double pairing, triple, or quadruple bubbling, which is a common happening in a very high gas flow rate.

Bubble pairing occurs when the second single bubble merges with the first bubble. This occurs only when the chamber volume is large.

Bubbling frequency increases with a decrease in chamber volumes. Double Bubbling occurs when the second bubble is sucked into the first one and the two bubbles then merge as one bigger bubble. See Fig. 5-8.

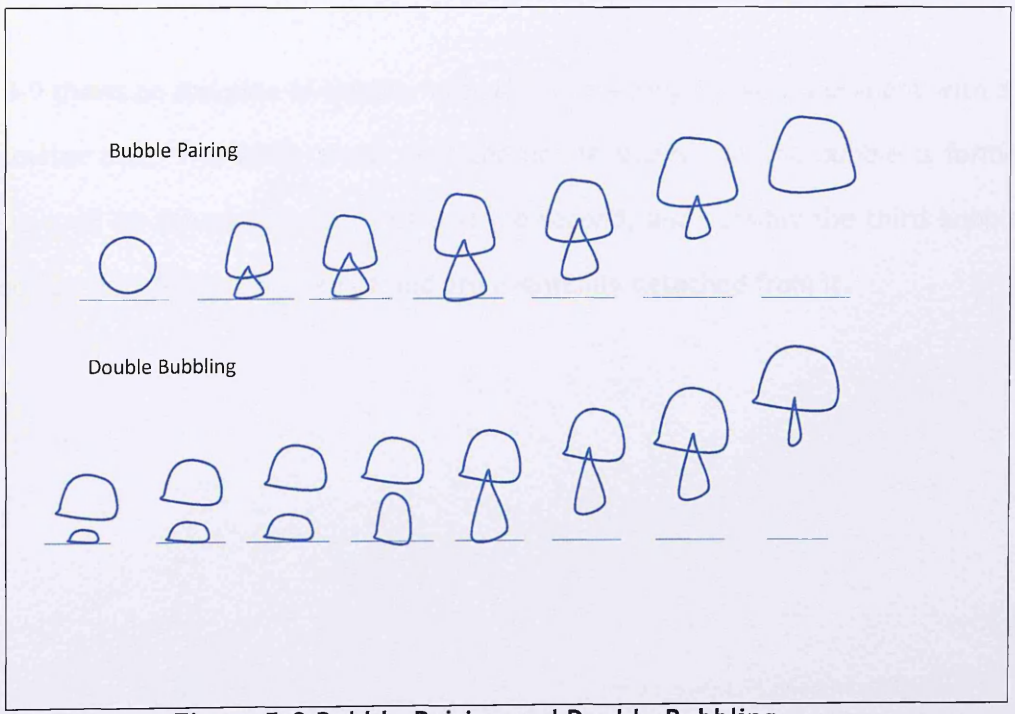

Figure 5.8 Bubble Pairing and Double Bubbling

(bubble pairing= second bubble touches the first bubble straight away when it is still on the nozzle plate, double bubbling= second bubble touches the second bubble after leaving the nozzle)

Under normal conditions, there are three types of bubble regimes commonly known, i.e. static regime, dynamic regime and turbulent regime. Static regime occurs when the gas flow rate is very small, the bubble volume remains constant and the bubble frequency is directly related to the gas flow rate. In a dynamic regime, bubble volume and frequency increase with increase in gas flow rate. (McCann, 1971).

In a turbulent regime which occurs when there is a very high gas flow rate, double pairing, triple, or quadruple or multiple bubbling types are formed. It is unstable and different bubble types appear randomly in any sequence. In this regime, bubbles are produced more frequently and these bubbles coalesce in a random pattern and create irregular shapes.

Figure 5-9 shows an example of bubble formation in the single-hole experiment with a 2 mm diameter hole. The white arrow near the nozzle shows how the bubble is formed and developed on the nozzle. The first and the second, and possibly the third bubbles attached to each other on the nozzle and are eventually detached from it.

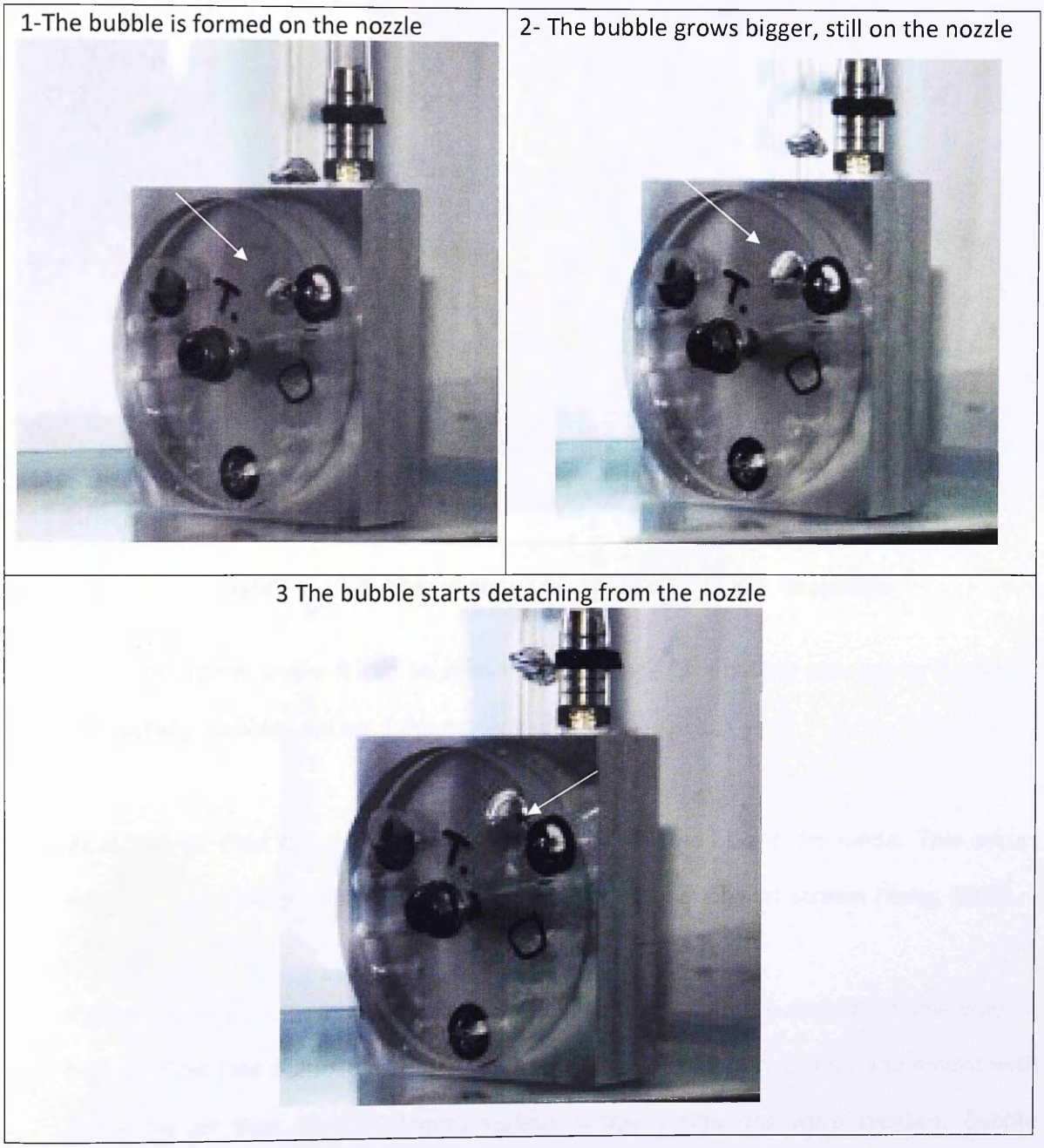

Figure 5.9 Multiple Bubble formation on the nozzle

Figure 5.10 Bubble changes its shape on the way to surface

From the figures above it can be seen how the shape of a bubble changes as it rises to the surface. Bubbles did not form perfect spherical shapes.

At a high air flow rate, the air injection regime may well be in jet mode. This occurs when surface tension controls the stability and breakup of the jet stream (Yang, 2001).

Figure 5-11 (a)-(c) shows an example of bubble formation in a turbulent regime when a high air flow rate occurs. For the various different holes (2 mm, 3 mm, and 4 mm) with the same air flow rate (16 l/min) various bubble formations were created. Bubble pairing occurred and this was followed by multiple bubbling.

The white arrows show the bubbles on the nozzle forming a jet stream before detachment.

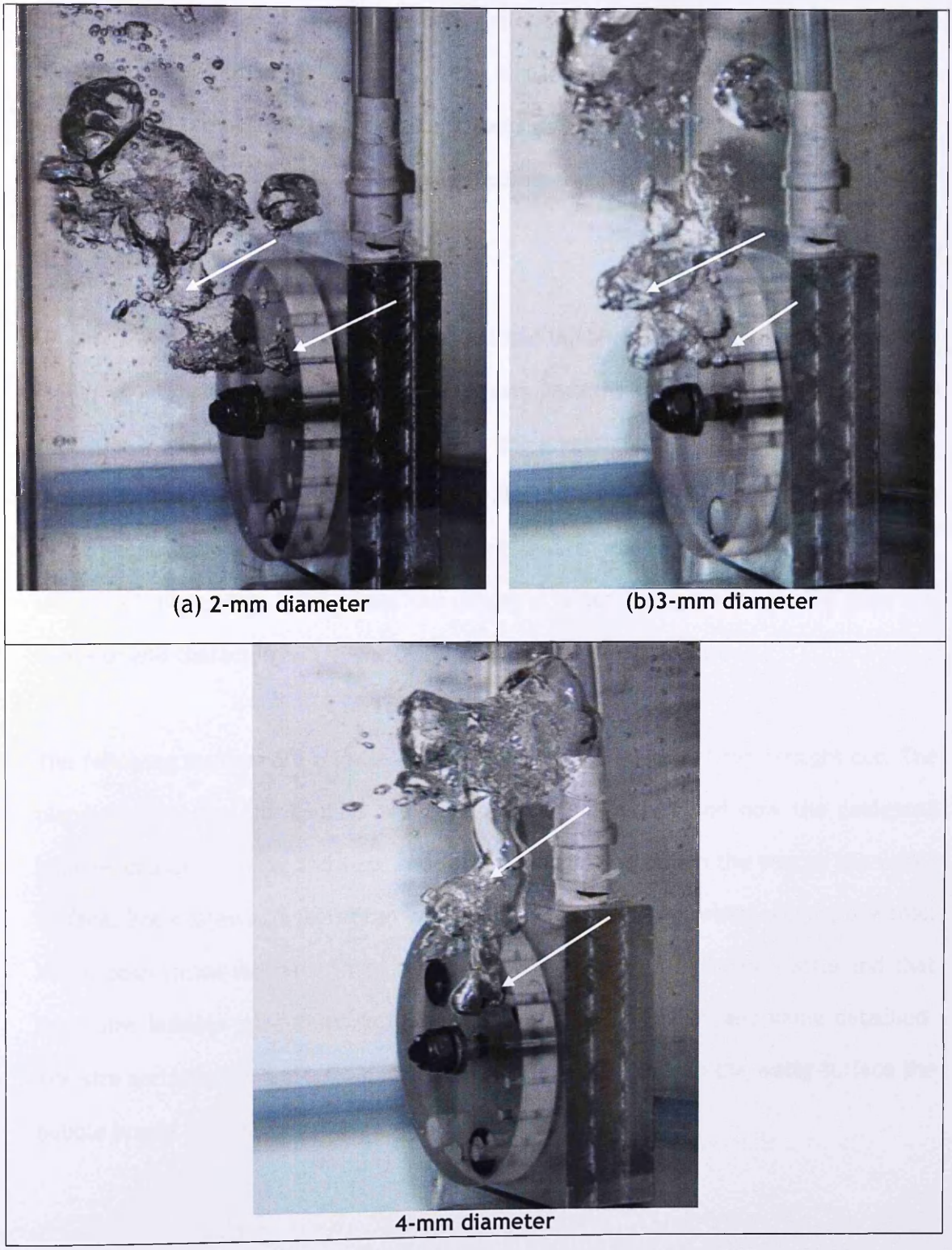

Figure 5.11 Bubble Formation in turbulent regime

It can be seen that with a 4 mm diameter hole, the delay in detachment is longer and multiple bubbling occurs. The stem is wider and longer compared to the smaller nozzle diameters. Visual observations indicate it looks as if a continuous jet mode of air flow comes out from the nozzle, then it is detached and forms a large irregular shape of coalesced bubbles.

On the way up to the water surface, the multiple bubbling form breaks into smaller size bubbles that may re-coalesce again into random patterns and shapes. At a high air flow rate, the bigger the diameter of the nozzle, the longer and bigger the jet stream of air that is formed (see figure 5-11, a, b, c). This means there is a longer delay in the detachment stage. Yang et al (2001) stated that on the vertical surface it remains unclear of how and to what extent the different forces acting on the bubble alter the behavior and characteristics of the bubble growth and detachment.

The following pictures are a series of shots of the orifice with a 3 mm straight cut. The pictures show how the bubbles are developed and detached and how the coalesced bubbles change in shape and size, and form a random pattern on the way to the water surface. The coalesced bubbles can break and re-coalesce again whilst moving upwards. Visual observation indicates there is a continuous jet stream from the nozzle and that large size bubbles are formed in multiple bubbling before eventually being detached. The size and shape of the bubble is not always the same. Close to the water surface the bubble breaks into smaller sizes.

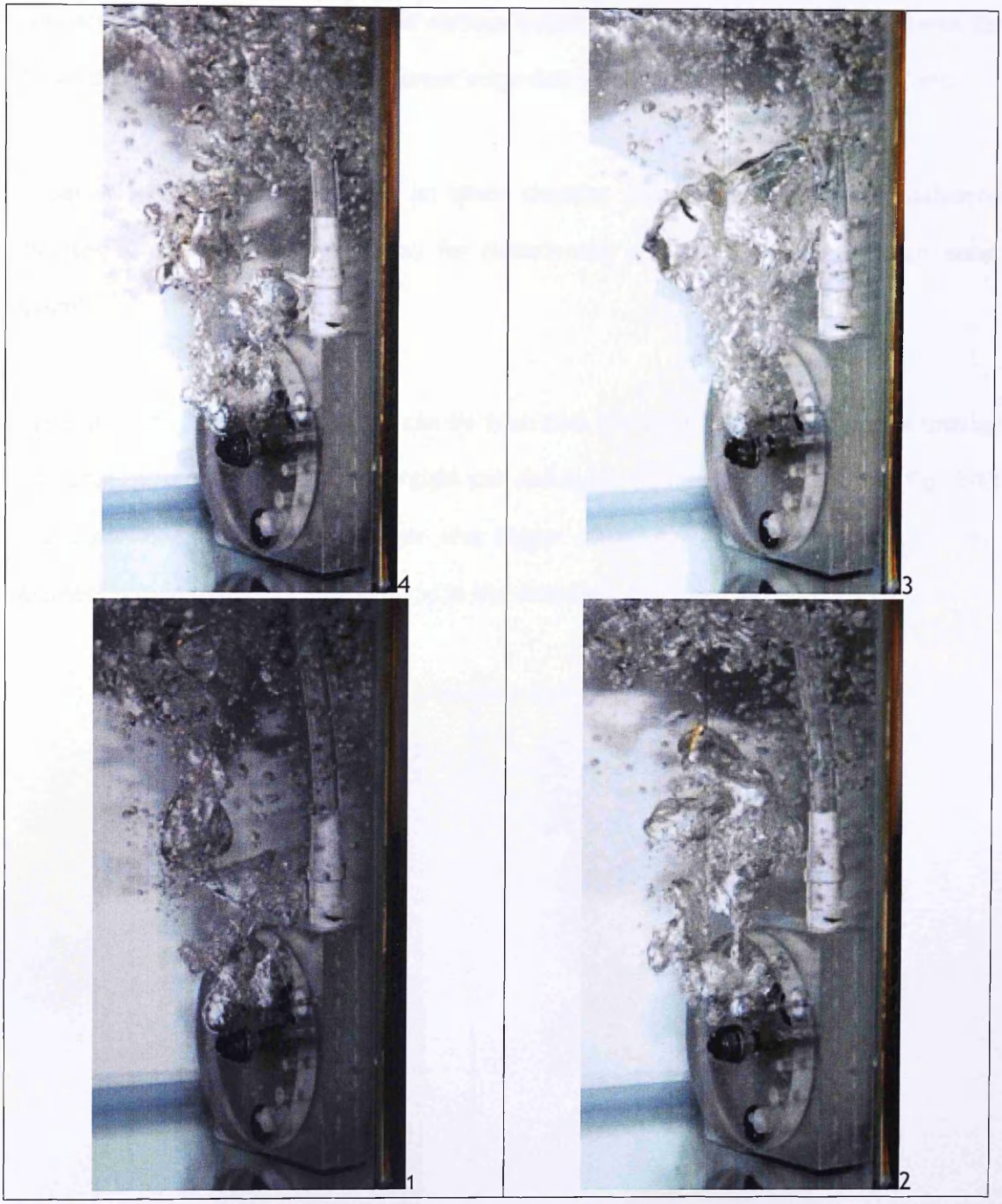

Figure 5.12 Series of Bubble formation in a second shot (3mm straight cut diameter)

The bubble formation is also determined by the shape of the edge of the orifice, depending on whether it is straight cut, or a hole with an inner chamfer or an outer chamfer. For the same diameter size, different random pattern due to different edge

cuts are visible. Figures 5-13 shows various bubble formations and random patterns for 3-mm diameter holes with the different edge cuts when the air flow rate is 14 l/min.

Visual observation indicates that an inner chamfer nozzle creates smaller coalesced bubbles with a shorter time delay for detachment compared to one with an outer chamfer.

For the 3 mm diameter orifice, it can be seen that the inner chamfer cut forms smaller size coalesced bubbles than the straight cut and outer chamfer. If, as shown in Fig. 5-13 the outer chamfer forms a longer and bigger stem, similar to 4 mm straight cut diameter, then there is a longer delay in the detachment stage (see Figure 5-11).

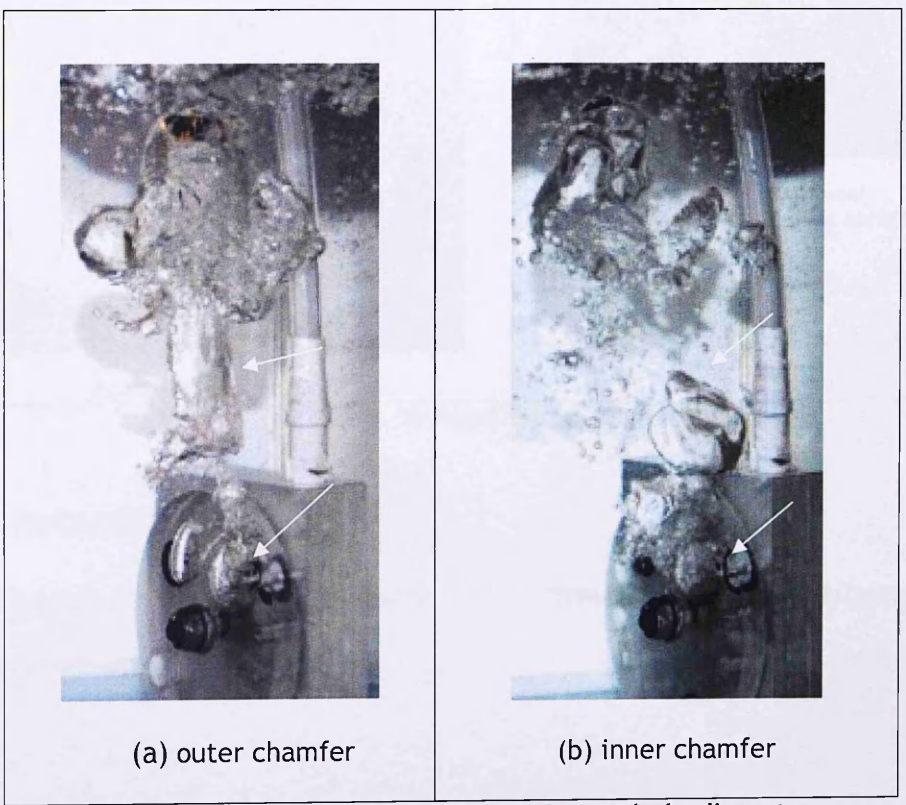

(a) outer chamfer (b) inner chamfer

Figure 5.13 Bubble formation - 3- mm hole diameter

Observation of the flow pattern and the bubble formation around the nozzle for multiple hole aerators as used in the siphon system, will be described in Chapter 7.

5.3. Air pressure loss

The air pressure drop during aeration is measured using a U-tube manometer, Fig 5-14.

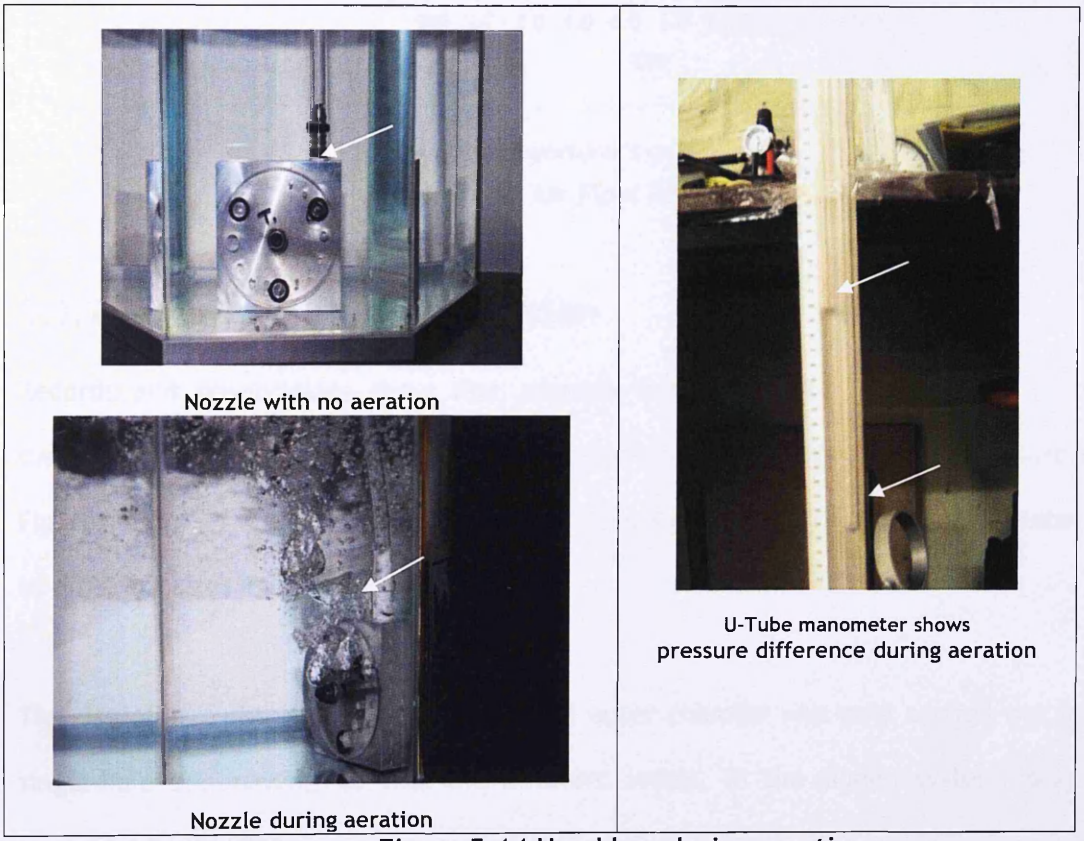

Figure 5.14 Head loss during aeration

5.3.1 Rotameter reading

The rotameter scale reads in cm, and this is converted into flow rate (l/minutes) using the conversion chart, Figure 5-15.

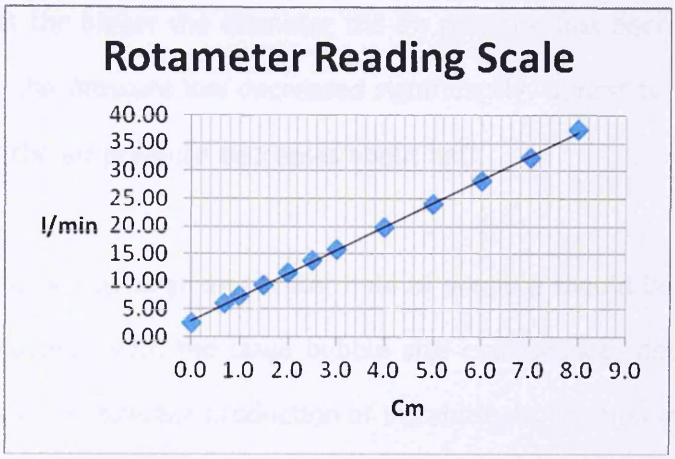

Source: Manufacturer's calibration

Figure 5.15 Air Flow Rate Chart

5.3.2 Air pressure loss observation

Records and observations show that pressure loss decreases with increase in inlet diameter. It was also found that using an inner chamfer will reduce the pressure loss. Figures 5-16, 5-17, and 5-18 show the pressure loss due to air release into the water due to different sizes and cuts of inlet holes.

The use of straight cut, inner chamfer and outer chamfer was only carried out in the single-hole experiments to find the different losses. In the siphon system, only the straight cut was used.

Air flow through rotameter (in l/s) against air pressure loss (in N/m^2) is shown in Figures 5-16 to 5-18 for various diameters size, 2 mm, 3 mm and 4 mm. These graphs also show the different air pressure loss for the same diameter size with different cut, i.e. sharp cut, inner chamfer and outer chamfer.

It can be seen that the bigger the diameter the air pressure loss decreases. From 2 mm to 4 mm diameter the pressure loss decreased significantly, almost ten times. From 3 m to 4 mm diameter the air pressure decreases about half.

Thus to minimize losses, as large an aerator hole as possible should be used, provided it does not cause problems with the large bubble size coalescence, delayed detachment from the nozzle, and the possible production of instability of the siphon flow continuity.

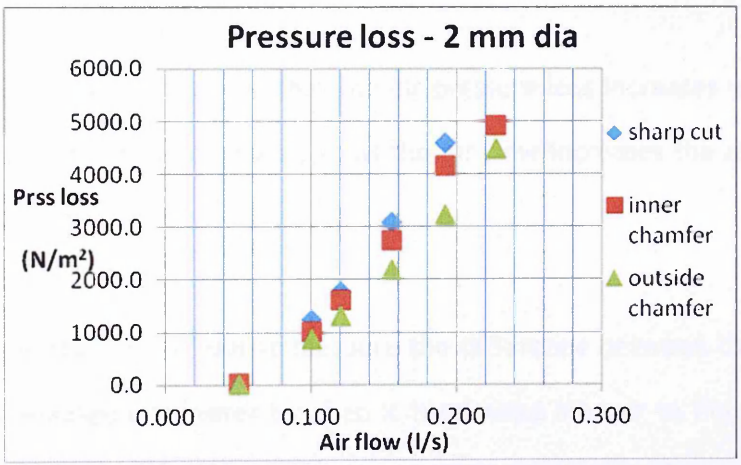

Figure 5.16 Air pressure loss for 2 mm inlet diameter

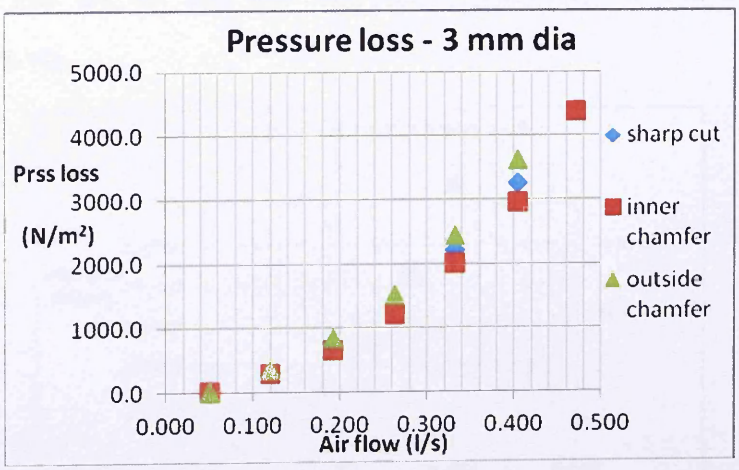

Figure 5.17 Air pressure head loss for 3 mm inlet diameter

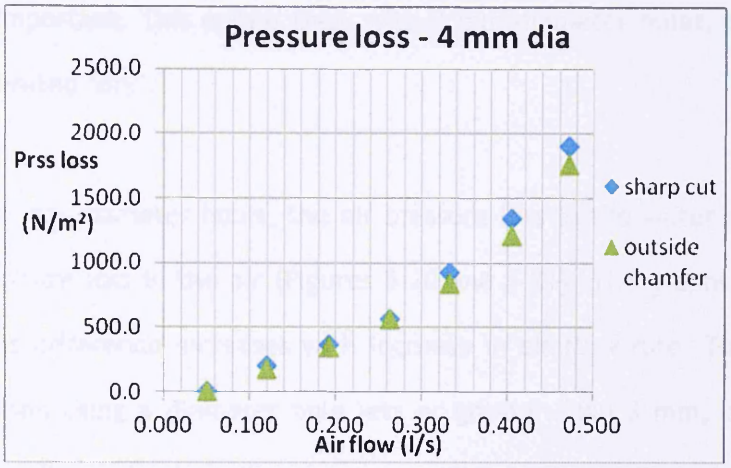

Figure 5.18 Air pressure head loss for 4 mm inlet diameter

From the graphs it also can be seen that the air pressure loss increases with increase in air flow. The relationship is not linear, so as the air flow increases the air pressure loss increases exponentially.

Experiments were also carried out to measure the difference between the pressure loss when the air is released into water to when it is released into air to find out how much difference. It was found that there was not very much difference of pressure loss due to release of air into the air and into the water, especially for the 3 mm diameter orifice.(Figure 5-19).

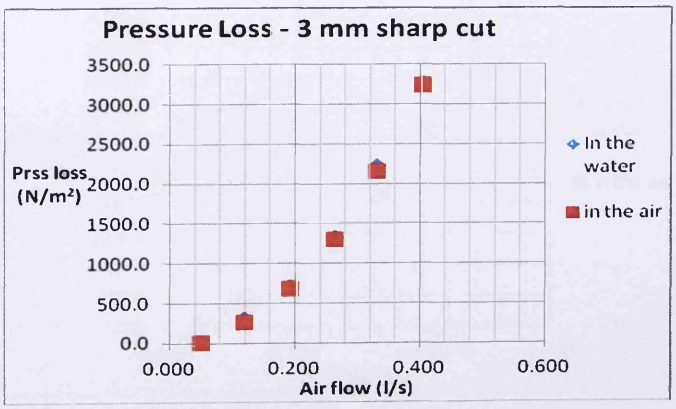

Figure 5.19 Pressure loss difference in the water and in the air - 3 mm

This finding is important. This means that, with 3 mm diameter holes, the air pressure loss can be calibrated 'dry'.

For 2 mm and 4 mm diameter holes, the air pressure loss in the water is slighty higher than the air pressure loss in the air (Figures 5-20 and 5-21). The graphs also show that the pressure loss difference increases with increase in air flow rate. Thus it has to be kept in mind when using a diameter hole less or greater than 3 mm, especially when applying a higher flow rate, that the air pressure loss is about 10% higher in the water than in the air for 4 mm hole diamater, and about 20% for 2 mm hole diameter.

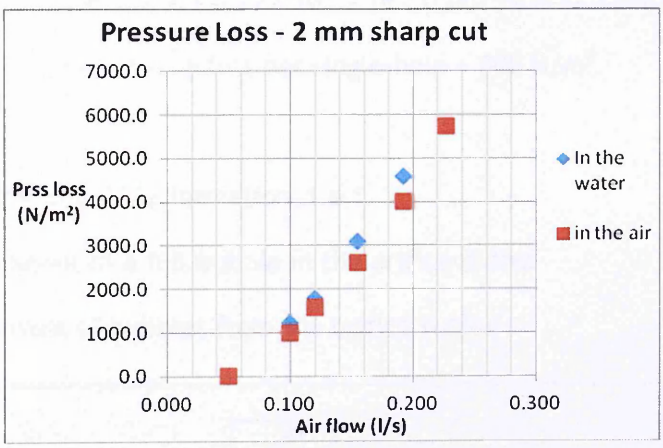

Figure 5.20 Pressure loss difference in the water and in the air - 2mm

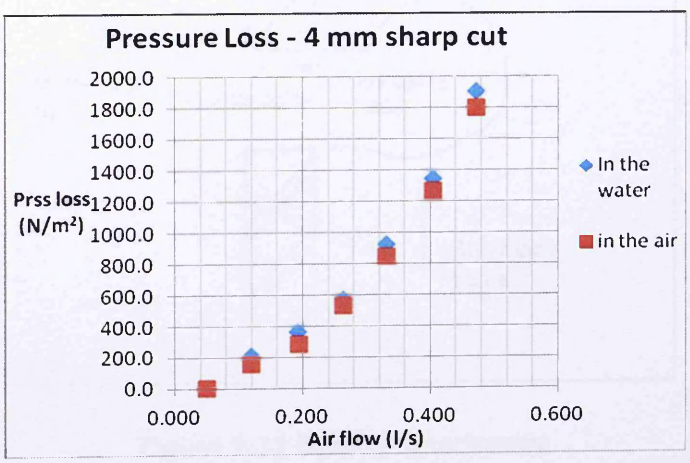

Figure 5.21 Pressure loss difference in the water and in the air - 4mm

5.4 Theoretical Calculation of Bubble Formation

In the siphon experimental rig, 3 mm diameter of straight cut sparger holes were used. The maximum air flow rate for aeration in the siphon (See Chapter 6) was approximately 600 l/min. There are 44 holes in the spargers. Assuming that the air flow rate is equally distributed to the 44 holes, thus the air flow rate for single hole:

$Q_{\text{single hole}}$ = (600 l/min)/44 = 13.636 l/min = 0.227 l/s = $0.227*10^{-3}$ m^3/s .

$(Q_{\text{single hole}})^2$ = $(13.636)^2$ = 185.95 $(l/min)^2$.

Air velocity for single hole = Q/A = $0.227*10^{-3}$ / (π * 0.0015^2) = 32.13 m/sec.

Refer to Fig 5-17, for the pressure loss per single-hole ≈ 800 N/m^2.

There are two stages in bubble formation, i.e.:

1) The development of a full bubble in the orifice outlet
2) The detachment of bubbles from the orifice outlet

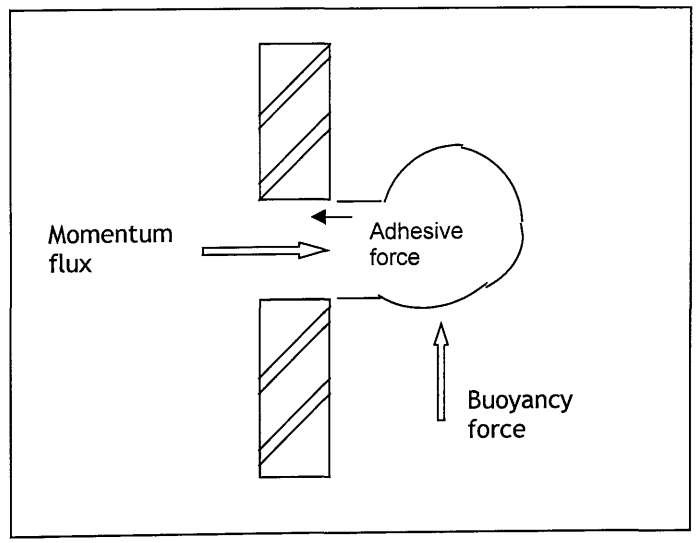

Figure 5.22 Bubble detachment

There are several forces working on bubble formation and detachment which need to be considered: Buoyancy force, Surface tension (adhesive) force, Momentum flux, Drag force, and Inertia force. The buoyancy force is the dominant force causing the detachment of the bubble from the orifice (Nahra and Kamotani, 2002). Bubble diameter decreases with increasing superficial fluid flow (Bhunia et al, 1998). The superficial fluid flow is the flow that occurs when no air is being injected (single phase).

In a turbulent regime when the gas flow rate is high, two bubbles frequently coalesce close to the orifice. These irregular bubbles rise in a rapid swirling motion and inertial forces become very high (Leibson in Mc Cann, 1970). The bubble volume increase is in proportion to the gas flow rate (McCann, 1970).

Buoyancy force:

$$F_B = V_B (\rho_w - \rho_a) g \qquad (5\text{-}1)$$

As the air density is relatively small compared with water density the later can be neglected. so

$$F_B = V_B \rho_w g \qquad (5\text{-}2)$$

Adhesive Force:

$$F_a = \pi (D_O) \sigma \qquad (5\text{-}3)$$

Momentum flux of gas

$$F_M = \rho_a (Q_a)^2 / [(\pi/4) (D_O)^2] \qquad (5\text{-}4)$$

Number of bubbles formed in a unit time is:

$$N_B = Q_a / V_B = Q_a / [(\pi/60/ (D_B)^3] \qquad (5)$$

Where:

V_B is volume of single bubble

D_B = diameter of bubble

D_o is hole diameter = 3 mm = 0.003 m

Q_a is air flow rate = 0.227 l/s.≈

ρ_w is water density = 1000 kg/m^3

σ is surface tension ≈ 7.4 * 10^{-2} N/m, at 10°C-20°C (Munson et al, p831).

5.4.1 Force Calculations

As the bubble diameter is the same or greater than the sparger diameter (D_O):

Adhesive force (Equation 5-3): $F_a = \pi * 0.003 * 74*10^{-3} = 6.97*10^{-3}$ N

Buoyancy force will have an effect in detaching the bubble if $F_B \geq F_a = 6.97*10^{-3}$ N

Bouyancy force (Equation 5-1): $F_B = V_B \rho_w g = 6.97*10^{-3}$ N →

$$V_B = 6.97*10^{-3} / (1000* 9.81) = 7.1 * 10^{-7} \text{ m}^3$$

$$= 0.71 \text{ cc}$$

Bubble volume = $V_B = [(4/3) * \pi r^3] = 0.71 \rightarrow r^3 = 0.71/[(4/3) * \pi]$

$r^3 = (0.71 * 3)/(4 * 3.14) = 0.17$ cm → r = 0.55 cm

D_B = 1.1 cm = 11 mm

The calculation above is based on a dynamic regime, where each bubble can be treated as a separate object (McCann, 1971), i.e. bubbles may be considered independently of one another (Buyevich and Webbon, 1996).

Observation showed that the diameter of a bubble near to the surface was greater than 10 mm. On the nozzle, the injected air appeared to form a jet stream before the bubbles were detached and formed into coalesced bubbles (See Figures 5-11, 5-12, 5-13).

For $Q_a = 0.227 * 10^{-3}$ m/s, number of bubble formed per unit time, N_B:

$N_B = Q_a / V_B = 0.227 * 10^{-3}/(7.1* 10^{-7}) = 320/sec$

$F_M = \rho_a (Q_a)^2/[(\pi/4) (D_O)^2$

Momentum flux of gas (Equation 4): $F_M = \rho_a (Q_a)^2/[(\pi/4) (D_O)^2]$

$= 0.0012 (0.227 * 10^{-3})^2/[(3.14/4) (0.003)^2$

$=8.75* 10^{-6}$ N

F_M is relatively small compared to surface tension, but it contributes to detaching bubbles.

5.5 Findings and Results

The experiment showed that a very high air flow rate produces multiple pairing and bubbling with a delayed detachment stage. This is characteristic of the higher gas velocity (McCann, 1971) when it may form into a jet stream.

Based on the above calculations the bubble diameter was 11 mm. The calculation was based on the dynamic regime, where bubbles are considered independent of one another.

Visual observation showed that close to the surface the bubble diameter was greater than 10 mm.

Based on the results from the single-hole experimental rig in still water, and using Fig 5-19 for a 0.227 l/sec air flow rate and for the 3 mm hole diameter, the pressure loss for single hole = 800 N/m^2.

In the siphon rig experiment, the two phase flow is vertically downward, so other elements of loss need to be taken into account. These are losses due to a bubble development zone in the downward leg siphon, the force required to break the coalesced bubbles, and the stream of air flow out from the nozzle (spargers) into single and smaller bubble sizes that creates a relatively dispersed bubbly pattern. There may also be an hydraulic jump effect.

5.6 Conclusion

This single-hole experimental rig has indicated how much pressure loss occurs in the formation and detachment of bubbles into the water chamber. It also showed that the higher air flow rate produced not just single, but multiple bubbling with delayed release. This appeared like an air jet stream before it detached from the nozzle and created random irregular shapes and sizes of bubbles.

Single bubble formation occurs only when there is a very small air flow rate (below 2 l/min for 2 mm nozzle diameter). Thus to create a bubbly flow pattern directly from the nozzle, nozzle diameter must be much smaller than 2 mm. In practice a smaller nozzle diameter will cause a large pressure loss (See Figures 5-16, 5-17, 5-18). Thus it is impractical to use such holes in the siphon system aerator.

Based on these experiments some points can be concluded with regard to pressure loss when a bubble is released into water:

- The bigger the diameter of the orifice, the less the pressure head loss needed to release the air into the water. This finding is useful when deciding what diameter will be used to design the aerator for the siphon experimental rig.
- With regard to the edge of the orifice, the inner chamfer cut produced less head loss than the straight cut and the outer chamfer cut. However it is not practical to make the sparger holes with inner cut chamfers.
- Overall, the pressure loss when using orifices with diameters of 3 mm or 4 mm is relatively small compared to that when a 2 mm diameter hole is used.
- There is very little difference in the pressure loss that occurs when a bubble is released into either air or water.

Chapter 6

Low-head hydro with aeration

6.1 Introduction

This chapter describes a laboratory experiment of low head hydropower generation using an aeration system with the intention of determining its performance. The research investigates the performance of selected aerator design to find which one has the best power output and efficiency.

There were two stages in this experiment. The first stage investigated aeration using a pumped system. In this stage three different aerator designs were tested. The aim was to find out the maximum air flow rate and the maximum void fraction that can be achieved by each aerator.

The second stage was a similar test using a natural siphon. Two versions of this experiment were carried out. One had the highest point of the siphon at the down leg part ($y_{A=}$ 3.5 m) than the other (y_A= 4.7m). The higher siphon had a larger suction pressure at its high point and this produced more power. As with the pumped system the aim was to establish the highest air flow rate before the siphon breaks, and to find the maximum void fraction that can be achieved. Based on the measurement of water flow,

air flow and the air pressure, the power output was calculated. The efficiency of the aerator was calculated by finding the ratio of the power output to the power input.

6.2 Aeration using a pumped system

The pumped system experiment was done to focus on the aeration process while avoiding the difficulties of creating a natural siphon that could break. With a pumped system, the water flow can be continuously maintained.

The behavior of the air inlet section is exactly the same in the pumped system as it is in the natural siphon system.

Figure 6-1 Rig using Pumped System

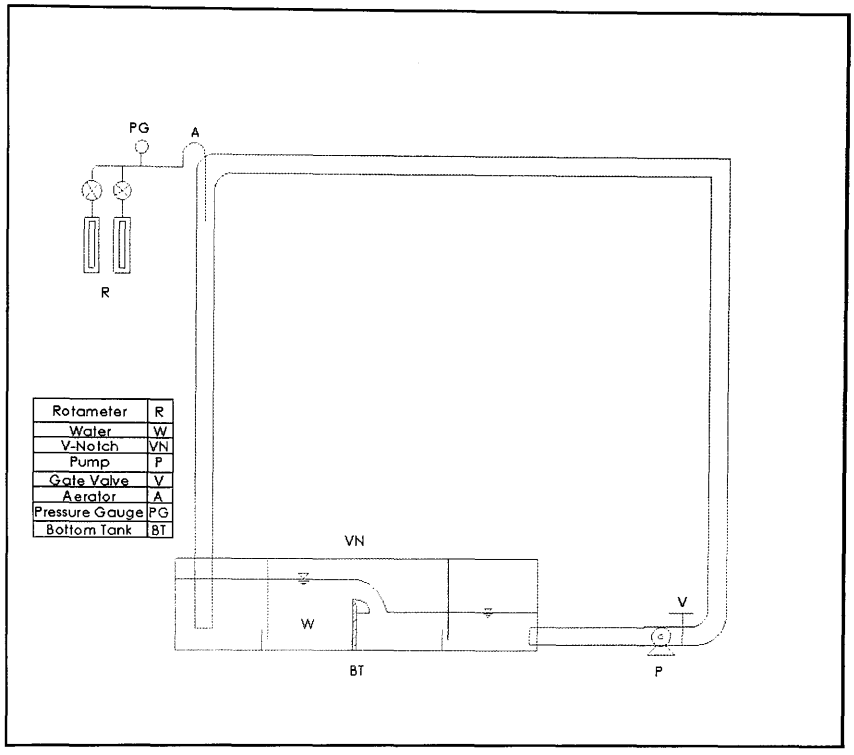

Figure 6-2 Schematic diagram of a pumped system

With the water flow initiated, air at atmospheric pressure passes through a rotameter and is induced into the flowing water through one of the various aerators. A valve was put between the rotameter and the aerator to control the air flow rate. Starting from zero aeration, the air flow was gradually increased until it reached the maximum rate that could be achieved before the siphon broke.

Three types of aerator design were tested, i.e.:

1. Aerator-1 - Copper tube spargers
2. Aerator-2 - Ring spargers using an air chamber
3. Aerator-3 - Horizontal spargers using an air chamber

Chapter 3 section 3.5 gave the detailed design of the aerators.

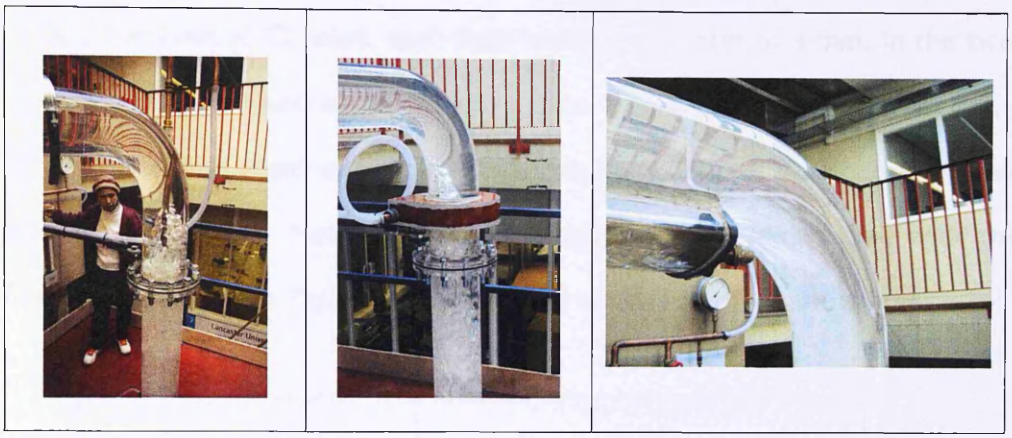

Figure 6-3 Three types of aerators design

6.2.1 Aerator 1 - Copper tube spargers

The copper tube spargers have a diameter of 20 mm, located near the top of the down pipe. There are three lines of holes along the copper tube, each of 3 mm diameter. The top hole is approximately 200 mm below the horizontal pipe level (See detailed design in section 3.5). Figure 6.4 shows the Copper tube sparger and the detail of the small holes.

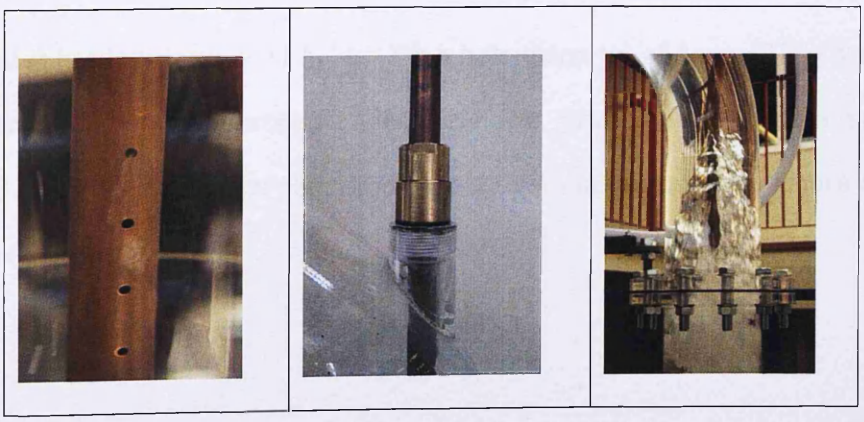

Figure 6.4 Aerator1 showing sparger details

6.2.2 Aerator 2 - ring spargers with an air chamber

These have two lines of 22 holes, each hole having a diameter of 3 mm, in the two ring spargers around a cross section of the down pipe (See detailed design in section 3.5). The air chamber is to disperse the air with a relatively uniform distribution, speed and pressure (Dhotre, 2006). Figure 6-5 shows a picture of the down pipe with the air chamber. As shown in this Figure the air inlet did not directly face the sparger holes.

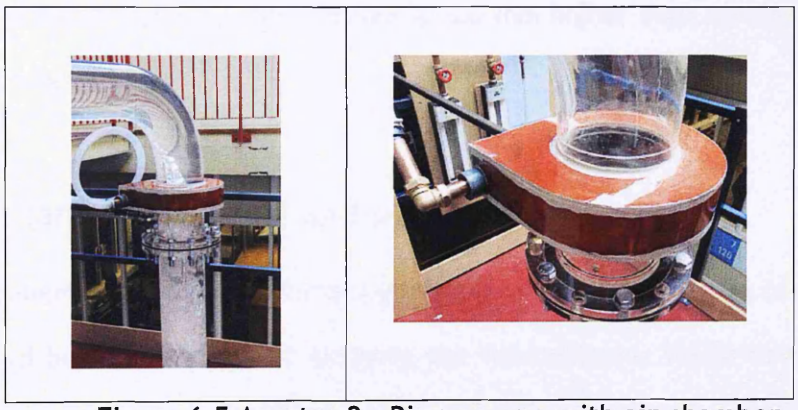

Figure 6-5 Aerator 2 - Ring sparger with air chamber

6.2.3 Aerator 3 - horizontal aerator using an air chamber

This aerator has four lines of 11 holes with a hole diameter of 3 mm. They are located at the bottom part of the horizontal pipe near the down pipe (See detailed design in section 3.5). The air chamber formed an arc shape around the pipe. Figure 6-6 shows a picture of Aerator 3.

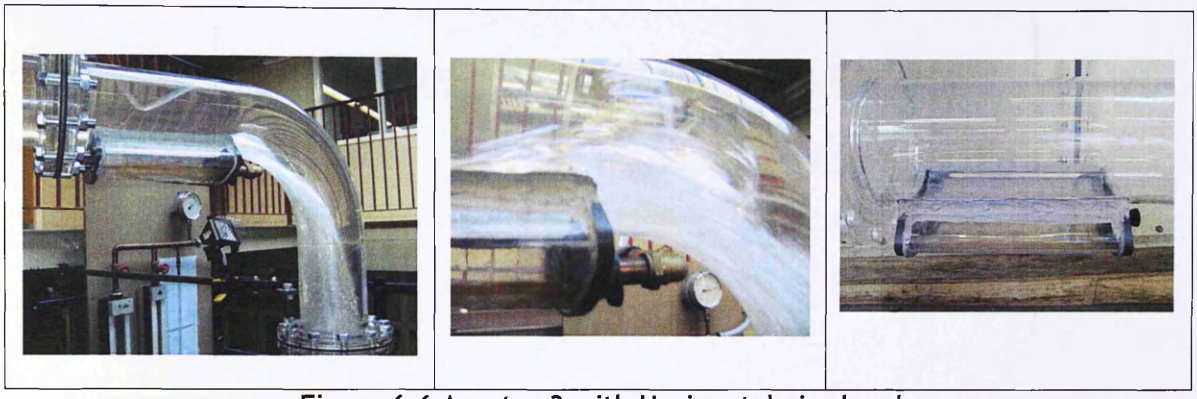

Figure 6-6 Aerator 3 with Horizontal air chamber

Aerator 3 was the highest at approximately 200 mm higher than Aerator 1, and 400 mm higher than Aerator 2.

6.2.4 Rotameter reading and observation

The experiment using the pumped system was focused on finding the maximum aeration which could be achieved and on studying the flow pattern. Water in the storage tank was pumped up the vertical PVC pipe, then it flowed through the horizontal transparent pipe and into the vertically downward transparent pipe. For the first test the air entered the water through the copper pipe sparger holes. The water flow rate was measured using the V-notch weir and the air flow rate by the rotameter. Various combinations of water flow rate and air flow rate were used in the tests.

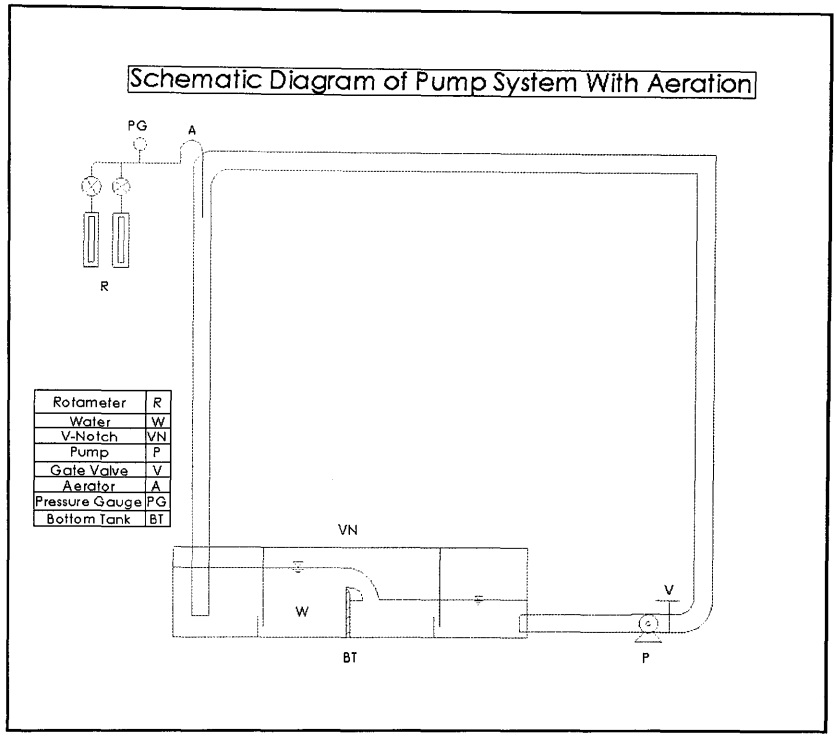

Figure 6-7 Aerator-1 in Pumped System

Initially a water flow rate was set and then air at atmospheric pressure was gradually induced into the pipe after passing through a rotameter. The air flow was adjusted and controlled by a valve. Two rotameters were used in parallel, the small one measured airflow rates up to 200 ml/min, and the larger one measured air flow rates up to 1000 ml/min. A pressure gauge was installed between the rotameter and the inlet of the aerator to measure the pressure at this location.

Three different initial water flow rates were used in the pumped system experiment. These were set by a control valve. Water was pumped into the fourth chamber of the tank (See Fig., 3-3 and 3-4). Once the water flow was stable, the reading of the water level above the V-Notch was recorded and converted to the flow rate using Figure 4-2.

Initially the water flow rate was set at 52.5 l/s. Gradually the rotameter valve was opened and air entered into the water flow. Water flow rate, air flow rate and the pressure gauge readings were recorded. This continued until the rotameter valve was fully opened and the reading reached its maximum. Then the water flow rate was set at 57.5 l/s and the above procedure completed for this rate. Then again it was completed for the 62.6 l/s flow rate.

Observations showed that as air is introduced into the system the water flow rate decreased. (See Figs. 6-9, 6-10 and 6-11) This was clearly visible in the free siphon experiment by an increase in the water level in the top tank (see Fig. 3-2) especially when the siphon is almost broken.

From the above readings, the void fraction was calculated.

6.2.5 Void fraction calculation

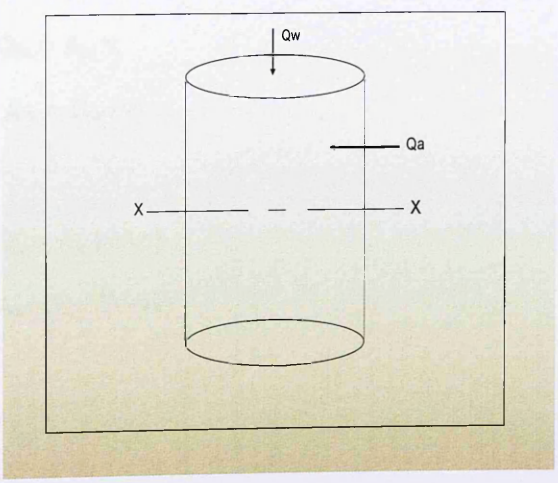

Figure 6-8 Schematic mixed flow in the tube

Below the sparger the water with velocity (v) in the vertical direction is mixed with the air entering from the orifices in the copper spargers. Due to **buoyancy** the air bubble will drift upwards with a drift velocity relative to the water of vs. Thus the actual air bubble velocity is (v-vs).

If the areas of pipe occupied by air and water are A_a and A_w, respectively, the void fraction (α):

$$\alpha = A_a/(A_a + A_w) = A_a/A_p \qquad (6.1)$$

where:

A_p = area of pipe cross section.

α = void fraction, volumetric ratio of air to mixed air and water

A_a = cross section area occupied by air

A_w= cross section area occupied by water

Volume flow rates for water and air:

$$Q_W = A_W v \qquad (6.2a)$$

Or, $A_W = Q_W/v$

$$Q_a = A_a (v\text{-}vs) \qquad (6.2b)$$

Or, $A_a = Q_a/(v\text{-}vs)$

Where:

Q_W = water flow rate

v = water velocity

vs = drift velocity

Here, the volume flow rate of air (Q_a) is the local value at level X-X (Fig. 6-8). As the pipe is short, it is assumed that Q_a has the same value as at the inlet, the value given by the rotameter.

Thus

$$v = Q_w/A_w = Q_w/(A_p-A_a) = Q_w/\{A_p-(Q_a/(v-vs)\} \qquad (6.3)$$

Rearranging the equations above gives:

$$v^2-(vs+(Q_a+Q_w)/A_p)v+(vsQ_w)/A_p)= 0 \qquad (6.4)$$

The assumption was made that Q_a and vs were constant in the down pipe; and that the drift velocity would be vs=0.24 m/sec (taken from Rice, 1976 in French Widden, 2001).

With pipe diameter = 0.2 m, the cross sectional area of the pipe (A_p) is:

$$A_p = \pi \times 0.1 \times 0.1 \text{ m}^2 = 0.0314 \text{ m}^2,$$

Thus Equation 6.4 becomes:

$$v^2- (0.24+(Q_a+Q_w)/0.0314)v+7.6433Q_w= 0 \qquad (6.5)$$

Since Q_a and Q_w were recorded from the experiment, then v could be calculated. To find the void fraction α, A_W and A_a were calculated and equation (6.1) was used.

Using this value of v, A_w and A_a were calculated from equation 6.2a and 6.2b, thus enabling the void fraction to be found from equation 6.1

6.2.6 Experimental findings and fresults

Figure 6-9 shows the relation between air flow rate, water flow rate and void fraction when the initial water flow rate is 52.5 l/s.

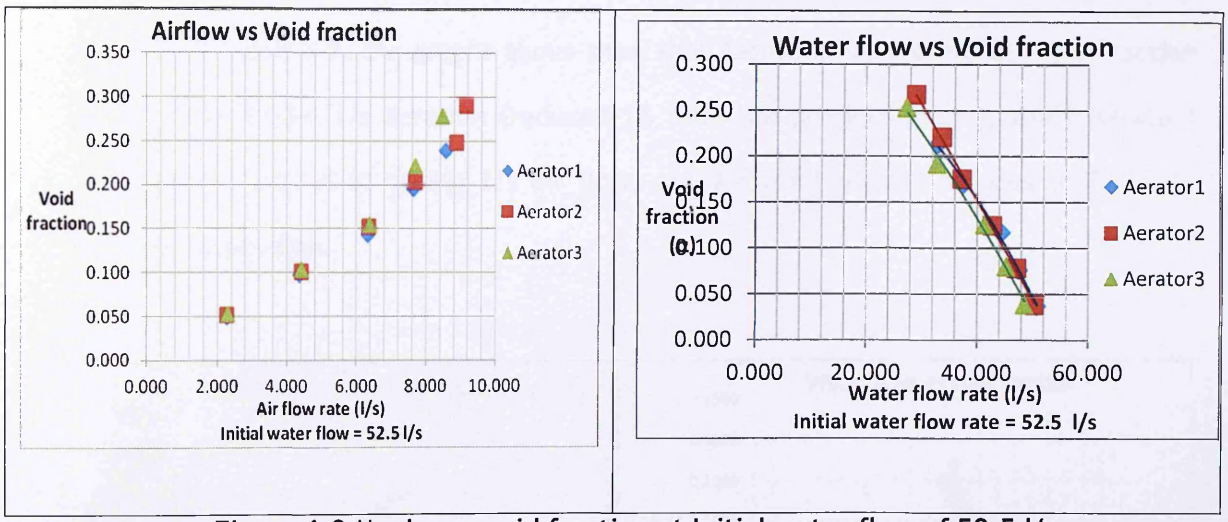

Figure 6-9 Maximum void fraction at Initial water flow of 52.5 l/s

When the air flow rate increases, the water flow rate decreases as is expected since the cross-sectional area in the pipe that is available for the water flow is reduced.

At the initial flow of 52.5 l/s, the graph above (Fig. 6-8) shows that Aerator2 produces the highest void fraction 29.1% at 9.153 l/s aeration, Aerator3 reaches 27.9 % at 8.458 l/s aeration and Aerator1 has the lowest value of 23.9% at 8.562 l/s aeration.

Figure 6-10 shows the void fractions for an initial water flow rate of 57.5 l/min.

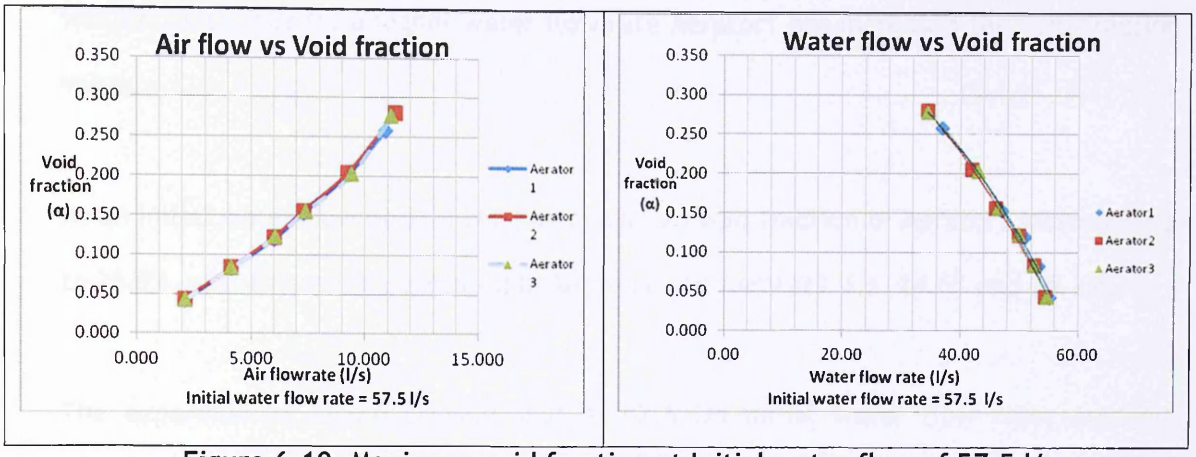

Figure 6-10. Maximum void fraction at Initial water flow of 57.5 l/s

Similar to Figure 6-9, the graphs above show that Aerator2 has the highest void fraction of 28.1% at 11.341 l/s aeration (reduced 1% from the previous graph), while Aerator1 increases to 25.7 % at 10.891 l/s air flow, and Aerator2 slightly reduces to 27.8% at 11.164 l/s aeration.

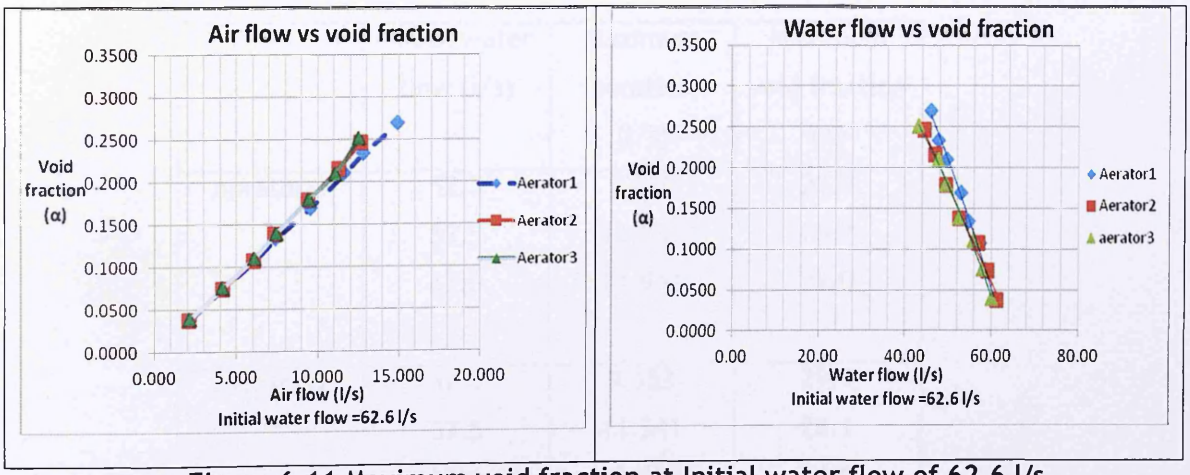

Figure 6-11 Maximum void fraction at Initial water flow of 62.6 l/s

At the initial water flow rate of 62.6 l/s, Aerator1 reached a maximum void fraction of 27.0%, 1.3% increase from the previous flow rates. Aerator-2 and Aerator-3 produced lower void fractions compared to the previous condition when the initial water flow rate

was 57.5 l/s. Thus for a higher water flow rate Aerator1 has increased the void fraction value.

At an Initial water flow of 62.6 l/s, the maximum void fraction of Aerator1 increased up to 26.9%, whilst its value decreased in Aerator2 and Aerator3, i.e. 24.6% and 25.13%

The experimental record showed that at 62.6 l/s initial water flow rate, Aerator1 achieved 14.941 l/s air flow, whilst Aerator 2 and Aerator-3 reached maximums of 12.629 l/s and 12.54 l/s respectively.

Table 6-1 shows the above data for different aerators.

Table 6-1 Maximum Aeration and Void Fraction for various Initial water flow rates

	Initial water flow (l/s)	Maximum aeration (l/s)	Maximum void fraction (%)
Aerator-1	52.5	8.560	23.9
	57.5	10.891	25.7
	62.6	14.941	27.0
Aerator-2	52.5	9.153	29.1
	57.5	11.341	28.1
	62.6	12.629	24.6
Aerator-3	52.5	8.458	27.9
	57.5	11.164	27.8
	62.6	12.540	25.1

As seen in Table 6-1 for Aerator1, the value of the void fraction increases as the initial water flow rates increases, whilst Aerator 2 and Aerator 3 show the opposite effect, i.e. the void fraction decreases as the initial water flow rate increases.

According to Jain (1988) and Joshi (2006) the void fraction will increase with the increase of water velocity up to a certain point and then it will decrease. This was an effect of the circulation that occurs when the water velocity is high and the flow is very turbulent. The circulation increases with an increase in water velocity and this will cause a decrease in void fraction to occur (ibid).

Appendices B-1a/b/c to B-3a/b/c show the detailed calculation of void fraction for each aerator with different initial water flow rates, i.e. 52.5 l/s, 57.5 l/s, and 62.6 l/s.

6.2.7. Conclusion

From the pumped system experiment it was found that at a very high air flow rate, Aerator1 was stable as indicated by the position of the rotameter pendulum, and that it produced the highest void fraction, 27%, at an air flow rate of 14.941 l/s aeration.

Aerator-2, at 12.629 l/s reached a 24.6% void fraction, and Aerator-3 at 12.54 l/s achieved 25.1% void fraction.

Since the intention of the experiment was to get the highest possible void fraction at full siphon flow, Aerator1 was selected for further investigation.

Also based on the experimental result from the pumped system, the natural siphon system focused on Aerator1.

It was expected that the maximum air flow rate using a pumped system would be higher than by using a natural siphon system, because the pumped system had an extra energy to pump the water flow in the pipe, so that more air suction can be produced. Also, in the pumped system, there was no 'siphon break' situation. The water flow kept running even though the rotameter valve was fully opened.

Observation showed that at full opening of the rotameter valve, the air flow reached up to a maximum between 750 l/min (Aerator 3) and 890 l/min (Aerator 1). Thus, in the pumped system, Aerator 1 produced the highest air flow. The similar performance was expected and occurred in the natural siphon condition, i.e. Aerator1 produced the highest air flow rate (see Section 6.4. and 6.5).

6.3. Site experiment

Part of the research work is to test how the siphon and the aerator work in the site experiment. Some surveys to find the suitable sites were conducted. To coordinate with the laboratory experiment, the sites must meet several criteria, i.e.:

- Enough driving head, i.e. at least about 2 m
- Accessibility
- Relatively clean water
- Security; to put and leave the equipment on the site
- Minimum cost, e.g. minimum extra civil work required
- Easy to get permission from the local authority

- If possible to be close to Lancaster

Several selected sites were visited as follows:

Heron Corn Mill

The weir is situated in River Bela at Beetham (Figure 6-12). The weir between the corn and paper mills is approximately 25m long. The fall over the main weir is about 4m. There is a fish pass on the left side of the weir on the downstream direction. It is a good location, about 30 minute driving from Lancaster, but the head is a little bit too high for a site experiment. Also it is in open area, so that it is not safe to leave all devices on site.

Figure 6.12 Heron Corn Mill Weir

(Source: http://www.visitcumbria.com/sl/heron-corn-mill/)

Staveley

The weir is about 2 m high, situated in the River Kent, behind a brewery factory and café (Figure 6-13). It is an ideal place and easy to access, and there will be somebody who can look after it. It needed to be discussed further with the owner.

Figure 6-13 Weir in Staveley

(Source: www.steveleymilyard.com ; www.geolocation.com)

Sedgwick-Kendal

The weir is about 1 m high, is located in River Kent near to the Caravan Park (Figure 6-14). Even though the place is easy to access, the head is too low for the site experiment.

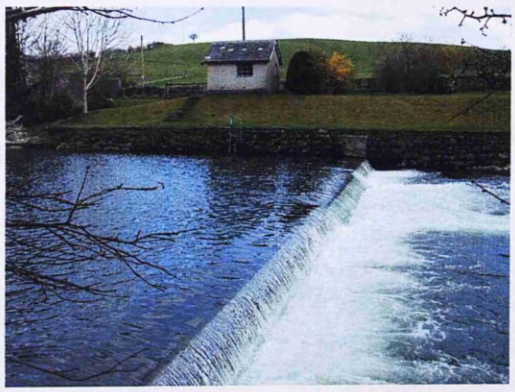

Figure 6-14 Sedgwick weir

Broad Raine Farm - Killington

The weir is situated in the River Lune on the north direction from Lancaster. The height of the weir is about 2 m (figure 6-15). It is a potential a place and easy to access and there is somebody there who is interested and willing to help to look after the siphon plant and to support site experiment.

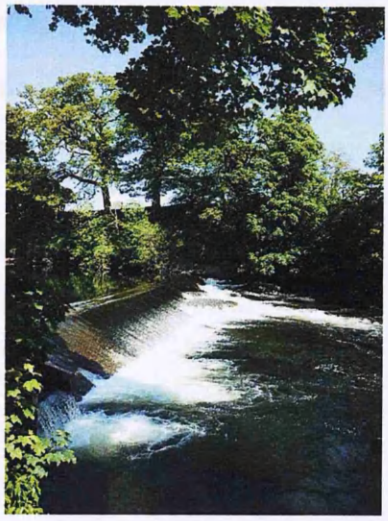

Figure 6-15 Broad raine farm Weir

(Sources: geograph.org.uk)

Halton Weir

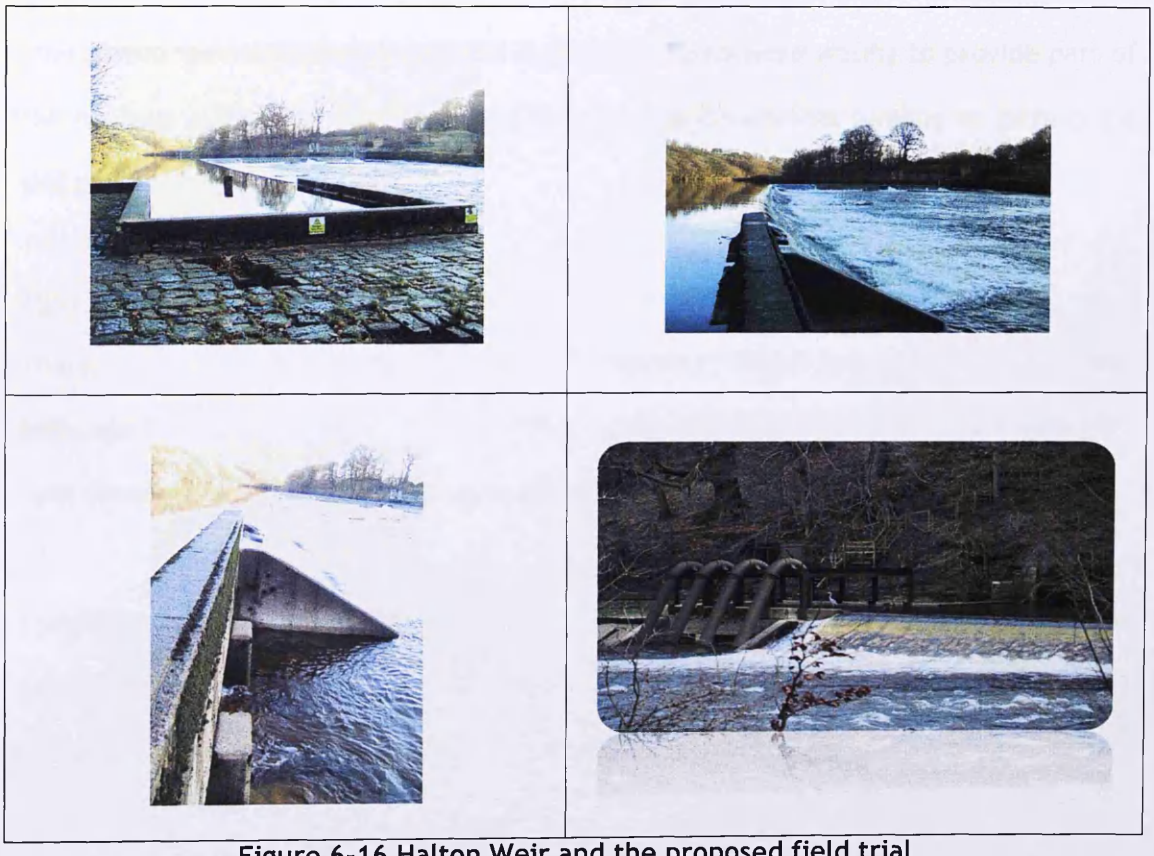

Figure 6-16 Halton Weir and the proposed field trial

Halton Weir is situated in the River Lune near to Lancaster. It is a very wide river with an abundant amount of water. There is a side weir part with under sluice, which is an ideal site to put the siphon (See Fig. 6-16). The head is about 2 m.

From the above potential sites, the Halton weir was considered the best location, because:

-The height is 2 m

-The water discharge is more than adequate

- It is very close to Lancaster

- There is a site weir where it is possible to place the siphon.

There were several meetings with the local people who were willing to provide part of the funding. Unfortunately, it turned out there was insufficient funding to carry out a site experiment here.

Sites under Yorkshire Water Authority

There were some potential sites owned by the Yorkshire Water Authority that could have been used for the site experiment. A visit to meet Yorkshire Water Representative (Mr. Ilyas Dawood) in July/August 2008 was made to discuss this possibility.

Yorkshire Water Treatment Plants (YWTP) through Mr. Ilyas Dawood offered collaboration and sites for the experiment. After several site visits and meetings, two potential locations were selected i.e. in Sandall and in Doncaster.

Based on the laboratory experiment, it was suggested that some improvement in the siphon system design was applied on site experiment, i.e.:

- Bell mouth shape for the siphon inlet and outlet
- No butterfly valve
- A bigger bend radius (r), with r/D = 4.6.
- Reduce the joints

Therefore, the improvement was carried out in developing the experimental rig on site. The site experiment was carried out by students with my supervision.

The onsite rig experiment was a fourth year student project based on the laboratory research results. It was using the same 200 mm siphon diameter and some improvement of the rig design as explained above. The students designed the site experimental rig, and a team of technicians organised by the Yorkshire Water built and installed the siphon on site.

Two groups of fourth-year students carried out an on-site siphon experiment at the Yorkshire Water Treatment plant in Doncaster. The first group used Aerator2. They managed to install the whole rig but due to problems with the downstream conditions of the weir, the test failed to prime the siphon. It was a very turbulent and frothy flow around the outlet which caused air to enter the siphon. Figure 6-17 shows the onsite experimental rig. The left photo is the inlet view and the right photo shows the outlet view, which is a very turbulent and frothy flow in the downstream weir.

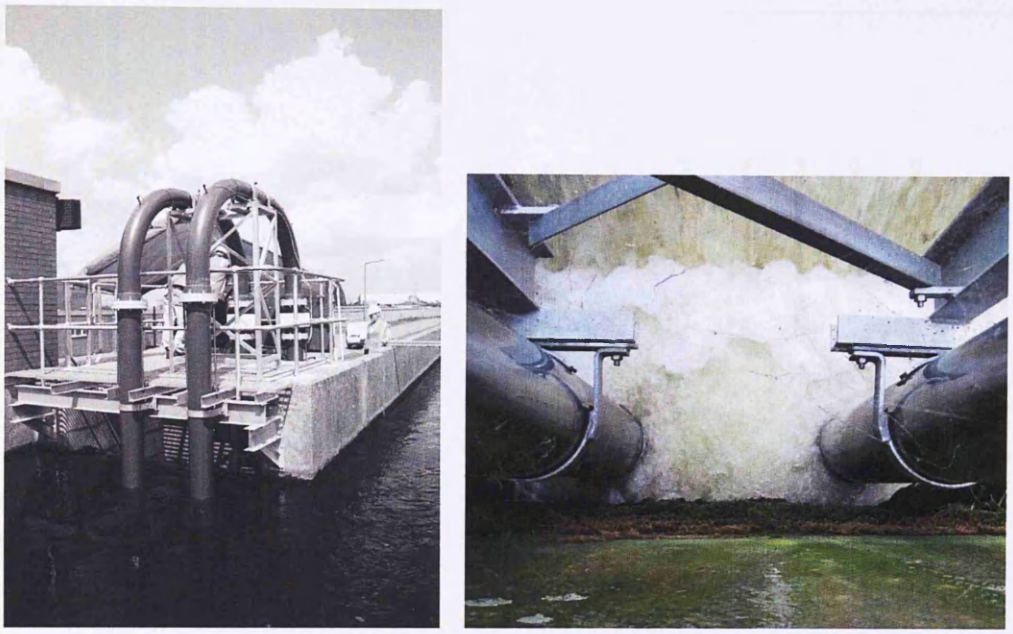

Figure 6-17 Site experiment using Aerator 2

(Sources: Final report 4th year students, 2009)

The second group improved the downstream conditions by putting a bell mouth and a deeper siphon to divert the frothy flow of the weir away from the siphon outlets as well as offering a slight depth increase. They used Aerator-1 and tested 6 configurations of spargers with 100 holes of 2 mm diameter. They found that the spiral configuration produced the highest void fraction.

The site experiments carried out by the fourth year students found that spiral configuration spargers produced the highest air flow rate. The maximum rate achieved on site was approximately 8.333 l/s with Aerator-1 with approximately 1.7 m of potential head and a siphon height (y_A) = 4.40 m (Earnshaw, 2010).

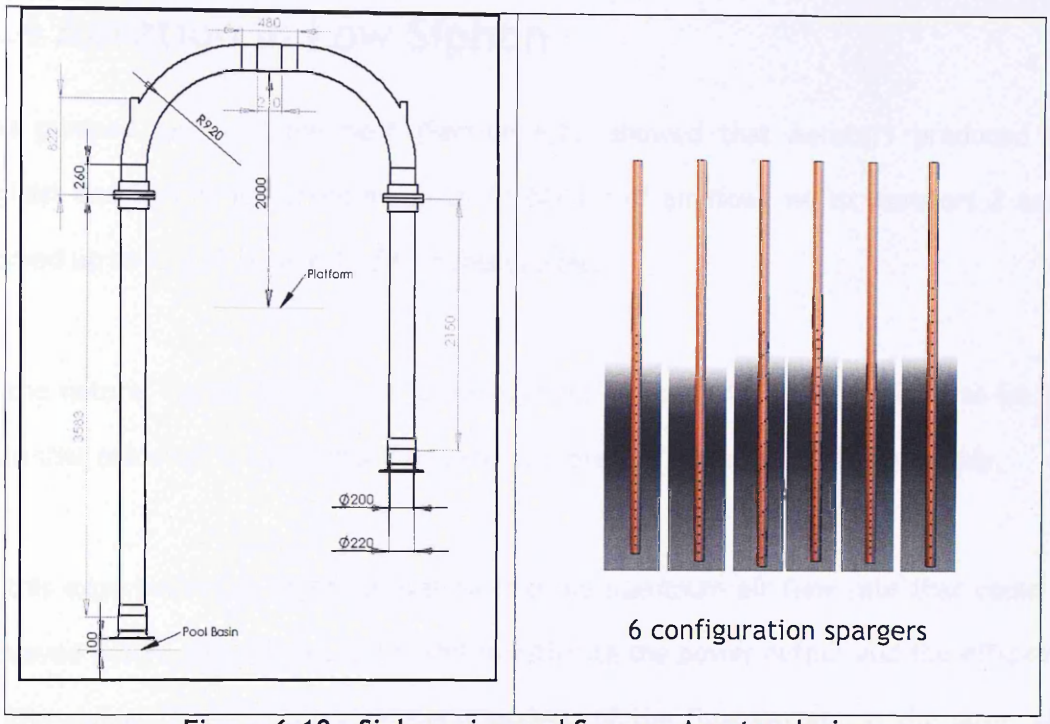

Figure 6-18 - Siphon pipe and Sparger Aerator design

(*Sources: Final report 4th year students, 2010)*

The siphon was left running for 3 months after the observations and continued to work. This showed that that the system was robust and reliable.

Based on the students' work, a spiral configuration sparger with 3 mm diameter holes was designed and then tested in the laboratory siphon experimental rig. Observation showed that the spiral spargers have a more stable performance at the higher air flow rate than do the other types.

The next stage of the experiment was carried out using a natural siphon and was focused more on Aerator1, however Aerators 2 and 3 were also tested.

6.4 Aeration in Low Siphon

The pumped system experiment (Section 6.2), showed that Aerator1 produced the highest aeration as it worked at up to 14.941 l/s of air flow, whilst Aerators 2 and 3 worked up to 12.629 l/s and 12.54 l/s respectively.

In the natural siphon experiment, the maximum airflow rate was estimated to be less than that achieved in the pumped system, as there was no external energy supply.

In this experiment the objective was to find the maximum air flow rate that could be achieved before the siphon breaks, and to estimate the power output and the efficiency of the siphon system. Observation and analysis of the flow pattern in the down pipe were made. These will be described separately and in more detail in Chapter 7.

The experiment was first carried out using a lower siphon height as seen in Figure 6-19, (y_A= 3.5 m) with Aerators 1 and 3, and then slightly lower for Aerator2 (y_A= 3.30 m). Later the siphon height was raised up to 4.70 m.

As stated in Chapter 3 the experimental rig was simulating the run-of-river condition, i.e. a weir or a hydraulic structure in the river with a siphon installed over the weir. The top tank simulates the upstream water source (weir) where the siphon inlet takes in the water. The storage (bottom) tank simulates the downstream location. This tank holds the water that will be re-circulated through the siphon. The difference in water levels between upstream and downstream (H) is approximately 2 m.

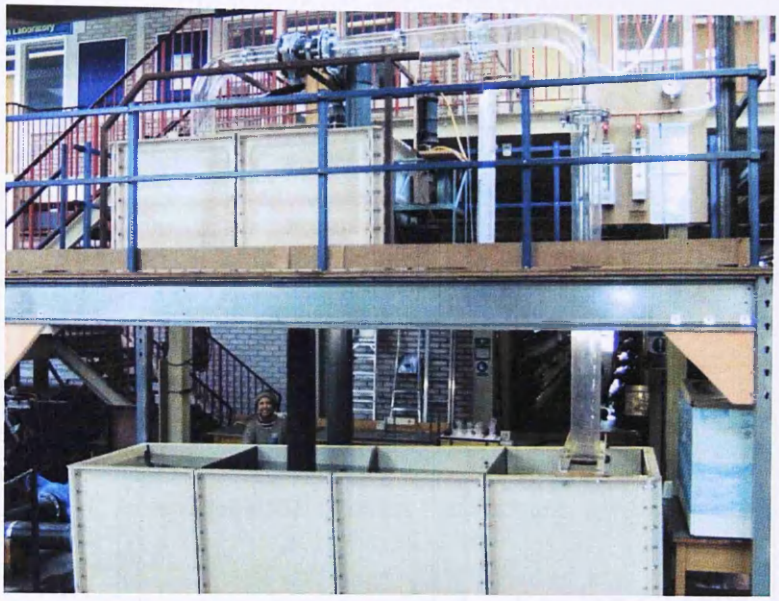

Figure 6-19 Lower Siphon Rig

As it was found that full siphon water flow would produce very high water velocity and cause overflowing in the system, a butterfly valve was installed in the horizontal part of the pipe system to control the flow rate. **(Figure 6-20).**

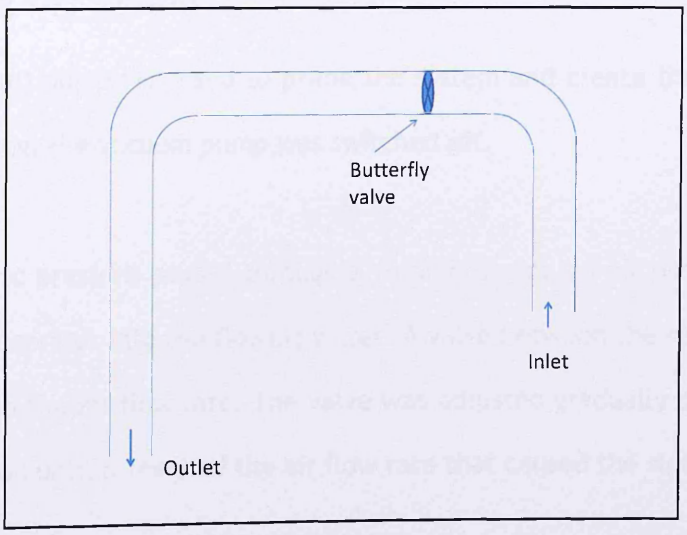

Figure 6-20 Butterfly valve position

Fig. 6-21 (similar to Fig. 3-2) shows a schematic diagram of the complete siphon system.

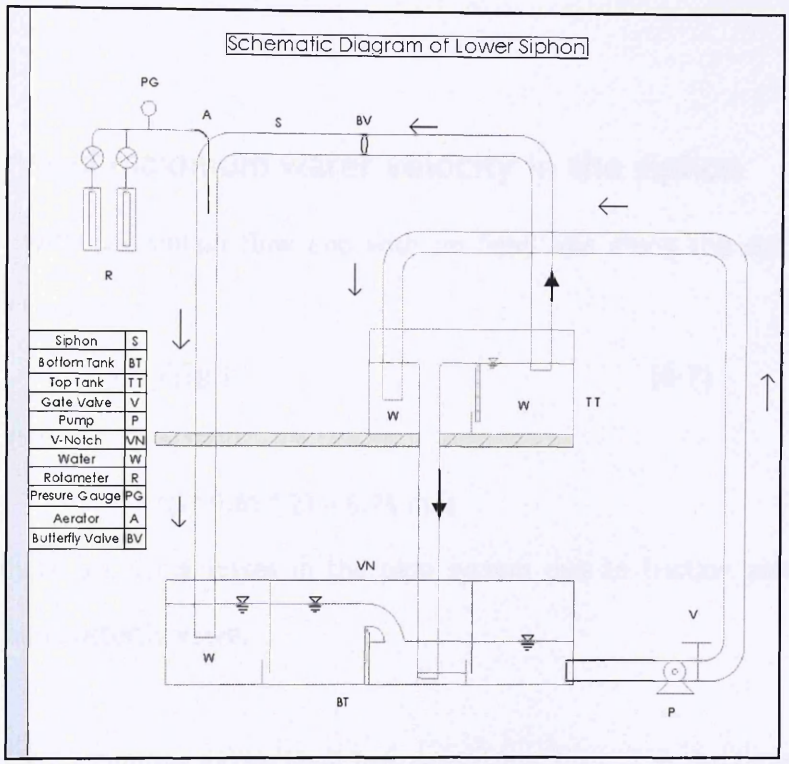

Figure 6-21 Schematic Diagram of Siphon Rig

6.4.1 Priming the siphon

A suction (vacuum) pump was used to prime the system and create the flow. Once the siphon was working, the vacuum pump was switched off.

Air at atmospheric pressure passed through a rotameter and an air pressure gauge and then through the aerator into the flowing water. A valve between the rotameter and the aerator controlled the air flow rate. The valve was adjusted gradually to allow more air to enter the siphon until it reached the air flow rate that caused the siphon to break.

The siphon was run with various butterfly valve settings, starting from 30° to 90° (full opening).

6.4.2 Estimated maximum water velocity in the siphon

Theoretically, with full siphon flow and with no head loss along the siphon pipe the water velocity would be:

$$v = \sqrt{(2gH)} \qquad (6\text{-}7)$$

For 2 m head (H):

$$v = \sqrt{(2 * 9.81 * 2)} = 6.26 \text{ m/s}$$

In practice, there are some losses in the pipe system due to friction along the pipe, bends, joints and butterfly valve.

Using **Table 4-5** (in Chapter 4) the total loss coefficient (K_{siphon}) in the lower siphon set up (L= 5 m, D= 0.20m) and without the butterfly valve would be:

$$K_{siphon} = K_f + 2K_{B\text{-}Perspex} + K_{inlet} + K_{outlet} + 4\,K_{joint} = 0.325 + 0.48 + 0.5 + 1.0 + 0.24 = 2.545$$

For H = 2 m, this gives total energy head:

$$H = v^2/2g + K\,(v^2/2g) = (1+K)(v^2/2g) \qquad (6\text{-}8)$$

For K = 2.545 → $v = \sqrt{[(2gH)/(3.545)]}$ → v = 3.33 m/s

For higher siphon (L=6.20m, D=0.20m) →

$K_f = f\,(L/D) = 0.013 * 6.2/0.2 = 0.403.$

Total loss coefficient (K_{siphon}) in the a higher siphon without butterfly valve:

$$K_{siphon} = K_f + 2K_{B\text{-}Perspex} + K_{inlet} + K_{outlet} + 7\,K_{joint} = 0.403+0.48+0.5+1.0+0.42=2.803$$

For H = 2 m, this gave:

$$H= v^2/2g + K\,(v^2/2g)= (1+K)(v^2/2g)$$

For $K = 2.803 \rightarrow v = \sqrt{[(2gH)/(2.803)]} \rightarrow v = 3.74$ m/s

With the presence of the butterfly valve in the siphon, there is another head loss. Thus, the maximum water velocity should be less than v = 3.74 m/s.

During the experiment the setup was only operated with the butterfly valve fully open when some air was being injected. Otherwise the bottom tank could not cope with the flow rate and overflowed.

6.4.3 Void fraction calculation

The void fraction (α) was calculated using Equation (6.1). The water velocity in the mixed flow of air and water was calculated using Equation (6.5). The air flow rate (Q_a) and the water flow rate (Q_w) data were recorded and the water velocity (v) was calculated.

Various butterfly valve openings were used and data recorded from the rotameter, the V-Notch weir and the pressure gauges. Figures 6-22 (a-c) show the relationship between

water flow rate and the void fraction for various openings of the butterfly valve for the three aerators.

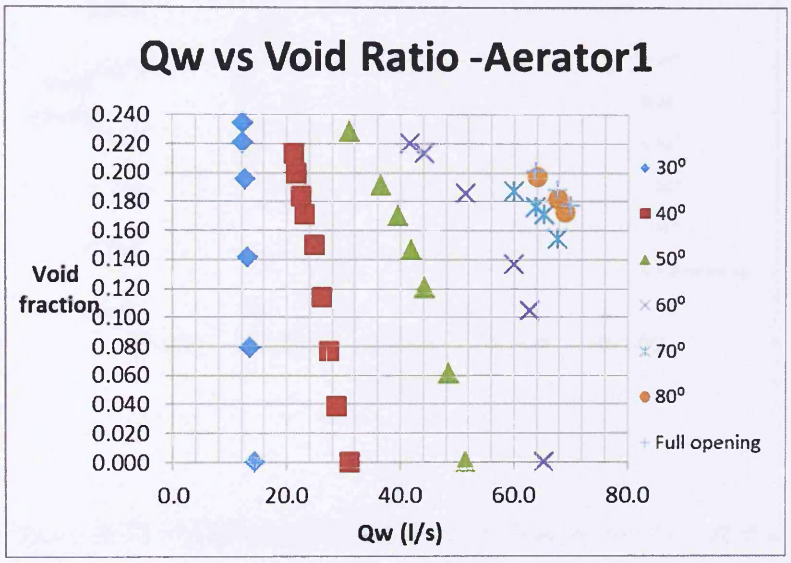

(a)

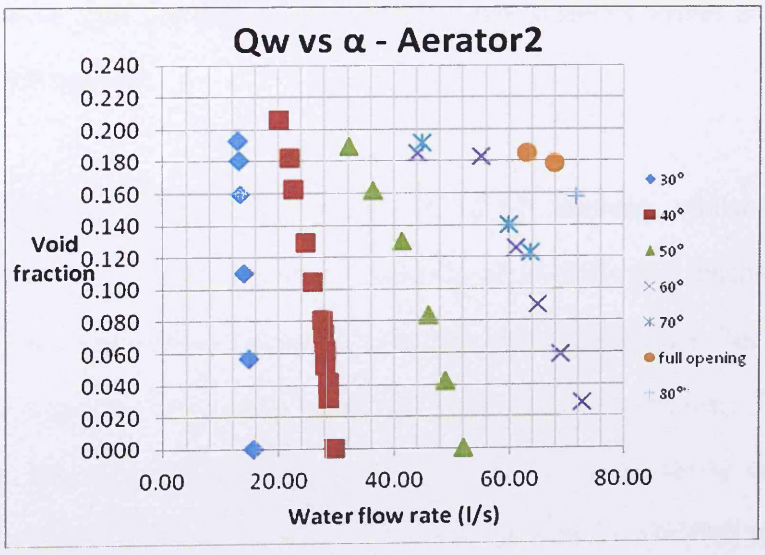

(b)

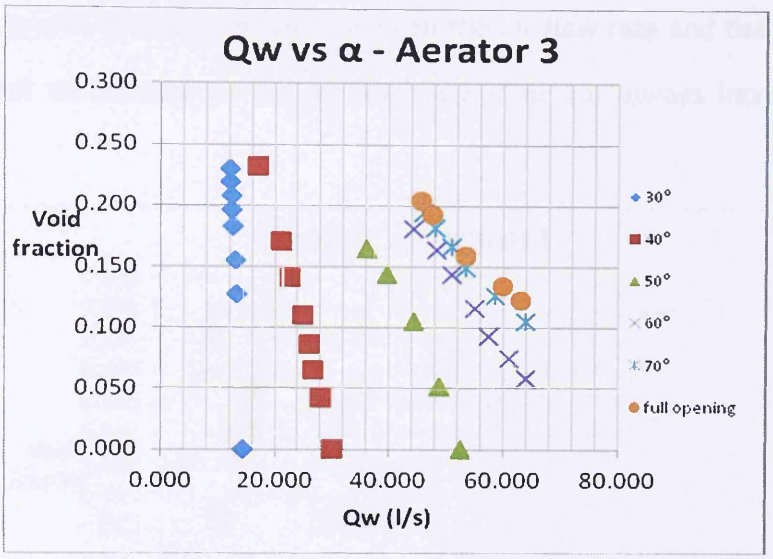

(c)

Figure 6-22 Void fraction vs Q_w for various butterfly opening

These graphs show that the degree of opening of the butterfly valves affects the void fractions for each aerator.

Aerator1 had the highest void fraction of 24% at 60° opening, whilst Aerator2 was relatively constant for various degrees of opening, about 19%, and reached the highest void fraction at 40° opening (at 20.6%). For Aerator3, the void fraction fluctuated up and down with the openings, indicating instability in the aeration process. This was most likely because Aerator3 was located relatively close to the butterfly valve, and the turbulence caused by the valve affected the flow pattern. It reached maximum void fraction of 23% at 30° opening.

The following graphs show the relation between the air flow rate and the void fraction. They show that an increase in the air flow rate does not always increase the void fraction.

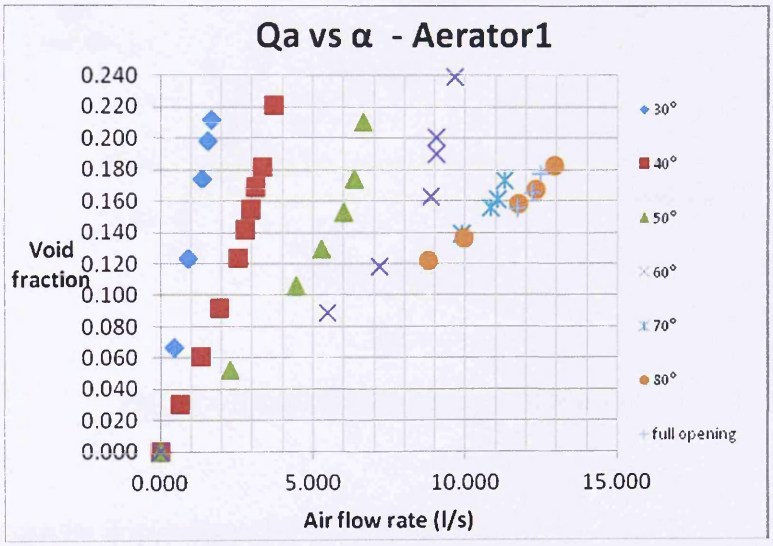

(a)

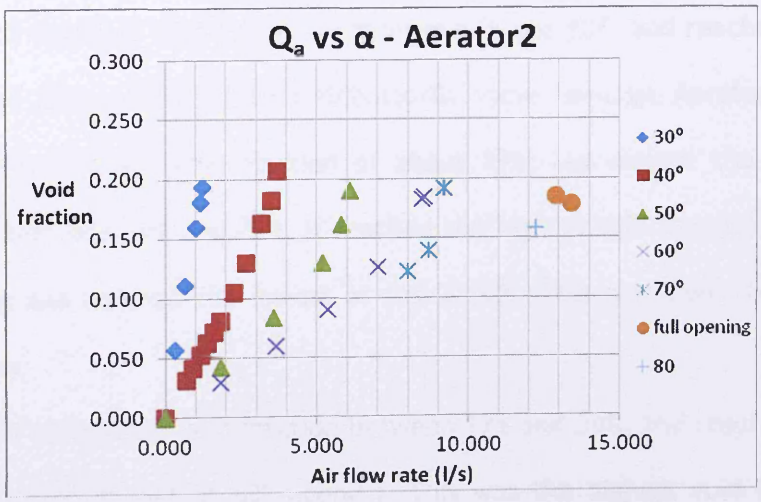

(b)

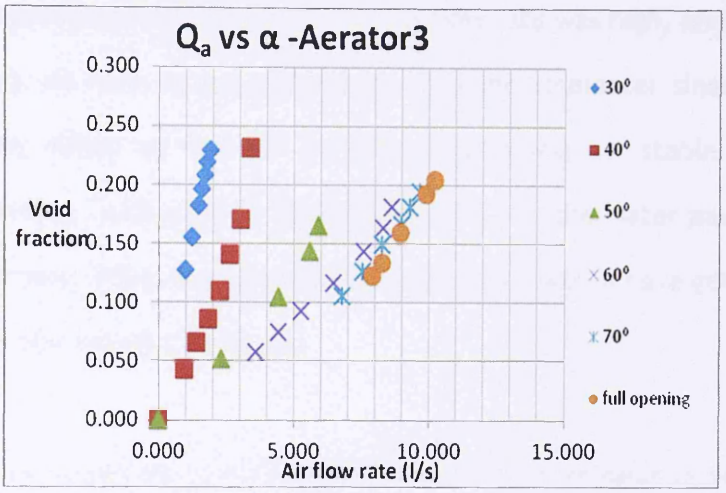

(c)

Figure 6-23 Air flow rate vs void fraction

Several points can be drawn from the three graphs:

1) Each aerator achieved the highest void fraction at a different opening, and it was not when the butterfly valve was fully open.
2) Aerator3 achieved a void fraction between17% and 23%, and reached the highest value of 23% at both 30° and 40°butterfly valve openings. Aerator2 achieved a relatively constant void fraction of about 19%, but overall the void fraction ranges between 16% and 21%. It reached the highest void fraction of 21% at 40° opening and reached the lowest of 16% at 80°. This was lower than the other aerators.
3) Aerator1 achieved a void fraction between 17% and 24%, and reached its highest void fraction of 24% at 60° opening. This was the highest void fraction value reached.

The aerators became very sensitive when the air flow rate was high, and the siphon flow started breaking. As well, it was difficult to read the rotameter since the pendulum fluctuated wildly indicating that the aeration process was not stable. This was most likely due to velocity fluctuation in the turbulent flow as the water passed the air exit holes in the spargers. The presence of the butterfly valve would have generated vortices that make the water velocity fluctuate.

From the graphs 6-23 (a-b-c), it was shown that the maximum value of void fraction was determined by the optimum combination of air flow and water flow. This combination varied according to the butterfly opening. In a certain degree of opening, the air flow increase with the increase of water flow, followed by the increase of the void fraction. Yet, as Jain (1988) reported, when water flow increased, the extent of turbulence in the water also increased. This turbulence has disturbed the air suction process and this stopped the void fraction increment.

Another factor that limited the maximum air flow rate was the water head. In section 6.3, we found that the air flow reached up to maximum of 750 l/min (Aerator2 and Aerator3) and 890 l/min (Aerator1). Even though the rotameter was gradually opened till fully opened the value of air flow remained constant at these values. This means that there is a maximum value of air flow which is limited by the water head (H). In turn, the maximum air flow produced a certain void fraction. Thus, the void fraction is also limited by the possible maximum air flow which can be attained. The experiment showed that it was not always the maximum void fraction which resulted.

Appendices B-4a, B-4b, and B-4c give the detailed calculation of the void fraction for the different aerators' designs with various butterfly openings.

6.4.4 Power output calculation

From the research carried out by Widden et al (2004), the aeration process within the system is assumed to be adiabatic because the air bubble temperature reached the same value as the water temperature in a very short time (see also Howey and Pullen, 2009).

The temperature ratio equation:

$$T_2/T_0 = (p_2/p_0)^{(\gamma-1)/\gamma} \qquad \textbf{(6-9a)}$$

$$T_2 = T_0(p_2/p_0)^{(\gamma-1)/\gamma} \qquad \textbf{(6-9b)}$$

Where:

T = absolute temperature

p = pressure

γ = Specific gas ratio = = C_p/C_v

C_p = Specific Heat at Constant Pressure, = 1.005 kJ/kg.K

C_v = Specific Heat at Constant Volume = 0.718 kJ/kg.K

Subscripts 2 and 0 represent the conditions within the aerator and in the atmosphere respectively.

Enthalpy (h) = energy per unit mass:

$$h = C_p\, dT = C_p\,(T_2 - T_o) \quad \textbf{(kJ/kg)} \qquad \textbf{(6-10)}$$

Power output equation:

$$P_{output} = p_A * h * Q_A \qquad \textbf{(6-11)}$$

Where :

ρ_A = air density (kg/m^3)

h = enthalpy = energy per unit mass (kJ/kg)

Q_A = air flow rate (l/s)

In the laboratory rig, as mentioned in the Chapter 3 and 4, due to limited space in the workshop, the siphon flow was controlled by a butterfly valve which causes a major energy loss. Also due to the narrow space in the upper and bottom tank, it was not using a bell mouth shape in the inlet and outlet entrance of the siphon. This also caused a significant loss. Therefore, in the laboratory experiment it was expected that the efficiency would be small, because the total loss coefficient in the siphon system (K) is high (See Table 6.2).

The following graphs show the power output vs the void fraction for the three aerators with various openings of the butterfly valve.

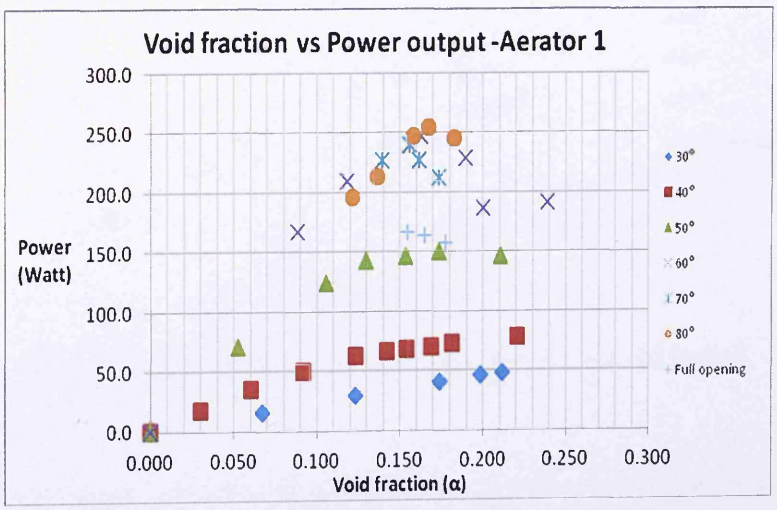

Figure 6-24 Void fraction vs Power output for Aerator-1

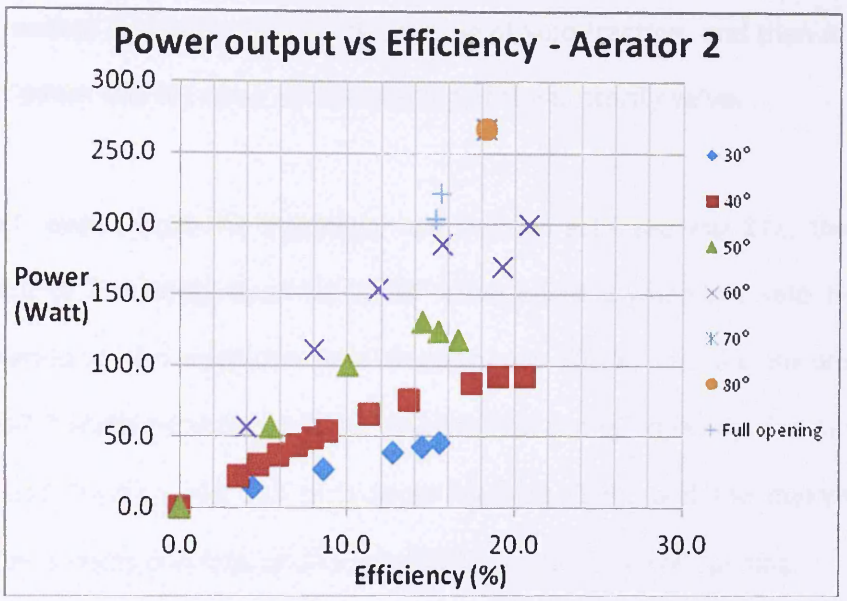

Figure 6-25 Void fraction vs Power output for Aerator-2

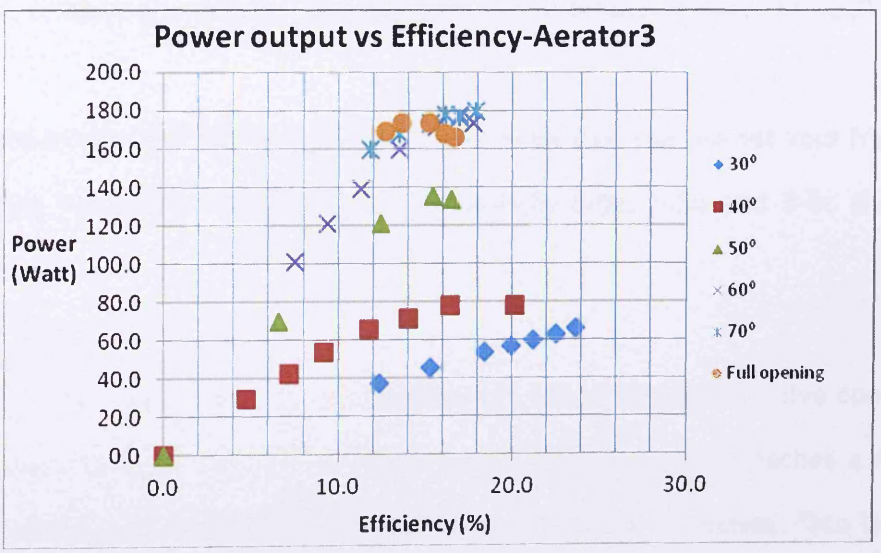

Figure 6-26 Void fraction vs Power output for Aerator-3

The three graphs above show a similar trend i.e. at a small degree opening, (30° and 40°) the power increases with increase in void fraction. At bigger openings, (above 50°),

the power reaches a maximum at a certain value of void fraction, and then it decreases. The highest power did not occur at full opening of the butterfly valve.

For Aerator1, even though the maximum void fraction achieved was 24%, the maximum power output of 254 Watts occurred at 80° valve opening when the void fraction was 17%. For Aerator2, the maximum void fraction was 20.6%, but the maximum power output of 267.5 Watts occurred at 15.8% void fraction and 80° opening. For Aerator3, the maximum void fraction was 23% at a lower opening (30°), and the maximum power output of 179.3 Watts occurred at 21% void fraction and 70° valve opening.

The results above show that Aerator3 produced the lowest maximum power, i.e. below 200 Watts, compared to Aerator1 and Aerator2, which produced more than 250 Watts.

With regard to the void fractions, the results showed that the highest void fraction did not produce the highest power output. Appendices B-5a, B-5b and B-5c show these results.

A similar pattern was found in all the Aerators i.e. for each butterfly valve opening, the power output increases with the increase in void fraction until it reaches a maximum value then it starts to decrease even though the void fraction increases. Thus there is an optimum value of void fraction to produce the maximum power output.

Henser (2005) explained that the increasing water flow will increase the 'void' causing more losses and a reduction of the air suction and air pressure. This reduction in air pressure suction reduces the power output.

The term 'void' in Henser work was a transition region, or a bubbly flow development zone, i.e. a region between an intensive air stream flow pattern around the aerator and the bubbly flow region at the lower part of the siphon. Chapter 7 describes in more detail about the changes in flow pattern along the downward leg of the siphon.

6.4.5 Aeration Efficiency

Calculation of system efficiency was carried out by comparing the power input due to the water flow with total head of 2 m and the power output produced by the air flow.

Power input: $P_{input} = \rho_W * g * Q_W * H$ (Watt) (6-11)

Where:

ρ_W = water density = 1000 kg/m^3

g = gravitation (m/s^2)

Q_W =water flow rate (m^3/s)

H = potential head ≈ 2 m

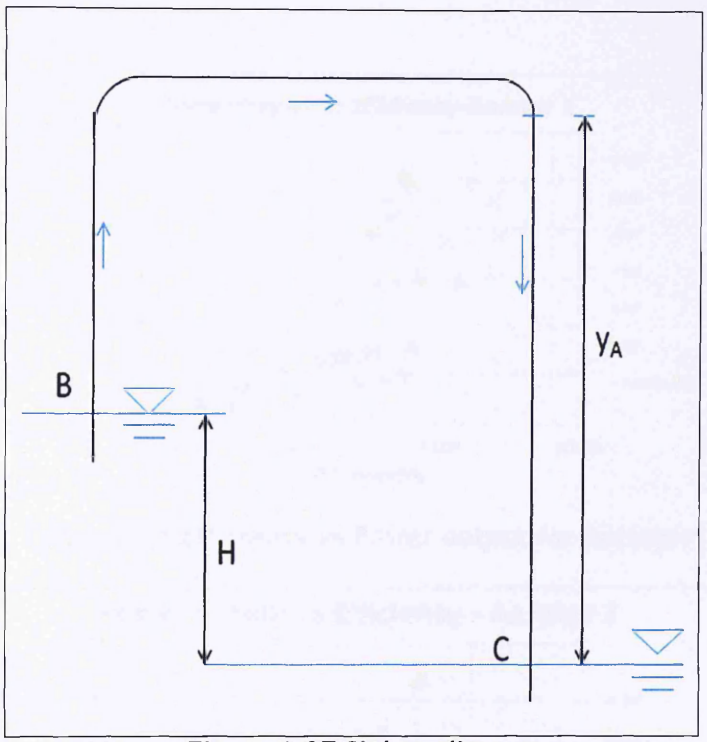

Figure 6-27 Siphon diagram

(A = Aerator, B= inlet, C=outlet, H = potential head, y_A = distance between water surface and Aerator)

It should be noticed that the calculation of power input was using the whole potential head (2 m), whilst the power output was calculated based on the record and measurement. This means it included all the losses in the siphon system due to inlet-outlet, frictions, bends, joints, the presences of the butterfly valve, and losses due to aerations.

Total efficiency: $$\eta = (P_{output} / P_{input}) * 100\% \quad (6\text{-}12)$$

The following graphs in Figure 6-28 to 6-30 show the relation between power output and siphon system efficiency for different butterfly valve openings. See Appendices B-6a, 6b and 6c for detailed calculations of power input and efficiency.

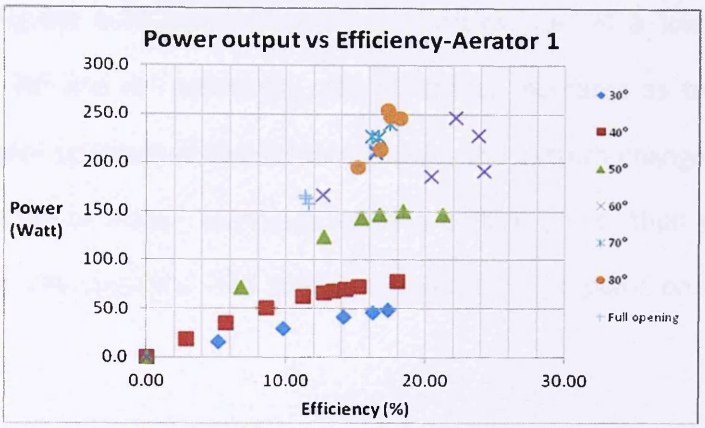

Figure 6-28 Efficiency vs Power output for Aerator-1

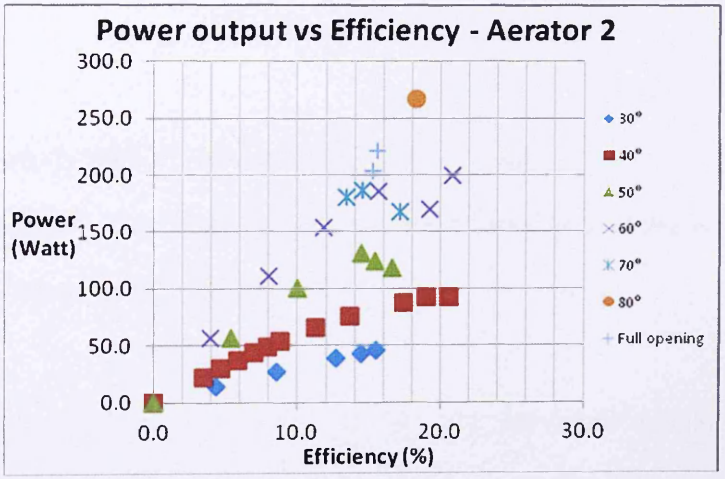

Figure 6-29 Efficiency vs Power output for Aerator-2

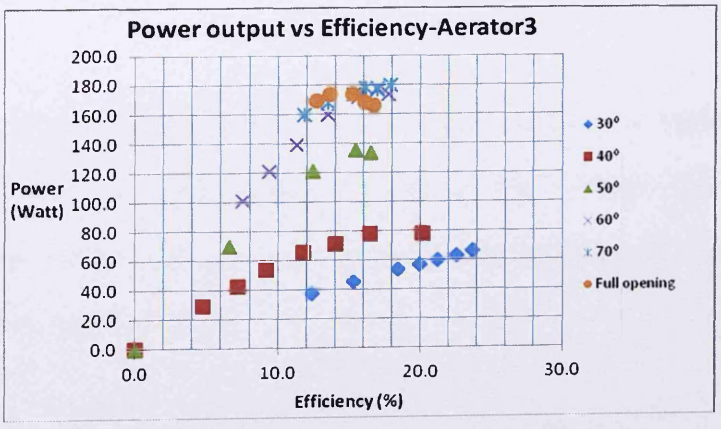

Figure 6-30 Efficiency vs Power output for Aerator-3

The graphs in Figures 6-28 and 6-30 show similarities, i.e. at a low opening of the butterfly valve (30° and 40° openings), the efficiency increases as the power output increases. At higher openings of the butterfly valve, the pattern changes, the efficiency increases as the power output increases up to a certain point, then efficiency either decreases or remains constant. The power output from this point on does not always decrease.

The graphs also show that the highest power output did not coincide with the highest efficiency.

Aerator1 reached its highest efficiency of 24% at a 60° valve opening with a power output of 185.5 Watts. The maximum power output was 254.2 Watts which occurred at an 80° opening with an efficiency of 17.3 %.

Aerator2 reached its highest efficiency of 21% at a 60° valve opening with a power output of 199.5 Watts. The maximum power output was 267.5 Watts at an 80° opening with an efficiency of 18.3%.

Aerator3 (Fig 6-30) reached the lowest value of power output. The highest efficiency of 17% at a 70° valve opening with a power output of 179.3 Watts. The butterfly valve opening had a very large effect on the efficiency, void fraction and pressure suction at the higher opening and flow rates.

6.5 Aeration in Higher Siphon

The objective of raising the siphon higher was to produce more power. In the higher siphon experiment the performance of Aerator1 using spiral spargers with 3 mm hole diameters was investigated. Spiral spargers were chosen based on the result of the on-site experiment. This sparger produced a slightly higher air flow rate than that achieved by the inline spargers.

In the higher siphon, the butterfly valve was located in the vertically upward leg of the siphon, just above the inlet. (See Fig. 6-31)

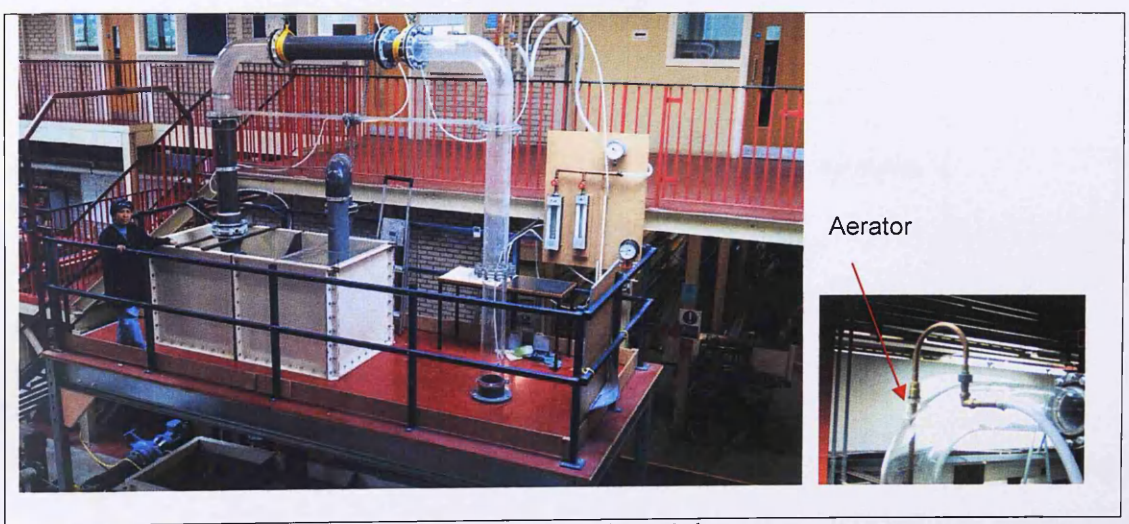

Figure 6-31 Higher siphon

The experiment was carried out using 60°, 70°, 80°, and full opening of the butterfly valve.

6.5.1 Void fraction

The void fraction (α) is calculated based on the Equation (6.1); the water velocity in the mixed area is calculated based on equation (6.4).

Q_a and Q_w are recorded and the velocity (v) is then calculated. Figures 6-32 and 6-33 show the relationship between the water flow rate and void fraction, and between the air flow rate and the void fraction for the different openings of the butterfly valve.

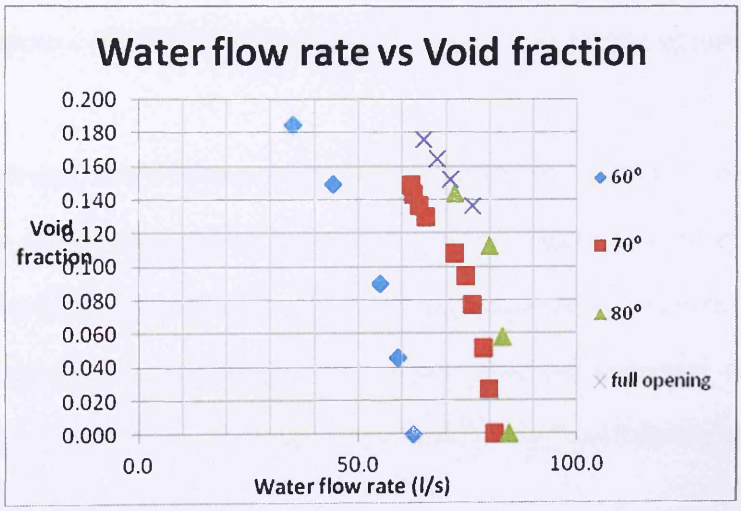

Figure 6-32 Void fraction vs Q_w for various butterfly opening

The graph above shows that as the water flow rate decreases the void fraction increases as more air and less water will flow in the pipe cross section. Void fraction reached its highest value, 18.5%, at 60^0 valve opening. At full opening the void fraction was 17.6%.

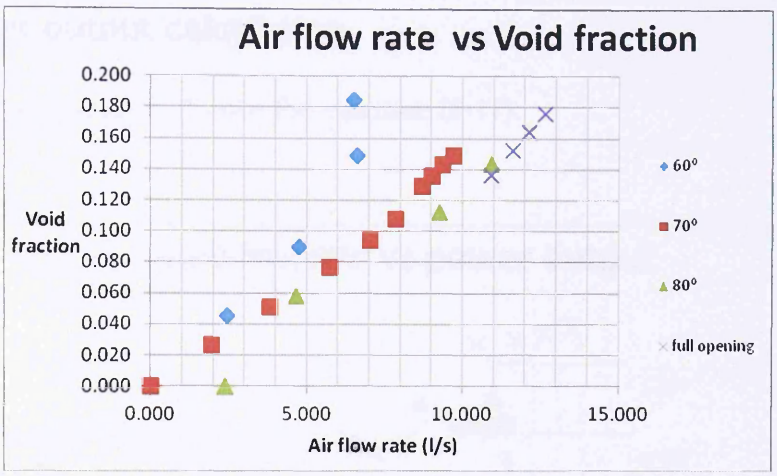

Figure 6-33 Void fraction vs Q_A for various butterfly opening

For the lower siphon, the maximum void fraction achieved was higher, 24%, at 60° valve opening. At the fully open position it was 18%. For the higher siphon, the void fraction was lower at the 60° valve opening due to the water flow being relatively less turbulent than was the case in the lower siphon. It appears that the closeness of the butterfly valve to the aerator in the lower siphon generated more turbulence and caused the higher void fractions.

The above graphs show that for the higher siphon the void fraction decreases with an increase in water flow rate.

6.5.2 Power output calculation

Power output was calculated using the equation (6-11):

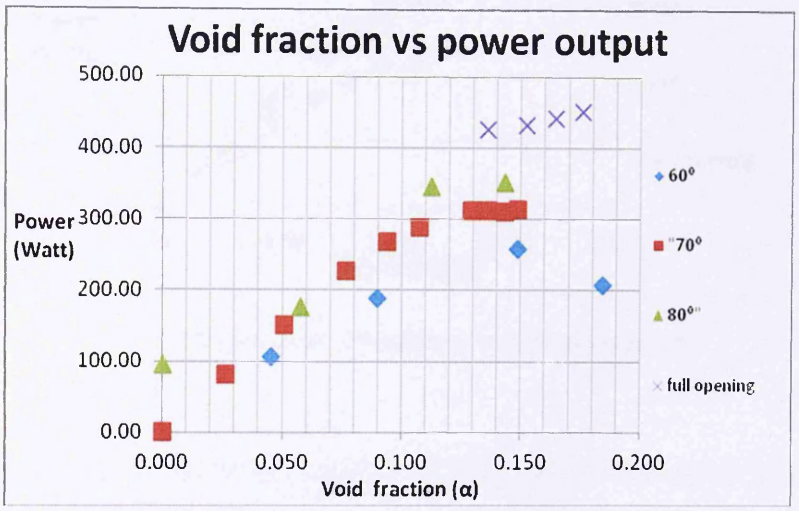

Figure 6-34 Void fraction vs Power output

The graph in Figure 6-34 shows that the maximum power output of 451.5 Watts was reached at full opening with a void fracion of 18%. This graph shows a similar trend to the results for the low siphon, i.e. that the power increases with an increase in water flow rate. Thus the power output increases with an increase in the void fraction until it reaches its maximum value. At higher void fraction it either remains constant or begins to decrease.

6.5.3 Efficiency

Efficiency of the aeration was calculated based on the equation 6-13. The following graph shows the relationship between power output and efficiency. The graph showed similar trends to the graph in Figure 6-34, i.e. the efficiency increases with an increase in the power output.

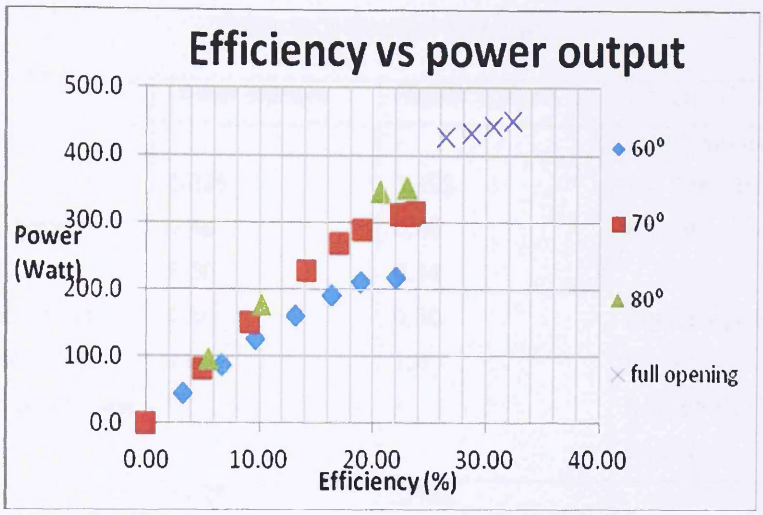

Figure 6-35 Efficiency vs Power output

The highest efficiency of 32.3% was reached at full opening with power output of 451.5 Watts. The maximum void fraction achieved was 19% at 60° opening with power output of 258 Watts. The higher siphon has a better performance in terms of the relation between power and efficiency. This is because the position of butterfly valve is further away from the aerator, so the influence of the butterfly valve which caused very turbulent flow is smaller than in the lower siphon. This is also evidence that the butterfly valve caused a very turbulent flow, with the implication of reducing void fraction ratio and a significant of energy loss.

6.5.4 Loss Coefficients in the siphon system

In both the lower and higher siphons, the butterfly valves contribute more head losses. The following table summarises the loss coefficients with a fully open value in both siphon systems.

Table 6-2 Overall K values

	Lower siphon	Higher siphon	Notes
Friction loss	0.325	0.403	Lower siphon: (L= 5 m, D=0.20m); 6 joints
Perspex bend (2 bends)	0.48	0.48	
Joints	0.30	0.54	
Inlet (sharp edge entry)	0.50	0.50	Higher siphon: (L= 6.2 m, D=0.20m); 9 joints
Outlet (sharp edge exit)	1.0	1.0	
Butterfly valve full opening	1	1	
Total K	3.605	3.923	

Several changes could be made to reduce losses along the pipe system:

- Use a bell mouth inlet (K= 0.10, refer to **Table 4-2- in Chapter 4 Section 4.3).**
- Use outlet diffuser (K= 0.20, refer to **Table 4-2- in Chapter 4 Section 4.3)**
- Use one round bend if it is possible instead of using two bends (K=0.24, refer to **Table 6-3.**

As mentioned in the previous section (section 6.3), that some improvements to the siphon system design was applied on the site experiment, i.e. using the bell mouth shape for the siphon inlet and outlet, a bigger bend radius, and no butterfly valve. With this improvement, the overall K values reduced significantly, i.e.:

Table 6-3 Improvement of K values

	K	Notes
Friction loss	0.403	L= 6.213 m, D= 0.20 m
Big radius bend, r/D = 4.6	0.40	
Joints (6 joints)	0.36	
Inlet (bell mouth)	0.10	
Outlet bell mouth	0.10	
Total K	1.36	

From Table 6-2 and Table 6-3, we can see that the loss coefficients reduced significantly, from K= 3.9 to K= 1.36, or almost one third from the K value in the laboratory experiment. As a consequence, the reduction in K value will have an impact on the increase in water flow velocity.

The following is the estimation of the increase in velocity in the siphon flow.

$v = \sqrt{2gH}$

$H = v/2g + K\, v^2/2g = v^2/2g\,(1+K)$

$v^2/2g = H/(1+K)$

$v = \sqrt{2gH/(1+K)}$

For $K = 3.9 \rightarrow v = 2.83$ m/s.

By using bell mouth inlet and outlet and the absence of the butterfly valve the value of K reduced, i.e. for $K = 1.36 \rightarrow v = 4.07$ m/s $\rightarrow$ Thus v increased by 43.8%. For v^2, v^2 increased by ≈ 20%.

Increase in water velocity will increase in water flow rate, and this will also have an impact on increase in air flow rate. In the Bernoulli equation, an increase in water velocity will decrease the pressure in the siphon:

$$p_1 g + v_1^2/2 + z_1 = p_2 g + v_2^2/2 + z_2$$

This means, it causes more air suction. Refer to Equation 6-11, the air power also increases proportionally with increase in air flow. Therefore, with this improvement, the site experiment produced more air power and also increased its efficiency.

If the v^2 increased by 20%, proportionally the pressure reduced about 20%. If the air flow (air suction) proportionally increased with the pressure reduction in the siphon, then the air flow increased by 20%. Thus, the power output and the efficiency also increased about the same figures.

The site experiment was carried at the Yorkshire Water Treatment plant in Doncaster (see Figure 6-13):

6.6. Experimental Findings and Results

The following section describes and summarises the results for the pumped experiment, the low siphon and the higher siphon.

All three tests showed that as the water flow rate is increased the air flow rate may be increased, but only until the void fraction reaches a certain point and then the void fraction starts to decrease or a siphon break may occur.

Another finding was that an increase in water flow will increase the power output. There is an optimum value to produce the highest power output (See Figures 6-24, 6-25, 6-26, 6-34).

Henser (2005) found that increasing the water flow rate caused a longer 'void'. This occurred in a segment of the vertically down pipe, from the aerator to the point where the bubbly zone starts. Chapter 7 will describe in more detail the flow pattern in the vertically down pipe.

The calculation of aeration efficiency showed that the efficiency changes according to the opening of the butterfly valve and also the increase in the water flow and air flow rates.

In the laboratory, Aerator1 reached its highest efficiency of 32.3% at full opening. These results were slightly better than those delivered by Bellamy (30%) and Pullen and Howey (10%).

On site experiment, this efficiency should be higher that this figures, because the designed was improved, i.e. by using bell mouth in the inlet and outlet and a bigger bend radius, and there was no butterfly valve.

In low siphon, Aerator1 reached its highest efficiency of 24% at 60° opening, and Aerator2 reached its highest efficiency of 21% at 60%, and Aerator 3 reach its highest efficiency of 23% at a low opening (30°).

An increase of siphon height increases the power output. Also, the effect of turbulence due to the butterfly valve is reduced, and this improved the efficiency. in Section 6.7 shows a theoretical calculation analysis based on research by French and Widden (2001)

which indicates that there is an optimum height to achieve the maximum power output for a given hydro power head (H).

6.7 Theoretical Calculation of Power Output

The following is a theoretical calculation based on research by French and Widden (2001). Using a different definition of the void fraction, they calculated the relationship between the power output (P) and the siphon height (y_A).

According to their work:

$$H = K\frac{v^2}{2g} + B \qquad \textbf{(6-13)}$$

H is the driving head. **$K(v^2/2g)$** is the total head loss in the siphon pipe (this includes the inlet and outlet losses, joints and bends, and the friction along the pipe). **B** is the buoyancy head of the air bubbles which is expressed as:

$$B = x_A\left(\frac{1}{r}\ln r\right)\frac{p_C}{\rho g} \qquad \textbf{(6-14)}$$

Figure 6-36 shows the schematic diagram of the siphon systems with aeration.

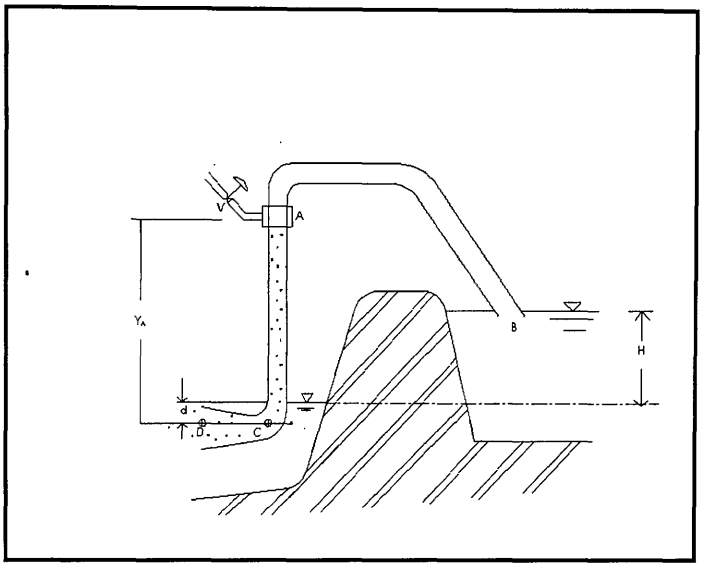

Figure 6-36 Siphon with aeration scheme

(H=potential head, B=inlet, A=Aeration, V=valve, C=bottom siphon, D=outlet, d=distance from D to downstream water surface, Y_A = height of earator)

Where:

x_A = the volume ratio between air and water,

p_C = the pressure at C and

r = the pressure ratio between point C and A.

If it is assumed that drift velocity of the bubbles (sv) is constant between point A and C, and that sv = 0.24 m/s (Rice, 1978 in French and Widden, 2001), then the value of the flow rate in the down pipe will be:

$$Q = (v - sv)(\pi R^2) \qquad \textbf{(6-15)}$$

Where,

v= water velocity,

sv =drift velocity,

s = slip ratio between water and air velocity,

R = siphon pipe radius

The power output will be:

$$Power = \rho_w gBQ \tag{6-16}$$

By substituting B and Q from equation (6-13) and (6-15),

$$Power = \rho_w g(H - K\frac{v^2}{2g})(v - vs)(\pi R^2) \tag{6-17}$$

The pressures at A and C were calculated using various values of y_A, i.e. from y_A = 3.0 m up to y_A = 8.0m. The height of the siphon (y_A) will determine the value of pressure at point A.

In two phase flow condition:

$$p_A = p_{Atm} - y_A * \rho_{Mixed} * g \tag{6-18}$$

$$p_C = p_{Atm} - d * \rho_{Mixed} * g \tag{6-19}$$

$$\rho Mixed = \rho_w \ (1+0.00123\ x_A)/\ (1+\ x_A) \tag{6-20}$$

Where:

p_A= pressure at A

p_C = pressure at C

ρ_w = *water density = 1000 kg/m^3*

ρMixed = mixed water and air density

x_A =*volumetric ratio of air to water above the datum*

Figure 6-37 shows the graph of power output (P) with respect to siphon height (y_A) for a 200 mm pipe diameter, with driving head (H)= 2 m for different values of the void fraction, α = 0.20 , 0.25, 0.27, 0.29, 0.30., and siphon height (y_A) from 3 m to 7 m. It was assumed that total loss coefficient due to friction and other minor losses K = 0.7.

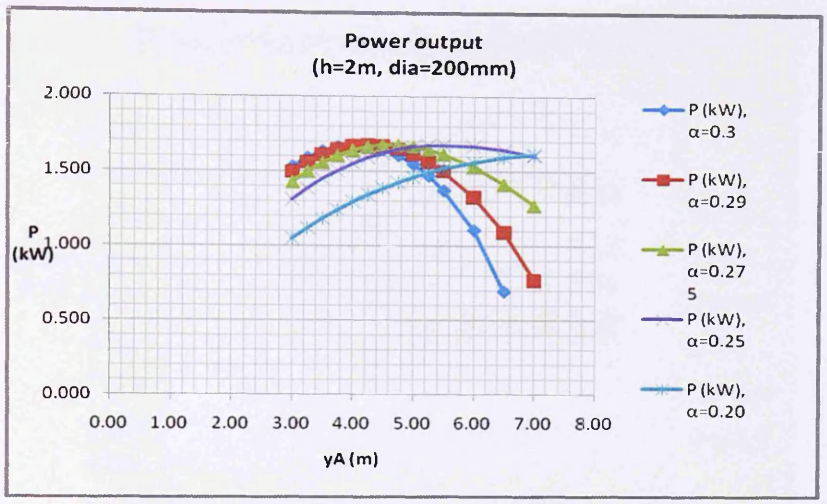

Figure 6-37 Power output vs siphon height for K=0.7

The above graph shows that for α = 0.25, the maximum power output is reached when y_A = 5.5 m. The power output increases with increase of siphon height (y_A) until at a certain height it reaches its maximum value. It then decreases even though the y_A increases. The graph also shows that the optimum siphon height increases with the decrease in void fraction, e.g. for α = 0.30, the optimum y_A = 4 m, and for α = 0.20, the optimum y_A is above 7 m.

An important conclusion that can be drawn from the graph in Figure 6-32 is that irrespective of the void fraction values the same maximum power is achieved. This shows that it is the driving head (H) that limits the value of the power output.

Figure 6-38 shows the graph of power output (P) versus siphon height (y_A) for void fraction α = 0.25 and loss coefficients K = 0.7, 1, 2, 3, 3.9.

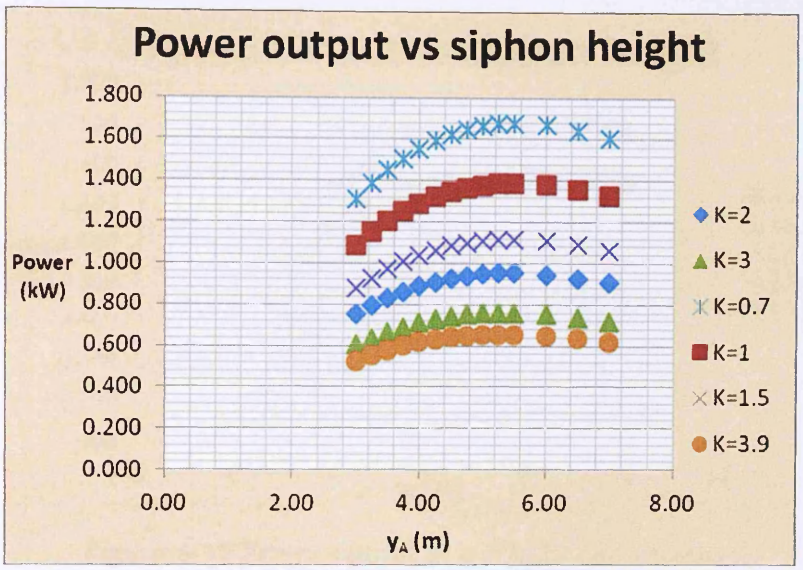

Figure 6-38 Power output at α = 0.25 and various K

The graph above shows the maximum power output occurs when y_A = 5.5 m, and this is independent of the value of K. Power output decreases as K increases. Thus reducing K does increase the power output as would be expected since the energy loss is reduced.(See Table 6-3).

60° valve opening.

Figure 6-39 shows the relation between the power output and the siphon height at α = 0.20. It is seen on the graph, a higher K values (K= 3-3.9), the maximum power out achieved at an optimum siphon height and the power output remains constant even though the siphon height is increased.

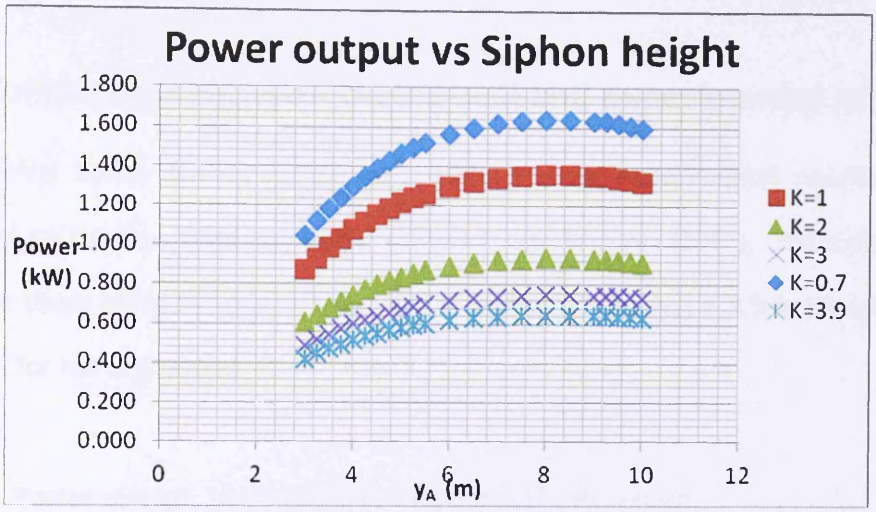

Figure 6-39 Power output at α = 0.20 and various K

The following graph (Figure 6-40) shows how changing the pipe diameter and thus increasing the flow rate will affect the power output. Theoretical calculation shows that a bigger diameter for the same height of driving head (H= 2 m) will produce a bigger power output. The graph is similar to that in Figure 6-37, showing there is an optimum height of siphon to reach the maximum power output for siphon diameter of 500 mm.

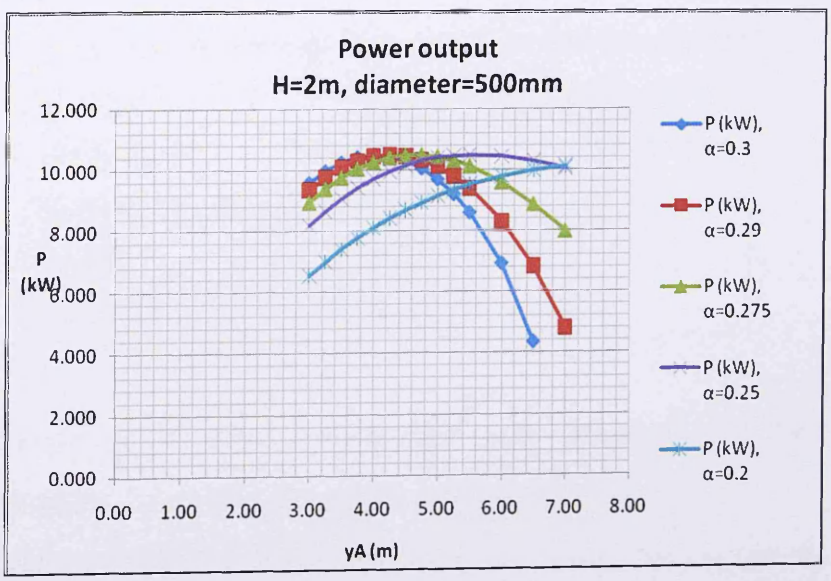

Figure 6-40 Power output vs siphon height

6.7.1 Comparison between theoretical and experimental results

The following tables give a comparison between some experimental results and the theoretical calculation from the work of French and Widden (2001). The experimental results are those using the driving head = 2 m, siphon height (y_A) = 3.5 m for low siphon, and 4.7 m for the higher siphon.

Table 6-4 Power output: Low siphon vs Theoretical calculation

Aerator1	Aerator2	Aerator3	Theoretical calculation
H ≈ 2 m ; K = 3.6 ; y_A = 3.5 m			H= 2 m ; K= 3.6; y_A = 3.5 m
254 Watts (α= 0.17, 80°)	267.5 Watts (α= 0.16, 80°)	179.3 Watts (α= 0.21, 70°)	520 Watt α = 0.20

Table 6-5 Power output: High siphon vs Theoretical calculation

Aerator1	Theoretical Calculation
451.5 Watt α= 0.18, full opening K= 3.9 y_A = 4.7 m	560 Watt α = 0.20 K= 3.9 y_A = 4.7 m

The experimental results show a lower value when compared with the French and Widden work (2001). This difference can be explained as follows:

- Theoretical formulation used by French and Widden did not include the losses due to the aeration process, namely;

1) Pressure loss due to bubble formation and detachment
2) Pressure loss due to bubbly flow development, or the presence of 'void'. (Henser, 2005)

6.8 Conclusions

Several points can be drawn from this experiment:

6.8.1 Low siphon

1) The highest void fraction of 24% was achieved using Aerator1 at 60° valve opening. Aerator1 achieved its highest power output of 254.2 Watts at 80° valve opening.
2) The highest power output, 267.5 Watts, was achieved using Aerator2 at 80° valve opening.
3) The highest efficiency of 24% was achieved using Aerator1 at 60° valve opening.
4) The highest efficiency did not occur when the highest power output was achieved.
5) The highest void fraction reached did not coincide with the highest power output.
6) Overall Aerator1 gave a better performance in terms of producing the highest void fraction, power output and efficiency.

6.8.2 Higher siphon

In the higher siphon using Aerator1 with spiral spargers:

1) The highest void fraction of 19% was achieved at full opening.
2) The highest power output, 451.5 Watts, was achieved at full opening

3) The highest efficiency of 32.3% was achieved at full valve opening.
4) The highest void fraction did not occur when the highest power output was achieved.

Overall the higher siphon produces a higher power output and a higher efficiency, but a lower void fraction compared to the low siphon.

Overall efficiency could be improved if the losses could be reduced.

Chapter 7

Qualitative Analysis of Flow Pattern

7.1 Introduction

This chapter discusses qualitatively the flow pattern of the two phase flow that results from the aeration. It analyses the air flow around the nozzle of the spargers, and the flow pattern of the mixed flow in the down pipe of the siphon.

As stated in Chapter-3 the spargers were designed with the aim of producing a homogenous bubbly flow in the end pipe section (below the spargers). When achieved, this type of flow is more likely to maintain a stable continuous flow that has a high void fraction. Thus more air is being drawn in and so a higher power output occurs, the latter being the real objective of this investigation.

7.2 Observation close to the Sparger holes

The following figures show the flow patterns. The pictures in Figure 7.1 show the pattern that occurred when the air exited from only one hole of the sparger at a very low flow rate.

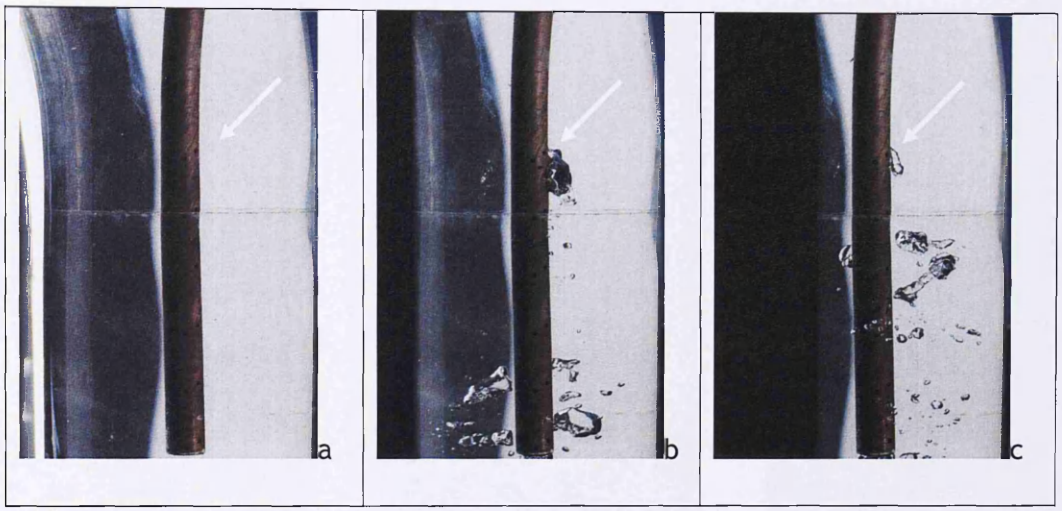

Figure 7-1 Air exits from one hole of the spargers

The white arrow in Figure 7-1a shows the top hole of the sparger. It can be seen in Figure 7-1b and 7-1c that it did not always form a single bubble. There could be bubble pairing (see Figure 5-8, in Chapter 5). The water flow detached the coalesced bubbles downward, breaking them into a combination of single bubbles, and coalesced bubbles in irregular shapes.

Figure 7-2 shows the development of the flow pattern around the nozzles starting with only one hole and continuing until all the sparger holes are operating.

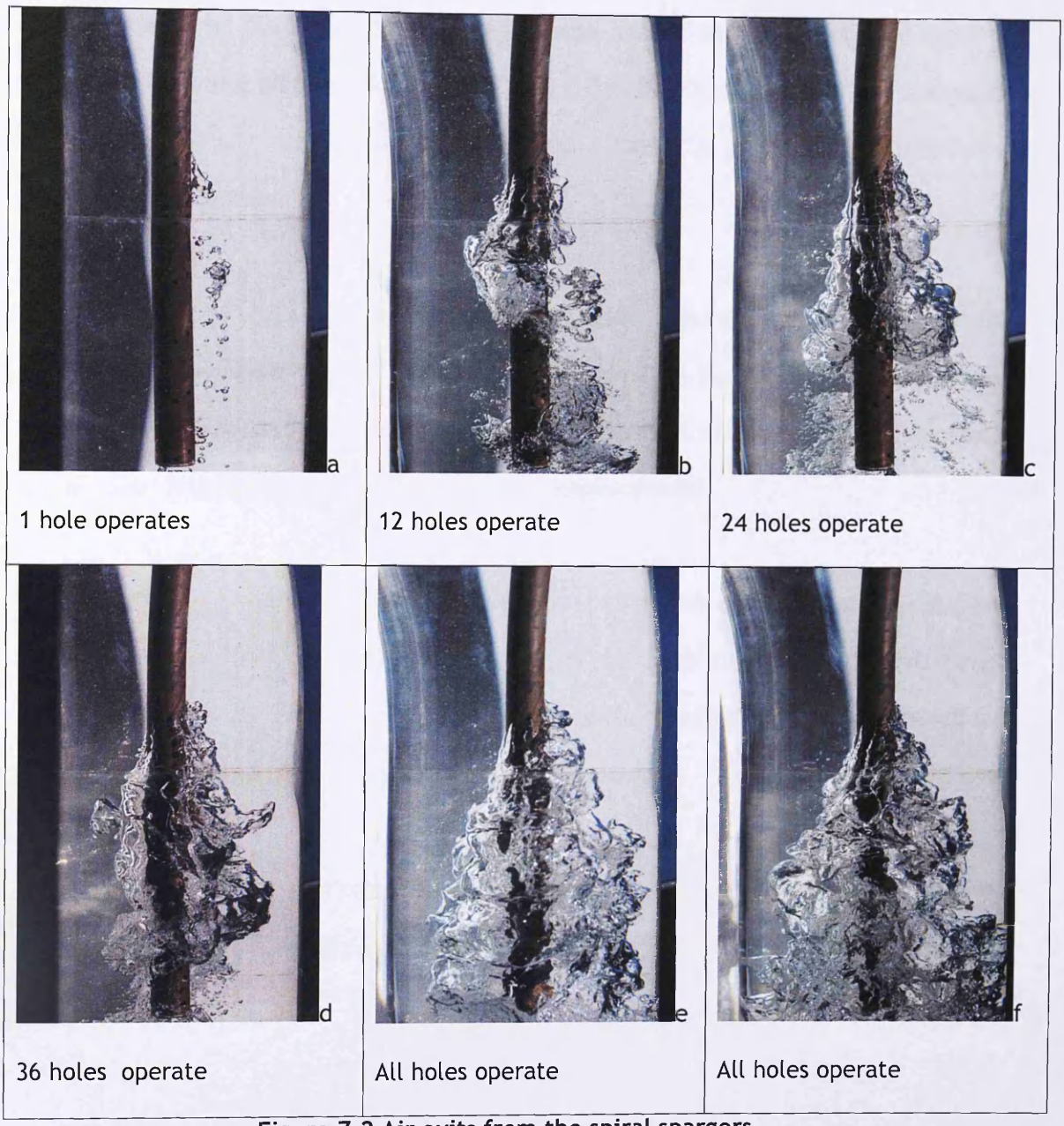

Figure 7-2 Air exits from the spiral spargers

Figures 7-2a to 7-2f show how air was entering the siphon. At the beginning, it started with the top hole operated. A small bubble or bubble pairing very quickly detached from the nozzle and flow downwards and then disintegrated into smaller bubbles of varying size and irregular shape. Gradually, when the air flow rate increased, the lower holes

started operating. It was no longer a small single bubble detached from the nozzle, instead, it formed a jet of air flow (Figure 7-2b -7-2d).Eventually all the holes operated and form a cone of air low surrounding the aerator tube. The air flow also rotated and swung on the way down.

At a very high air flow rate, the flow became fully turbulent. An air cone formed surrounding the copper pipe of the Aerator (Figures 7-2e Figure 7-2f). The air cone diameter increased with an increase in the air flow rate. At the bottom of the aerator, the air cone detached and a vigorous swirling motion occurred.

Yang et al (2001, page 2003-2004) reported that 'it *remains unclear that how and to what extent, the different forces acting on the gas bubble alter the behavior and characteristics of the bubble growth and detachment on vertical surfaces, compared to that of the bubbles on horizontal surfaces'.*

When the air flow rate increased, the air exited from more holes of the sparger until it looked like a stream of air (shown by the white arrow in Figure 7-3).

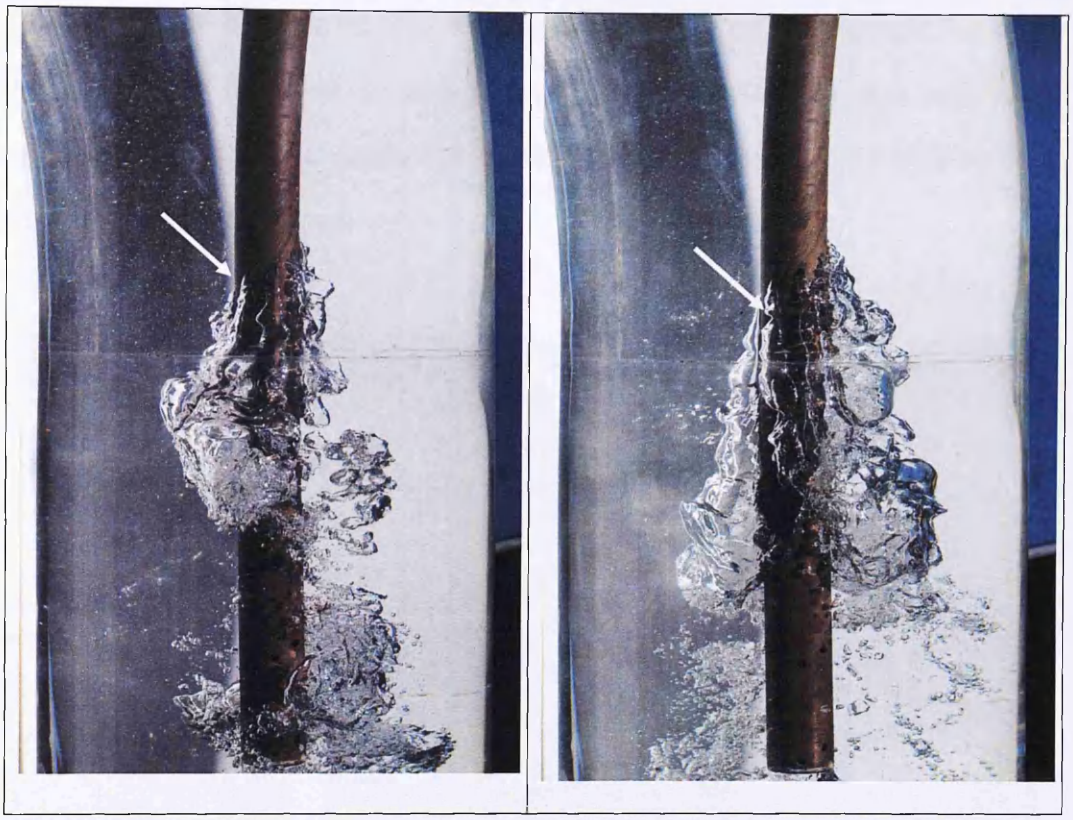

Figure 7-3 Air stream exits from the spiral spargers

7.2.1 Observation at 60^0 valve opening

There are two types of sparger configuration, i.e. straight line spargers, and spiral spargers, each type creating different flow patterns. The spargers are located just below the pipe bend, the inner side of the bend being located above and on the left side of the photos.

Figure 7-4 shows the flow pattern around the straight line spargers of Aerator1 for air flow rates from 200 l/min to 400 l/min with a 60^0 butterfly valve opening. As the air exited from the holes of the sparger it formed a cone shape that moved towards the right side of the pipe. This happened because the water pressure on the inside of the

bend (the left side in the figures) is lower than the pressure on the outside. The cone got larger as the air flow rate increased. Eventually it touched the pipe wall (blue arrows) on the outside of the bend (right side). When this happened it indicated that very soon the siphon would break.

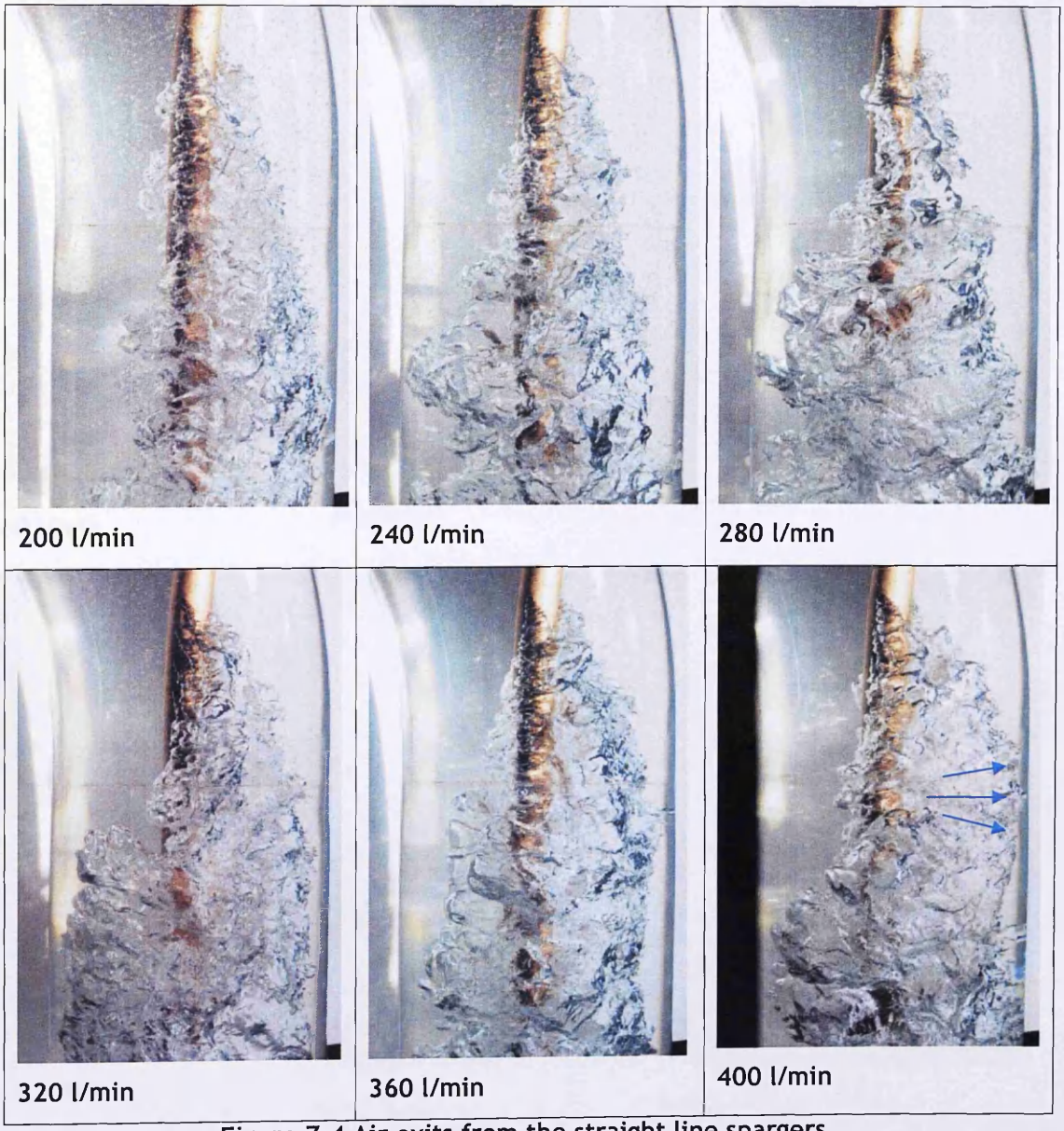

Figure 7-4 Air exits from the straight line spargers

Figure 7-5 shows the flow patterns around a spiral sparger at a 60^0 butterfly valve opening in the copper pipe. It moves away from the pipe and becomes detached. It then continues revolving in the siphon pipe before breaking into a bubbly flow.

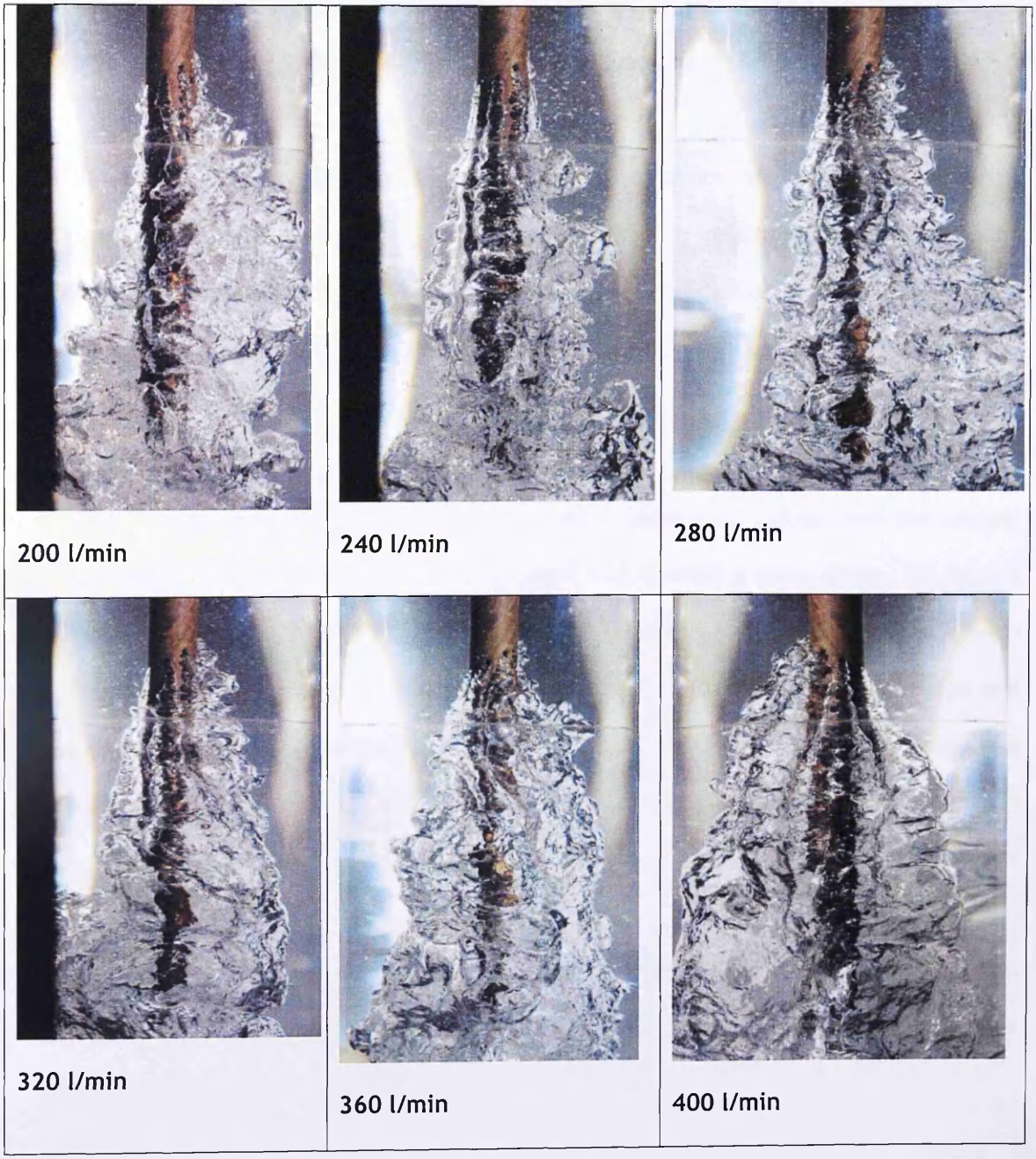

Figure 7-5 Air exits from the spiral spargers

These patterns are similar to those from a straight line sparger. As seen, the air exits the sparger holes in the form of air jets. These accumulate and form a conical shape that looks symmetrical. The cone oscillates and rotates around the copper pipe as it moves downward, and gradually detaches from the lower part of the pipe. When it is completely detached it continues revolving before breaking into a bubbly flow.

In the spiral hole configuration the air flow seems to move downwards faster than it does for the straight line sparger. The cone takes longer to expand and touch the siphon pipe. Thus flow does not form a break so quickly. This observation is consistent with the test results that showed, both in the lab and on the site, that the spiral sparger achieved a better result.

It is still similar to the straight line one. In a spiral sparger air exited from the sparger holes in the forms of jet air and accumulated and formed a cone shape. By eyes it looked relatively symmetrical and created a wavy air flow rather than curly flow as seen in the straight line spargers. The air cone swung and rotated around the copper pipe and moved downward, and gradually detached at the lower part. When it completely detached it started to swirl in the down leg pipe, and gradually broke into smaller bubbles and eventually created a bubbly flow zone.

The spiral holes configuration helped the air flow moving downward faster compared to the straight line spargers. In the spiral spargers the air also swings around the copper pipe and is more dynamic than in the straight one.

Similar to the straight line spargers, when the air cone started to touch the pipe wall of the outside bend, it pushed the water upward, moving back to the siphon inlet direction. At this stage, it was a sign that the siphon would break very soon.

Since the tendency of shifting to the outer bend was reduced in the spiral sparger (see Figure 7-5), this means that it would delay the air cone touching the wall. As we understand that when the air cone touches the wall it will trigger the siphon break, so it is good to produce a relatively symmetrical air cone rather than it is heavy to the right side. That is why a spiral sparger produces more of an air flow rate.

7.2.2. Observation at full opening

Figure 7-6 shows the flow pattern around the straight line spargers when the butterfly valve was fully open and with high air flow rates ranging from 500l/min to 620 l/min.

They demonstrate that the air cone around the sparger becomes larger with the increase in the air flow rate. The air cone was seen to rotate rapidly around the sparger and tended to shift to the right side (outer bend) of the pipe due to centrifugal force (white arrows).

The butterfly valve on the horizontal segment of the siphon has created what is called a "Karman Vortex Street" (Fig. 7-7) downstream of the valve. As the velocity of the flow increases the effect of these vortices becomes magnified. This causes very unstable flow patterns (Wood and Clark, 1988).

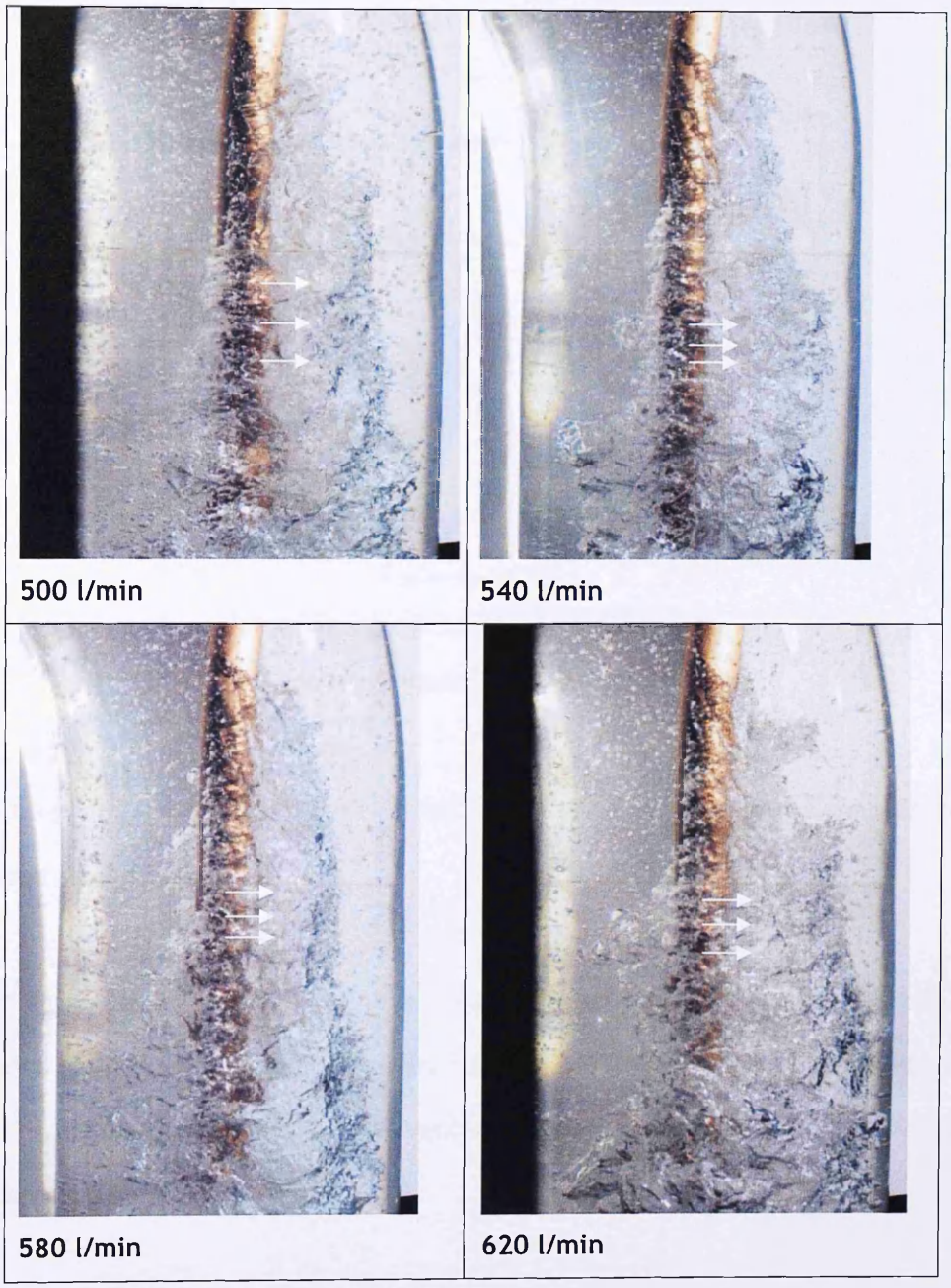

Figure 7-6 Flow pattern around the straight line spargers - full opening

The presence of equipment that generates such flow would be very detrimental to the establishment of conditions suitable for a bubbly flow as well as causing additional energy losses.

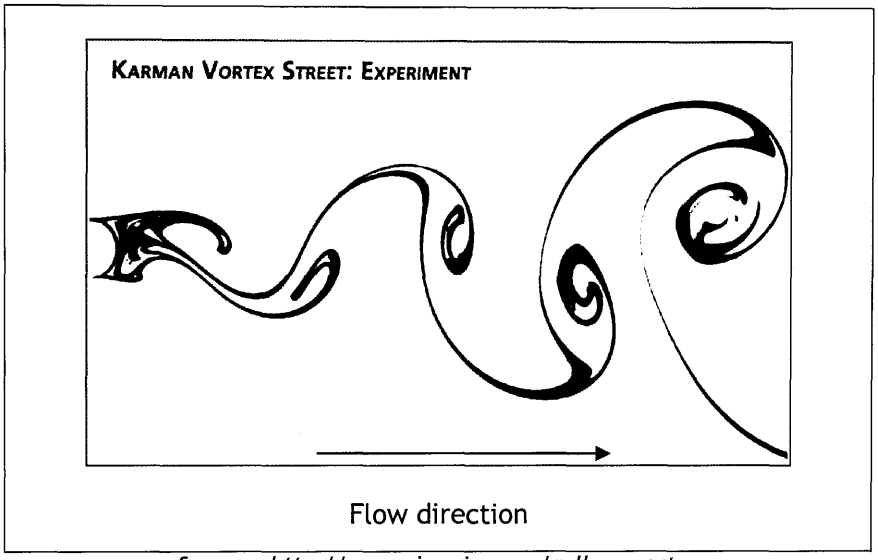

Sources: http://www.simerics.com/gallery_vortex

Figure 7-7 Karman Vortex Street

The pictures in Figure 7-8 show the pattern of aeration at 620 l/min flow with a fully open valve.

The air flow direction of the air cone bubble is shown by the white arrows. The movement of the outer edge of the cone towards and away from the right side of the pipe is readily observable. If the cone touches the pipe it can create the conditions for a siphon break. This is discussed below.

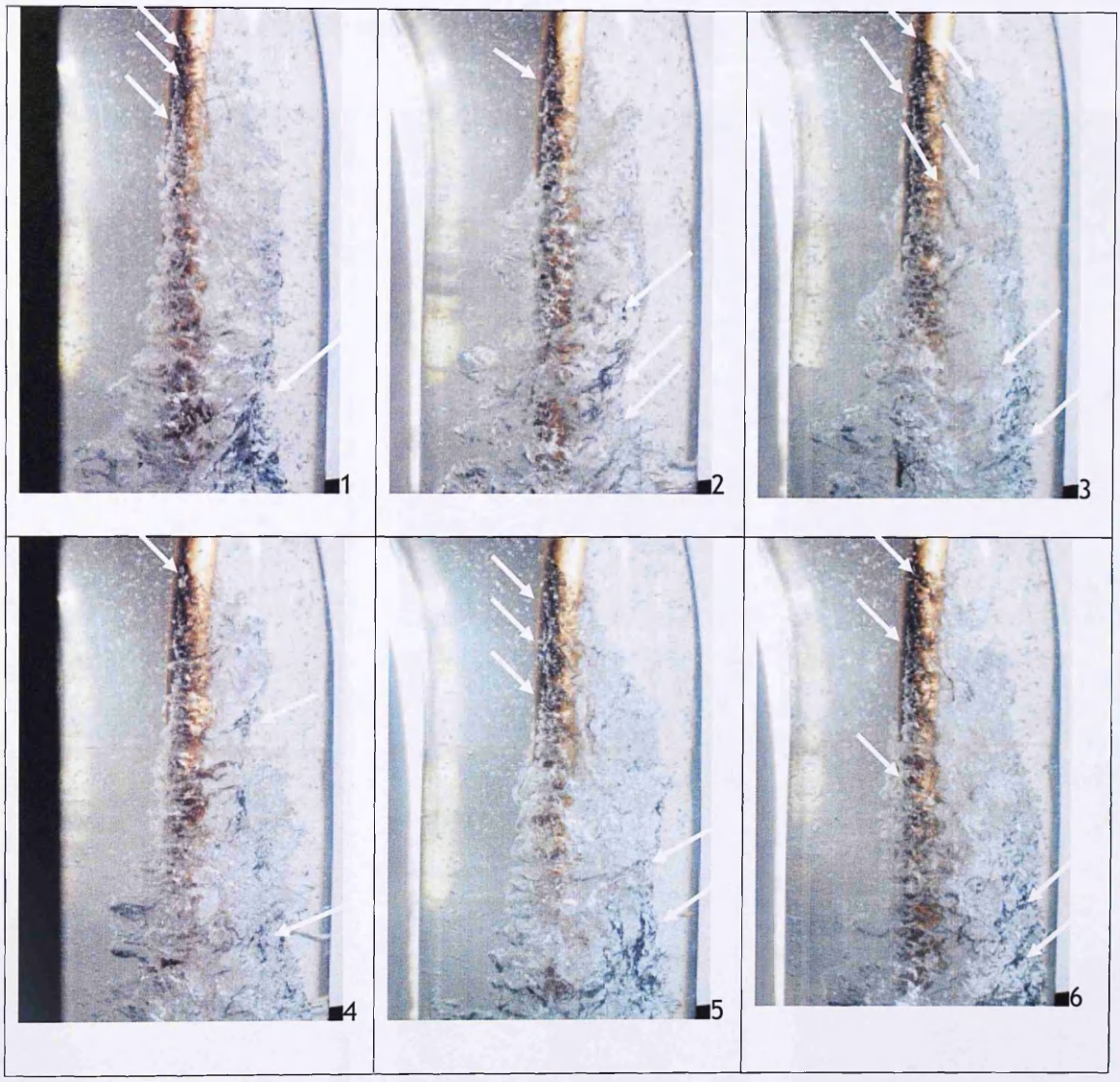

Figure 7-8 Aeration sequences - full opening -straight at 620 l/min

7.3 Observation when the siphon breaks

The siphon breaks at a high air flow rate when the air cone starts to touch the wall of the outside bend of the pipe (Figure 7-9-1). It then extends up the pipe wall (shown by the blue arrows in Figure 7-9-2). Next the cone touches the aerator pipe (white arrows) and creeps up (Figure 7-9-3). Eventually, the whole aerator is covered by a cloud of air

which extends towards the siphon inlet and a break occurs. (Figure 7-9-4 to 7-9-6).

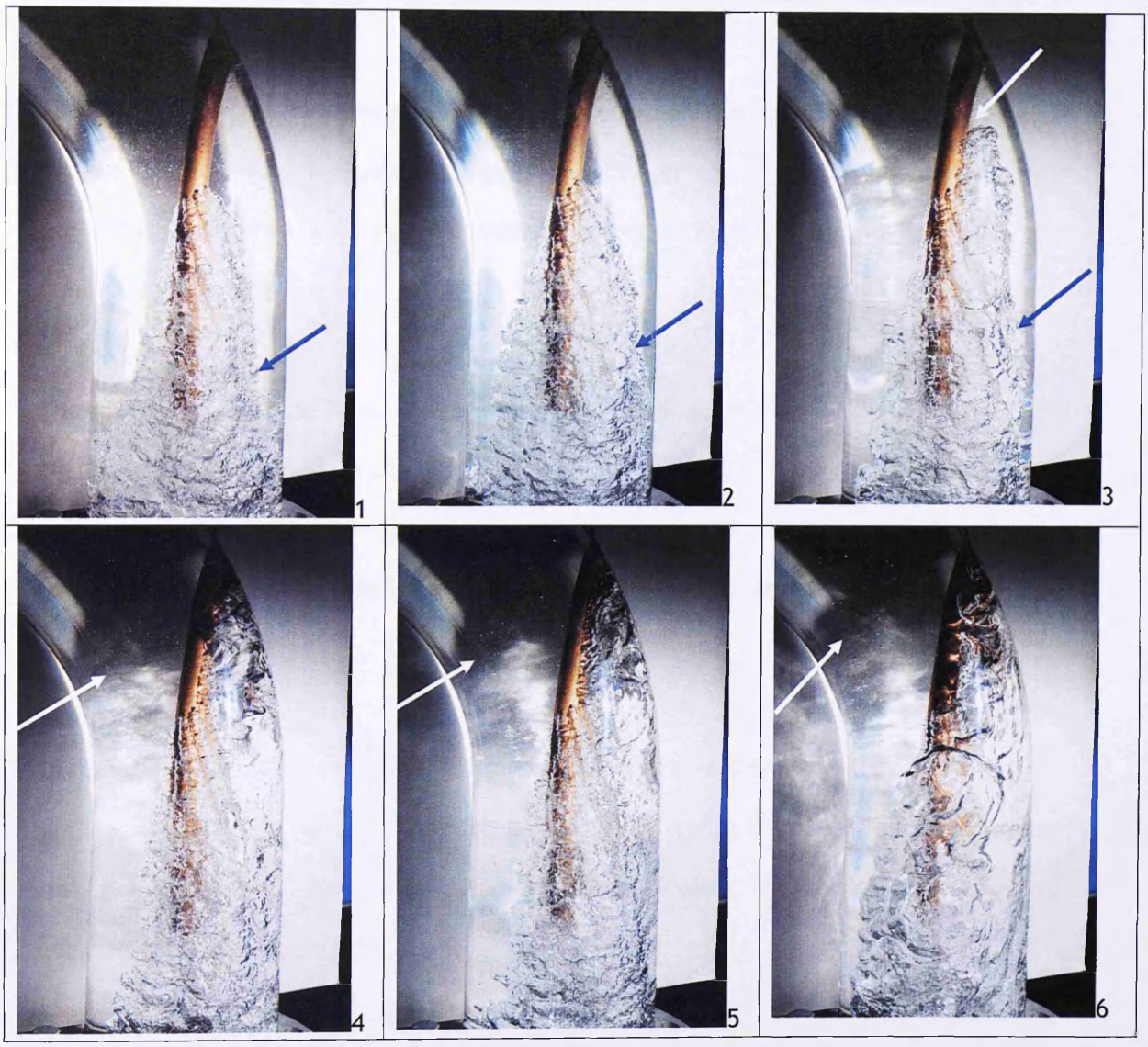

Figure 7-9 Sequence when the siphon breaks

Another sign when the siphon is in critical condition, i.e. to the direction of breaking was that the pendulum of the rotameter fluctuated up and down, instable. This would trigger the instability inside of the siphon around the aerator, as indicated the air cone

touched the outer bend siphon wall. In this situation, the air flow must be reduced by adjusting the rotameter valve opening slightly, so that the pendulum was stable again.

The sign that the siphon broke was also identified when the water level in the top tank increased. This was because the water velocity in the siphon dropped and then eventually the siphon flow stopped, whilst the water from the bottom tank was still pumped to fill in the top tank.

Therefore, in order to keep the siphon flow continuously, we have to control the position of the water level of the top tank, to maintain it in the stable position. The same thing with the rotameter pendulum, need to be maintained in a stable position, not fluctuated wildly to prevent the air surrounding the aerator not touching the pipe wall.

Observation showed that care needed to be taken so that this critical situation did not occur in the higher siphon (y_A= 4.7 m) when the airflow rate increased to values greater than 600 l/min and in the lower siphon (y_A= 3.5 m) when air flow rate increased to values greater than 500 l/min.

Figure 7-10 shows more patterns of the siphon break. The blue arrows show the back water and air flow to the direction of the siphon inlet.

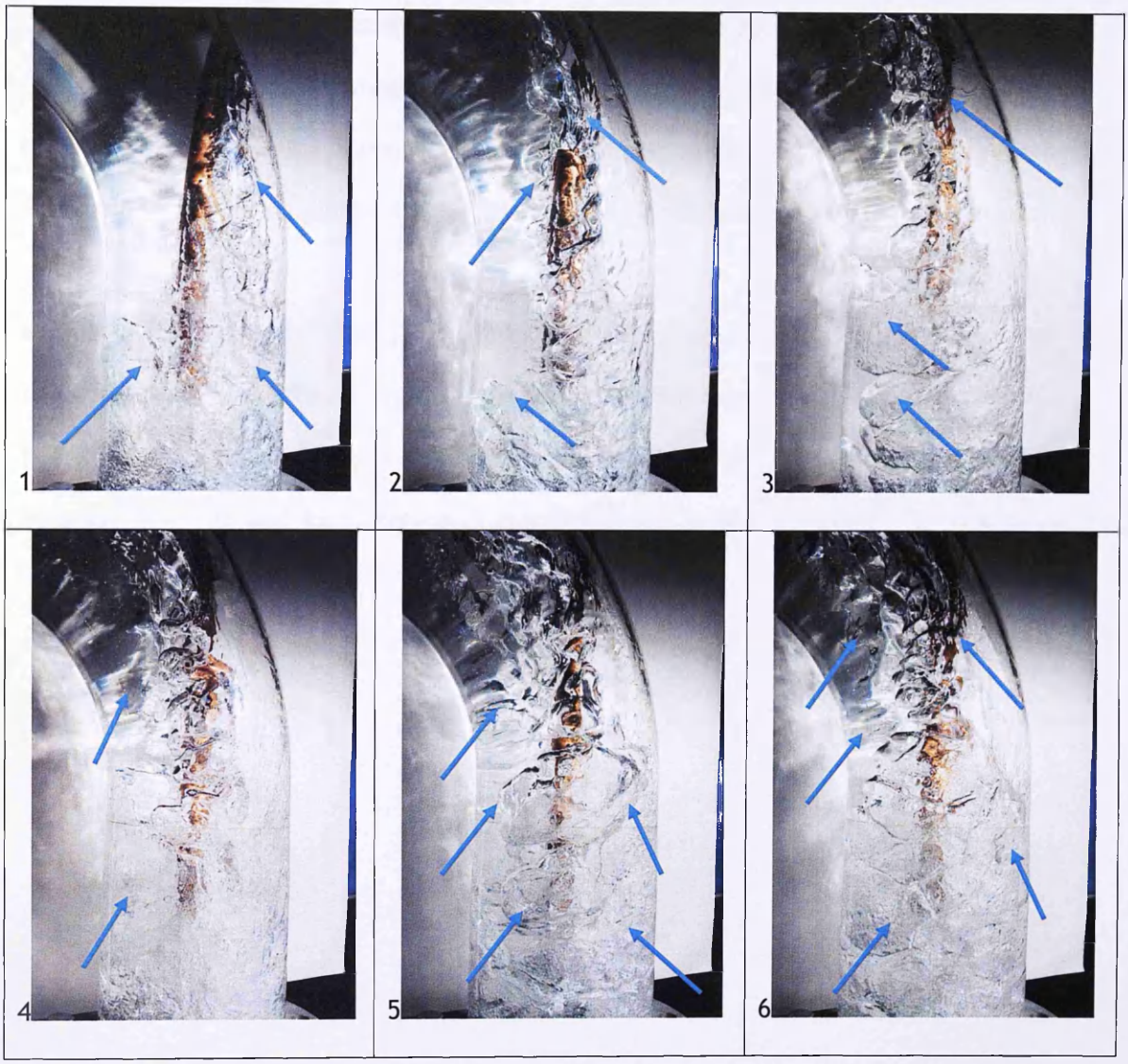

Figure 7-10 Sequence when the siphon breaks

7.4 Flow Pattern in the Down Pipe

Figure 7-11 shows the flow pattern for the 100 l/min air flow rate in the down pipe of the siphon. The flow pattern changes along the pipe. Figure 7-11 a, b, and c.

The flow pattern looks like a cloud of coalesced bubbles around the exit holes of the spargers. The entering air created a jet stream and formed a cone shape shown by a

white arrow (A). Once it detached from the aerator, it coalesced into large bubbles and then gradually broke into smaller bubble sizes (B). Eventually it formed a bubbly flow (C). This was relatively homogenous and uniformly dispersed along the pipe cross section. The bubble size in the bubbly zone was estimated to be approximately 5-6 mm.

At this air flow rate, the bubbly flow occurred 60 cm below the top hole of the sparger. The bubble concentration increased along the down flow (see Figure 7-11: d, e, and f). The white arrows with (D) symbols show that not all of the pipe cross section filled with bubbles. This indicates the presence of circulation and a spiral turbulent flow due to the bend and the butterfly valve.

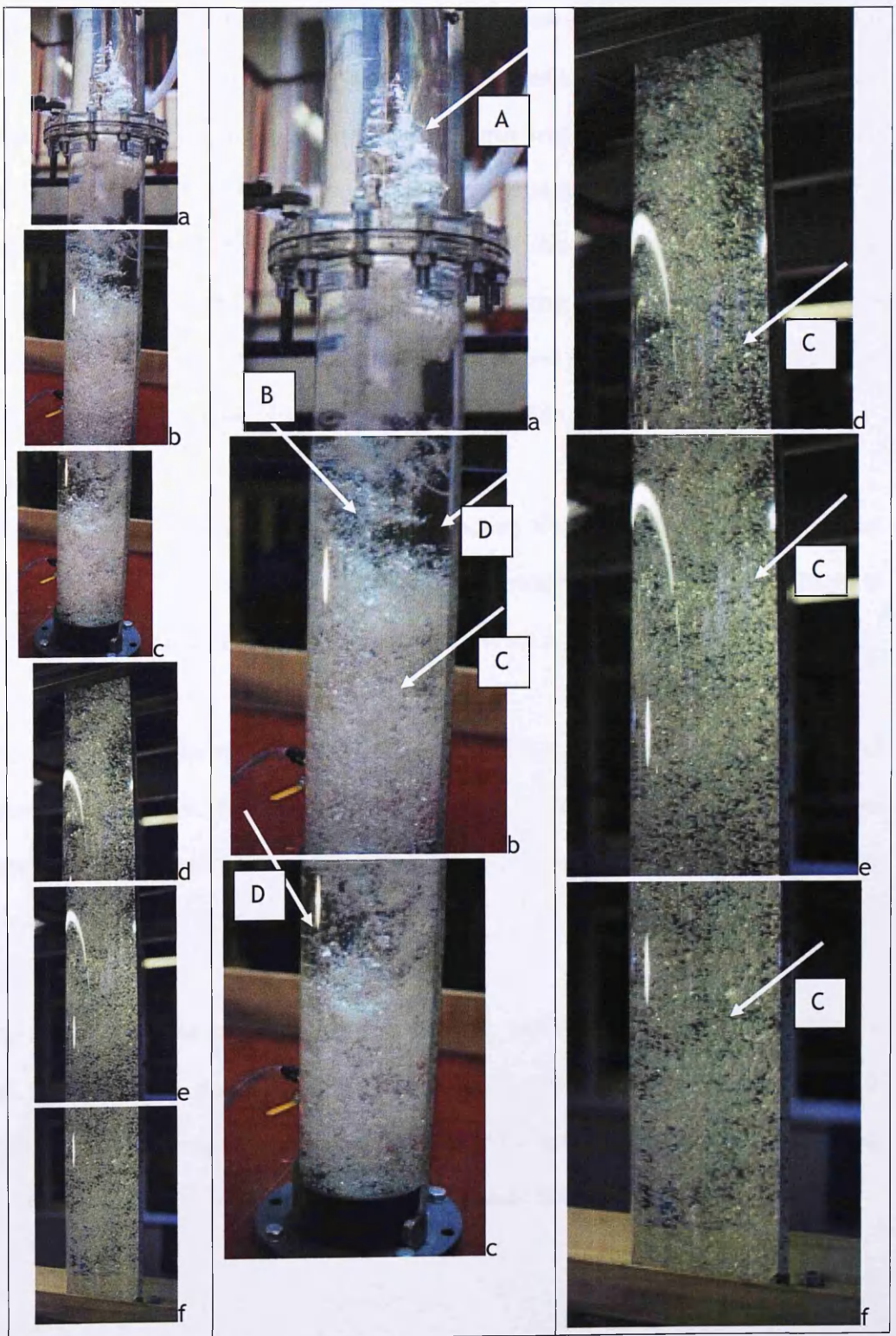

Figure 7-11 Flow pattern -100 l/min aeration

Figure 7-12 shows the flow pattern with a bigger air flow rate, i.e. 600 l/min. As the flow rate was increasing, the cloud of coalesced bubbles were continuing flowing downward further and it gradually disintegrated into smaller bubbles in various size further down, below the platform. Along the down leg pipe, the mean diameter of the bubbles decreased. This is because at the lower part of the down leg pipe, the pressure is higher than the upper part. This pressure compresses the air bubbles. Aissa et al have carried out an experiment using various air tube length and diameter to find the bubbles mean diameter along the down pipe which showed a similar result.

Yet, because the air flow was turbulent and caused the swirling and spiral motion downwards, we could not treat the bubbles as individual entities. That is why it is difficult to model the turbulent regime reliably (Buyevich and Webbon,1996).

Similar to Figure 7-11, the flow pattern started as a cloud of coalesced bubbles around the nozzles of the sparger. This formed an air jet that transformed into a cone as shown by a white arrow (A). After the coalesced bubbles were completely detached from the nozzles they moved downward (Arrow B).

Gradually they broke into individual smaller bubbles (white arrow C) in various shapes and sizes. In the bubbly zone, the single bubble size ranged between 4.5 mm and 7.5 mm of diameter in an irregular oval shape rather than a sphere. Because of the swirling motion of the flow it was not possible to track individual bubbles.

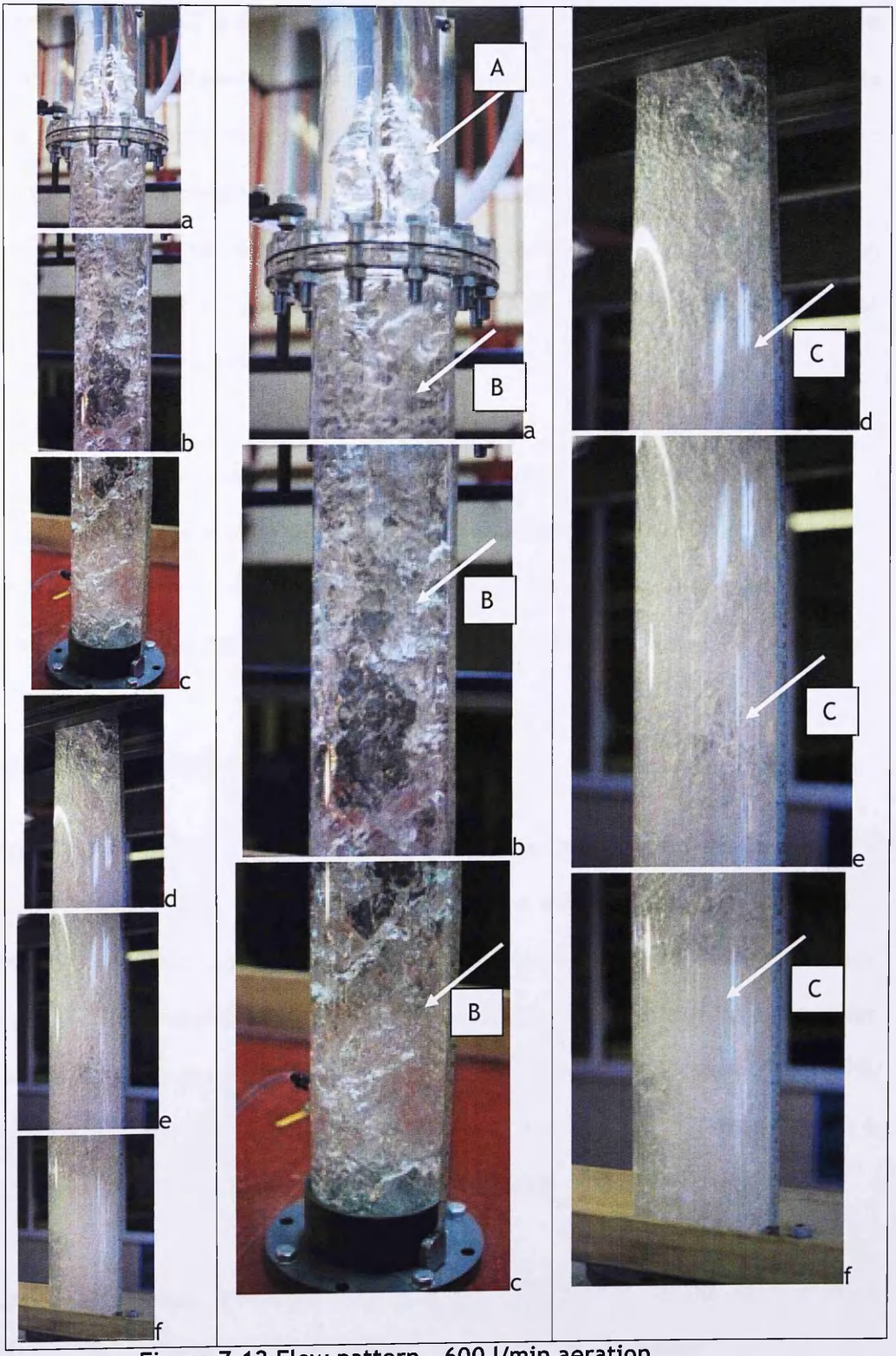

Figure 7-12 Flow pattern - 600 l/min aeration

From Figure 7-11 and 7-12 it can be concluded that the length required to change from the coalesced bubble pattern (slug or churn flow) into relatively homogenous bubbly flow varies according to the magnitude of the air flow rate. The higher the air flow rate the longer the transition length needed to affect this change.

Hasan (1995) reported that the transition between bubbly flow and slug flow in an upward vertical pipe occurs at a void fraction, $\alpha = 0.25$. He proposed that the same criteria could apply to downward flow as well.

Similar flow patterns were also found in Aerators 2 and 3. In the upper part of the down pipe and the siphon there was an accumulation of coalesced bubbles. Going downward, the coalesced bubble size was smaller and eventually these broke into single bubbles and created a bubbly flow pattern (See photographs in **Appendices C1 - C4).**

7.5 Findings and results

It was stated in the Chapter 3 the major objective of this investigation was to design an Aerator with a lot of small holes that would create a bubbly flow in the siphon. Observation showed that spargers with 3 mm diameter holes could not immediately create a bubbly flow pattern. There was a transition of the flow pattern from the upper part of the down pipe to the bottom part. The flow started as a cloud of air. This changed into a slug, or churn flow when the air flow rate was high, or wispy flow in a high mass water flow rate, and eventually into bubbly flow.

In the bubbly flow regime, it was not possible to track the bubbles as individual entities because the swirling motion due to the turbulence and the vortex motion.

Thus, in a sparger, holes of 3 mm diameter are not small enough to create a bubbly flow pattern.

Creating a smaller bubble size can be achieved by reducing the diameter of the holes (Bhunia et al, 1998; Aissa et al, 2010), because smaller holes produce smaller bubbles which are easy to be detached by the liquid drag force. With smaller diameter holes the number of holes must be increased so that the total opening area is the same as the cross section area of the copper pipe.

However, reducing the hole's diameter to a smaller size may cause more pressure head loss (see Chapter 5) and a reduction in power output.

Proposed changes in the design to achieve more aeration will be supplied in Chapter 8.

Chapter 8

Conclusions and Recommendations

The main contributions of the present works towards low head hydro power using aeration i.e. based on conversion from water to air pressure are summarised here. It is then followed by suggestion on future research directions based on the findings obtained from this study.

8.1 Conclusions

This research established the following results.

- In the laboratory, with relatively high overall coefficient (K = 3.9) in the pipe system due to the restricted space, it is possible to harvest above 30% of the energy available at a low head hydro site. On site experiment, with some improvement, i.e. using bell mouth inlet-outlet, large bend radius, and no butterfly valve, the K reduced significantly up to one fourth (K≈1). This increased power output as well as efficiency. This is a marked improvement over previous research findings.
- The copper tube spargers with the holes cut in a spiral pattern along the pipe performed the best.
- There is a specific combination of siphon height (y_A in the above material) and air flow rate that gives the best result. This finding from a full scale experimental rig is consistent with the theoretical research accomplished by French and Widden (2001)

- It is very difficult to produce the bubbly flow pattern (considered to be ideal for this process) when 3mm diameter sparger holes are used in the aerator. The lack of this flow regime is considered to be a major reason why at low siphon, the highest power output was not achieved at the highest void fraction.
- Any part of the equipment that contributed to producing more turbulence in the flow (e.g. the butterfly valve) should be removed or modified.
- The aeration process would improve the water quality down stream of the siphon as it would add oxygen to the water.
- If larger pipe sizes were used the siphons may provide a passage for fish migration. The presence of the sparger pipe may be an obstacle to fish movement in smaller diameter pipes.

8.2 Recommendations for future research

It is recommended that further investigations incorporate the following features.

- Sparger orifice holes of 3 mm diameter (or less) should be used, and the total cross-sectional area of these holes should be at least 20% than the current aerator design. Since the total area must be equal or less than the area of the nozzle, the nozzle diameter needs to be increased 20% or more.
- Any future experimental rig should be like that in Fig 8.1 but with the following modifications - all of which are designed to reduce the turbulence level in the flow.

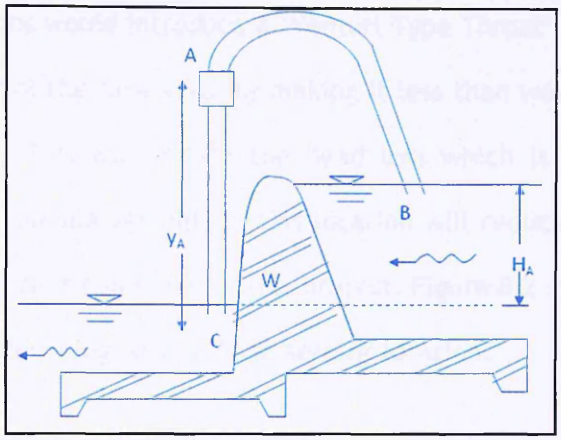

Figure 8-1 Siphon system

(H_A= driving head, S=siphon, A= aerator, B= inlet, C= outlet, W = weir, y_A= aerator height)

Bell mouth entry at B and C

(a) Pipe diameter from B to A to be 300mm

(b) A 300mm length (A to A_1) of conical pipe section, reducing in diameter from 300mm to 200mm

(c) A 300mm length of 200mm diameter pipe from the section A_1 to A_2. This section of the pipe to be where the sparger is located.

(d) A second conical section, 500mm in length and expanding from 200mm to 300mm from A_2 to A_3

(e) The remainder of the pipe to be 300mm in diameter, exiting in a bell mouth

(f) The sparger pipe to enter the siphon at point A_3 and project upwards against the flow rather than enter it as in the current system.

(g) The water flow rate should be set flexibly according to the upstream water level rather than using a butterfly valve.

(h) The height of the aerator (y_A) should be the optimum height, referred to the theoretical calculation based on French and Widden (2001). See Chapter 6.7.

The suggested modifications would introduce a 'Venturi Type Throat' into the pipe. The diameter of this will control the flow velocity making it less than would occur if all the pipe is 300mm diameter. This will reduce the head loss which is a function of the velocity squared. Placing the sparger pipe in this location will reduce the turbulence it would create if placed where it had been for this project. Figure 8.2 show in more detail the Venturi Throat in the down leg part and the aerator location.

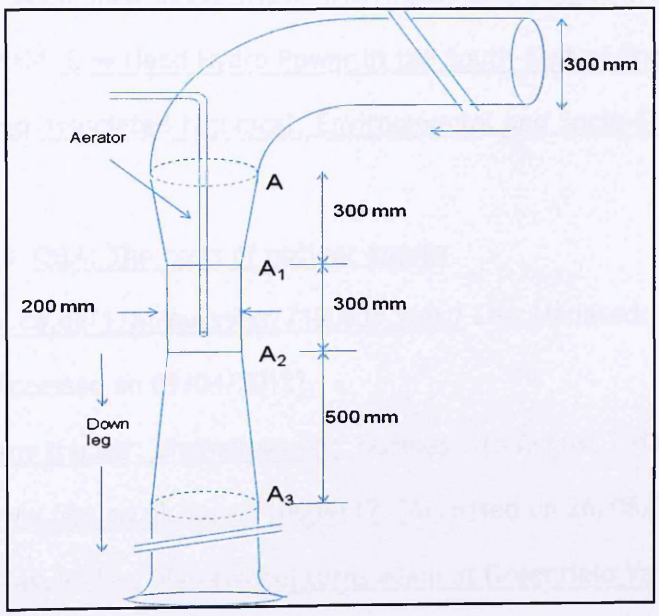

Figure 8-2 Venturi around aerator

References

Aissa, W.A et al, 2010. Performance Analysis of Low head Hydraulic Air Compressor. Smart Grid Renewable Energy, 2010, No. 1, pp 15-24.

Alternative Technology Centre. Power from the Landscape. http://www.powerfromthelandscape.co.uk/. 01 June 2011

Arnott, Sarah. 2010. Lord Turner: 'We must act now to meet energy targets'. The Independent, 10 September 2010. http://www.independent.co.uk. 11 January 2011

Bacon, I., Davison, I., 2004. Low Head Hydro Power in the South-East of England - A review of the Resources and Associated technical, Environmental and Socio-Economic Issues. TV Energy

BBC News Channel, 2008. Q&A: The costs of nuclear energy http://news.bbc.co.uk/1/hi/business/7180539.stm./ Last Updated: Thursday, 10 January 2008. [Accessed on 09/04/2012].

BBC News, 2012. Economy tracker: Unemployment. Business. 15 August 2012 Last updated at 12:03. http://www.bbc.co.uk/news/10604117. [Accessed on 26/08/2012].

BBC, 2010. BBC -North East Wales. Waterwheel turns again at Greenfield Valley Heritage Park. 26 March 2010 http://news.bbc.co.uk/local/northeastwales/hi/people_and_places/newsid_8589000/8589713.stm

Bedard, R, Epri (Ed), 2005. Tidal in Stream Energy Conversion (TISEC) Devices. http://oceanenergy.epri.com/attachments/streamenergy/reports/004TISECDeviceReportFinal111005.pdf

Bellamy, N.W.,1995. The Syfogen Low-head Pneumatic Hydroelectric System. Conference on: Hydropower into the Next Century, Barcelona.

Bhunia, A. et al, 1998. Bubble Formation in a Coflow Configuration in Normal an Reduce Gravity. AlChe Journal. July 1998. Vol 4, No. 7, pp 1499-1509.

British Hydro Association, 2005. A guide for UK Mini Hydro Development. Technology http://www.british-hydro.org/mini-hydro/infopagef10a.html?infoid=362 [Accessed 17/04/2012]

Buyevich, Y.A., Webbon, B.W., 1996. Bubble formation at a submerged orifice in reduced gravity. Chemical Engineering Science. Vol. 51,. No. 21, pp 4843-4857.

Chisholm, D., 1983. Two phase flowing pipe lines and heat exchangers. Essex: longman Group Limited.

Coe, T., Kibel, P., 2012. Forge Weir/River Lune Fisheries Assesment. First Draft. 8 May 2012. Fishtek Consulting Ltd. Dartington.

Crow, C.T., et al, 2001. Engineering Fluid Mechanics. Seventh edition. New York: John Wiley and Sons, Inc.

Das, D., 2010. Developing Small Hydroelectric Projects in the Indian Himalayas - Issues and Option. Proceeding on 16th International Seminar on Hydropower plants. Vienna University of Technology.

Date, A., Akhbarzadeh., A.,2009. Design and cost analysis of low head simple reaction hydro turbine for remote area power supply. Renewable energy34 (2009) 409-415

Department of Energy and Climate Change, 2010. Electricity Statistics. Digest of United Kingdom Energy Statistics (DUKES) 2010. Last updated 28 July 2011.http://www.decc.gov.uk/en/content/cms/statistics/energy_stats/source/electricity/electricity.aspx. [Accessed on 12/04/2012].

Department of Energy and Climate Change, 2010.England and Wales Hydropower resourcse Assemnet. Final report, October 2010

Department of Trade and Industry, 2007. Meeting the Energy Challenge. A White Paper on Energy. May 2007.

Dhotre, M.T., Joshi, J.B. 2006. Design of gas distributor: Three -dimensional CFD simulation of a coupled system consisting a gas chamber and bubble column. Chemical Engineering Journal.125 (2007) 149-163

Dragu, C., et al, 2001. Small Hydro Power, State of The Art and Applications. International Conference Power Generation and Sustainable Development (pp 265-270), Liege.

Earnshaw, M. et al, 2010. Development of Siphonic Hydro power and aeration systems. Project report. Master degree program. Engineering Department Lancaster University.

Environment Agency, 2010. Opportunity and environmental sensitivity Mapping for Hydro Power in England and Wales. Bristol. 4 March 2010

Environment Blog, 2010. What are your top green books?. http://www.guardian.co.uk/environment/blog/2010/jan/27/top-50-green-books. [Accessed on14/04/2012].

Experiment Resources.Com. How to Make an Archimedes Screw. *http://www.experiment-resources.com/archimedes-screw.html.* Accessed 19/10/11

Fox, R.W., McDonald, A.T (2001). Introduction to Fluid Mechanics. New York: John Wiley and Sons.

French, M.J., Widden, M.B., 2001, 2004. The Exploitation of Low-head Hydropower by Pressure Interchange with Air, using Siphons. Proceedings of International Conference on Mechanical Engineering Vol 215 Part A.

Friends of the Earth, 2012. Hydro Power: How Hydro power works: The Archimedes Screw. http://www.foe.co.uk/campaigns/climate/how_hydro_power_works_8280.html. [Accessed on July 2012]

Grossetete, C., 1995. Caracterissation Experimentaleet Simulation de l'Evolution d'un Ecoulment diphasique a Bulles Ascendant dans Une Conduit Verticale. PhD thesis, Ecole Central Paris.

Guy-Jobson, T , 2011. Giant screw in place for river hydro project. The Northern Echo News. 24 March 2011 http://www.thenorthernecho.co.uk/news/8928356.Giant_screw_in_place_for_river_hydro_project/ [Accessed on 16/04/2012]

Hanser, Steven, 2005. Low head hydro power. Final year project. Engineering Department Lancaster University.

Hartenberg, R.S., Denavit, J, 1960. The Fabulous of Air Compressor. Machine Design. Volume 32 No. 15. July 1960

Hasan, A.R., 1995. Void Fraction in Bubbly and Slug Flow in Downward Vertical and Inclined SPE Production and Facilities, August 1995. pp 172-176.

Hetsroni, Gad, 1982. Handbook of Multiphase Systems. New York: McGraw Hill Book Company

Hibiki et al (2004). Structure of Vertical downward Bubbly Flow. International journal of Heat and Mass Transfer 47 (2004) 1857-1862

Hibiki, T., Ishii, M. (2002). Distribution Parameter and Drift velocity in Bubbly Flow using Drift Flux Model. International Journal of Heat and Mass Transfer 45 (2002) 707-721.

Highlands & Islands Community Energy Company, 2006. Stornoway waterwheel turns history around. Community Energy News. Issue One January 2006. http://www.communityenergyscotland.org.uk/assets/0000/3724/Community_Energy_News_Jan_2006.pdf. [Accessed on 13/04/2012]

Howey, DA, Pullen, KR, 2008. Hydraulic Air Compressors for Low Head Hydro-power.City University, London. http://www.ieahydro.org/uploads/files/annexii_fish_passage_smallhydrosites.pdf.

[Accessed on 20/08/2012].

International Energy Agency, 2010. World Energy Outlook 2010 Factsheet. OECD/IEA 2010

Jain, S.C.,1988. Air Transport in Vortex-Flow Drop Shaft. Journal of Hydraulic Engineering. Volume 114, No.12, December 1988.

Jean Therrien, J., Bourgeois, G., 2000. Fish Passage at Small Hydro Sites. The International Energy Agency - Implementing Agreement for Hydropower Technology and Programmes. March 2000. Québec: Genivar Consulting Group Inc.

Joule Centre, 2008. Low head hydro power - new opportunities in the UK water industry. Wednesday, 01 October 2008. http://www.joulecentre.org. [Accessed on 10/04/2012].

Kalkach-Navaro, S., 1992.The mathematical Modeling of Flow Regime Transition in Bubbly Two phase Flow. PhD thesis, Rensselaer Polytechnic Institute, USA

Kashinsky, O.N., Randin, V.V., 1999. Downward Bubbly Gas-Liquid Flow in a Vertical Downward Pipe. International Journal of Multiphase Flow 25 (1999) 109-138.

Kippax, V., 2011. http://www.waterworld.com, 2011

Kirk, 1999. Small-Scale Hydro Power in the UK. Journal CIWEM, 13 June 1999.

Kundu, et al, 1995. Experimental Studies on a Co-current Gas-liquid Down flow Bubble column. International Journal Multiphase Flow. Vol. 21, No.5, pp.893-906.

Liu, T.J., 1989. Experimental Investigation of Turbulent Structure in Twophase Bubbly Flow. PhD thesis, North Western University, USA.

Majumder et al, 2006. Bubble size distribution and gas -liquid interfacial area in modified down flow bubble column. Chemical engineering Journal 122 (2006) 1-10.

McCann, D.J., 1971. Regimes of Bubbling at a Submerged Orifice. Chemical Engineering Science, 1971, Vol. 26, pp 1505-1512.

McKinney, Daene. Elementary Mechanics of Fluids: Flow in Pipe. Lecture Note: CE 319 F. www.ce.utexas.edu/prof/mckinney/ce319f/Overhead-Pages/Fluids16.ppt. [Accessed on 7/13/2011].

Miller, D.S., 1996. Internal flow Systems. Second edition. Bedford: BHR Group Limited.

Müller, Gerald. Water wheel as a power source. http://hmf.enseeiht.fr/travaux/CD0708/beiere/3/html/bi/3/fichiers/Muller_histo.pdf [Accessed on 26/09/2012].

Munson, Bruce et al, 2002. Fundamental of Fluid Mechanics. New York: John Wiley and Sons, Inc.

Nahra, H.K., Kamotani, Y., 2002. Prediction of bubble diameter at detachment from a wall orifice in liquid cross-flow under reduced and normal gravity conditions. Chemical Engineering Science 58 (2003) pp. 55-69

North West Development Agency, 2006. Reported by Quantum Strategy & Technology Limited. Feasibility Study for the Establishment of a Centre of Excellence for Installers, Final Report. 18 August 2006 http://www.skills4business.org.uk/. 7 July 2008

Paish, O., 2002. Small Hydro Power: Technology and Current Status. Renewable and Sustainable Energy Review. Elsevier Science Ltd. 6 (2002) 537-556

Pico Energy Ltd, 2012. Longeller Mill. Case study 7. http://www.picoenergy.co.uk/longaller_mill. .[Accessed on 13/04/2012]

Process and Control Today, 2012. Archimedes Screw Powers Rivers Dart Country Park. Case Study. 20/12/2010 http://www.pandct.com/media/shownews.asp?ID=27528. [Accessed on 16/04/2012]

Renewable First, 2012. Archimedean Screw Hydropower Turbines. http://www.renewablesfirst.co.uk/archimedean-screws.html. [Accessed on 16/04/2012].

Rice, W., 1976. Performance of Hydraulic Gas Compressor. Journal of Fluid Engineering. ASME. December 1976.

Rogers, G., Mayhew, Y., 1992. Engineering Thermodynamics Work and Heat Transfer. Fourth Edition. Essex: Pearson Education Limited.

Salford Civil Engineering Ltd, 1989. Small-scale Hydro-electric generation potential of the UK. Report No. ETSU-SSH-4063-P3 Volume 3.

Sastraatmadja, 1981. Mekanika Fluida Hirolika. Bandung: Nova.

Serizawa, A., et al, 1991. Phase distribution in Bubbly Flow, in: G.F Hewitt, J.M. Delhaye, N Zuber (Eds.). Multiphase Science and Technology. Vol.6, pp. 257-301. Hemisphere, Washington DC.

Shapiro, J.L, 1994. The Hydraulic Air compressor Combustion Turbine. IGTI-Vol9, ASME Cogen-Turbo. ASME 1994.

Shelly, T, 2009. Water wheels begin their come back. Eureka magazine 17/02/2009. *http://www.eurekamagazine.co.uk/article/17130/Water-wheels-begin-their-come-back.aspx*. [Accessed on 13/04/2012]

Shen, Xiuzhong et al, 2005. Two-phase distribution in a vertical large diameter pipe. International Journal of Heat and Mass Transfer 48 (2205) 211-225.

Sleigh, A., Goodwill, I., 2009. CIVE 2400: Fluid Mechanics. School of Engineering, Faculty of Engineering, University of Leeds. Eee.efm.leedsac.uk/CIVE/Fluids

Subramanya, K., 1982. Flow in Open Channels. New Delhi: McGraw -Hill Publishing Company.

Sustainable Energy Research Group. Southampton University. Water Wheels as Hydraulic Energy Converters for Low Head Hydro Power. *http://www.energy.soton.ac.uk/hydro/waterwheels.html*. [Accessed on 13/04/2012].

Sustainable Guernsey. Wind power increasing contribution to UK's renewable energy supply. March 31st, 2012 by RenewableUK. http://www.sustainableguernsey.info/

Taitel,.Y., Borne, D., Dekler, AE., 1980. Modeling Flow Pattern Transitions for Steady Upward Gas-Liquid in Vertical Tube. AChE J. 26, 345(1980)

The Engineer, 1911. A Large Hydraulic Air Compressing Plant. The Engineer, Volume 112, November 10, 1911

Tung, T. et al 2006. Emerging Canadian Technology for Small Hydropower. HCI Publications.

Wakayama, N.I., Zhong, C., 2001. AICE journal, December 201. Volume 47, No. 12, pp 2640-2643.

Western Renewable Energy, 2007-2012. Archimedes Screw Turbines. http://www.westernrenew.co.uk/wre/hydro_basics/machines/archimedes_screw_turbineseseed . [Accessed on 16/04/2012].

Whalley, P.B. 1996.Two phase flow and heat transfer. Oxford: Oxford University Press.

Wiemann, P., et al, 2007. Review of Current Developments in Low-head, Small Hydropower. 32rd IAHR Conference 2007, Venice Italy, 01-06 July 2007.

Wood. W.A., Clark, D.G., 1988. Editor. Visuaized Flow. Fluid in basic and engineering situations reveled by flow visualization. Complied by: The Japan Society of Mechanical Engineers. Oxford: Pergamon Press.

Yang, Z.L., et al, 2000. Numerical investigation of bubble growth and detachment by lattice-Boltzmann method. International Journal of Heat and Mass Transfer 44(2000), pp 195-206.

Young, D.F. et al, 1997. A Brief Introduction to Fluid Mechanics. New York: John Wiley and Sons, Inc.

Bibliography

Hansgate, A., 2008. Book Review: Small is Beautiful: Economics as if People Mattered. Strategic Sustainability Consulting. 21 August 2008. http://sustainabilytyconsulting.wordpress.com/2008/08/21/book-review-small-book–review-small-is-beautiful-economics-as-if-people-mattered-by-ef-schumacher/. Accessed 14/04/2012

Majumder, S.K., et al, 2007. Pressure drop and bubble - liquid interfacial shear stress in a modified non-Newtonian liquid downflow bubble column. Chemical Engineering Science 62 (2007), pp 2482-2490.

Soo, S.L., 1990. Multiphase Fluid Dynamics. Beijing: Science Press.

Widden. M.B., 1996. Fluid Mechanics. Foundation of Engineering Series. London: Macmillan Press Limited.

Appendix A

Datasets used in Chapter 4

A.1 Moody Diagram

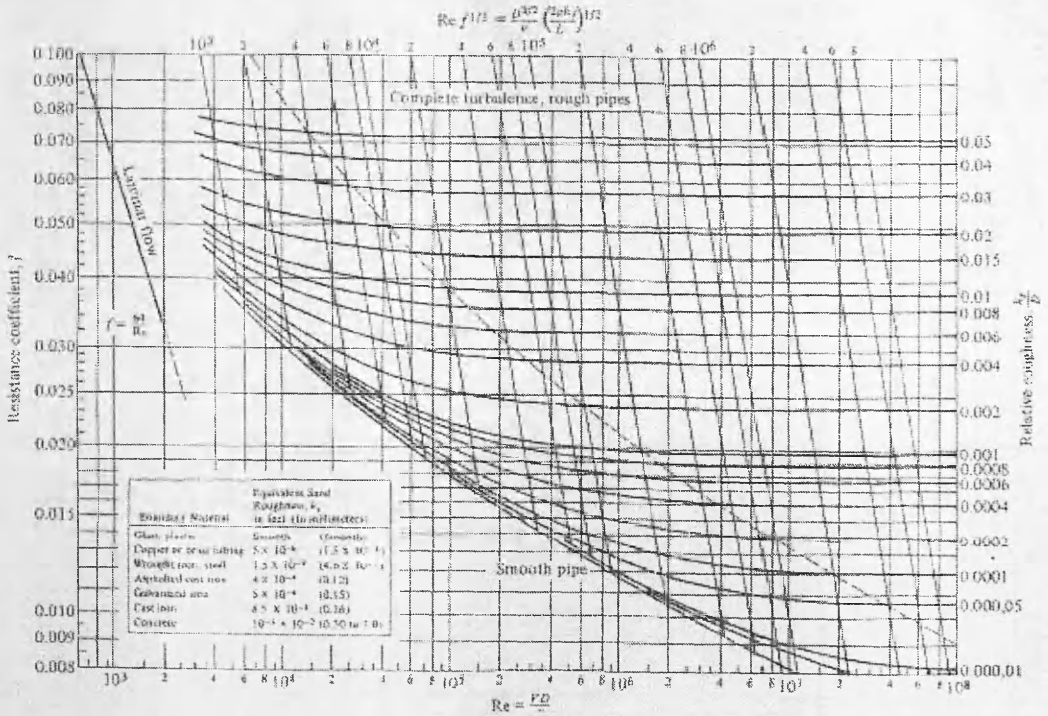

A.2 Loss in straight Perspex pipe

L = 0.8m **D=0.20 m**

v= 0.000001 m/s^2 at 20°C

Manometer						
Reading 1	**Reading 2**	**ΔH_f (m)**	**over V-notch**	**Q m^3/s**	**V (m/s)**	**Ref $^{1/2}$ = $(D^{3/2}/V)(2gH_f/L)^{1/2}$**
mm	mm		cm			
460	490	0.030	28	0.0573	1.8232	76720
460	490	0.030				76720
460	490	0.030				76720
						0
460	480	0.020	27	0.0525	1.6720	62642
460	480	0.020				62642
460	480	0.020				62642
						0
468	485	0.017	26	0.0488	1.5525	57753
463	480	0.017				57753
463	480	0.017				57753
464	480	0.016	25	0.0443	1.4092	56029
464	480	0.016				56029
464	480	0.016				56029
463	478	0.015	24	0.0400	1.2739	54249
463	478	0.015				54249
460	475	0.015				54249
461	474	0.013	23	0.0360	1.1465	50503
461	475	0.014				52410
461	475	0.014				52410
462	473	0.011	22	0.0320	1.0191	46456
462	474	0.012				48522
462	474	0.012				48522
460	470	0.010	21	0.0286	0.9108	44294
460	470	0.010				44294
460	470	0.010				44294
460	468	0.008	20	0.0246	0.7834	39618

460	468	0.008				39618
460	468	0.008				39618
462	467	0.005	19	0.0217	0.6911	31321
462	467	0.005				31321
462	467	0.005				31321
462	465	0.003	18	0.0194	0.6162	24261
462	465	0.003				24261
462	465	0.003				24261
461	463	0.002	17	0.0170	0.5414	19809
461	463	0.002				19809
461	463	0.002				19809
461	462	0.001	16	0.0144	0.4586	14007
461	462	0.001				14007
461	462	0.001				14007
460	461	0.001	15	0.0123	0.3917	14007
460	461	0.001				14007
460	461	0.001				14007
459	460	0.001	14	0.0104	0.3312	14007
459	460	0.001				14007
459	460	0.001				14007
458	459	0.001	13	0.0086	0.2739	14007
458	459	0.001				14007
458	459	0.001				14007

A.3 Loss due to Butterfly Valve

Butterfly Valve	Different pressure loss (reading)	Different pressure (Δp)	Δp/γ	Pressure Loss		Total loss	Butterfly Valve loss	K_{but}
opening	bar	N/m^2	m	bar	N/m^2	m	m	
20	0.300	30000.00	3.06	0.22544	22544.00	2.30	2.2915	166.1
30	0.290	29000.00	2.96	0.21544	21544.00	2.20	2.1840	86.3
40	0.270	27000.00	2.75	0.19544	19544.00	1.99	1.9700	42.3
50	0.235	23500.00	2.40	0.16044	16044.00	1.64	1.5983	20.5
60	0.180	18000.00	1.83	0.10544	10544.00	1.07	1.0245	9.7
65	0.150	15000.00	1.53	0.07544	7544.00	0.77	0.7102	5.8
Q water	v	$v^2/2g$	Friction loss	bend loss	Joint			
l/s	m/s	m	$K_f(v^2/2g)$	$K_B(v^2/2g)$	$K_J(v^2/2g)$			
8.500	0.271	0.014	0.0016	0.0033	0.0017			
15.60	0.497	0.025	0.0030	0.0061	0.0030			
28.70	0.914	0.047	0.0055	0.0112	0.0056			
48.00	1.529	0.078	0.0091	0.0187	0.0093			
65.00	2.070	0.106	0.0123	0.0253	0.0127			
75.30	2.398	0.122	0.0143	0.0293	0.0147			

Total loss = $(v^2/2g)$ $(K_f + K_B + K_J + K_{but})$

Butterfly loss = Pressure gauge reading - static pressure difference

(p_A-p_B)

(p_A-p_B)= 1000x9.8x0.76 = 7455.6 N/m^2= 0.07456 bar

Barometer = 755 mmHg

100628.5888 N/m^2

1.006285888 bar

1 bar = 10^5 N/m^2

1 bar = 750.2838 mmHg

$\gamma=\rho g$=1000*9.81 N/m^3

K_f = f (L/D)

f=friction coefficient= 0.013

L= length between manometer reading = 66+95+20=180 cm = 1.80m

D=pipe diameter = 0.20 m

K_B = 0.24 1 bend

K_J= 0.06 2 joints

Appendix B

Datasets used in Chapter 6

B.1a Void Fraction Calculation 27cm V-Notch - Aeration 1

Pumped system

Appendix 6-1a Void Fraction Calculation - Aeration 1

Vnotch=27cm

$v2 - (vs+(Qw+Q_A)/A_p)\,v + vsQ_w/A_p = 0$

Initial water flow = 52.5 l/s

vs=0.24 m/s

Pipe area, A_p = 0.031 m2

Reading gauge bar	Ratio pressure pAtm/pMeasrd		
-0.375	1.60	-0.26	1.356
-0.340	1.52	-0.24	1.312
-0.300	1.43	-0.21	1.266
-0.245	1.32	-0.17	1.207
-0.205	1.26	-0.14	1.168

Vnotch cm	Qw l/s	l/min	Q_A l/s	Q_{A1} l/s	Q_w+Q_{A1} l/s	$((Q_w+Q_{A1})/1000)/A_p$ m/s	$vs+((Q_w+Q_{A1})/1000)/A_p$ b	$vs(Q_w/1000)/A_p$ c	√(b2-4ac)	v1 m/s	v2 m/s
26.50	50.80	100	1.667	2.260	53.060	1.68981	1.9298	0.3883	1.47344	1.702	0.338
25.75	47.50	200	3.333	4.374	51.874	1.65205	1.8921	0.3631	1.45864	1.675	0.329
25.00	44.40	300	5.000	6.329	50.729	1.61558	1.8556	0.3394	1.44420	1.650	0.321
23.40	37.40	400	6.333	7.644	45.044	1.43453	1.6745	0.2859	1.28865	1.482	0.311
22.25	33.00	440	7.333	8.562	41.562	1.32363	1.5636	0.2522	1.19834	1.381	0.302

$Aw=Q_w/v$	$A_A=Q_{A1}/(v-vs)$	$\alpha=A_A/(A_A+A_w)$
29.8539	1.54615	0.049
28.3523	3.04766	0.097
26.9109	4.48909	0.143
25.2431	6.15688	0.196
23.8960	7.50402	0.239

B.1b Void Fraction Calculation 27cm V-Notch - Aeration 2

Pumped system

Appendix 6-1b Void Fraction Calculation - Aeration 2

Vnotch=27cm

Initial water flow = 52.5 l/s

vs=0.24 m/s

Pipe area, A_P = 0.0314 m2

$$v2 - (vs+(Qw+Q_A)/A_P)\,v + vsQw/A_P = 0$$

Reading gauge bar	Press Ratio	Callib press	Ratio
-0.385	1.63	-0.27	1.369
-0.350	1.54	-0.25	1.325
-0.305	1.44	-0.21	1.271
-0.250	1.33	-0.18	1.212
-0.220	1.28	-0.15	1.182
-0.180	1.22	-0.13	1.144

Qw		QA	QA1	Qw+QA1 l/s	((Qw+QA1)/1000)/Ap m/s	vs+((Qw+QA1)/1000)/Ap b	vs(Qw/1000)/Ap c	√(b2-4ac)	v1 m/s	v2 m/s
50.40	100	1.667	2.282	52.682	1.6778	1.9178	0.3852	1.06845	1.49	0.425
47.200	200	3.333	4.415	51.615	1.6438	1.8838	0.3608	1.05280	1.47	0.415
42.800	300	5.000	6.357	49.157	1.5655	1.8055	0.3271	0.97568	1.39	0.415
37.300	400	6.333	7.677	44.977	1.4324	1.6724	0.2851	0.82824	1.25	0.422
33.700	450	7.500	8.865	42.565	1.3556	1.5956	0.2576	0.75778	1.18	0.419
29.000	480	8.000	9.153	38.153	1.2151	1.4551	0.2217	0.61531	1.04	0.420

$A_W=Q_W/v$ m2	$A_A=Q_{A1}/(v-vs)$ m2	$\alpha = A_A/(A_A+A_W)$
33.75522	1.82072	0.0512
32.14608	3.59442	0.1006
30.77809	5.52519	0.1522
29.83261	7.59843	0.2030
28.63988	9.46454	0.2484
28.01416	11.51084	0.2912

B.1c Void Fraction Calculation 27cm V-Notch - Aeration 3

Pumped system

Appendix 6-1c Void Fraction Calculation - Aeration 3

Vnotch=27cm

Initial water flow = 52.5 l/s

vs=0.24 m/s

Pipe area, A_p = 0.0314 m2

$v2 - (vs+(Qw+Q_A)/A_p)\,v + vsQ_w/A_p = 0$

Reading gauge bar	Press Ratio		
-0.39	1.64	-0.27	1.376
-0.35	1.54	-0.25	1.325
-0.31	1.45	-0.22	1.277
-0.25	1.33	-0.18	1.212
-0.19	1.23	-0.13	1.153

Qw l/s	l/min	Q_A l/s	Q_{A1} l/s	Q_w+Q_{A1} l/s	$((Q_w+Q_{A1})/1000)/A_p$ m/s	$vs+((Q_w+Q_{A1})/1000)/A_p$ b	$vs(Q_w/1000)/A_p$ c	√(b2-4ac)	v1 m/s	v2 m/s
48.60	100	1.667	2.293	50.893	1.6208	1.8608	0.3715	1.40593	1.63	0.23
45.30	200	3.333	4.415	49.715	1.5833	1.8233	0.3462	1.39262	1.61	0.22
41.40	300	5.000	6.386	47.786	1.5218	1.7618	0.3164	1.35585	1.56	0.20
32.80	400	6.333	7.677	40.477	1.2891	1.5291	0.2507	1.15553	1.34	0.19
27.30	440	7.333	8.458	35.758	1.1388	1.3788	0.2087	1.03268	1.21	0.17

$A_w=Q_w/v$	$A_A=Q_{A1}/(v-vs)$ m2	$\alpha = A_A/(A_A+A_w)$
29.75467	1.64533	0.0524
28.17253	3.22747	0.1028
26.55812	4.84188	0.1542
24.43568	6.96432	0.2218
22.64167	8.75833	0.2789

B.2a Void Fraction Calculation 28cm V-Notch - Aeration 1

Pumped system

Appendix 6-2a Void Fraction Calculation - Aeration 1

Vnotch=28cm

$v2-(vs+(Qw+Q_A)/A_p)v+vsQw/A_p=0$

Initial water flow = 57.5 l/s

vs=0.24 m/s

Pipe area, A_p = 0.0314 m2

Aerator1

Callib pressure	Pressure bar	prss ratio	ratio
-0.214	-0.305	1.44	1.271
-0.196	-0.280	1.39	1.244
-0.168	-0.240	1.32	1.202
-0.133	-0.190	1.23	1.153
-0.105	-0.150	1.18	1.117
-0.067	-0.095	1.10	1.071

cm	Qw		Q_A	Q_{A1}	Q_w+Q_{A1}	$((Q_w+Q_{A1})/1000)/A_p$	$vs+((Q_w+Q_{A1})/1000)/A_p$	$vs(Q_w/1000)/A_p$		v1	v2
	l/s	l/min	l/s		l/s	m/s	b	c	√(b2-4ac)	m/s	m/s
27.45	55.20	100	1.667	2.119	57.319	1.8254	2.0654	0.4219	1.60575	1.84	0.230
27.00	53.30	200	3.333	4.146	57.446	1.8295	2.0695	0.4074	1.62887	1.85	0.220
26.40	51.00	300	5.000	6.010	57.010	1.8156	2.0556	0.3898	1.63286	1.84	0.211
25.45	47.00	400	6.333	7.305	54.305	1.7295	1.9695	0.3592	1.56263	1.77	0.203
24.40	42.50	500	8.333	9.311	51.811	1.6500	1.8900	0.3248	1.50758	1.70	0.191
22.60	37.00	610	10.167	10.891	47.891	1.5252	1.7652	0.2828	1.40879	1.59	0.178

$A_w=Q_w/v$	$A_A=Q_{A1}/(v-vs)$	$\alpha=A_A/(A_A+A_w)$
0.0301	0.00133	0.042
0.0288	0.00258	0.082
0.0277	0.00375	0.119
0.0266	0.00479	0.152
0.0250	0.00638	0.203
0.0233	0.00809	0.257

B.2b Void Fraction Calculation 28cm V-Notch - Aeration 2

Pumped system

Appendix 6-2b Void Fraction Calculation - Aeration 2

Vnotch=28cm

Initial water flow = 57.5 l/s

vs=0.24 m/s

Pipe area, A_p = 0.0314 m2

Aerator1

$v2 - (vs+(Qw+Q_A)/A_p)\,v + vsQ_w/A_p = 0$

	Pressure bar	prss ratio	Ratio
-0.221	-0.315	1.46	1.28
-0.196	-0.280	1.39	1.24
-0.168	-0.240	1.32	1.20
-0.133	-0.190	1.23	1.15
-0.102	-0.145	1.17	1.11
-0.060	-0.085	1.09	1.06

Qw l/s	l/min	Q_A l/s	Q_{A1}	Q_w+Q_{A1} l/s	$((Q_w+Q_{A1})/1000)/A_p$ m/s	$vs+((Qw+Q_{A1})/1000)/A_p$ b	$vs(Qw/1000)/A_p$ c	√(b2-4ac)	v1 m/s	v2 m/s
54.500	100	1.667	2.138	56.638	1.8038	2.0438	0.4166	1.58453	1.81	0.230
52.500	200	3.333	4.146	56.646	1.8040	2.0440	0.4013	1.60402	1.82	0.220
50.000	300	5.000	6.010	56.010	1.7837	2.0237	0.3822	1.60215	1.81	0.211
46.000	400	6.333	7.305	53.305	1.6976	1.9376	0.3516	1.53230	1.73	0.203
42.000	500	8.333	9.274	51.274	1.6329	1.8729	0.3210	1.49125	1.68	0.191
34.500	640	10.667	11.341	45.841	1.4599	1.6999	0.2637	1.35460	1.53	0.173

$Aw=Q_w/v$	$A_A=Q_{A1}/(v-vs)$	$\alpha = A_A/(A_A+A_w)$
	m2	
0.03004	0.00136	0.043
0.02878	0.00262	0.083
0.02758	0.00382	0.122
0.02651	0.00489	0.156
0.02497	0.00643	0.205
0.02259	0.00881	0.281

B.2c Void Fraction Calculation 28cm V-Notch - Aeration 3

Pumped system

Appendix 6-2c Void Fraction Calculation - Aeration 3

Vnotch=28cm

Initial water flow = 57.5 l/s

vs=0.24 m/s

Pipe area, A_p = 0.031 m2

Aerator1

$v2 - (vs+(Qw+Q_A)/A_p)\,v + vsQ_w/A_p = 0$

	Pressure	prss ratio	
	bar		Ratio
-0.221	-0.315	1.46	1.283
-0.196	-0.280	1.39	1.244
-0.175	-0.250	1.33	1.212
-0.144	-0.205	1.26	1.168
-0.116	-0.165	1.20	1.131
-0.060	-0.085	1.09	1.063

Qw		Q_A	Q_{A1}	Q_w+Q_{A1}	$((Q_w+Q_{A1})/1000)/A_p$	$vs+((Q_w+Q_{A1})/1000)/A_p$	$vs(Q_w/1000)/A_p$		v1	v2
l/s	l/min	l/s		l/s	m/s	b	c	√(b2-4ac)	m/s	
54.70	100	1.667	2.138	56.838	1.8101	2.0501	0.4181	1.59081	1.82	0.23
52.50	200	3.333	4.146	56.646	1.8040	2.0440	0.4013	1.60402	1.82	0.22
50.00	300	5.000	6.061	56.061	1.7854	2.0254	0.3822	1.60420	1.81	0.21
46.50	400	6.333	7.394	53.894	1.7164	1.9564	0.3554	1.55106	1.75	0.20
43.00	500	8.333	9.421	52.421	1.6695	1.9095	0.3287	1.52689	1.72	0.19
34.50	630	10.500	11.164	45.664	1.4543	1.6943	0.2637	1.34751	1.52	0.17

$A_w=Q_w/v$	$A_A=Q_{A1}/(v-vs)$	$\alpha = A_A/(A_A+A_w)$
0.03005	0.00135	0.043
0.02878	0.00262	0.083
0.02755	0.00385	0.123
0.02652	0.00488	0.156
0.02503	0.00637	0.203
0.02268	0.00872	0.278

B.3a Void Fraction Calculation 29cm V-Notch - Aeration 1

Pumped system

Appendix 6-3a Void Fraction Calculation - Aeration 1

Vnotch=29cm

Initial water flow = 62.6 l/s

vs=0.24 m/s

Pipe area, A_p = 0.0314 m2

$$v2 - (vs+(Qw+Q_A)/A_p)\,v + vsQ_w/A_p = 0$$

Callib prs bar	Pressure bar	prss ratio	Ratio
-0.217	-0.310	1.45	1.277
-0.200	-0.285	1.40	1.249
-0.175	-0.250	1.33	1.212
-0.147	-0.210	1.27	1.172
-0.126	-0.180	1.22	1.144
-0.105	-0.150	1.18	1.117
-0.077	-0.110	1.12	1.083
-0.063	-0.090	1.10	1.067

Vnotch cm	Qw l/s	QA l/min	Q_A l/sec	Q_{A1}	Qw+Q_{A1} l/s	((Qw+Q_{A1})/1000) / A_p m/s	vs+((Qw+Q_{A1})/1000) / A_p b	vs(Qw/1000)/A_p c	√(b2-4ac)	v1 m/s	v2 m/s
28.55	60.60	100	1.667	2.129	62.729	1.9977	2.2377	0.4632	1.77614	2.01	0.231
28.25	58.50	200	3.333	4.164	62.664	1.9957	2.2357	0.4471	1.79156	2.01	0.222
27.95	57.30	300	5.000	6.061	63.361	2.0179	2.2579	0.4380	1.82922	2.04	0.214
27.40	54.60	400	6.330	7.421	62.021	1.9752	2.2152	0.4173	1.79938	2.01	0.208
26.95	53.00	500	8.333	9.534	62.534	1.9915	2.2315	0.4051	1.83286	2.03	0.199
26.30	49.70	600	10.420	11.642	61.342	1.9536	2.1936	0.3799	1.81447	2.00	0.190
25.80	47.80	710	11.833	12.821	60.621	1.9306	2.1706	0.3654	1.80279	1.99	0.184
25.40	46.00	840	14.000	14.941	60.941	1.9408	2.1808	0.3516	1.83018	2.01	0.175

Aw=Qw/v	A_A=QA1/(v-vs)	α=AA/(AA+Aw)
30.1953	1.2047	0.0384
29.0522	2.3478	0.0748
28.0396	3.3604	0.1070
27.2010	4.1990	0.1337
26.0801	5.3199	0.1694
24.8001	6.5999	0.2102
24.0601	7.3399	0.2338
22.9370	8.4630	0.2695

B.3b Void Fraction Calculation 29cm V-Notch Aeration 2

Pumped system

Appendix 6-3b Void Fraction Calculation - Aeration 2

Vnotch=29cm

$v2 - (vs+(Qw+Q_A)/A_p)\,v + vsQ_w/A_p = 0$

Initial water flow = 62.6 l/s

vs=0.24 m/s

Pipe area, A_p = 0.0314 m2

	Pressure	prss ratio	
	bar		ratio
-0.210	-0.300	1.43	1.266
-0.196	-0.280	1.39	1.244
-0.175	-0.250	1.33	1.212
-0.140	-0.200	1.25	1.163
-0.112	-0.160	1.19	1.126
-0.077	-0.110	1.12	1.083
-0.063	-0.090	1.10	1.067

V-notch	Qw		Q_A	Q_{A1}	Qw+Q_{A1}	((Qw+QA1)/1000) / Ap	vs+((Qw+QA1)/1000) / Ap	vs(Qw/1000)/Ap		v1	v2
cm	l/s	l/min	l/s		l/s	m/s	b	c	√(b2-4ac)	m/s	m/s
28.75	61.200	100	1.667	2.110	63.310	2.0162	2.2562	0.4678	1.79430	2.03	0.231
28.40	59.200	200	3.333	4.146	63.346	2.0174	2.2574	0.4525	1.81269	2.04	0.222
27.90	57.000	300	5.000	6.061	63.061	2.0083	2.2483	0.4357	1.81994	2.03	0.214
27.00	52.500	400	6.330	7.360	59.860	1.9064	2.1464	0.4013	1.73259	1.94	0.207
26.30	49.500	500	8.333	9.384	58.884	1.8753	2.1153	0.3783	1.72077	1.92	0.197
25.55	47.000	600	10.420	11.289	58.289	1.8563	2.0963	0.3592	1.71980	1.91	0.188
25.00	44.400	710	11.833	12.629	57.029	1.8162	2.0562	0.3394	1.69427	1.88	0.181

Aw=Qw/v	AA=QA1/(v-vs)	α = AA/(AA+Aw)
30.218	1.182	0.0376
29.090	2.310	0.0736
28.022	3.378	0.1076
27.069	4.331	0.1379
25.808	5.592	0.1781
24.632	6.768	0.2155
23.677	7.723	0.2460

B.3c Void Fraction Calculation 29cm V-Notch - Aerator 3

Pumped system

Appendix 6-3c Void Fraction Calculation - Aeration 3

Vnotch=29cm

Initial water flow = 62.6 l/s

vs=0.24 m/s

Pipe area, A_p 0.0314 m2

$$v2 - (vs+(Qw+Q_A)/A_p)\,v + vsQ_w/A_p = 0$$

Pressure bar	prss ratio	cal. Prss	Ratio
-0.315	1.46	-0.221	1.283
-0.285	1.40	-0.200	1.249
-0.255	1.34	-0.179	1.217
-0.210	1.27	-0.147	1.172
-0.170	1.20	-0.119	1.135
-0.130	1.15	-0.091	1.100
-0.090	1.10	-0.063	1.067

Vnotch cm	Qw l/s	l/min	QA l/s	QA1	Q_w+Q_{A1} l/s	$((Q_w+Q_{A1})/1000)/A_p$ m/s	$vs+((Q_w+Q_{A1})/1000)/A_p$ b	$vs(Q_w/1000)/A_p$ c	√(b2-4ac)	v1 m/s	v2 m/s
28.50	60.0	100	1.667	2.138	62.1381	1.9789	2.2189	0.45860	1.76	1.988	0.231
28.10	57.9	200	3.333	4.164	61.2333	1.9501	2.1901	0.44255	1.74	1.965	0.225
27.65	55.8	300	5.000	6.086	60.8000	1.9363	2.1763	0.42650	1.74	1.959	0.218
27.00	52.5	400	6.333	7.425	58.8333	1.8737	2.1137	0.40127	1.69	1.903	0.211
26.20	49.5	500	8.333	9.459	57.8330	1.8418	2.0818	0.37834	1.68	1.881	0.201
25.80	47.8	605	10.083	11.093	57.8833	1.8434	2.0834	0.36535	1.70	1.890	0.193
24.75	43.1	705	11.750	12.540	54.8500	1.7468	1.9868	0.32943	1.62	1.804	0.183

$A_w=Q_w/v$	$A_A=Q_{A1}/(v-vs)$ m2	$\alpha = A_A/(A_A+A_w)$
30.1770	1.2230	0.0389
29.4675	2.4141	0.0757
28.4906	3.5416	0.1106
27.5911	4.4653	0.1393
26.3209	5.7652	0.1797
25.2893	6.7224	0.2100
23.8883	8.0167	0.2513

B.4a Low Siphon - Aerator 1 - Void Fraction Calculation

Butterfly opening: 30°

Aeration-1 | Butterfly opening =30 ° | *Siphon break at 80 l/min aeration*

V-notch cm	Qwater l/s		Over weir cm	YA m	H m	Air flow l/min	Airflow l/s	Press. Gauge bar	Press. Ratio	callib prss	ratio
16.00	14.500		0	3.425	2.300	0	0.000	-0.435	1.770	-0.305	1.44
15.60	13.600		1	3.425	2.314	20	0.333	-0.420	1.724	-0.294	1.42
15.40	13.200		1	3.425	2.316	40	0.667	-0.400	1.667	-0.280	1.39
15.20	12.700		1	3.425	2.318	60	1.000	-0.380	1.613	-0.266	1.36
15.10	12.400		1	3.425	2.319	70	1.167	-0.370	1.587	-0.259	1.35
15.00	12.200		1	3.425	2.320	75	1.250	-0.365	1.575	-0.256	1.34

Pipe area, A_P 0.0314 m2

$v^2 - (v_s + (Q_W + Q_A)/A_P)v + v_s Q_W / A_P = 0$

Qw l/s	l/min	QA l/s	QA1	Qw+QA1 l/s	((Qw+QA1)/1000)/Ap m/s	vs+((Qw+QA1)/1000)/Ap b	vs(Qw/1000)/Ap c	√(b2-4ac)	v1 m/s	v2 m/s
14.500	0	0.000	0.000	14.500	0.4618	0.7018	0.1108	0.22178	0.4618	0.2400
13.600	20	0.333	0.472	14.072	0.4482	0.6882	0.1039	0.24034	0.4642	0.2239
13.200	40	0.667	0.926	14.126	0.4499	0.6899	0.1009	0.26899	0.4794	0.2104
12.700	60	1.000	1.362	14.062	0.4478	0.6878	0.0971	0.29130	0.4896	0.1983
12.400	70	1.167	1.574	13.974	0.4450	0.6850	0.0948	0.30030	0.4927	0.1924
12.200	75	1.250	1.679	13.879	0.4420	0.6820	0.0932	0.30354	0.4928	0.1892

$A_W = Q_W/v$ m2	$A_A = Q_{A1}/(v-v_s)$ m2	$\alpha = A_A/(A_A+A_W)$
31.400	0.0000	0.0000
29.295	2.1054	0.0671
27.533	3.8672	0.1232
25.941	5.4589	0.1739
25.169	6.2312	0.1984
24.758	6.6422	0.2115

Butterfly opening: 40°

Butterfly opening = 40° Siphon break at 180 l/min aeration

V-notch	Qwater	Over weir	YA	H	Air flow	Airflow	Press. Gauge	Press. Ratio	Calib press	ratio
cm	l/s	cm	cm	m	l/min	l/s	bar			
21.60	31	0.0	3.425	2.244	0.00	0.000	-0.355	1.55	-0.249	1.331
21.00	28.6	1.0	3.425	2.260	30.00	0.500	-0.350	1.54	-0.245	1.325
20.60	27.4	1.5	3.425	2.269	60.00	1.000	-0.340	1.52	-0.238	1.312
20.40	26.1	1.7	3.425	2.273	90.00	1.500	-0.330	1.49	-0.231	1.300
20.00	24.9	2.0	3.425	2.280	120.00	2.000	-0.315	1.46	-0.221	1.283
19.50	23.2	2.5	3.425	2.290	130.00	2.167	-0.310	1.45	-0.217	1.277
19.30	22.6	2.8	3.425	2.295	140.00	2.333	-0.300	1.43	-0.210	1.266
19.00	21.7	2.9	3.425	2.299	150.00	2.500	-0.290	1.41	-0.203	1.255
18.80	21.2	3.0	3.425	2.302	160.00	2.667	-0.285	1.40	-0.200	1.249
17.70	19.0	4.5	3.425	2.328	180.00	3.000	-0.275	1.38	-0.193	1.238

Pipe area, 0.0314 m2

$v^2 - (vs+(Qw+QA)/Ap)\, v + vsQw/Ap = 0$

Water flowrate / Air flowrate

Qw		QA	QA1	Qw+QA1	((Qw+QA1)/1000)/Ap	vs+((Qw+QA1)/1000)/Ap	vs(Qw/1000)/Ap		v1	v2
l/s	l/min	l/s		l/s	m/s	b	c	V(b2-4ac)	m/s	m/s
31	0	0.000	0.000	31.000	0.98726	1.22726	0.23694	0.74726	0.987	0.24
28.6	30	0.500	0.662	29.262	0.93192	1.17192	0.21860	0.70640	0.939	0.23
27.4	60	1.000	1.312	28.712	0.91441	1.15441	0.20943	0.70352	0.929	0.23
26.1	90	1.500	1.951	28.051	0.89333	1.13333	0.19949	0.69748	0.915	0.22
24.9	120	2.000	2.566	27.466	0.87471	1.11471	0.19032	0.69375	0.904	0.21
23.2	130	2.167	2.767	25.967	0.82698	1.06698	0.17732	0.65509	0.861	0.21
22.6	140	2.333	2.954	25.554	0.81381	1.05381	0.17274	0.64773	0.851	0.20
21.7	150	2.500	3.137	24.837	0.79098	1.03098	0.16586	0.63204	0.832	0.20
21.2	160	2.667	3.331	24.531	0.78125	1.02125	0.16204	0.62833	0.825	0.20
19.0	180.000	3.000	3.715	22.715	0.72341	0.96341	0.14522	0.58930	0.776	0.19

Aw=Qw/v	A_A=QA1/(v-vs)	$\alpha = A_A/(A_A+A_W)$
m2	m2	
31.400	0.00000	0.0000
30.453	0.94721	0.0302
29.495	1.90479	0.0607
28.512	2.88802	0.0920
27.537	3.86274	0.1230
26.944	4.45568	0.1419
26.564	4.83584	0.1540
26.097	5.30296	0.1689
25.704	5.69649	0.1814
24.473	6.92669	0.2206

Butterfly opening: 50°

Aerator1 | Butterfly opening = 50° | Siphon break at 340 l/min aeration

V-notch	Qwater	Over weir	Head	YA	Air flow	Airflow	Press. Gauge	Press. Ratio	callib prss	ratio
cm	l/s	cm	m	m	l/min	l/s	bar		bar	
26.60	51.5	-0.5	2.189	3.425	0	0.000	-0.426	1.74	-0.298	1.42
25.95	48.6	1.0	2.211	3.425	100	1.667	-0.391	1.64	-0.274	1.38
25.00	44.3	3.0	2.240	3.425	200	3.333	-0.356	1.55	-0.249	1.33
24.50	42.0	3.5	2.250	3.425	240	4.000	-0.346	1.53	-0.242	1.32
23.80	39.5	4.5	2.267	3.425	280	4.667	-0.316	1.46	-0.221	1.28
23.10	36.5	5.0	2.279	3.425	300	5.000	-0.306	1.44	-0.214	1.27
21.60	31.0	2.0	2.264	3.425	320	5.333	-0.286	1.40	-0.200	1.25

Ap= 0.0314 m2

$v^2 - (vs+(Qw+QA)/Ap)\, v + vs\, Qw/Ap = 0$

Qw		QA	QA1	Qw+QA1	((Qw+QA1)/1000)/Ap	vs+((Qw+QA1)/1000)/Ap	vs(Qw/1000)/Ap		v1	v2
l/s	l/min	l/s		l/s	m/s	b	c	√(b2-4ac)	m/s	m/s
51.5	0	0.000	0.000	51.500	1.6401	1.8801	0.39363	1.40013	1.64	0.24
48.6	100	1.667	2.295	50.895	1.6209	1.8609	0.37146	1.40603	1.63	0.23
44.3	200	3.333	4.440	48.740	1.5522	1.7922	0.33860	1.36296	1.58	0.21
42.0	240	4.000	5.278	47.278	1.5057	1.7457	0.32102	1.32791	1.54	0.21
39.5	280	4.667	5.992	45.492	1.4488	1.6888	0.30191	1.28233	1.49	0.20
36.5	300	5.000	6.363	42.863	1.3651	1.6051	0.27898	1.20843	1.41	0.20
31.0	320	5.333	6.668	37.668	1.1996	1.4396	0.23694	1.06055	1.25	0.19

Aw=Qw/v	AA=QA1/(v-vs)	α = AA/(AA+Aw)
m2	m2	
31.400	0.00000	0.0000
29.753	1.64682	0.0524
28.081	3.31919	0.1057
27.330	4.07038	0.1296
26.589	4.81077	0.1532
25.946	5.45358	0.1737
24.798	6.60174	0.2102

Butterfly opening: 60°

Butterfly opening = 60° Siphon break at 480 l/min aeration

V-notch	Qwater	Over weir	Head	YA	Air flow	Airflow	Press. Gauge	Press. Ratio	Calib prss	ratio
cm	l/s	cm	m	cm	l/min	l/s	bar			
29.50	65.3	-6.0	2.105	3.425	160	0.000	-0.410	1.69	-0.287	1.40
29.00	62.8	-2.5	2.145	3.425	240	4.000	-0.385	1.63	-0.270	1.37
28.50	60.0	-0.5	2.170	3.425	320	5.333	-0.370	1.59	-0.259	1.35
26.75	51.5	1.0	2.203	3.425	400	6.667	-0.355	1.55	-0.249	1.33
25.00	44.3	0.0	2.210	3.425	420	7.000	-0.325	1.48	-0.228	1.29
24.40	41.5	2.0	2.236	3.425	440	7.333	-0.270	1.37	-0.189	1.23
23.10	36.0	1.0	2.239	3.425	475	7.917	-0.260	1.35	-0.182	1.22

Ap= 0.0314 m2

$v^2 - (vs+(Qw+QA)/Ap)\, v + vs\,Qw/Ap = 0$

Qw		QA	QA1	Qw+QA	((Qw+QA1)/1000)/Ap	vs+((Qw+QA1)/1000)/Ap	s(Qw/1000)/Ap		v1	v2
l/s	l/min	l/s		l/s	m/s	b	c	V(b2-4ac)	m/s	m/s
65.3	160	0.000	0.000	65.300	2.0796	2.3196	0.49911	1.83962	2.08	0.24
62.8	240	4.000	5.477	68.277	2.1744	2.4144	0.48000	1.97724	2.20	0.22
60.0	320	5.333	7.197	67.197	2.1400	2.3800	0.45860	1.95710	2.17	0.21
51.5	400	6.667	8.871	60.371	1.9226	2.1626	0.39363	1.76140	1.96	0.20
44.3	420	7.000	9.061	53.361	1.6994	1.9394	0.33860	1.55142	1.75	0.19
41.6	440	7.333	9.042	50.642	1.6128	1.8528	0.31796	1.47006	1.66	0.19
36.0	460	7.917	9.678	45.678	1.4547	1.6947	0.27516	1.33095	1.51	0.18

Aw=Qw/v	AA=QA1/(v-vs)	α = AA/(AA+Aw)
m2	m2	
31.400	0.00000	0.0000
28.600	2.80044	0.0892
27.668	3.73203	0.1189
26.248	5.15158	0.1641
25.381	6.01925	0.1917
25.039	6.36141	0.2026
23.796	7.60358	0.2422

Butterfly opening: 70°

Total head = (80+4+127+35)+ Over weir-V-Notch level						80+4+127+35				
Initial pressure (no flow):	-0.068 bar		with flow =			-0.354 bar		V-notch =		
Pump valve opening: 9.2 cm										
Inlet setting =43 Hz		Butterfly opening = 70°				Siphon break at 580 l/min aeration				

V-notch	Qwater	Over weir	Head	YA	Air flow	Airflow	Press. Gauge	Press. Ratio	callib prss	ratio
cm	l/s	cm	m	cm	l/min	l/s	bar			
30.00	67.60	-4.5	2.115	3.425	470	7.833	-0.298	1.42	-0.209	1.26
29.50	65.30	-1.5	2.150	3.425	520	8.667	-0.288	1.40	-0.202	1.25
29.20	63.90	0.0	2.168	3.425	540	9.000	-0.268	1.37	-0.188	1.23
28.50	60.00	2.5	2.200	3.425	560	9.333	-0.248	1.33	-0.174	1.21

Ap= 0.0314 m2

$v^2 - (vs+(Qw+QA)/Ap)\, v + vs\, Qw/Ap = 0$

Qw		QA	QA1	Qw+QA1	((Qw+QA1)/1000)/Ap	vs+((Qw+QA1)/1000)/Ap	s(Qw/1000)/Ap		v1	v2
l/s	l/min	l/s		l/s	m/s	b	c	√(b2-4ac)	m/s	m/s
67.60	470	7.833	9.898	77.498	2.4681	2.7081	0.51669	2.29500	2.50	0.21
65.30	520	8.667	10.855	76.155	2.4253	2.6653	0.49911	2.25998	2.46	0.20
63.90	540	9.000	11.078	74.978	2.3878	2.6278	0.48841	2.22529	2.43	0.20
60.00	560	9.333	11.294	71.294	2.2705	2.5105	0.45860	2.11383	2.31	0.20

Aw=Qw/v	AA=QA1/(v-vs)	α = AA/(AA+Aw)
m2	m2	
27.023	4.37669	0.1394
26.516	4.88383	0.1555
26.333	5.06652	0.1614
25.950	5.45032	0.1736

Butterfly opening: 80°

Butterfly opening = 80° Siphon break at 640-660 l/min aeration

V-notch	Qwater	Over weir	Head	YA	Air flow	Airflow	Actual prss	Press. Ratio	callib prss	ratio
cm	l/s	cm	m	cm	l/min	l/s	bar			
30.50	70.00	-10.50	2.050	3.425	420	7.000	-0.290	1.41	-0.203	1.25
30.40	69.60	0.00	2.156	3.425	480	8.000	-0.280	1.39	-0.196	1.24
30.25	69.00	-1.50	2.143	3.425	570	9.500	-0.275	1.38	-0.193	1.24
30.00	67.60	-2.00	2.140	3.425	600	10.000	-0.270	1.37	-0.189	1.23
29.25	64.00	-2.00	2.148	3.425	640	10.667	-0.250	1.33	-0.175	1.21

Ap= 0.0314 m2

$v^2 - (vs + (Qw+QA)/Ap)\, v + vs\,Qw/Ap = 0$

Qw		QA	QA1	Qw+QA1	((Qw+QA1)/1000)/Ap	vs+((Qw+QA1)/1000)/Ap	vs(Qw/1000)/Ap		v1	v2
l/s	l/min	l/s		l/s	m/s	b	c	√(b2-4ac)	m/s	m/s
70.00	420	7.000	8.783	78.783	2.5090	2.7490	0.53503	2.32743	2.54	0.21
69.60	480	8.000	9.950	79.550	2.5334	2.7734	0.53197	2.35884	2.57	0.21
69.00	570	9.500	11.765	80.765	2.5721	2.8121	0.52739	2.40801	2.61	0.20
67.60	600	10.000	12.330	79.930	2.5456	2.7856	0.51669	2.38591	2.59	0.20
64.00	640	10.667	12.929	76.929	2.4500	2.6900	0.48917	2.29767	2.49	0.20

Aw=Qw/v	AA=QA1/(v-vs)	α = AA/(AA+Aw)
m2	m2	
27.578	3.82162	0.1217
27.122	4.27758	0.1362
26.436	4.96388	0.1581
26.143	5.25655	0.1674
25.663	5.73660	0.1827

Butterfly opening: 90° (full)

		full opening				Siphon break at 680 l/min aeration				
V-notch	Qwater	Over weir	Head	YA	Air flow	Airflow	Press. Gauge	Press. Ratio	Calib prss	ratio
cm	l/s	cm	m	cm	l/min	l/s	bar			
30.50	70.00	-2.50	2.130	3.425	610	10.167	-0.190	1.23	-0.133	1.153
30.00	67.60	-0.50	2.155	3.425	640	10.667	-0.180	1.22	-0.126	1.144
29.25	63.80	0.00	2.168	3.425	660	11.000	-0.170	1.20	-0.119	1.135

Ap= 0.0314 m2

Water Air $v^2 - (vs+(Qw+QA)/Ap)\, v + vs\,Qw/Ap = 0$

Qw		QA	QA1	Qw+QA1	((Qw+QA1)/1000)/Ap	vs+((Qw+QA1)/1000)/Ap	(Qw/1000)/Ap		v1	v2
l/s	l/min	l/s		l/s	m/s	b	c	√(b2-4ac)	m/s	m/s
70.00	420	10.167	11.7263	81.726	2.6027	2.8427	0.53503	2.43743	2.64	0.20
67.60	600	10.667	12.2044	79.804	2.5415	2.7815	0.51669	2.38122	2.58	0.20
63.80	640	11.000	12.4858	76.286	2.4295	2.6695	0.48764	2.27499	2.47	0.20

Aw=Qw/v	AA=QA1/(v-vs)	α = AA/(AA+Aw)
m2	m2	
26.514	4.88576	0.1556
26.188	5.21249	0.1660
25.807	5.59341	0.1781

B.4b Low Siphon - Aerator2 - Void Fraction Calculation

Butterfly opening: 30°

Butterfly opening =30 ° *Siphon break at 80 l/min aeration*

V-notch cm	Qwater l/s	Over weir cm		H m	Air flow l/min	Airflow l/s	Press. Gauge bar	Press. Ratio	callib prss bar	ratio
16.50	15.600	0.3		2.298	0	0.000	-0.408	1.689	-0.286	1.40
16.10	14.800	0.6		2.305	20	0.333	-0.395	1.653	-0.277	1.38
15.80	14.000	1.7		2.319	40	0.667	-0.380	1.613	-0.266	1.36
15.50	13.400	0.5		2.310	60	1.000	-0.365	1.575	-0.256	1.34
15.35	13.200	0		2.307	70	1.167	-0.355	1.550	-0.249	1.33
15.30	13.000	0		2.307	75	1.250	-0.352	1.543	-0.246	1.33

Pipe area, A_P 0.0314 m2

$v^2 - (v_s + (Q_w + Q_A)/A_P)v + v_s Q_w/A_P = 0$

Water flowrate	Air flowrate									
Qw l/s	l/min	QA l/s	QA1	Qw+QA1 l/s	((Qw+QA1)/1000)/Ap m/s	vs+((Qw+QA1)/1000)/Ap b	vs(Qw/1000)/Ap c	√(b2-4ac)	v1 m/s	v2 m/s
15.600	0	0.000	0.000	15.600	0.4968	0.7368	0.1192	0.25682	0.4968	0.2400
14.800	20	0.333	0.461	15.261	0.4860	0.7260	0.1131	0.27314	0.4996	0.2264
14.000	40	0.667	0.908	14.908	0.4748	0.7148	0.1070	0.28791	0.5013	0.2134
13.400	60	1.000	1.343	14.743	0.4695	0.7095	0.1024	0.30618	0.5079	0.2017
13.200	70	1.167	1.552	14.752	0.4698	0.7098	0.1009	0.31667	0.5132	0.1966
13.000	75	1.250	1.659	14.659	0.4668	0.7068	0.0994	0.31964	0.5132	0.1936

$A_W = Q_W/v$ m2	$A_A = Q_{A1}/(v - v_s)$ m2	$\alpha = A_A/(A_A + A_W)$
31.400	0.00000	0.0000
29.625	1.77490	0.0565
27.925	3.47530	0.1107
26.385	5.01457	0.1597
25.719	5.68146	0.1809
25.329	6.07057	0.1933

Butterfly opening: 40°

Butterfly opening = 40°

Siphon break at 180 l/min aeration

V-notch cm	Qwater l/s	Over weir cm	YA cm	H m	Air flow l/min	Airflow l/s	Press. Gauge bar	Press. Ratio	Calib prss	Ratio
21.30	29.7	0.5		2.252	0.00	0.000	-0.404	1.68	-0.283	1.39
21.00	28.7	1.0		2.260	30.00	0.500	-0.400	1.67	-0.280	1.39
20.90	28.6	1.1		2.262	40.00	0.667	-0.400	1.67	-0.280	1.39
20.80	28.0	1.0		2.262	50.00	0.833	-0.398	1.66	-0.279	1.39
20.80	28.0	1.2		2.264	60.00	1.000	-0.395	1.65	-0.277	1.38
20.70	27.7	1.5		2.268	70.00	1.167	-0.386	1.63	-0.270	1.37
20.60	27.5	1.6		2.270	80.00	1.333	-0.378	1.61	-0.265	1.36
20.30	26.0	1.9		2.276	100.00	1.667	-0.370	1.59	-0.259	1.35
19.90	24.6	2.3		2.284	120.00	2.000	-0.360	1.56	-0.252	1.34
19.30	22.6	0.9		2.276	142.50	2.375	-0.355	1.55	-0.249	1.33
19.00	21.9	0.0		2.270	160.00	2.667	-0.340	1.52	-0.238	1.31
18.30	20.1	0.4		2.281	170.00	2.833	-0.325	1.48	-0.228	1.29

Pipe area, Ap 0.0314 m2

$v^2 - (vs+(Qw+QA)/Ap)\, v + vsQw/Ap = 0$

Qw l/s	l/min	QA l/s	QA1	Qw+QA1 l/s	((Qw+QA)/1000) / Ap m/s	vs+((Qw+QA)/1000) / Ap b	vs(Qw/1000)/Ap c	V(b2-4ac)	v1 m/s	v2 m/s
29.7	0.0	0.0000	0.0000	29.700	0.94586	1.18586	0.22701	0.70586	0.946	0.240
28.7	30.0	0.5000	0.6944	29.394	0.93613	1.17613	0.21936	0.71121	0.944	0.232
28.6	40.0	0.6667	0.9259	29.526	0.94032	1.18032	0.21860	0.72024	0.950	0.230
28.0	50.0	0.8333	1.1552	29.155	0.92851	1.16851	0.21401	0.71370	0.941	0.227
28.0	60.0	1.0000	1.3822	29.382	0.93574	1.17574	0.21401	0.72547	0.951	0.225
27.7	70.0	1.1667	1.5986	29.299	0.93308	1.17308	0.21172	0.72748	0.950	0.223
27.5	80.0	1.3333	1.8131	29.313	0.93354	1.17354	0.21019	0.73241	0.953	0.221
26.0	100.0	1.6667	2.2492	28.249	0.89966	1.13966	0.19873	0.70987	0.925	0.215
24.6	120.0	2.0000	2.6738	27.274	0.86859	1.10859	0.18803	0.69056	0.900	0.209
22.6	142.5	2.3750	3.1603	25.760	0.82039	1.06039	0.17274	0.65839	0.859	0.201
21.9	160.0	2.6667	3.4996	25.400	0.80890	1.04890	0.16739	0.65623	0.853	0.196
20.1	170.0	2.8333	3.6677	23.768	0.75693	0.99693	0.15363	0.61592	0.806	0.191

Aw=Qw/v m2	AA=QA1/(v-vs) m2	$\alpha = A_A/(A_A+A_W)$
31.400	0.00000	0.0000
30.413	0.98689	0.0314
30.096	1.30361	0.0415
29.752	1.64764	0.0525
29.455	1.94506	0.0619
29.149	2.25068	0.0717
28.857	2.54297	0.0810
28.115	3.28466	0.1046
27.346	4.05381	0.1291
26.298	5.10234	0.1625
25.687	5.71293	0.1819
24.925	6.47523	0.2062

Butterfly opening: 50°

Butterfly opening = 50° Siphon break at 310 l/min aeration

V-notch	Qwater	Over weir	Head		Air flow	Airflow	Press. Gauge	Press. Ratio	Callib prss	Ratio
cm	l/s	cm	m		l/min	l/s	bar			
26.90	52.00	-1.0	2.181		0.000	0.000	-0.393	1.65	-0.275	1.380
26.00	48.80	0.7	2.207		80	1.333	-0.390	1.64	-0.273	1.376
25.40	46.0	2.0	2.226		160	2.667	-0.360	1.56	-0.252	1.337
24.30	41.3	1.5	2.232		240	4.000	-0.325	1.48	-0.228	1.294
23.20	36.4	3.0	2.258		280	4.667	-0.280	1.39	-0.196	1.244
22.00	32.1	1.5	2.255		300	5.000	-0.255	1.34	-0.179	1.217

Ap= 0.0314 m2

$v^2 - (vs + (Qw+QA)/Ap)\, v + vs\, Qw/Ap = 0$

Water flowrate / Air flowrate

Qw		QA	QA1	Qw+QA1	((Qw+QA1)/1000)/Ap	vs+((Qw+QA)/1000)/Ap	vs(Qw/1000)/Ap		v1	v2
l/s	l/min	l/s		l/s	m/s	b	c	√(b2-4ac)	m/s	m/s
52.00	0	0.000	0.000	52.000	1.6561	1.8961	0.39745	1.41605	1.66	0.24
48.80	80	1.333	1.834	50.634	1.6125	1.8525	0.37299	1.39282	1.62	0.23
46.0	160	2.667	3.565	49.565	1.5785	1.8185	0.35159	1.37862	1.60	0.22
41.3	240	4.000	5.178	46.478	1.4802	1.7202	0.31567	1.30245	1.51	0.21
36.4	280	4.667	5.804	42.204	1.3441	1.5841	0.27822	1.18172	1.38	0.20
32.1	300	5.000	6.086	38.186	1.2161	1.4561	0.24535	1.06720	1.26	0.19

Aw=Qw/v	AA=QA1/(v-vs)	α = AA/(AA+Aw)
m2	m2	
31.400	0.0000	0.0000
30.074	1.3264	0.0422
28.776	2.6241	0.0836
27.327	4.0729	0.1297
26.321	5.0786	0.1617
25.443	5.9574	0.1897

Butterfly opening: 60°

Butterfly opening = 60°

Siphon break at 430 l/min aeration

V-notch	Qwater	Over weir	Head	YA	Air flow	Airflow	Press. Gauge	Press. Ratio	Callib prss	ratio
cm	l/s	cm	m	cm	l/min	l/s	bar			
31.0	72.8	-9	2.060		0	0	-0.388	1.63	-0.272	1.37
30.3	69.0	-6.5	2.093		80	1.333	-0.385	1.63	-0.270	1.37
29.5	65.0	0.5	2.170		160	2.667	-0.365	1.57	-0.256	1.34
28.8	61.3	0.0	2.173		240	4.000	-0.340	1.52	-0.238	1.31
27.5	55.2	0.9	2.194		320	5.333	-0.305	1.44	-0.214	1.27
24.9	44.0	1.0	2.221		400	6.667	-0.260	1.35	-0.182	1.22
24.0	40.0	2.0	2.240		420	7.000	-0.254	1.34	-0.178	1.22

Water flowrate | Air flowrate

Ap= 0.0314 m2

$v^2 - (vs + (Qw+QA)/Ap)\, v + vs\, Qw/Ap = 0$

Qw		QA	QA1	Qw+QA1	((Qw+QA1)/1000)/Ap	vs+((Qw+QA)/1000)/Ap	vs(Qw/1000)/Ap		v1	v2
l/s	l/min	l/s		l/s	m/s	b	c	√(b2-4ac)	m/s	m/s
69.0	80.0	1.333	1.830	70.830	2.2557	2.4957	0.52739	2.02958	2.26	0.23
65.0	160.0	2.667	3.650	68.650	2.1863	2.4263	0.49682	1.97478	2.20	0.23
61.3	240.0	4.000	5.373	66.673	2.1233	2.3633	0.46854	1.92645	2.14	0.22
55.2	320.0	5.333	6.999	62.199	1.9809	2.2209	0.42191	1.80128	2.01	0.21
44.0	400.0	6.667	8.476	52.476	1.6712	1.9112	0.33631	1.51906	1.72	0.20
40.0	420.0	7.000	8.557	48.557	4.0000	4.2400	0.30573	4.09325	4.17	0.07

Aw=Qw/v	AA=QA/(v-vs)	α = AA/(AA+Aw)
m2	m2	
30.495	0.90499	0.0288
29.538	1.86196	0.0593
28.580	2.82049	0.0898
27.448	3.95192	0.1259
25.654	5.74614	0.1830
9.600	2.17934	0.1850

Butterfly opening: 70°

			Butterfly opening = 70°			Siphon break at 580 l/min aeration				
V-notch	Qwater	Over weir	Head	YA	Air flow	Airflow	Press. Gauge	Press. Ratio	callib prss	ratio
cm	l/s	cm	m	cm	l/min	l/s	bar			
29.25	63.80	-1.0	2.158		380	6.333	-0.295	1.42	-0.207	1.26
28.60	60.0	1.5	2.189		420	7.000	-0.280	1.39	-0.196	1.24
25.10	45.0	0.0	2.209		460	7.667	-0.240	1.32	-0.168	1.20

Ap= 0.0314 m2

$v^2 - (vs+(Qw+QA)/Ap)\, v + vs\,Qw/Ap = 0$

Qw		QA	QA1	Qw+QA1	((Qw+QA1)/1000)/Ap	+((Qw+QA1)/1000)/A	s(Qw/1000)/Ap		v1	v2
l/s	l/min	l/s		l/s	m/s	b	c	√(b2-4ac)	m/s	m/s
63.8	380	6.333	7.982	71.782	2.2860	2.5260	0.48764	2.10482	2.32	0.21
60.0	420	7.000	8.706	68.706	2.1881	2.4281	0.45860	2.01527	2.22	0.21
45.0	460	7.667	9.215	54.215	1.7266	1.9666	0.34395	1.57850	1.77	0.19

Aw=Qw/v	AA=QA1/(v-vs)	α = AA/(AA+Aw)
m2	m2	
27.554	3.84572	0.1225
27.007	4.39347	0.1399
25.387	6.01272	0.1915

Butterfly opening: 80°

Initial pressure (no flow): -0.07 bar with flow = -0.34 bar
Pump valve opening: 9.2 cm
Inlet setting = 43.5-45 Hz

Butterfly opening = 80° Siphon break at 640-660 l/min aeration

V-notch	Qwater	Over weir	Head	YA	Air flow	Airflow	Press. Gauge	Press. Ratio	callib prss	ratio
cm	l/s	cm	m	cm	l/min	l/s	bar			
30.75	71.60	-7.00	2.083		600	10.000	-0.260	1.35	-0.182	1.22

Ap= 0.0314 m2

$v^2 - (vs+(Qw+QA)/Ap)\, v + vs\,Qw/Ap = 0$

Qw		QA	QA1	Qw+QA1	((Qw+QA1)/1000)/Ap	vs+((Qw+QA1)/1000)/Ap	vs(Qw/1000)/Ap		v1	v2
l/s	l/min	l/s		l/s	m/s	b	c	√(b2-4ac)	m/s	m/s
71.60	600	10.000	12.225	83.825	2.6696	2.9096	0.54726	2.50532	2.71	0.20

Aw=Qw/v	AA=QA1/(v-vs)	α = AA/(AA+Aw)
m2	m2	
26.446	4.95448	0.1578

Butterfly opening: 90° (full)

full opening Siphon break at 680 l/min aeration

V-notch	Qwater	Over weir	Head	YA	Air flow	Airflow	Press. Gauge	Press. Ratio	callib prss	ratio
cm	l/s	cm	m	cm	l/min	l/s	bar			
29.00	63.00	-1.50	2.155		660	11.000	-0.210	1.27	-0.147	1.17
30.00	67.80	-2.50	2.135		680	11.333	-0.220	1.28	-0.154	1.18

Ap= 0.0314 m2

$v^2 - (vs+(Qw+QA)/Ap)\, v + vs\,Qw/Ap = 0$

Qw		QA	QA1	Qw+QA1	((Qw+QA1)/1000)/Ap	vs+((Qw+QA1)/1000)/Ap	vs(Qw/1000)/Ap		v1	v2
l/s	l/min	l/s		l/s	m/s	b	c	√(b2-4ac)	m/s	m/s
63.00	660	11.000	12.8957	75.896	2.4171	2.6571	0.48153	2.26580	2.46	0.20
67.80	680	11.333	13.3964	81.196	2.5859	2.8259	0.51822	2.43160	2.63	0.20

Aw=Qw/v	AA=QA1/(v-vs)	α = AA/(AA+Aw)
m2	m2	
25.595	5.8051	0.1849
25.792	5.6081	0.1786

B.4c Low Siphon – Aerator 3 – Void Fraction Calculation

Butterfly opening: 30°

Butterfly opening = 30° *Siphon break at 85 l/min aeration*

V-notch	Qwater	Velocity	Over weir		H	Air flow	Airflow	Press. Gauge	Press. Ratio	callib prss	ratio
cm	l/s	m/s	cm		m	l/min	l/s	bar			
16.00	14.500	0.470	0		2.300	0	0	-0.496	1.98	-0.347	1.53
15.50	13.300	0.425	1		2.315	40	0.6667	-0.466	1.87	-0.326	1.48
15.30	13.000	0.420	1		2.317	50	0.8333	-0.456	1.84	-0.319	1.47
15.20	12.700	0.415	1		2.318	60	1.0000	-0.451	1.82	-0.316	1.46
15.15	12.500	0.410	1		2.319	65	1.0833	-0.446	1.81	-0.312	1.45
15.10	12.400	0.405	1		2.319	70	1.1667	-0.441	1.79	-0.309	1.45
15.05	12.300	0.395	1		2.320	75	1.2500	-0.436	1.77	-0.305	1.44
15.00	12.200	0.385	1		2.320	80	1.3333	-0.430	1.75	-0.301	1.43

Pipe area, 0.0314 m2

$v2 - (vs + (Qw + QA)/Ap)v + vsQw/Ap = 0$

Qw		QA	QA1	Qw+QA1	((Qw+QA1)/1000)/Ap	vs+((Qw+QA1)/1000)/Ap	vs(Qw/1000)/Ap		v1	v2
l/s	l/min	l/s		l/s	m/s	b	c	√(b2-4ac)	m/s	m/s
14.500	0	0	0.000	14.500	0.4618	0.7018	0.1108	0.22178	0.4618	0.2400
13.330	40	0.667	0.989	14.319	0.4560	0.6960	0.1019	0.27734	0.4867	0.2093
13.000	50	0.833	1.224	14.224	0.4530	0.6930	0.0994	0.28773	0.4904	0.2026
12.700	60	1.000	1.461	14.161	0.4510	0.6910	0.0971	0.29866	0.4948	0.1962
12.500	65	1.083	1.575	14.075	0.4483	0.6883	0.0955	0.30253	0.4954	0.1929
12.400	70	1.167	1.688	14.088	0.4487	0.6887	0.0948	0.30843	0.4985	0.1901
12.300	75	1.250	1.799	14.099	0.4490	0.6890	0.0940	0.31415	0.5016	0.1874
12.200	80	1.333	1.907	14.107	0.4493	0.6893	0.0932	0.31956	0.5044	0.1849

$Aw = Qw/v$	$AA = QA1/(v-vs)$	$\alpha = AA/(AA+Aw)$
m2	m2	
31.400	0.0000	0.0000
27.389	4.0108	0.1277
26.511	4.8891	0.1557
25.665	5.7346	0.1826
25.233	6.1673	0.1964
24.872	6.5275	0.2079
24.522	6.8777	0.2190
24.186	7.2138	0.2297

Butterfly opening: 40°

Butterfly opening = 40° Siphon break at 180 l/min aeration

V-notch	Qwater	Over weir	Head		Air flow	Airflow	Press. Gauge	Press Ratio	callib prss	ratio
cm	l/s	cm	m		l/min	l/s	bar			
21.40	30.0	-1.0	2.236		0	0.000	-0.420	1.72	-0.29	1.42
20.80	28.0	0.0	2.252		40	0.667	-0.400	1.67	-0.28	1.39
20.50	26.6	0.3	2.258		60	1.000	-0.390	1.64	-0.27	1.38
20.40	26.1	0.8	2.264		80	1.333	-0.375	1.60	-0.26	1.36
20.00	24.9	1.4	2.274		100	1.667	-0.370	1.59	-0.26	1.35
19.30	22.6	2.0	2.287		120	2.000	-0.345	1.53	-0.24	1.32
18.60	21.0	2.5	2.299		140	2.333	-0.330	1.49	-0.23	1.30
17.10	17.0	3.0	2.319		160	2.667	-0.300	1.43	-0.21	1.27

Pipe area, Ap 0.0314 m2

v2- (vs+(Qw+QA)/Ap) v + vsQw/Ap = 0

Qw		QA	QA1	Qw+QA1	((Qw+QA1)/1000)/Ap	vs+((Qw+QA1)/1000) / Ap	vs(Qw/1000)/Ap		v1	v2
l/s	l/min	l/s		l/s	m/s	b	c	√(b2-4ac)	m/s	m/s
30.0	0	0.0000	0.000	30.000	0.9554	1.1954	0.2293	0.7154	0.955	0.240
28.0	40	0.6667	0.926	28.926	0.9212	1.1612	0.2140	0.7017	0.931	0.230
26.6	60	1.0000	1.376	27.976	0.8909	1.1309	0.2033	0.6825	0.907	0.224
26.1	80	1.3333	1.808	27.908	0.8888	1.1288	0.1995	0.6901	0.909	0.219
24.9	100	1.6667	2.249	27.149	0.8646	1.1046	0.1903	0.6774	0.891	0.214
22.6	120	2.0000	2.637	25.237	0.8037	1.0437	0.1727	0.6312	0.837	0.206
21.0	140	2.3333	3.034	24.034	0.7654	1.0054	0.1605	0.6073	0.806	0.199
17.0	160	2.6667	3.376	20.376	0.6489	0.8889	0.1299	0.5200	0.704	0.184

Aw=Qw/v	AA=QA1/(v-vs)	α = AA/(AA+Aw)
m2	m2	
31.400	0.000	0.0000
30.061	1.339	0.0426
29.337	2.063	0.0657
28.699	2.701	0.0860
27.945	3.455	0.1100
26.987	4.413	0.1406
26.043	5.357	0.1706
24.132	7.268	0.2315

Butterfly opening: 50°

Butterfly opening = 50°

Siphon break at 300 l/min aeration

V-notch	Qwater	Over weir	Head		Air flow	Airflow	Press. Gauge	Press ratio	callib prss	ratio
cm	l/s	cm	m		l/min	l/s	bar			
27.00	52.50	-1.2	2.178		0	0.000	-0.415	1.71	-0.29	1.41
26.00	48.80	-0.8	2.192		100	1.667	-0.385	1.63	-0.27	1.37
25.00	44.30	3.0	2.240		200	3.333	-0.350	1.54	-0.25	1.32
23.80	39.50	4.5	2.267		260	4.333	-0.315	1.46	-0.22	1.28
23.00	36.00	6.0	2.290		280	4.667	-0.295	1.42	-0.21	1.26

Pipe area, Ap 0.0314 m2

$v2-(vs+(Qw+QA)/Ap)v+vsQw/Ap=0$

Qw		QA	QA1	Qw+QA1	((Qw+QA1)/1000)/Ap	vs+((Qw+QA1)/1000)/Ap	vs(Qw/1000)/Ap		v1	v2
l/s	l/min	l/s		l/s	m/s	b	c	√(b2-4ac)	m/s	m/s
52.50	0	0.000	0.000	52.500	1.672	1.912	0.4013	1.43197	1.672	0.240
48.80	100	1.667	2.282	51.082	1.627	1.867	0.3730	1.41173	1.639	0.228
44.30	200	3.333	4.415	48.715	1.551	1.791	0.3386	1.36192	1.577	0.215
39.50	260	4.333	5.559	45.059	1.435	1.675	0.3019	1.26412	1.470	0.205
36.00	280	4.667	5.881	41.881	1.334	1.574	0.2752	1.17311	1.373	0.200

Aw=Qw/v	AA=QA1/(v-vs)	α = AA/(AA+Aw)
m2	m2	
31.400	0.000	0.0000
29.769	1.631	0.0519
28.097	3.303	0.1052
26.879	4.521	0.1440
26.211	5.189	0.1652

Butterfly opening: 60°

Butterfly opening = 60°

Siphon break at 420 l/min aeration

V-notch cm	Qwater l/s	Over weir cm		H m	Air flow l/min	Airflow l/s	Press. Gauge bar	Press ratio	callib prss	ratio
29.25	64.0	-3.5		2.133	160.00	2.667	-0.360	1.56	-0.252	1.34
28.75	61.0	-2.5		2.148	200.00	3.333	-0.350	1.54	-0.245	1.32
28.00	57.5	-0.5		2.175	240.00	4.000	-0.340	1.52	-0.238	1.31
27.50	55.0	1.0		2.195	300.00	5.000	-0.320	1.47	-0.224	1.29
26.50	51.0	0.0		2.195	360.00	6.000	-0.295	1.42	-0.207	1.26
25.80	48.2	1.5		2.217	400.00	6.667	-0.280	1.39	-0.196	1.24
25.00	44.4	3.0		2.240	420.00	7.000	-0.265	1.36	-0.186	1.23

Pipe area, Ap 0.0314 m2

v2- (vs+(Qw+QA)/Ap) v + vsQw/Ap = 0

Qw l/s	l/min	QA l/s	QA1	Qw+QA1 l/s	((Qw+QA1)/1000)/Ap m/s	vs+((Qw+QA1)/1000)/Ap b	vs(Qw/1000)/Ap c	√(b2-4ac)	v1 m/s	v2 m/s
64.0	160	2.667	3.565	67.565	2.15175	2.39175	0.48917	1.94005	2.1659	0.22585
61.0	200	3.333	4.415	65.415	2.08328	2.32328	0.46624	1.87954	2.1014	0.22187
57.5	240	4.000	5.249	62.749	1.99839	2.23839	0.43949	1.80344	2.0209	0.21747
55.0	300	5.000	6.443	61.443	1.95679	2.19679	0.42038	1.77324	1.9850	0.21178
51.0	360	6.000	7.561	58.561	1.86501	2.10501	0.38981	1.69465	1.8998	0.20518
48.2	400	6.667	8.292	56.492	1.79910	2.03910	0.36841	1.63839	1.8387	0.20036
44.4	420	7.000	8.594	52.994	1.68771	1.92771	0.33936	1.53578	1.7317	0.19597

Aw=Qw/v m2	AA=QA1/(v-vs) m2	α = AA/(AA+Aw)
29.549	1.851	0.0590
29.028	2.372	0.0755
28.452	2.948	0.0939
27.708	3.692	0.1176
26.844	4.556	0.1451
26.214	5.186	0.1652
25.639	5.761	0.1835

Butterfly opening: 70°

Butterfly opening = 70°

Siphon break at 500 l/min aeration

V-notch	Qwater	Over weir		H	Air flow	Airflow	Press. Gauge	Press ratio	callib prss	ratio
cm	l/s	cm		m	l/min	l/s	bar			
29.25	64.0	-2.5		2.143	320.00	5.333	-0.305	1.44	-0.21	1.27
28.25	58.5	-2.0		2.158	360.00	6.000	-0.290	1.41	-0.20	1.25
27.25	53.5	-2.5		2.163	400.00	6.667	-0.275	1.38	-0.19	1.24
26.50	51.0	0.0		2.195	440.00	7.333	-0.260	1.35	-0.18	1.22
25.80	48.0	0.5		2.207	460.00	7.667	-0.250	1.33	-0.18	1.21
25.40	46.0	1.5		2.221	480.00	8.000	-0.245	1.32	-0.17	1.21

Pipe area, Ap 0.0314 m2

$v2 - (vs+(Qw+QA)/Ap)\, v + vsQw/Ap = 0$

Qw		QA	QA1	Qw+QA1	((Qw+QA1)/1000)/Ap	vs+((Qw+QA1)/1000)/Ap	vs(Qw/1000)/Ap		v1	v2
l/s	l/min	l/s		l/s	m/s	b	c	√(b2-4ac)	m/s	m/s
64.0	320	5.333	6.781	70.781	2.25418	2.49418	0.48917	2.06500	2.28	0.21
58.5	360	6.000	7.528	66.028	2.10281	2.34281	0.44713	1.92360	2.13	0.21
53.5	400	6.667	8.256	61.756	1.96675	2.20675	0.40892	1.79835	2.00	0.20
51.0	440	7.333	8.965	59.965	1.90971	2.14971	0.38981	1.74986	1.95	0.20
48.0	460	7.667	9.293	57.293	1.82462	2.06462	0.36688	1.67186	1.87	0.20
46.0	480	8.000	9.656	55.656	1.77248	2.01248	0.35159	1.62595	1.82	0.19

Aw=Qw/v	AA=QA1/(v-vs)	α = AA/(AA+Aw)
m2	m2	
28.075	3.325	0.1059
27.424	3.976	0.1266
26.716	4.684	0.1492
26.157	5.243	0.1670
25.693	5.707	0.1818
25.286	6.114	0.1947

Butterfly opening: 90° (full)

Butterfly opening = full — Siphon break at 540 l/min aeration

V-notch	Qwater	Over weir		H	Air flow	Airflow	Press. Gauge	Press. Ratio	callib prss	ratio
cm	l/s	cm		m	l/min	l/s	bar			
29.00	63.0	-2.0		2.150	380	6.333	-0.280	1.39	-0.196	1.24
28.50	60.0	-1.0		2.165	400	6.667	-0.275	1.38	-0.193	1.24
27.25	53.5	-2.5		2.163	440	7.333	-0.255	1.34	-0.179	1.22
25.75	47.6	2.5		2.228	500	8.333	-0.225	1.29	-0.158	1.19
25.25	46.0	0.5		2.213	520	8.667	-0.216	1.28	-0.151	1.18

Pipe area, Ap = 0.0314 m2

$v^2 - (vs+(Qw+QA)/Ap)\, v + vsQw/Ap = 0$

Qw		QA	QA1	Qw+QA1	((Qw+QA1)/1000)/Ap	vs+((Qw+QA1)/1000)/Ap	vs(Qw/1000)/Ap		v1	v2
l/s	l/min	l/s		l/s	m/s	b	c	√(b2-4ac)	m/s	m/s
63.0	380	6.333	7.877	70.877	2.25724	2.49724	0.48153	2.07607	2.2867	0.21058
60.0	400	6.667	8.256	68.256	2.17376	2.41376	0.45860	1.99795	2.2059	0.20790
53.5	440	7.333	8.927	62.427	1.98811	2.22811	0.40892	1.82451	2.0263	0.20180
47.6	500	8.333	9.891	57.491	1.83093	2.07093	0.36382	1.68329	1.8771	0.19382
45.7	520	8.667	10.210	55.910	1.78059	2.02059	0.34930	1.63877	1.8297	0.19091

Aw=Qw/v	AA=QA1/(v-vs)	α = AA/(AA+Aw)
m2	m2	
27.551	3.849	0.1226
27.200	4.200	0.1337
26.403	4.997	0.1592
25.358	6.042	0.1924
24.977	6.423	0.2046

B.5a Low Siphon - Aerator 1 - Power Calculation

Butterfly opening: 30°

					Gas equation:	T2/T1 = (p2/p1) ^ (γ-1)/γ	
Pipe dia 200 mm							
					(γ-1)/γ=	0.2857	
					Cp=	1.005	kJ/kg.K
Inlet pressure (p1)= 1 bar					**Constant pressure, h= Cp (T2-T1)**		
Outlet pressure (p2) = 1 bar - actual presure in side of the siphon							
Inlet temperature (T1) = 20°C		293 °K			T2=(p2/p1)^0.286		
Specific heat rati	**1.4**				1.4		
Density of air =	1.204	Kg/m3					

p2/p1 bar	(γ-1)/γ	T2/T1	T2 °K	h= CpT m	QA1 l/s	Power Watt
0.696	0.2860	0.90	264.10	29.05	0.000	0.000
0.706	0.2860	0.91	265.23	27.91	0.472	15.864
0.720	0.2860	0.91	266.73	26.41	0.926	29.438
0.734	0.2860	0.92	268.20	24.93	1.362	40.886
0.741	0.2860	0.92	268.93	24.19	1.574	45.860
0.745	0.2860	0.92	269.29	23.83	1.679	48.168

Butterfly opening: 40°

					Gas equation:	T2/T1 = (p2/p1) ^ (γ-1)/γ	
Pipe dia	200 mm						
					(γ-1)/γ=	0.2857	
					Cp=	1.005	kJ/kg.K
Inlet pressure (p1)= 1 bar					**Constant pressure, h= Cp (T2-T1)**		
Outlet pressure (p2) = 1 bar - actual presure in side of the siphon							
Inlet temperature (T1) = 20°C =		293	°K		T2=(p2/p1)^0.286		
Specific heat ratio =		**1.4**			1.4		
Density of air =		1.204	Kg/m3				

p2/p1	(γ-1)/γ	T2/T1	T2	h= CpT	QA1	Power
bar			°K	m	l/s	Watt
0.752	0.2860	0.92	270.01	23.10	0.000	0.000
0.755	0.2860	0.92	270.37	22.74	0.6623	18.133
0.762	0.2860	0.93	271.09	22.02	1.3123	34.799
0.769	0.2860	0.93	271.80	21.31	1.9506	50.047
0.780	0.2860	0.93	272.85	20.25	2.5657	62.552
0.783	0.2860	0.93	273.20	19.90	2.7671	66.290
0.790	0.2860	0.93	273.90	19.20	2.9536	68.268
0.797	0.2860	0.94	274.59	18.50	3.1368	69.876
0.801	0.2860	0.94	274.93	18.16	3.3313	72.821
0.808	0.2860	0.94	275.62	17.47	3.7152	78.132

Butterfly opening: 50°

				Gas equation:	T2/T1 = (p2/p1) ^ (γ-1)/γ	
Pipe dia	200 mm					
$H=(1+K_{tota})v^2/2g$				(γ-1)/γ	0.2857	
$K=(2gH/v2)-1$				Cp=	1.005	kJ/kg.K
Inlet pressure (p1)= 1 bar				**Constant pressure, h= Cp (T2-T1)**		
Outlet pressure (p2) = 1 bar - actual presure in side of the siphon						
Inlet temperature (T1) = 20°C =	293 °K			T2=(p2/p1)^0.286		
Specific heat ratio =	**1.4**			1.4		
Density of air =	1.204 Kg/m3					

p2/p1	(γ-1)/γ	T2/T1	T2	h= CpT	QA1	Power
bar			°K	m	l/s	Watt
0.702	0.2860	0.90	264.78	28.36	0.000	0.000
0.726	0.2860	0.91	267.39	25.74	2.295	71.108
0.751	0.2860	0.92	269.94	23.18	4.440	123.880
0.758	0.2860	0.92	270.66	22.45	5.278	142.701
0.779	0.2860	0.93	272.78	20.32	5.992	146.594
0.786	0.2860	0.93	273.48	19.62	6.363	150.284
0.800	0.2860	0.94	274.87	18.23	6.668	146.324

Butterfly opening: 60°

		Gas equation:	T2/T1 = (p2/p1) ^ (γ-1)/γ
Pipe dia	200 mm		
		(γ-1)/γ=	0.2857
		Cp=	1.005 kJ/kg.K
Inlet pressure (p1)= 1 bar		**Constant pressure, h= Cp (T2-T1)**	
Outlet pressure (p2) = 1 bar - actual presure in side of the siphon			
Inlet temperature (T1) = 20°C =	293 °K	T2=(p2/p1)^0.286	
Specific heat ratio =	**1.4**	1.4	
Density of air =	1.204 Kg/m3		

p2/p1 bar	(γ-1)/γ	T2/T1	T2 °K	h= CpT m	QA1 l/s	Power Watt
0.713	0.2860	0.91	265.98	27.15	0.000	0.000
0.730	0.2860	0.91	267.81	25.31	5.477	166.938
0.741	0.2860	0.92	268.93	24.19	7.197	209.647
0.752	0.2860	0.92	270.01	23.10	8.871	246.758
0.773	0.2860	0.93	272.15	20.96	9.061	228.624
0.811	0.2860	0.94	275.96	17.12	9.042	186.431
0.818	0.2860	0.94	276.64	16.44	9.678	191.586

Butterfly opening: 70°

		Gas equation:	T2/T1 = (p2/p1) ^ (γ-1)/γ
Pipe dia	200 mm		
$H=(1+K_{tota})v^2/2g$		(γ-1)/γ=	0.2857
K=(2gH/v2)-1		Cp=	1.005 kJ/kg.K
Inlet pressure (p1)= 1 bar		**Constant pressure, h= Cp (T2-T1)**	
Outlet pressure (p2) = 1 bar - actual presure in side of the siphon			
Inlet temperature (T1) = 20°C =	293 °K	T2=(p2/p1)^0.286	
Specific heat ratio	**1.4**	1.4	
Density of air =	1.204 Kg/m3		

p2/p1 bar	(γ-1)/γ	T2/T1	T2 °K	h= CpT m	QA1 l/s	Power Watt
0.791	0.2860	0.94	274.04	19.06	9.898	227.120
0.798	0.2860	0.94	274.73	18.36	10.855	240.001
0.812	0.2860	0.94	276.10	16.99	11.078	226.583
0.826	0.2860	0.95	277.45	15.63	11.294	212.511

Butterfly opening: 80°

					Gas equation:	T2/T1 = (p2/p1) ^ (γ-1)/γ	
Pipe dia	200 mm						
$H=(1+K_{tota})v^2/2g$					(γ-1)/γ	0.2857	
$K=(2gH/v2)-1$					Cp=	1.005	kJ/kg.K
Inlet pressure (p1)= 1 bar					**Constant pressure, h= Cp (T2-T1)**		
Outlet pressure (p2) = 1 bar - actual presure in side of the siphon							
Inlet temperature (T1) = 20°C =		293	°K		T2=(p2/p1)^0.286		
Specific heat ratio	**1.4**				1.4		
Density of air =	1.204	Kg/m3					

p2/p1 bar	(γ-1)/γ	T2/T1	T2 °K	h= CpT m	QA1 l/s	Power Watt
0.797	0.2860	0.94	274.59	18.50	8.783	195.653
0.804	0.2860	0.94	275.28	17.81	9.950	213.378
0.808	0.2860	0.94	275.62	17.47	11.765	247.417
0.811	0.2860	0.94	275.96	17.12	12.330	254.225
0.825	0.2860	0.95	277.32	15.76	12.929	245.386

Butterfly Opening: 90° (full)

					Gas equation:	T2/T1 = (p2/p1) ^ (γ-1)/γ	
Pipe dia	200 mm						
$H=(1+K_{tota})v^2/2g$					(γ-1)/γ	0.2857	
$K=(2gH/v2)-1$					Cp=	1.005	kJ/kg.K
Inlet pressure (p1)= 1 bar					**Constant pressure, h= Cp (T2-T1)**		
Outlet pressure (p2) = 1 bar - actual presure in side of the siphon							
Inlet temperature (T1) = 20°C =		293	°K		T2=(p2/p1)^0.286		
Specific heat ratio	**1.4**				1.4		
Density of air =	1.204	Kg/m3					

p2/p1 bar	(γ-1)/γ	T2/T1	T2 °K	h= CpT m	QA1 l/s	Power Watt
0.867	0.2860	0.96	281.28	11.78	11.726	166.275
0.874	0.2860	0.96	281.93	11.13	12.204	163.491
0.881	0.2860	0.96	282.57	10.48	12.486	157.531

B.5b Low Siphon - Aerator 2 - Power Calculation

Butterfly opening: 30°

					Gas equation:	T2/T1 = (p2/p1) ^ (γ-1)/γ	
Pipe dia	200 mm						
					(γ-1)/γ=	0.2857	
					Cp=	1.005	kJ/kg.K
Inlet pressure (p1)= 1 bar					**Constant pressure, h= Cp (T2-T1)**		
Outlet pressure (p2) = 1 bar - actual presure in side of the siphon							
Inlet temperature (T1) = 20°C =		293	°K		T2=(p2/p1)^0.286		
Specific heat ratio		**1.4**			1.4		
Density of air =		1.204	Kg/m3				

p2/p1	(γ-1)/γ	T2/T1	T2	h= CpT	QA1	Power
bar			°K	m	l/s	Watt
0.714	0.2860	0.91	266.13	27.00	0.000	0.000
0.724	0.2860	0.91	267.10	26.03	0.461	14.441
0.734	0.2860	0.92	268.20	24.93	0.908	27.257
0.745	0.2860	0.92	269.29	23.83	1.343	38.535
0.752	0.2860	0.92	270.01	23.10	1.552	43.183
0.754	0.2860	0.92	270.23	22.89	1.659	45.705

Butterfly opening: 40°

					Gas equation:	T2/T1 = (p2/p1) ^ (γ-1)/γ	
					(γ-1)/γ=	0.2857	
					Cp=	1.005	kJ/kg.K
Inlet pressure (p1)= 1 bar					**Constant pressure, h= Cp (T2-T1)**		
Outlet pressure (p2) = 1 bar - actual presure in side of the siphon							
Inlet temperature (T1) = 20°C =		293	°K		T2=(p2/p1)^0.286		
Specific heat ratio =	**1.4**				1.4		
Density of air =	1.204	Kg/m3					

p2/p1	(γ-1)/γ	T2/T1	T2	h=CpT	QA1	Power
bar			°K	m	l/s	Watt
0.717	0.2860	0.91	266.43	26.70	0.0000	0.000
0.720	0.2860	0.91	266.73	26.41	0.6944	22.078
0.720	0.2860	0.91	266.73	26.41	0.9259	29.438
0.721	0.2860	0.91	266.87	26.26	1.1552	36.518
0.724	0.2860	0.91	267.10	26.03	1.3822	43.324
0.730	0.2860	0.91	267.76	25.37	1.5986	48.825
0.735	0.2860	0.92	268.34	24.78	1.8131	54.090
0.741	0.2860	0.92	268.93	24.19	2.2492	65.515
0.748	0.2860	0.92	269.65	23.46	2.6738	75.539
0.752	0.2860	0.92	270.01	23.10	3.1603	87.907
0.762	0.2860	0.93	271.09	22.02	3.4996	92.797
0.773	0.2860	0.93	272.15	20.96	3.6677	92.538

Butterfly opening: 50°

					Gas equation:	T2/T1 = (p2/p1) ^ (γ-1)/γ	
Pipe dia	200 mm						
					(γ-1)/γ=	0.2857	
					Cp=	1.005	kJ/kg.K
Inlet pressure (p1)= 1 bar					**Constant pressure, h= Cp (T2-T1)**		
Outlet pressure (p2) = 1 bar - actual presure in side of the siphon							
Inlet temperature (T1) = 20°C		293 °K			T2=(p2/p1)^0.286	Power =	
Specific heat ratio	**1.4**				1.4		
Density of air =	1.204	Kg/m3					

p2/p1 bar	(γ-1)/γ	T2/T1	T2 °K	h= CpT m	QA1 l/s	Power Watt
0.725	0.2860	0.91	267.24	25.89	0.000	0.000
0.727	0.2860	0.91	267.46	25.66	1.834	56.668
0.748	0.2860	0.92	269.65	23.46	3.565	100.719
0.773	0.2860	0.93	272.15	20.96	5.178	130.642
0.804	0.2860	0.94	275.28	17.81	5.804	124.470
0.822	0.2860	0.95	276.98	16.10	6.086	117.997

Butterfly opening: 60°

		Gas equation:	T2/T1 = (p2/p1) ^ (γ-1)/γ	
Pipe dia	200 mm			
		(γ-1)/γ=	0.2857	
		Cp=	1.005	kJ/kg.K
Inlet pressure (p1)= 1 bar		**Constant pressure, h= Cp (T2-T1)**		
Outlet pressure (p2) = 1 bar - actual presure in side of the siphon				
Inlet temperature (T1) = 20°C =	293 °K	T2=(p2/p1)^0.286		
Specific heat ratio	**1.4**	1.4		
Density of air =	1.204 Kg/m3			

p2/p1 bar	(γ-1)/γ	T2/T1	T2 °K	h= CpT m	QA1 l/s	Power output Watt
0.728	0.2860	0.91	267.61	25.52	1.830	56.233
0.731	0.2860	0.91	267.83	25.29	3.650	111.169
0.745	0.2860	0.92	269.29	23.83	5.373	154.139
0.762	0.2860	0.93	271.09	22.02	6.999	185.593
0.787	0.2860	0.93	273.55	19.55	8.476	199.486
0.818	0.2860	0.94	276.64	16.44	8.557	169.402

Butterfly opening: 70°

		Gas equation:	T1 = (p2/p1) ^ (γ-1)/γ	
Pipe dia	200 mm			
		(γ-1)/γ=	0.2857	
		Cp=	1.005	kJ/kg.K
Inlet pressure (p1)= 1 bar		**Constant pressure, h= Cp (T2-T1)**		
Outlet pressure (p2) = 1 bar - actual presure in side of the siphon				
Inlet temperature (T1) = 20°C =	293 °K	T2=(p2/p1)^0.286		
Specific heat ratio =	**1.4**	1.4		
Density of air =	1.204 Kg/m3			

p2/p1 bar	(γ-1)/γ	T2/T1	T2 °K	h= CpT m	QA1 l/s	Power Watt
0.794	0.2860	0.94	274.24	18.85	7.982	181.136
0.804	0.2860	0.94	275.28	17.81	8.706	186.706
0.832	0.2860	0.95	277.99	15.09	9.215	167.407

Butterfly opening: 80°

					Gas equation:	2/T1 = (p2/p1) ^ (γ-1)/γ	
Pipe dia	200 mm						
					(γ-1)/γ=	0.2857	
					Cp=	1.005	kJ/kg.K
Inlet pressure (p1)= 1 bar					**Constant pressure, h= Cp (T2-T1)**		
Outlet pressure (p2) = 1 bar - actual presure in side of the siphon							
Inlet temperature (T1) = 20°C =		293	°K		T2=(p2/p1)^0.286		
Specific heat ratio =	**1.4**				1.4		
Density of air =		1.204	Kg/m3				

p2/p1 bar	(γ-1)/γ	T2/T1	T2 °K	h= CpT m	QA1 l/s	Power Watt
0.818	0.2860	0.94	276.64	16.44	13.514	267.512

Butterfly opening: 90° (full)

					Gas equation:	T2/T1 = (p2/p1) ^ (γ-1)/γ	
Pipe dia	200 mm						
					(γ-1)/γ=	0.2857	
					Cp=	1.005	kJ/kg.K
Inlet pressure (p1)= 1 bar					**Constant pressure, h= Cp (T2-T1)**		
Outlet pressure (p2) = 1 bar - actual presure in side of the siphon							
Inlet temperature (T1) = 20°C =		293	°K		T2=(p2/p1)^0.286		
Specific heat ratio	**1.4**				1.4		
Density of air =		1.204	Kg/m3				

p2/p1 bar	(γ-1)/γ	T2/T1	T2 °K	h= CpT m	QA1 l/s	Power Watt
0.853	0.2860	0.96	279.97	13.09	12.896	203.244
0.846	0.2860	0.95	279.32	13.75	13.396	221.819

B.5c Low Siphon - Aerator 3 - Power Calculation

Butterfly opening: 30°

					Gas equation:	T2/T1 = (p2/p1) ^ (γ-1)/γ	
Pipe dia	200 mm						
					(γ-1)/γ	0.2857	
					Cp=	1.005	kJ/kg.K
Inlet pressure (p1)= 1 bar					**Constant pressure, h= Cp (T2-T1)**		
Outlet pressure (p2) = 1 bar - actual presure in side of the siphon							
Inlet temperature (T1) = 20°C =			293	°K	T2=(p2/p1)^0.915		
Specific heat ratio					1.4		
Density of air =		1.204	Kg/m3				
			Power = h*Q_A*1.204				
					Vel from calculation (v1)		

p2/p1	(γ-1)/γ	T2/T1	T2	h= CpT	QA1	Power output
bar			°K	m	l/s	Watt
0.653	0.2860	0.89	259.36	33.81	0.000	0.000
0.674	0.2860	0.89	261.71	31.44	0.989	37.456
0.681	0.2860	0.90	262.49	30.66	1.224	45.191
0.684	0.2860	0.90	262.87	30.28	1.461	53.270
0.688	0.2860	0.90	263.26	29.89	1.575	56.684
0.691	0.2860	0.90	263.64	29.51	1.688	59.954
0.695	0.2860	0.90	264.02	29.12	1.799	63.084
0.699	0.2860	0.90	264.48	28.67	1.907	65.834

Butterfly opening: 40°

					Gas equation:	T2/T1 = (p2/p1) ^ (γ-1)/γ	
Pipe dia	200 mm						
					(γ-1)/γ	0.286	
					Cp=	1.005	kJ/kg.K
Inlet pressure (p1)= 1 bar					**Constant pressure, h= Cp (T2-T1)**		
Outlet pressure (p2) = 1 bar - actual presure in side of the siphon							
Inlet temperature (T1) = 20°C =		293	°K				
Specific heat ratio= 1.4					1.4		
Density of air =		1.204	Kg/m3				
			Power = h*Q_A*1.204				

p2/p1	(γ-1)/γ	T2/T1	T2	h= CpT	QA1	Power
bar				m	l/s	Watt
0.706	0.2860	0.91	265.23	27.91	0.0000	0.000
0.720	0.2860	0.91	266.73	26.41	0.9259	29.438
0.727	0.2860	0.91	267.46	25.66	1.3755	42.501
0.738	0.2860	0.92	268.56	24.56	1.8079	53.457
0.741	0.2860	0.92	268.93	24.19	2.2492	65.515
0.759	0.2860	0.92	270.73	22.38	2.6368	71.057
0.769	0.2860	0.93	271.80	21.31	3.0342	77.852
0.790	0.2860	0.93	273.90	19.20	3.3755	78.021

Butterfly opening: 50°

Gas equation: $T2/T1 = (p2/p1)^{(\gamma-1)/\gamma}$

Pipe dia 200 mm

$(\gamma-1)/\gamma$ = 0.286

Cp = 1.005 kJ/kg.K

Inlet pressure (p1)= 1 bar

Constant pressure, h= Cp (T2-T1)

Outlet pressure (p2) = 1 bar - actual presure in side of the siphon

Inlet temperature (T1) = 20°C = 293 °K

Specific heat ratio= 1.4 1.4

Density of air = 1.204 Kg/m3

Power = $h * Q_A * 1.204$

p2/p1 bar	$(\gamma-1)/\gamma$	T2/T1	T2	h= CpT m	QA1 l/s	Power Watt
0.710	0.2860	0.91	265.61	27.53	0.000	0.000
0.731	0.2860	0.91	267.83	25.29	2.282	69.481
0.755	0.2860	0.92	270.37	22.74	4.415	120.889
0.780	0.2860	0.93	272.85	20.25	5.559	135.529
0.794	0.2860	0.94	274.24	18.85	5.881	133.469

Butterfly opening: 60°

Gas equation: $T2/T1 = (p2/p1)^{(\gamma-1)/\gamma}$

Pipe dia 200 mm

$(\gamma-1)/\gamma$ 0.286

Cp= 1.005 kJ/kg.K

Inlet pressure (p1)= 1 bar

Constant pressure, h= Cp (T2-T1)

Outlet pressure (p2) = 1 bar - actual presure in side of the siphon

Inlet temperature (T1) = 20°C = 293 °K

Specific heat ratio= 1.4 1.4 N/m3

Density of air = 1.204 Kg/m3

Power = $h * Q_A * 1.204$

p2/p1 bar	$(\gamma-1)/\gamma$	T2/T1	T2	h= CpT m	QA1 l/s	Power Watt
0.748	0.2860	0.92	269.65	23.46	3.565	100.7
0.755	0.2860	0.92	270.37	22.74	4.415	120.9
0.762	0.2860	0.93	271.09	22.02	5.249	139.2
0.776	0.2860	0.93	272.50	20.60	6.443	159.8
0.794	0.2860	0.94	274.24	18.85	7.561	171.6
0.804	0.2860	0.94	275.28	17.81	8.292	177.8
0.815	0.2860	0.94	276.30	16.78	8.594	173.7

Butterfly opening: 70°

Gas equation: $T2/T1 = (p2/p1)^{(\gamma-1)/\gamma}$

$(\gamma-1)/\gamma$ = 0.286

Cp = 1.005 kJ/kg.K

Pipe dia 200 mm

Inlet pressure (p1)= 1 bar

Constant pressure, h= Cp (T2-T1)

Outlet pressure (p2) = 1 bar - actual presure in side of the siphon

Inlet temperature (T1) = 20°C = 293 °K

Specific heat ratio= 1.4 1.4 N/m3

Density of air = 1.204 Kg/m3

Power = $h*Q_A*1.204$

p2/p1 bar	$(\gamma-1)/\gamma$	T2/T1	T2	h= CpT m	QA1 l/s	Power Watt
0.787	0.2860	0.93	273.55	19.55	6.781	159.6
0.797	0.2860	0.94	274.59	18.50	7.528	167.7
0.808	0.2860	0.94	275.62	17.47	8.256	173.6
0.818	0.2860	0.94	276.64	16.44	8.965	177.5
0.825	0.2860	0.95	277.32	15.76	9.293	176.4
0.829	0.2860	0.95	277.65	15.43	9.656	179.3

Butterfly opening: 90° (full)

Gas equation: $T2/T1 = (p2/p1)^{(\gamma-1)/\gamma}$

Pipe dia 200 mm

$H=(1+K_{tota})v^2/2g$

$(\gamma-1)/\gamma$ = 0.286

$K=(2gH/v2)-1$

Cp = 1.005 kJ/kg.K

Inlet pressure (p1)= 1 bar

Constant pressure, h= Cp (T2-T1)

Outlet pressure (p2) = 1 bar - actual presure in side of the siphon

Inlet temperature (T1) = 20°C = 293 °K

Specific heat ratio= 1.4 1.4

Density of air = 1.204 Kg/m3

Power = $h*Q_A*1.204$

p2/p1 bar	$(\gamma-1)/\gamma$	T2/T1	T2	h= CpT m	QA1 l/s	Power Watt
0.804	0.286	0.94	275.28	17.81	7.877	168.9
0.808	0.286	0.94	275.62	17.47	8.256	173.6
0.822	0.286	0.95	276.98	16.10	8.927	173.1
0.843	0.286	0.95	278.98	14.09	9.891	167.7
0.849	0.286	0.95	279.58	13.49	10.210	165.8

B.6a Low Siphon - Aerator 1 - Efficiency Calculation

Butterfly opening: 30°

Efficiency calculation

Efficiency=Pout/Pin

Power in = $\rho_W * g * Q_W * H$

$\rho W = 1000\ kg/m^3$

H	Qw	Power in	Efficiency
m	l/s	Watt	%
2.300	14.500	327.2	0.00
2.314	13.600	308.7	5.14
2.316	13.200	299.9	9.82
2.318	12.700	288.8	14.16
2.319	12.400	282.1	16.26
2.320	12.200	277.7	17.35

Butterfly opening: 40°

Efficiency calculation

Efficiency=Pout/Pin

Power in = $\rho_W * g * Q_W * H$

$\rho W = 1000\ kg/m^3$

H	Qw	Power in	Efficiency
m	l/s	Watt	%
2.244	31.0	682.4	0.00
2.260	28.6	634.1	2.86
2.269	27.4	609.9	5.71
2.273	26.1	582.0	8.60
2.280	24.9	556.9	11.23
2.290	23.2	521.2	12.72
2.295	22.6	508.8	13.42
2.299	21.7	489.4	14.28
2.302	21.2	478.8	15.21
2.328	19.0	433.9	18.01

Butterfly opening: 50°

Power in = $\rho_W * g * Q_W * H$

$\rho_W = 1000\ kg/m^3$

Efficiency=Pout/Pin

H	Qw	Power in	Efficiency
m	l/s	Watt	%
2.189	51.5	1105.9	0.00
2.211	48.6	1053.9	6.75
2.240	44.3	973.5	12.73
2.250	42.0	927.0	15.39
2.267	39.5	878.5	16.69
2.279	36.5	816.0	18.42
2.264	31.0	688.5	21.25

Butterfly opening: 60°

Power in = $\rho_W * g * Q_W * H$

$\rho W = 1000\ kg/m^3$

Efficiency=Pout/Pin

H	Qw	Power in	Efficiency
m	l/s	Watt	%
2.11	65.30	1348.4	0.00
2.15	62.80	1321.5	12.63
2.17	60.00	1277.3	16.41
2.20	51.50	1112.7	22.18
2.21	44.30	960.4	23.80
2.24	41.60	912.5	20.43
2.24	36.00	790.7	24.23

Butterfly opening: 70 °

Power in = $\rho_W * g * Q_W * H$

$\rho W = 1000\ kg/m^3$

H	Qw	Power in	Efficiency
m	l/s	Watt	%
2.12	67.60	1402.6	16.19
2.15	65.30	1377.3	17.43
2.17	63.90	1359.0	16.67
2.20	60.00	1294.9	16.41

Butterfly opening: 80°

Power in = $\rho_W * g * Q_W * H$

$\rho W = 1000\ kg/m^3$

H	Qw	Power in	Efficiency
m	l/s	Watt	%
2.05	70.00	1407.7	15.16
2.16	69.60	1472.1	16.81
2.14	69.00	1450.2	17.53
2.14	67.60	1419.2	17.29
2.15	64.00	1348.3	18.20

Butterfly opening: 90° (full)

Power in = $\rho_W * g * Q_W * H$

$\rho W = 1000\ kg/m^3$

H	Qw	Power in	Efficiency
m	l/s	Watt	%
2.13	70.00	1462.7	11.37
2.16	67.60	1429.1	11.44
2.17	63.80	1356.3	11.61

B.6b Low Siphon - Aerator 2 - Efficiency Calculation

Butterfly opening: 30°

Power in = $\rho_W * g * Q_W * H$

$\rho W = 1000\ kg/m^3$

H	Qw	Power in	Efficiency
m	l/s	Watt	%
2.298	15.600	351.677	0.00
2.305	14.800	334.658	4.32
2.319	14.000	318.491	8.56
2.310	13.400	303.659	12.69
2.307	13.200	298.738	14.46
2.307	13.000	294.212	15.53

Butterfly opening: 40°

Power in = $\rho_W * g * Q_W * H$

$\rho W = 1000\ kg/m^3$

H	Qw	Power in	Efficiency
m	l/s	Watt	%
2.25	29.7	656.136	0.00
2.26	28.7	636.296	3.47
2.26	28.6	634.640	4.64
2.26	28.0	621.326	5.88
2.26	28.0	621.876	6.97
2.27	27.7	616.300	7.92
2.27	27.5	612.389	8.83
2.28	26.0	580.517	11.29
2.28	24.6	551.189	13.70
2.28	22.6	504.603	17.42
2.27	21.9	487.685	19.03
2.28	20.1	449.770	20.57

Butterfly opening: 50°

Power in = $\rho_W * g * Q_W * H$

$\rho W = 1000\ kg/m^3$

H	Qw	Power in	Efficiency
m	l/s	Watt	%
2.252	52.0	1148.79	0.00
2.207	48.8	1056.55	5.36
2.226	46.0	1004.50	10.03
2.232	41.3	904.30	14.45
2.258	36.4	806.30	15.44
2.255	32.1	710.10	16.62

Butterfly opening: 60°

Power in = $\rho_W * g * Q_W * H$

$\rho W = 1000\ kg/m^3$

H	Qw	Power in	Efficiency
m	l/s	Watt	%
2.093	69.0	1416.392	3.97
2.175	65.0	1386.889	8.02
2.173	61.3	1306.439	11.80
2.194	55.2	1188.077	15.62
2.221	44.0	958.672	20.81
2.240	40.0	878.976	19.27

Butterfly opening: 70°

Power in = $\rho_W * g * Q_W * H$

$\rho W = 1000\ kg/m^3$

H	Qw	Power in	Efficiency
m	l/s	Watt	%
2.158	63.8	1350.3	13.41
2.185	60.0	1286.1	14.52
2.210	45.0	975.6	17.16

Butterfly opening: 80°

Power in = $\rho_W * g * Q_W * H$

$\rho W = 1000\ kg/m^3$

H	Qw	Power in	Efficiency
m	l/s	Watt	%
2.08	71.60	1462.740	18.29

Butterfly opening: 90° (full)

Power in = $\rho_W * g * Q_W * H$

$\rho W = 1000\ kg/m^3$

H	Qw	Power in	Efficiency
m	l/s	Watt	%
2.155	63.00	1331.855	15.26
2.135	67.80	1420.027	15.62

B.6c Low Siphon - Aerator 3 - Efficiency Calculation

Butterfly opening: 30°

Power in = $\rho_W * g * Q_W * H$

$\rho W = 1000\ kg/m^3$

Eff= Power out/power in

H m	Qw l/s	Power in Watt	Efficiency %
2.300	14.500	327.164	0.00
2.315	13.330	302.726	12.37
2.317	13.000	295.487	15.29
2.318	12.700	288.793	18.45
2.319	12.500	284.306	19.94
2.319	12.400	282.092	21.25
2.320	12.300	279.878	22.54
2.320	12.200	277.662	23.71

Butterfly opening: 40°

Power in = $\rho_W * g * Q_W * H$

$\rho W = 1000\ kg/m^3$

Eff= Power out/power in

H m	Qw l/s	Power in Watt	Efficiency %
2.236	30.0	658.1	0.00
2.252	28.0	618.6	4.76
2.258	26.6	589.2	7.21
2.264	26.1	579.7	9.22
2.274	24.9	555.5	11.79
2.287	22.6	507.0	14.01
2.299	21.0	473.6	16.44
2.319	17.0	386.7	20.17

Butterfly opening: 50°

Power in = $\rho_W * g * Q_W * H$

$\rho W = 1000\ kg/m^3$

H	Qw	Power in	Efficiency
m	l/s	Watt	%
2.18	52.50	1121.72	0.00
2.19	48.80	1049.37	6.62
2.24	44.30	973.47	12.42
2.27	39.50	878.45	15.43
2.29	36.00	808.74	16.50

Butterfly opening: 60°

Power in = $\rho_W * g * Q_W * H$

$\rho W = 1000\ kg/m^3$

H	Qw	Power in	Efficiency
m	l/s	Watt	%
2.133	64.0	1338.9	7.52
2.148	61.0	1285.1	9.41
2.175	57.5	1226.9	11.35
2.195	55.0	1184.3	13.49
2.195	51.0	1098.2	15.63
2.217	48.2	1048.3	16.96
2.240	44.4	975.7	17.80

Butterfly opening: 70°

Power in = $\rho_W * g * Q_W * H$

$\rho W = 1000\ kg/m^3$

H	Qw	Power in	Efficiency
m	l/s	Watt	%
2.143	64.0	1345.1	11.86
2.158	58.5	1238.2	13.54
2.163	53.5	1135.0	15.30
2.195	51.0	1098.2	16.16
2.207	48.0	1039.2	16.97
2.221	46.0	1002.2	17.89

Butterfly opening: 90° (full)

Power in = $\rho_W * g * Q_W * H$

$\rho W = 1000\ kg/m^3$

H	Qw	Power in	Efficiency
m	l/s	Watt	%
2.150	63.0	1328.8	12.71
2.165	60.0	1274.3	13.62
2.163	53.5	1135.0	15.25
2.228	47.6	1040.1	16.13
2.213	45.7	991.9	16.72

B.7 New Spiral -Higher Siphon - Void Fraction Calculation

Butterfly opening: 60°

Butterfly opening = 60° Siphon break at 320 l/min aeration

V-notch	Qwater	Over weir	Head		Air flow	Airflow	Press. Gauge	Press. Ratio	Callib prss	ratio
cm	l/s	cm	m		l/min	l/s	bar			
29.00	62.5	1.0	2.180		0	0.000	-0.516	2.066	-0.361	1.57
28.35	59.0	0.0	2.177		100	1.667	-0.462	1.859	-0.323	1.48
27.50	55.0	1.5	2.200		200	3.333	-0.428	1.748	-0.300	1.43
25.00	44.2	2.0	2.230		280	4.667	-0.420	1.724	-0.294	1.42
22.70	35.0	2.5	2.258		300	5.000	-0.335	1.504	-0.235	1.31

Ap= 0.0314 m2

v2- (vs+(Qw+QA)/Ap) v + vs Qw/Ap = 0

Qw		QA	QA1	Qw+QA1	((Qw+QA1)/1000)/Ap	+((Qw+QA1)/1000)/A	vs (Qw/1000)/Ap		v1	v2
l/s	l/min	l/s		l/s	m/s	b	c	√(b2-4ac)	m/s	m/s
62.5	0	0.000	0	62.500	1.9904	2.2304	0.47771	1.75045	1.99	0.24
59.0	100	1.667	2.463	61.463	1.957	2.197	0.451	1.739	1.97	0.23
55.0	200	3.333	4.759	59.759	1.903	2.143	0.420	1.706	1.92	0.22
44.2	280	4.667	6.610	50.810	1.618	1.858	0.338	1.450	1.65	0.20
35.0	300	5.000	6.532	41.532	1.323	1.563	0.268	1.171	1.37	0.20

Aw=Qw/v	AA=QA1/(v-vs)	α = AA/(AA+Aw)
m2	m2	
31.400	0.000	0.000
29.975	1.425	0.045
28.575	2.825	0.090
26.725	4.675	0.149
25.604	5.796	0.185

Butterfly opening: 70°

diameter = 3mm Butterfly opening = 70° Siphon break at 460 l/min aeration

V-notch	Qwater	Over weir	Head		Air flow	Airflow	Press. Gauge	Press. Ratio	callib prss	ratio
cm	l/s	cm	m		l/min	l/s	bar	bar		
32.50	81.30	-5.0	2.085		0	0.000	-0.535	2.151	-0.375	1.5987
32.25	80.00	-3.0	2.108		80	1.333	-0.455	1.835	-0.319	1.4674
32.00	78.70	-1.0	2.130		160	2.667	-0.432	1.761	-0.302	1.4335
31.50	76.00	0.5	2.150		240	4.000	-0.432	1.761	-0.302	1.4335
31.25	74.70	0.0	2.148		300	5.000	-0.415	1.709	-0.291	1.4094
30.75	72.00	-1.0	2.143		340	5.667	-0.400	1.667	-0.280	1.3889
29.50	65.30	1.0	2.175		380	6.333	-0.390	1.639	-0.273	1.3755
29.25	64.00	0.0	2.168		400	6.667	-0.375	1.600	-0.263	1.3559
29.00	62.5	0.0	2.170		420	7.000	-0.360	1.563	-0.252	1.3369
28.80	62.00	0.0	2.172		440	7.333	-0.350	1.538	-0.245	1.3245

Ap= 0.0314 m2

v2- (vs+(Qw+QA)/Ap) v + vs Qw/Ap = 0

Water flowrate Qw	Air flowrate	QA	QA1	Qw+QA1	((Qw+QA1)/1000)/Ap	vs+((Qw+QA1)/1000)/Ap	vs (Qw/1000)/Ap		v1	v2
l/s	l/min	l/s		l/s	m/s	b	c	√(b2-4ac)	m/s	m/s
81.30	0	0.000	0.000	81.300	2.5892	2.8292	0.62140	2.34917	2.59	0.24
80.00	80	1.333	1.956	81.956	2.6101	2.8501	0.61146	2.38266	2.62	0.23
78.70	160	2.667	3.823	82.523	2.6281	2.8681	0.60153	2.41245	2.64	0.23
76.00	240	4.000	5.734	81.734	2.6030	2.8430	0.58089	2.39980	2.62	0.22
74.70	300	5.000	7.047	81.747	2.6034	2.8434	0.57096	2.40856	2.63	0.22
72.00	340	5.667	7.870	79.870	2.5436	2.7836	0.55032	2.35529	2.57	0.21
65.30	380	6.333	8.712	74.012	2.3571	2.5971	0.49911	2.17905	2.39	0.21
64.00	400	6.667	9.040	73.040	2.3261	2.5661	0.48917	2.15132	2.36	0.21
62.5	420	7.000	9.358	71.858	2.2885	2.5285	0.47771	2.11716	2.32	0.21
62.00	440	7.333	9.713	71.713	2.2839	2.5239	0.47389	2.11525	2.32	0.20

Aw=Qw/v	AA=QA1/(v-vs)	α = AA/(AA+Aw)
m2	m2	
31.400	0.00000	0.000
30.577	0.82330	0.026
29.807	1.59258	0.051
28.992	2.40781	0.077
28.446	2.95358	0.094
28.021	3.37862	0.108
27.344	4.05558	0.129
27.133	4.26653	0.136
26.907	4.49308	0.143
26.729	4.67072	0.149

Butterfly opening: 80°

Butterfly opening = 80° Siphon break above 500 l/min aeration

V-notch	Qwater	Over weir	Head		Air flow	Airflow	Press. Gauge	Press. Ratio	Cllib prss	ratio
cm	l/s	cm	m		l/min	l/s	bar			
33.00	84.5	-5.0	2.080		100	0.000	-0.430	1.754	-0.301	1.43
32.75	83.0	-2.5	2.108		200	3.333	-0.405	1.681	-0.284	1.40
32.25	80.0	-0.5	2.133		400	6.667	-0.400	1.667	-0.280	1.39
30.75	72.0	1.0	2.163		500	8.333	-0.340	1.515	-0.238	1.31

Ap= 0.0314 m2

v2- (vs+(Qw+QA)/Ap) v + vs Qw/Ap = 0

Qw		QA	QA1	Qw+QA1	((Qw+QA1)/1000)/Ap	vs+((Qw+QA1)/1000)/Ap	vs (Qw/1000)/Ap		v1	v2
l/s	l/min	l/s		l/s	m/s	b	c	√(b2-4ac)	m/s	m/s
84.5	100	1.667	2.384	86.167	2.7442	2.9842	0.64586	2.51431	2.75	0.23
83.0	200	3.333	4.652	86.333	2.7495	2.9895	0.63439	2.52969	2.76	0.23
80.0	400	6.667	9.259	86.667	2.7601	3.0001	0.61146	2.56021	2.78	0.22
72.0	500	8.333	10.936	80.333	2.5584	2.7984	0.55032	2.37270	2.59	0.21

Aw=Qw/v	AA=QA1/(v-vs)	α = AA/(AA+Aw)
m2	m2	
30.736	0.950	0.0300
30.077	1.846	0.0578
28.775	3.645	0.1124
27.847	4.663	0.1434

Butterfly opening: 90° (full)

full opening — Siphon break at 620 l/min aeration

V-notch	Qwater	Over weir	Head		Air flow	Airflow	Press. Gauge	Press. Ratio	Callib prss	ratio
cm	l/s	cm	m		l/min	l/s	bar			
31.50	76.00	2	2.165		500	8.333	-0.340	1.515	-0.238	1.31
30.50	71.00	1.00	2.165		540	9.000	-0.320	1.471	-0.224	1.29
30.00	68.00	1.00	2.170		570	9.500	-0.310	1.449	-0.217	1.28
29.50	65.00	2.50	2.190		600	10.000	-0.300	1.429	-0.210	1.27

Ap= 0.0314 m2

Qw		QA	QA1	Qw+QA1	((Qw+QA1)/1000)/Ap	vs+((Qw+QA1)/1000)/Ap	vs(Qw/1000)/Ap		v1	v2
l/s	l/min	l/s		l/s	m/s	b	c	√(b2-4ac)	m/s	m/s
76.00	500	8.333	10.9361	86.936	2.7687	3.0087	0.58089	2.59394	2.80	0.21
71.00	540	9.000	11.5979	82.598	2.6305	2.8705	0.54268	2.46356	2.67	0.20
68.00	570	9.500	12.1328	80.133	2.5520	2.7920	0.51975	2.39088	2.59	0.20
65.00	600	10.000	12.6582	77.658	2.4732	2.7132	0.49682	2.31822	2.52	0.20

callibrated pressure

Aw=Qw/v	AA=QA1/(v-vs)	α = AA/(AA+Aw)
m2	m2	
27.130	4.2698	0.136
26.621	4.7787	0.152
26.240	5.1597	0.164
25.838	5.5623	0.177

B.8 New Spiral - Higher Siphon - Power Calculation

Butterfly opening: 60°

				Gas equation:	T2/T1 = (p2/p1) ^ (γ-1)/γ		
Pipe dia	200 mm						
$H=(1+K_{tota})v^2/2g$				(γ-1)/γ	0.2857		
K=(2gH/v2)-1				Cp=	1.005	kJ/kg.K	
Inlet pressure (p1)= 1 bar				**Constant pressure, h= Cp (T2-T1)**			
Outlet pressure (p2) = 1 bar - actual presure in side of the siphon							
Inlet temperature (T1) = 15°C =		288 °K		T2=(p2/p1)^0.286		P=h*QA*ρA	
Specific heat ratio =	**1.4**			1.4			
Density of air =	1.204	Kg/m3					

p2/p1 bar	(γ-1)/γ	T2/T1	T2 °K	h= CpT m	QA1 l/s	Power Watt
0.639	0.2860	0.88	253.35	39.84	0.000	0.00
0.677	0.2860	0.89	257.55	35.62	2.463	105.65
0.700	0.2860	0.90	260.11	33.05	4.759	189.39
0.706	0.2860	0.91	260.71	32.46	6.610	258.30
0.766	0.2860	0.93	266.81	26.32	6.532	207.00

Butterfly opening: 70°

			Gas equation:	T2/T1 = (p2/p1) ^ (γ-1)/γ	
Pipe dia	200 mm				
$H=(1+K_{tota})v^2/2g$			(γ-1)/γ=	0.2857	
$K=(2gH/v2)-1$			Cp=	1.005	kJ/kg.K
Inlet pressure (p1)= 1 bar			**Constant pressure, h= Cp (T2-T1)**		
Outlet pressure (p2) = 1 bar - actual presure in side of the siphon					
Inlet temperature (T1) = 15.6°C =	288.6 °K		T2=(p2/p1)^0.286		
Specific heat ratio =	**1.4**		1.4		
Density of air =	1.204 Kg/m3				

p2/p1	(γ-1)/γ	T2/T1	T2	h= CpT	QA1	Power
bar			°K	m	l/s	Watt
0.626	0.2860	0.87	252.36	40.85	0.000	0.000
0.682	0.2860	0.90	258.62	34.55	1.956	81.382
0.698	0.2860	0.90	260.36	32.81	3.823	150.993
0.698	0.2860	0.90	260.36	32.81	5.734	226.489
0.710	0.2860	0.91	261.62	31.54	7.047	267.597
0.720	0.2860	0.91	262.72	30.43	7.870	288.364
0.727	0.2860	0.91	263.45	29.70	8.712	311.512
0.738	0.2860	0.92	264.53	28.61	9.040	311.397
0.748	0.2860	0.92	265.60	27.53	9.358	310.241
0.755	0.2860	0.92	266.31	26.82	9.713	313.674

Butterfly opening: 80°

					Gas equation:	T2/T1 = (p2/p1) ^ (γ-1)/γ	
Pipe dia	200 mm						
$H=(1+K_{total})v^2/2g$					(γ-1)/γ	0.2857	
$K=(2gH/v2)-1$					Cp=	1.005	kJ/kg.K
Inlet pressure (p1)= 1 bar					**Constant pressure, h= Cp (T2-T1)**		
Outlet pressure (p2) = 1 bar - actual presure in side of the siphon							
Inlet temperature (T1) = 15°C =		288 °K			T2=(p2/p1)^0.286		
Specific heat ratio =	**1.4**				1.4		
Density of air =	1.204 Kg/m3						

p2/p1 bar	(γ-1)/γ	T2/T1	T2 °K	h= CpT m	QA1 l/s	Power Watt
0.699	0.2860	0.90	259.96	33.20	2.384	95.313
0.717	0.2860	0.91	261.81	31.35	4.652	175.585
0.720	0.2860	0.91	262.17	30.98	9.259	345.371
0.762	0.2860	0.93	266.46	26.67	10.936	351.206

Butterfly opening: 90° (full)

					Gas equation:	T2/T1 = (p2/p1) ^ (γ-1)/γ	
Pipe dia	200 mm						
$H=(1+K_{total})v^2/2g$					(γ-1)/γ=	0.2857	
$K=(2gH/v2)-1$					Cp=	1.005	kJ/kg.K
Inlet pressure (p1)= 1 bar					**Constant pressure, h= Cp (T2-T1)**		
Outlet pressure (p2) = 1 bar - actual presure in side of the siphon							
Inlet temperature (T1) = 8.9°C =		281.9 °K			T2=T1(p2/p1)^0.286	Power = Cp(T2-T1)* QA*pA	
Specific heat ratio (γ)=	**1.4**				1.4		
Density of air =	1.204 Kg/m3						

p2/p1 bar	(γ-1)/γ	T2/T1	T2 °K	h= Cp(T2-T1) m	QA1 l/s	Power Watt
0.762	0.2860	0.93	260.82	32.34	10.936	425.9
0.776	0.2860	0.93	262.18	30.98	11.598	432.6
0.783	0.2860	0.93	262.85	30.30	12.133	442.6
0.790	0.2860	0.93	263.52	29.63	12.658	451.5

B.9 New Spiral - Higher Siphon - Efficiency Calculation

Butterfly opening: 60°

Power in = ρW*g*QW*H

ρW= 1000 kg/m3

H	Qw	Power in	Efficiency
m	l/s	Watt	%
2.180	62.5	1336.6	0.0
2.177	59.0	1259.7	8.4
2.200	55.0	1187.0	16.0
2.230	44.2	966.9	26.7
2.258	35.0	775.3	26.7

Butterfly opening: 70°

Power in = ρW*g*QW*H

ρW= 1000 kg/m3

H	Qw	Power in	Efficiency
m	l/s	Watt	%
2.085	81.30	1662.90	0.0
2.108	80.00	1653.97	4.9
2.130	78.70	1644.46	9.2
2.150	76.00	1602.95	14.1
2.148	74.70	1573.70	17.0
2.143	72.00	1513.29	19.1
2.175	65.30	1393.29	22.4
2.168	64.00	1360.84	22.9
2.170	62.5	1330.48	23.3
2.172	62.00	1321.05	23.7

Butterfly opening: 80°

Power in = ρW*g*QW*H

ρW= 1000 kg/m3

H	Qw	Power in	Efficiency
m	l/s	Watt	%
2.080	84.5	1724.2	5.5
2.1075	83.0	1716.0	10.2
2.1325	80.0	1673.6	20.6
2.1625	72.0	1527.4	23.0

Butterfly opening: 90° (full)

Power in = ρW*g*QW*H

ρW= 1000 kg/m3

H	Qw	Power in	Efficiency
m	l/s	Watt	%
2.165	76.00	1614.14	26.4
2.165	71.00	1507.94	28.7
2.170	68.00	1447.56	30.6
2.190	65.00	1396.45	32.3

Appendix C

Datasets used in Chapter 7

C.1 Bubbly flow pattern - Aerator2

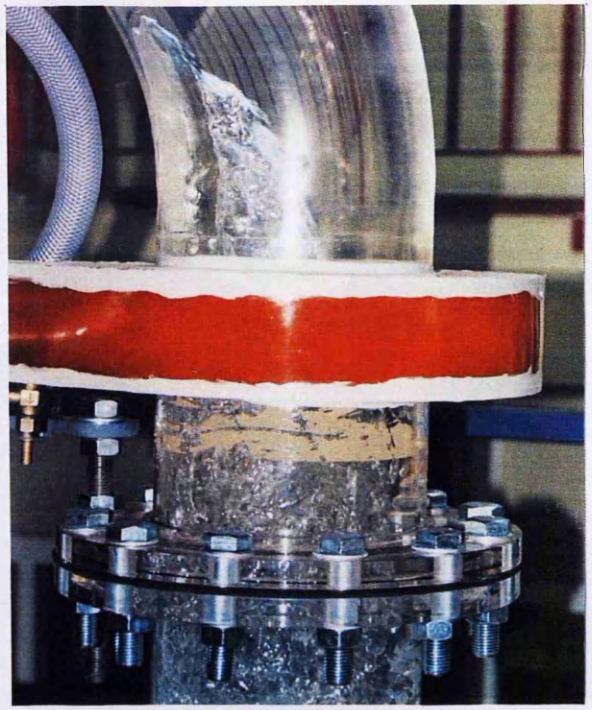

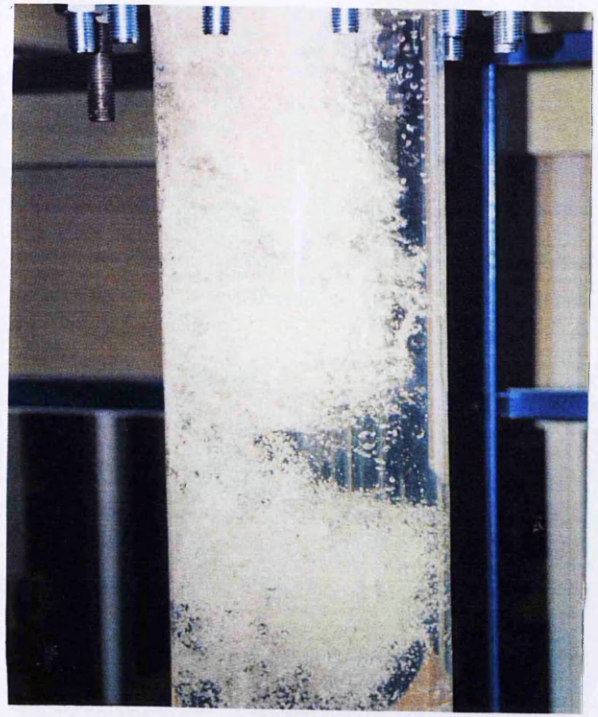

C.1 Bubbly flow pattern - Aerator2

C.2 Bubbly flow pattern - Aerator3

C.2 Bubbly flow pattern - Aerator3